8-9-2014

EFFECTS OF HIV-1 TAT PROTEIN ON STRUCTURE, FUNCTION AND TRAFFICKING OF THE DOPAMINE TRANSPORTER

Narasimha Murty Midde
University of South Carolina - Columbia

EFFECTS OF HIV-1 TAT PROTEIN ON STRUCTURE, FUNCTION AND TRAFFICKING OF THE DOPAMINE TRANSPORTER

by

Narasimha Murty Midde

Bachelor of Science
Andhra University, 2003

Master of Science
Andhra University, 2005

Professional Science Master
University of South Carolina, 2009

Submitted in Partial Fulfillment of the Requirements

For the Degree of Doctor of Philosophy in

Pharmaceutical Sciences

College of Pharmacy

University of South Carolina

2014

Accepted by:

Jun Zhu, Major Professor

Douglas Pittman, Committee Member

Campbell McInnes, Committee Member

Kennerly Patrick, Committee Member

Rosemarie Booze, Committee Member

Lacy Ford, Vice Provost and Dean of Graduate Studies

DEDICATION

To my wife Elisha, for her immeasurable sacrifices, love and encouragement during this roller coaster ride….

ACKNOWLEDGEMENTS

First and foremost, I would like to express my deep gratitude to my mentor Dr. Jun Zhu who has been wonderful mentor and motivator. Dr. Zhu has been the best guide imaginable and working in his lab provided me great training to tackle research questions from different perspectives. From the bottom of my heart, I thank you for your support and encouragement throughout the years.

I would like to thank the members of dissertation committee: Drs. Douglas Pittman, Campbell McInnes, Rosemarie Booze and Kennerly Patrick for their help, accessibility and valuable critiques of this research work. Especially, I extend my grateful thanks to Dr. Rosemarie Booze, for her advice and support in keeping my research progress on schedule. I would like to express my gratitude for Dr. Chang-Guo Zhan and members of his research group at University of Kentucky for providing me computational data on tight timescales. Further, I extend my appreciation to Dr. Kim E. Creek for allowing me to use his laboratory facilities.

I would like to thank all the members of Zhu lab, past and present, for their help and making my life lively in the lab. Particularly, I acknowledge my colleague and good friend, Adrian Gomez, for his friendship and great discussions on endless topics. I would like to recognize all the people from Department of Drug Discovery and Biomedical Sciences for their help to complete my graduate work. I have been fortunate to have amazing group of friends in and outside the department. Thank you all for making my graduate life memorable. Finally, I wish to thank my wonderful family – parents Nageswara Rao and Saraswathi, wife Elisha, Uncle Mahipal Bandlamudi and our adorable little ones Charan and Amuktha for their endless support, patience and unwavering love. I love you all.

ABSTRACT

The alarming rise in HIV-1 associated neurocognitive disorder (HAND) is, at least in part, associated with HIV-1 viral proteins shed from infected macrophages, including transactivator of transcription (Tat) despite the success of anti-retroviral therapies. The dopamine (DA) system is greatly involved in the progression of HAND and is influenced by psychostimulants like cocaine. The DA transporter (DAT), a key regulator of neurocognitive functions, is a major molecular target for both Tat and cocaine. Our lab previously reported that exposure to Tat decreases DA uptake through allosteric regulation and alters cocaine binding sites in DAT.

In this research project the hypothesis 'HIV-1 Tat protein via allosteric modulation of DAT induces inhibition of DA transport, leading to dysfunction of the DA system' was tested. Initially, it was shown that Tat protein directly interacts with DAT to impair DA translocation. Based on the predictions of computational modeling and simulations, Y470, Y88 and K92 residues of the human DAT (hDAT) are essential to stabilize the compact structure of DAT and potentially recognize Tat. Mutating these residues in hDAT – Y470H, Y88F, and K92M attenuated Tat-induced inhibition of DA uptake. Additional substitutions Y470A and Y470F at 470 displayed attenuated or no effect on Tat-induced inhibition of DA uptake respectively, indicating the significant role of aromatic ring of Y470 in DAT and Tat interaction. Pharmacological characterization showed that compared to wild type hDAT, Y470H and K92M but not Y88F reduce V_{max} with no change in the K_m values for DA uptake. Moreover, Y470H, K92M, and Y88F mutants exhibited no alterations in IC_{50} values

of DA to inhibit [^{3}H]DA uptake but increased [^{3}H]DA uptake potency or [^{3}H]WIN35,428 binding potency for cocaine and GBR12909, suggesting that these three Tat-recognition residues do not overlap with substrate DA binding but influence binding of small molecule inhibitors. Besides, all five mutants reversed zinc-induced increase of [^{3}H]WIN35,428 binding and differentially altered basal DA efflux properties of the DAT, indicating that Tat protein through interaction at these recognition residues disrupts intermolecular interactions that are critical for maintenance of the outward-facing conformation of DAT.

Another study was conducted to determine the effects of Tat on DAT phosphorylation, trafficking and its influence on sequestration of [^{3}H]DA by vesicular monoamine transporter 2 (VMAT2). We found that protein kinase C (PKC) inhibitor, bisindolylmaleimide-I eliminates Tat effects on DA uptake and Tat increases intracellular DAT immunoreactivity. Moreover, Tat also produced inhibitory effects on VMAT2 function. Collectively, these findings revealed that Tat inhibits DAT function through PKC and trafficking- dependent mechanisms; besides, both DAT and VMAT2 proteins may involve in Tat-induced dysregulation of the DA system.

In conclusion, Tat inhibits DA translocation process principally by altering the conformational states of the DAT through interaction at specific recognition residues. Furthermore, regulatory pathways that control the functional attributes of DAT may play a vital role in Tat-mediated impairment of the DA system. Future studies will be necessary to identify and characterize other recognition residues for Tat binding and these molecular insights will be helpful to develop adjunctive therapies to restore the impaired DA system in HIV-1 positive individuals.

TABLE OF CONTENTS

LIST OF TABLES

LIST OF FIGURES

List of Abbreviations

3D.....Three dimensional

AMPH.....d-Amphetamine

ANOVA.....Analysis of Variance

ART.....Anti retroviral therapy

BD..... Brownian dynamics

BIM-1.....Bisindolyl maleimide -1

B_{max} ..... Binding capacity

CNS.....Central nervous system

Co-IP.....Co-Immunoprecipitation

CREB ..... Cyclic AMP response element binding protein

CSF .....Cerebrospinal fluid

DA.....Dopamine

DAT .....Dopamine transporter

Dox.....Doxycycline

ERK.....Extracellular regulated kinase

FBS .....Fetal bovine serum

Flot-1.....Flotillin/Reggie-1

Gag..... Group specific antigen

GBR12909 .....1-[2-(bis[4-fluorophenyl]methoxy)ethyl]-4-[3-phenylpropyl] piperazine

GFAP ..... Glial fibrillary acidic protien

GFP .....Green fluorescent protein

GST .....Glutathione S-transferase

HAND .....HIV-1 associated neurocognitive disorder

hDAT .....Human dopamine transporter

HIV-1 ..... Human Immunodeficiency Virus-1

HIV-1 Tg.....HIV-1 transgenic

HVA .....Homovanillic acid

IB.....Immunoblotting

IC_{50}.....The half maximal inhibitory concentration

IP .....Immunoprecipitation

IPTG..... Isopropyl beta-D-1-thiogalactopyranoside

K_d ..... Dissociation constant

K_m.....Michaelis-Menten constant

KRH ..... Krebs-Ringer-HEPES

LTR .....Long terminal repeat

MAPK .....Mitogen-activated protein kinase

MD .....Molecular dynamics

MPP.....1-methyl-4-phenylpyridinium

NAc .....Nucleus accumbens

NIH .....National Institute of Health

NMR ..... Nuclear magnetic resonance

PAGE ..... Polyacrylamide gel electrophoresis

PFC .....Prefrontal cortex

PKC.....Protein kinase - C

RRE..... Rev response element

RTI-55..... 3beta-(4'-iodophenyl)tropan-2beta-carboxylic acid methyl ester

SDS .....Sodium dodecyl sulfate

SEM .....Standard error of mean

SLCA3 ..... Solute carrier 6 family

SoRI-20040 ..... N-(2,2-diphenyl ethyl)-2-phenyl-4-quinazolinamine

SoRI-20041 .....N-(3,3-diphenylpropyl)-2-phenyl-4-quinazolinamine

SoRI-9804 .....N-(Diphenylmethyl)-2-phenyl-4-quinazolinamine

SPR .....Surface plasmon resonance

TAR..... Transactivation response element

Tat .....Trans-activator of transcription

TBZ.....Tetrabenazine

TH .....Tyrosine hydroxylase

VMAT2.....Vesicular monoamine transporter - 2

V_{max} ..... Maximal velocity

VTA ..... Ventral tegmental area

WIN 35,428.....2beta-carbomethoxy-3beta-(4-fluorophenyl) tropane

WT .....Wild type

CHAPTER 1

INTRODUCTION

1.1 HIV-ASSOCIATED NEUROCOGNITIVE DISORDER (HAND)

The devastating effects of Human Immunodeficiency Virus-1 (HIV-1) infection were substantially reduced in HIV-infected individuals with the introduction of antiretroviral therapies (ARTs) in 1996 (Carpenter et al., 1996; Deeks et al., 2013). This resulted in reclassification of HIV-1 from life threatening disease to a manageable chronic illness (Clifford and Ances, 2013). However, HIV-1 has the propensity to have broad effects on central nervous system (CNS) and impairs CNS functions which results in serious consequences that lead to HIV-associated neurocognitive disorder (HAND). Approximately 70% of HIV-1 positive adults and children exhibit a neurological disease at one point during the course of their infection (Grovit-Ferbas and Harris-White, 2010; Simioni et al., 2010; Bilgrami and O'Keefe, 2014). The spectrum of neurological complications in HAND ranges from asymptomatic neurocognitive impairment, to mild neurocognitive disorder, to the more severe form HIV-associated dementia (Antinori et al., 2007). The clinical impairments in HAND include attention, memory, learning, motor functioning and behavioral changes. ARTs improve the survival rate of infected people but cannot eliminate the virus from their brain (Antiretroviral Therapy Cohort, 2008; Heaton et al., 2010) meaning that these therapies do not offer complete cure. In addition, the incidences and progression of HAND are further compounded by the consumption of recreational drugs like cocaine and methamphetamine

(Buch et al., 2011; Nair and Samikkannu, 2012). If HAND can be prevented at early infection stage, quality of patient's life will be improved and economic burden will be lessened on the health care system.

During the course of HAND, HIV-1 infected monocytes infiltrates the brain by crossing the blood-brain barrier at the early infection stage approximately 2-3 weeks after primary infection (Davis et al., 1992; Nath and Clements, 2011; Williams et al., 2013). Subsequently, virus spreads to perivascular macrophages and microglia and establishes a reservoir within the brain. These infected cells release large number of viral particles daily which ultimately increase the viral load in the CNS. Moreover, these cells secrete neurotoxic HIV-1 viral proteins that include structural protein gp120 and nonstructural protein Tat (*trans*-activator of transcription) as well as proinflammatory cytokines and chemokines (Mattson et al., 2005). Several studies observed that HIV-1 cannot directly infect dopaminergic neurons but extracellularly discharged viral proteins through direct interaction progressively destruct the neurons and cause subsequent neurodegeneration (Nath et al., 2000b; Ferris et al., 2008). Among these proteins, Tat has been highly linked to progressive neuronal dysegulation leading to the development of HAND. Lastly, dopamine (DA) dysregulation has been associated with cognitive deficits in HIV-1 positive people (Purohit et al., 2011; Jacobs et al., 2013). Long-term viral proteins exposure can accelerate the damage in the DA system (Del Valle et al., 2000; Ferris et al., 2008; Hudson et al., 2010; Nath, 2010). Considering the oxidative stress-induced damage to the dopaminergic neurons, long lasting exposure to viral proteins and elevated DA eventually lead to DA deficits which enhance the severity and acceleration of the HAND (Purohit et al., 2011). For the purpose of this dissertation, the following literature review broadly discusses HIV-1 viral proteins, DA

transporter (DAT) structure, function and regulation, and general effects of Tat protein on dopaminergic neurons through impairment of DAT function.

1.1.1 HIV-1 Viral Proteins

The proviral DNA of HIV-1 is composed of at least nine genes flanked by a repeated sequence called the long terminal repeats (LTRs). These genes encode proteins that can principally be divided into three categories: (1) major structural proteins – Gag, Pol and Env, (2) regulatory proteins – Tat and Rev, (3) accessory proteins – Vpu, Vpr, Vif and Nef (Gallo et al., 1988). These proteins are required at various stages of virus life cycle.

Structural proteins

The Gag (group-specific antigen) codes for Gag precursor protein (p55) which is associated with cell membrane after post-translational modifications. Viral protease processes this p55 to generate the following proteins: matrix protein (p17) – facilitates nuclear transport of viral genome, capsid (p24) protein – forms conical core of the viral particle, nucleocapsid (p9) – recognizes packaging signal and helps in reverse transcription, and p6 protein – aids in interaction of p55 and vpr, and release of viral particles from infected cells (Göttlinger et al., 1989; King, 1994; Lee et al., 2012). The pol gene expresses four essential enzymes that include, reverse transcriptase – transcribes DNA from RNA template, RNase H – facilitates complementary DNA strand synthesis by cleaving original RNA template, integrase – required for integration of proviral DNA into the host genome, protease – necessary to p55 protein (Lee et al., 2012). Furthermore, Env (for 'envelope') codes for gp160 protein and this protein is glycosylated in the endoplasmic reticulum before being processed by a cellular protease to produce gp41 and gp120 proteins. While gp41 acts as an anchor in the viral envelope, gp120 mediates HIV-1 infection by interacting with CD4 receptor that is present on the lymphocytes (King, 1994; Merk and Subramaniam, 2013).

Regulatory proteins

Tat, an RNA-binding protein is absolutely required for the HIV-1 replication. Tat acts as the transcriptional activator by interacting with transactivation response element (TAR) at the 5' terminus of HIV-1 RNA template (Ruben et al., 1989; Feinberg et al., 1991). Rev (regulator of expression of virion proteins) is an RNA-binding protein that binds at Rev response element (RRE) within the second intron of the HIV-1 genome. Rev is essential to activate late genes and thus for synthesis of viral proteins to produce virions (Zapp and Green, 1989; Vercruysse and Daelemans, 2014).

Accessory proteins

The other four viral genes such as Nef, Vpu, Vif and Vpr encode accessory proteins. These proteins perform multiple functions at different stages of viral infection (Trono, 1995; Strebel, 2013). It appears that they mostly work toward evasion of innate and adaptive immune systems. Specifically, Nef and Vpu proteins manipulate the localization and functional aspects of host cell membrane proteins. These alterations greatly influence viral replication and also help the virus to escape the immunity shield. Vif and Vpr proteins protect the virus by inhibiting cytoplasmic host defense molecules and by modifying host cell intracellular environment.

1.1.2 HIV-1 TAT PROTEIN

Tat is a key early regulatory protein for viral gene expression and replication. It is a small polypeptide encoded from two separate exons, length varies from 86 to 101 amino acids depending on the viral strain (Ratner et al., 1985; Jeang et al., 1999). Tat protein has been divided into five different protein domains. The first exon encodes the first four well conserved domains that include acidic domain (residues 1-21), cysteine rich domain

(residues 22-37), hydrophobic core (residues 38-48) and basic domain (residues 49-72), whereas sixth domain (residues 73-101) is encoded by second exon (Li et al., 2012). Clinical isolates from HIV-infected patients' display the presence of Tat_{1-101} or its truncated form, Tat_{1-86} in different target organs (Jeang et al., 1999; Barré-Sinoussi et al., 2004; Strazza et al., 2011). Besides its canonical function as a transcriptional activator, Tat is actively secreted from infected cells and can be detected in cell culture supernatants, in serum and in cerebrospinal fluid of HIV-1 infected individuals (Ensoli et al., 1990; Westendorp et al., 1995; New et al., 1997; Bachani et al., 2013; Midde et al., 2013). Westendorp et al. (1995) reported ~1 to 3 ng/mL and ~16 ng/mL of Tat levels in the plasma and the cerebrospinal fluid (CSF) of HIV-1 infected patients respectively. Furthermore, another study using 80 anonymous HIV-1 positive patients' sera found that soluble Tat levels range from 2 ng/ml to 40 ng/ml (Xiao et al., 2000). However, authors argued that these estimations may be lower than the actual concentration present in the system (Westendorp et al., 1995; Xiao et al., 2000). Although the precise Tat concentration in the brain is not yet known, one could expect that this level to be markedly elevated in CSF than plasma because of close proximity of HIV-1-infected cells in the brain (Hayashi et al., 2006). This secreted Tat can act as neurotoxin by effecting bystander cells including neurons (Del Valle et al., 2000) . The precise mechanism by which Tat damages neurons is not clear. However, it has been suggested that Tat can interact with specific cell surface proteins or can be taken up by neurons to manipulate intracellular signaling and trafficking events (Ensoli et al., 1990; Nath et al., 2000a; Chang et al., 2011).

1.1.3 Effect of HIV-1 Tat protein on dopaminergic neurons

DA, a key catecholamine neurotransmitter is involved in a variety of functions including cognition, locomotion, reward and neuroendocrine secretion (Lyon et al., 2011; Money and Stanwood, 2013). A plethora of investigations suggest that HIV-1 infection damages DA-rich regions in the brain that include substantia nigra, caudate nucleus, basal ganglia and globus pallidus. Interestingly, studies using animal models and human subjects revealed that HIV-mediated damage to the DA neurons occurs at the early infection stage of the disease (Lopez et al., 1999; Koutsilieri et al., 2002). Moreover, *in vitro* studies showed that increased levels of DA enhances the replication of the virus in the infected lymphocytes and macrophages (Scheller et al., 2000; Gaskill et al., 2009) and promotes oxidative stress which subsequently causes neuronal death. In this backdrop, DAT, a crucial player to maintain DA homeostasis in the brain, is central focus for this dissertation for the following reasons (1) DAT is the primary regulator for the termination of the DA neurotransmission at the synapse; (2) it has been reported that DAT density is strikingly reduced in HIV-1 infected patients and Tat protein inhibits DAT function (Wang et al., 2004; Chang et al., 2008; Ferris et al., 2009a; Zhu et al., 2009); and (3) DAT is a major target for highly addictive psychostimulants like cocaine and methamphetamines. Studies demonstrated that HIV-1 viral protiens in concert with these abused drugs have additive or synergistic effects to elevate the extracellular synaptic DA levels. This escalation of DA concentration leads to increased viral load and DA metabolism which ultimately cause neuronal death (Nath et al., 2000b; Gaskill et al., 2009; Gannon et al., 2011). While some investigators worked broadly on connections of HIV-1 infection, dysregulation of the DA system and drugs of abuse, limited studies have focused on the influence of Tat protein on DAT. This project is focused

to understand the effects of Tat protein on structure and functional regulation of DAT.

Neurotoxic effects of Tat protein were first described in a study using neurblastoma cells (Sabatier et al., 1991). Although these cells are not dopaminergic, they provided basic idea of Tat protein interaction with the neurons and associated neurotoxicity. Application of synthetic Tat to the striatal regions of rat brain *in vivo* causes deleterious effects on the neurons (Hayman et al., 1993). Studies using Tat exposed cultured human fetal neurons and microinjection of Tat into striatal neurons showed that Tat protein promotes neurotoxicity by triggering inflammatory cascades that eventually induce neuronal death by apoptosis (New et al., 1997; Jones et al., 1998; Zauli et al., 2000; Aksenov et al., 2001), suggesting that the dopaminergic neurons are predominantly susceptible to Tat protein. Moreover, Tat protein direct interaction with dopaminergic neurons increases intracellular calcium levels which in turn activate the caspases and generation of reactive oxygen species leading to neuronal injury (Kruman et al., 1998; Bonavia et al., 2001; Haughey and Mattson, 2002; Mattson et al., 2005). Elevated levels of Tat mRNA have been detected in the brain tissue extracts of HIV-1 infected patients (Wiley et al., 1996; Hudson et al., 2000) and these brain derived Tat sequences showed mutations at second exon region (Bratanich et al., 1998; Cowley et al., 2011), indicating that the Tat protein exhibits significant molecular diversity and this heterogeneity may render the neuronal cells vulnerable to this protein. Extracellular Tat uses neuronal transport to reach different anatomical pathways that are distant from viral replication site (Bruce-Keller et al., 2003) and its passage to the spinal cord through cerebrospinal fluid (Pocernich et al., 2005) clearly implicate secreted Tat as a major contributor to HIV-1 associated dementia. Along these lines, an *in vivo* microdialysis study showed compromised DA levels in the striatum of the Tat-treated animals (Ferris et al.,

2009b). Specifically, Tat protein contributed to the alterations in the dopaminergic markers expression levels that include tyrosine hydroxylase and dopamine receptor like-1 (Zauli et al., 2000; Silvers et al., 2006; Silvers et al., 2007). Thus, the above findings suggest that Tat protein directly or indirectly causes injury to dopaminergic pathways which are highly correlated with the dementia and motor deficits observed in HIV-1 positive individuals (Fig. 1.1).

1.1.4 Animal models of HIV-infected brains

Animal models for HAND are critical to understand the disease onset and progression, and to develop and test adjunctive therapies along with retroviral drugs. Non-human primates such as chimpanzees are logical models to mimic HIV-1 infection and disease progression due to their genetic similarities to humans (van Maanen and Sutton, 2003). However, financial considerations, maintenance, difficulty to obtain sufficient numbers to achieve statistically significant outcomes and public apprehensions limit their use in HAND research. Rodent models in contrast are extensively used to study HIV-1 and associated neurological dysfunctions despite the need of quite challenging efforts to generate disease in rodents because of species-specific nature of HIV-1 infection. These models offer several advantages that include low cost, easy maintenance during housing and subsequent experimental stage and well characterized genome that can be exploited to alter a particular cell or region of interest (Gorantla et al., 2012). These models may be created by employing several approaches that include stereotactic injection of viral proteins directly into the brain, expressing viral transgenes in animals, and transplantation of infected human cells into immunodeficient rodents (Van Duyne et al., 2009; Barreto et al., 2014).

In vivo mouse model was initially developed by introducing human neurofilament promoter controlled the whole HIV-1 proviral DNA into a mouse genetic background (Thomas et al., 1994). The transgene was expressed in anterior thalamic and spinal motor neurons, and animals exhibited neurological complications both in central and peripheral nervous systems. Another proviral mouse model that expresses gap-pol deleted mutant of the HIV-1 full length genome demonstrated that viral proteins and accessory genes may be sufficient to produce neurotoxicity and motor abnormalities observed in HIV-1 positive patients (Santoro et al., 1994). Further studies showed that individual viral components that include gp120/gp160, gp140, Tat, Nef, Vpr and Rev are capable of eliciting neurotoxicity in the brain (Nath, 2002; Li et al., 2005). Efforts were made to determine the role of Tat and gp120 in producing neurotoxic effects by direct injection of these proteins into the rodent brains (Jones et al., 1998; Bansal et al., 2000).

In advanced approaches, transgenic models were generated by inserting gp120 or Tat coding genes into the animal genome. Transgenic expression of HIV-1 env gene that encodes for gp120 revealed that extracellularly released gp120 is neurotoxic and produces alterations in neuronal and glial cells. These modifications are similar to the changes in HIV-1 infected human brains (Toggas et al., 1994). These transgenic animals also showed impairment in open filed activity and spatial reference memory in an age-dependent manner suggesting the role of gp120 in cognitive and motor decline observed in HIV-1 positive patients (D'Hooge et al., 1999). Another study created a transgenic mouse model that expresses Tat protein under the control of both GFAP promoter and doxycycline (Dox) inducible promoter (Kim et al., 2003). Interestingly, findings from these studies suggest that presence of Tat expression is adequate to attain neuronal damage in the brain and this neurotoxicity is severe than that

observed in gp120 transgenic animals (Toggas et al., 1994; Kim et al., 2003). Thus, these transgenic animal models are quite useful to study the HIV-associated neuropathogenesis. However, there are certain limitations to fully utilize these models to understand the HIV-1 mediated neurocognitive dysfunctions. For example, these models can replicate certain features of the disease but do not represent the whole spectrum of neuropathology associated with HIV-1 (Nath, 2010; Jaeger and Nath, 2012).

For the purpose of our project-2, to study whether HIV-1 viral proteins and nicotine together produce molecular changes in mesolimbic structures that mediate psychomotor behavior, we used HIV-1 transgenic (HIV-1 Tg) rat as small animal model that was developed by reid et al. (2001). HIV-1 Tg rats are derived from Fisher344/ BHsd strain and carry proviral DNA that is devoid of Gag and Pol genes. Expressing only seven of nine HIV- 1 genes makes this model as noninfectious, and displays immune, motor and behavioral abnormalities (Reid et al., 2001). Deficits in learning and cognition that are associated with asymptomatic HIV-1 infection have been reported in these animals (Vigorito et al., 2007; Lashomb et al., 2009). Observed dopaminergic alteration, neuroinflammation and deficits in several synaptic proteins (Persidsky and Fox, 2007; Webb et al., 2010; Rao et al., 2011) make HIV-1 Tg rat as a suitable animal model to study the effects of HIV-1 viral proteins on nicotine induced behavioral sensitization and associated signaling protein changes. Furthermore, HIV-1 Tg rats have also been successfully employed to study the concerted effects of HIV-1 viral proteins and drugs of abuse (Liu et al., 2009; Kass et al., 2010; Moran et al., 2012).

1.2 DOPAMINE TRANSPORTER (DAT)

1.2.1 STRUCTURE AND FUNCTION

The DAT, a member of the Solute Carrier 6 family (SLCA3), comprises of 620 amino acids with 12 putative transmembrane domains with both amino and carboxy termini located in the cytoplasmic side of the cells (Kristensen et al., 2011). The DAT, clears extracellular DA via rapid reuptake, is a primary determinant for the regulation of DA neurotransmission and maintaining DA homeostasis in the brain (Fig. 1.2). In addition to DA transport, DAT can move endogenous trace amines tyramine and β-phenethylamine; neurotoxin 1-methyl-4-phenylpyridinium (MPP+) and amphetamines (Sulzer, 2011) into presynaptic terminal. Great insights into structure and function relations of DAT come from the mutagenesis analysis, engineering of zinc binding sites, substituted-cysteine accessibility method and homology modeling to bacterial leucine transporter LeuT, a prokaryotic homolog of DAT (Kitayama et al., 1992; Javitch, 1998; Chen and Reith, 2000; Loland et al., 2003; Loland et al., 2004; Lin and Uhl, 2005; Yamashita et al., 2005). DAT uses Na^+ and Cl^- dependent process to translocate DA back into dopaminergic neurons against its concentration gradient. Active substrate translocation by DAT follows the alternating access model (Jardetzky, 1966; Yamashita et al., 2005). This model suggests that the transporter cycles through at least three conformational states: outward, occluded and inward, in order to re-accumulate DA into cell interiors. Correspondingly, recent studies suggest that substrate translocation is a dynamic process and it requires multiple interaction sites within DAT (Schmitt and Reith, 2011; Shan et al., 2011).

Different chemical classes of ligands induce specific conformations in DAT to achieve a particular physiological or behavioral effect. For example, cocaine-like inhibitors

have inclination to outward facing conformation (Beuming et al., 2008; Reith et al., 2012) whereas benztropine and related analogs preferentially interact with inward facing conformation of the transporter (Loland et al., 2008; Schmitt and Reith, 2011). It is worth noting that benztropine was established as an anticholinergic agent in the management of Parkinson's disease (Katzenschlager et al., 2003) and, it may also be used to treat extrapyramidal reactions caused by use of antipshycotics (Teoh et al., 2002; González-Lugo et al., 2010). Consistent with these findings, a recently solved X-ray crystal structure of DAT shows that tricyclic antidepressant nortriptyline occupies the substrate binding site and stabilizes the *Drosophila melanogaster* transporter in outward conformation and thus preventing substrate translocation (Penmatsa et al., 2013). Substrate efflux or reversal of transport is mechanistically distinct from the translocation process. Recent studies implied that synthetic compounds like N-(3,3-diphenylpropyl)-2-phenyl-4-quinazolinamine (SoRI-20041) and point mutations at specific residues in DAT cause subtle alterations in the transporter conformation which in turn have differential effects on inward transport and efflux properties (Guptaroy et al., 2009; Rothman et al., 2009; Guptaroy et al., 2011). Thus, conformational transitions in the transporter protein and associated structural changes provide a basic framework for ligand binding and have a great impact on transport kinetics and functionality of the DAT.

1.2.2 REGULATION

DAT regulation is a complex and vital process for the spatial and temporal management of DA concentration in the brain. DAT mediated behavioral and physiological functions are dynamically controlled by multitude of exogenous factors, macromolecules and signaling cascades. Many of these check points work interactively while exerting their

actions. Although there is a lack of complete understanding of regulation of DAT, available information suggest that the diverse set of DAT-affecting molecules achieve their function through ligand-transporter interactions, trafficking, post-translational modifications and protein-protein interactions (Fig. 1.3). In recent years, several reviews comprehensively presented extensive details about DAT regulation (Chen et al., 2010; Eriksen et al., 2010; Schmitt and Reith, 2011; Vaughan and Foster, 2013) and for the purpose of this dissertation, I briefly discuss some of these DAT regulatory processes that are relevant to HIV-1 Tat protein and DAT interaction.

1.2.2.1 ALLOSTERIC MECHANISM DEPENDENT REGULATION

Initial evidence for the existence of allosteric binding site for DA, a modulatory binding site on the transporter that is topographically distinct from the primary binding site comes from molecular dynamics and simulation studies (Shi et al., 2008; Shan et al., 2011). These studies suggest that direct interaction of substrates and ions at allosteric sites elicit progressive rearrangements in the transporter structure that help to shift the conformational state in order to transport substrate DA (Fig. 1.4). Furthermore, different structural classes of DAT ligands that include tricyclic antidepressants and selective reuptake inhibitors have been shown to influence this allosteric binding site (Zhou et al., 2007; Zhou et al., 2009). Likewise, investigations conducted by schmitt and reith (2010) further supported the presence of allosteric binding by using bivalent phenethylamines (two substrate like molecules connected with aliphatic spacer) that act as potent inhibitor rather than substrate molecule. In addition to the secondary binding site for DA, the existence of allosteric binding sites for synthetic DAT ligands were reported (Pariser et al., 2008). According to this study, N-(Diphenylmethyl)-2-phenyl-4-quinazolinamine (SoRI-9804), N-(2,2-diphenyl ethyl)-2-

phenyl-4-quinazolinamine (SoRI-20040), and SoRI-20041 compounds inhibit the binding of [^{125}I]3beta-(4'-iodophenyl) tropan-2beta-carboxylic acid methyl ester ([^{125}I]RTI-55) by following allosteric inhibitory patterns, meaning that these compounds do not follow classical dose dependent competitive inhibition paradigm irrespective of the concentration of [^{125}I]RTI-55. These modulators also slowed down the dissociation rate of prebound [^{125}I]RTI-55 and presented a decrease in B_{max} and increase in K_d values for [^{125}I]RTI-55 binding, further confirming the allosteric binding of these 4-quinazolinamine derivatives with the DAT. Taken together, these investigations strongly imply that various ligands allosterically regulate local rearrangements in the structural elements of the DAT that finally contribute to the formation of functionally unique conformation of the transporter to achieve targeted function.

1.2.2.2 Trafficking and Post-translational dependent regulation

Post-translational modifications, in particular phosphorylation of the transporter or its binding partners are the key strategy for controlling the function and distribution of the transporter. Numerous studies have showed that DAT trafficking to and away from plasma membrane is precisely regulated by various protein kinases that include protein kinase C (PKC), Ca^{2+}/calmodulin kinase, phosphoinositide 3-kinase, protein tyrosine kinase and members of mitogen-activated protein kinase (MAPK) family (Foster et al., 2006; Ramamoorthy et al., 2011). Of these, PKC-mediated processes are most well characterized. Activation of PKC causes decrease in V_{max} without effecting K_m value by directing active transporter population to intracellular regions (Melikian, 2004). This mode of internalization controls short and long-term availability of the transporter on the surface. While acute endocytic regulation targets DAT to early and recycling endosomes, long-term endocytosis

triggers lysosomal degradation of the protein (Chen et al., 2010; Rao et al., 2011; Hong and Amara, 2013; Sorkina et al., 2013). Interestingly, it has also been reported that PKC-stimulated direct phosphorylation of DAT does not require for internalization (Granas et al., 2003; Pramod et al., 2013) indicating the involvement of accessory proteins for the regulation of DAT endocytosis. Correspondingly, protein-protein interactions have been implicated as the crucial regulators that dictate DAT function (Eriksen et al., 2010; Sager and Torres, 2011). For example membrane raft protein Flotillin-1/Reggie-1 (Flot-1) has been shown to be required for the PKC-mediated internalization of DAT (Cremona et al., 2011). Besides eliciting DAT endocytosis, PKC also induces DAT down regulation in the presence of endocytotic blockers (Foster et al., 2008; Foster and Vaughan, 2011), indicating phosphorylation led intrinsic kinetic alterations in the transporter. On the other hand, MAPK family kinases enhance the functionality of the DAT by potentially phosphorylating serine and threonine residues in the transporter (Schmitt and Reith, 2010; Vaughan and Foster, 2013). Overall, these studies reveal that a plethora of convergent and divergent pathways regulate DAT activities: substrate translocation, substrate efflux and ion conductance through alterations in conformational states and endocytosis of the transporter.

1.2.3 DAT AND HIV-1 TAT PROTEIN

The apparent indirect evidence for dysregulation of the DAT in HIV-1 positive patients comes from reduced DA levels observed in infected brains. Decreased DA and its major metabolite homovanillic acid (HVA) were observed in post mortem brain samples and CSF (Larsson et al., 1991; Berger et al., 1994; Sardar et al., 1996; Kumar et al., 2009). These DA deficits differ from region to region in the brain, however, greater neuronal loss is associated with dopaminergic neurons especially at the subcortical area. These claims were

further substantiated by imaging studies and neuropsychological performance tests (Aylward et al., 1993; Kieburtz et al., 1996; Kumar et al., 2011). Although the above studies do not explain the underlying mechanism of HIV-infection and impairment of DA system, the possible explanation would be dysregulation of DAT that results from HIV-1 viral proteins. Because HIV-1 viral proteins load is usually peak in the dopaminergic rich areas, where the highest density of DAT protein is situated, it is reasonable to hypothesize that Tat protein impairs DAT function to promote neuronal injury. However, we cannot exclude the possibility of involvement of other HIV-1 neurotoxic proteins like coat glyco protein gp120, HIV-induced host chemokines and free radicals for the loss of dopaminergic neurons (Purohit et al., 2011). Indeed, significantly reduced DAT levels were reported in HIV-1 associated dementia patients' using positron emission tomography (Wang et al., 2004; Sporer et al., 2005; Chang et al., 2008). In contrary to these imaging studies, a recent biochemical characterization on human brain specimen collected from HIV-1 encephalitis subjects demonstrated elevated levels of DAT protein (Gelman et al., 2006). Furthermore, a single photon emission tomography imaging on treatment naïve HIV-1 patients showed enhanced DA levels with no change in the DAT density (Scheller et al., 2010). These contradictory outcomes for DAT levels suggest that the stage of the disease, treatment condition of the patient and host as well as viral factors may play a defining role in dopaminergic neuronal degeneration. Taken together, these findings indicate the altered regulation of DAT function in HIV-1 infected individuals. Although these studies clearly show the pivotal role of DAT in Tat-induced DA system impairment, mechanisms underlying alterations in the DAT activity remain elusive.

1.3 OBJECTIVES OF THE RESEARCH

The overall objective of this research is to understand how Tat protein interacts with DAT at specific recognition sites and thereby modulating transporter structure-function coordination in DA translocation process. This study provides valuable information of Tat binding residues and mechanistic understanding of Tat action on DAT at the molecular level, which is important to study Tat induced DA deficits in the animal models. This project seeks to delineate structural and molecular basis of how Tat protein interacts with DAT through conceptual and technical innovations. First, this work aims to address the novel concept of allosteric influence of Tat on DAT via interaction at specific binding sites. Second, our study is technically innovative because combining computational modeling and neuro-pharmacology represent a novel approach that allowed us to define potential Tat interacting residues on DAT. While previous studies broadly established Tat mediated dysfunction of the DAT, they have fallen short in precisely locating the molecular determinants of Tat recognition sites on DAT. This is the first time that this state-of-art-technique, integrated with conventional approaches was used to determine Tat and DAT protein interaction. We also employed molecular biological and cell surface biotinylation techniques to answer the fundamental question how Tat protein controls dynamic surface expression and trafficking of the DAT. Findings of this work lay a platform to study the relationship between Tat interaction and associated changes in DAT structure-function, and open the door to rational drug development to treat cognitive and motor deficits associated with neuroAIDS.

1.4 SPECIFIC AIMS

Our lab previously reported that Tat inhibits DAT function and that inhibition is due to a protein-protein interaction (Zhu et al., 2009). Recently, we have also demonstrated that Tat protein allosterically inhibits DAT function and influences cocaine binding sites on DAT

(Zhu et al., 2011). Moreover, our preliminary three dimensional computational modeling predicts that amino acid Tyr470 of human DAT is an important residue for favorable intermolecular interaction between DAT and HIV-1 Tat. Our initial pharmacological data for Tyr470His (Y470H) mutant DAT revealed significant attenuation of Tat-induced effects on DA uptake without changes in the binding affinity of DA to the DAT. This is consistent with the observed attenuated effects of Cys22Gly mutant Tat on DA transport (Zhu et al., 2009). Collectively, these observations ascertain the critical role of recognition sites for Tat-mediated influence on DAT structure and function.

Therefore, we ***hypothesized that HIV-1 Tat protein via allosteric modulation of DAT induces inhibition of DA transport, leading to dysfunction of the DA system.*** This central hypothesis was tested with the specific aims outlined below.

Aim 1: To create and validate computational modeling predicted HIV-1 Tat recognition sites (Y88, K92 and Y470) on human DAT. (Chapter 2 and 3)

Aim 2: To determine whether Tat has any influence on the trafficking and phosphorylation dependent regulation of DAT. (Chapter 4)

In addition to the above stated aims, the findings from my second project, combined effects of HIV-1 viral proteins and nicotine on nicotine-induced behavioral sensitization and associated changes in the expression of intracellular signaling proteins were described in Chapter 5. Finally, Chapter 6 provides overall summary and conclusions for the dissertation followed by the future directions for this research.

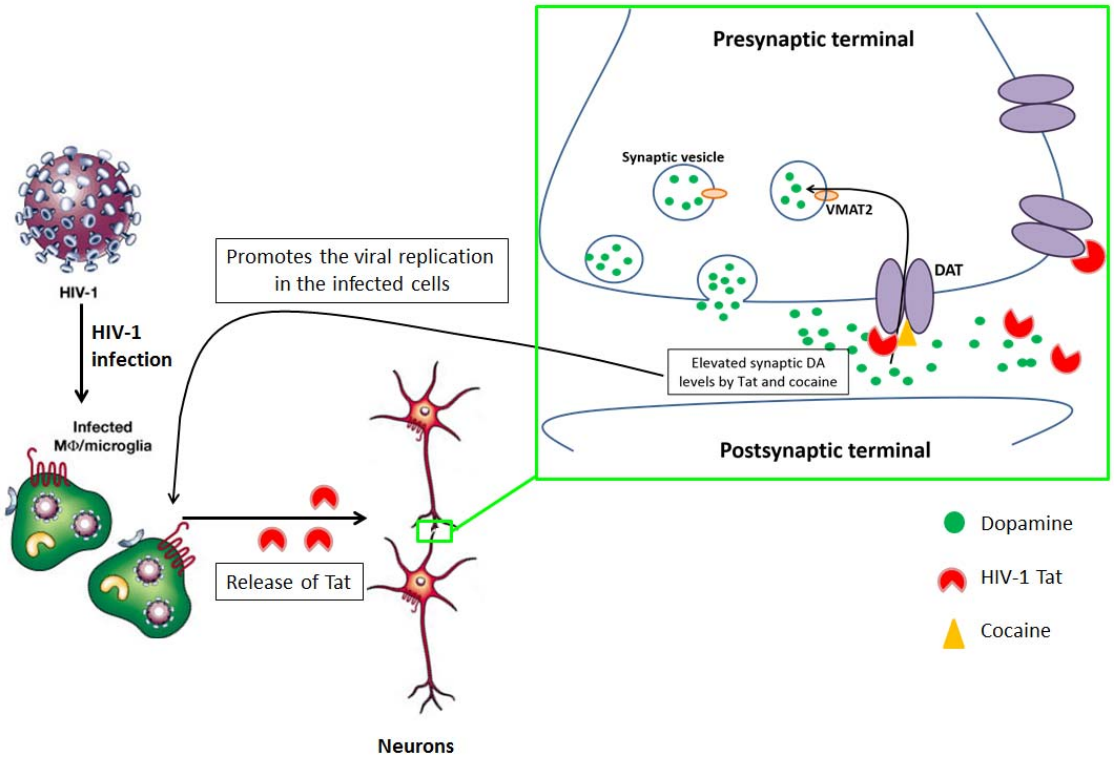

Figure 1.1 Overview of HIV-1 Tat and cocaine synergistic or additive effects on dopamine neurotransmission in HIV-1 infected individuals. HIV-1 penetrates the brain at the early infection stage and infects macrophages and microglial cells. These cells exude viral proteins that including Tat and other neurotoxic factors. Cocaine, a major psycho stimulant blocks DAT to inhibit DA translocation. Both Tat and cocaine elevate synaptic DA levels by inhibiting DA reuptake into presynaptic terminal. This increased DA induces further replication of virus in infected cells. Persistent exposure to the viral proteins, oxidative stress induced by increased DA levels and other chemokines aggravate the severity of the neurocognitive deficits in HIV-1 positive population.

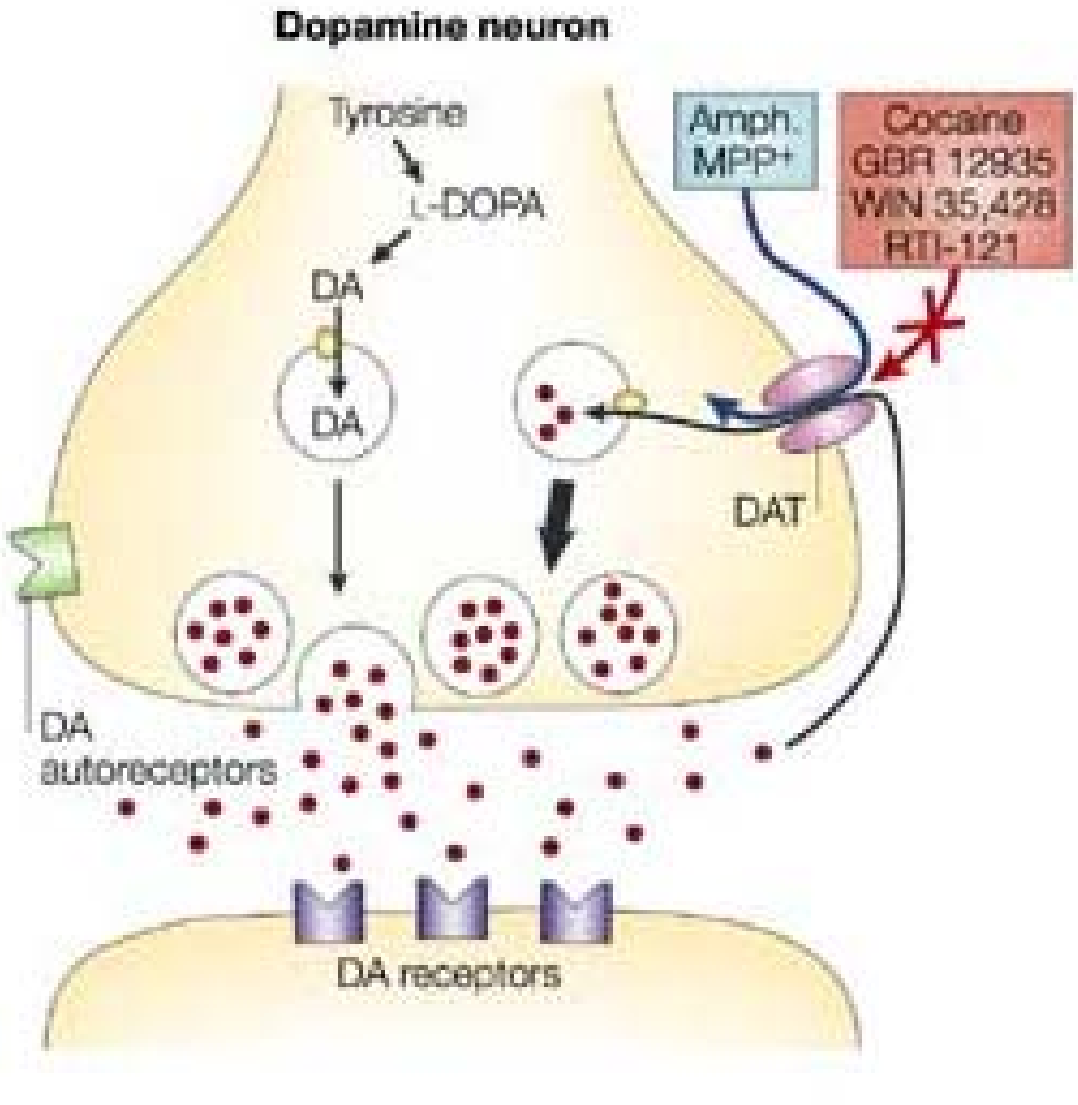

Figure 1.2 DAT is localized to the presynaptic terminal of the dopaminergic neurons. It regulates the DA availability at the synapse by rapid reuptake into the terminal. In addition to the DA, amphetamine and MPP+ (1-methyl-4-phenylpyridinium) act as substrates for DAT. Selective pharmacological inhibitors for DAT such as cocaine, GBR12909, WIN 35,428 and RTI-121 were also shown. The image was taken from Torres et al. (2003).

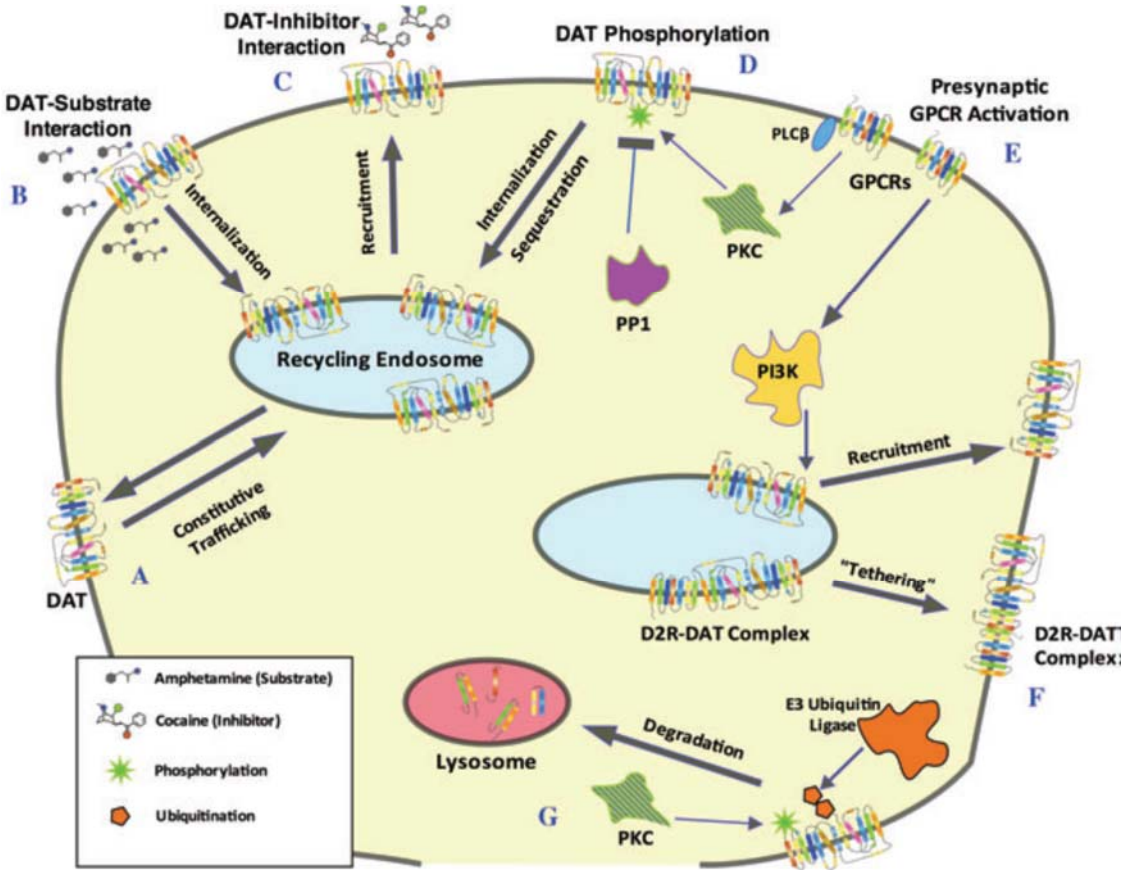

Figure 1.3 Illustration of potential regulatory pathways that control the function and availability of the DAT. **(A)** The surface localization of DAT is maintained by trafficking and endocytosis to and from the surface of the membrane. **(B and C)** Direct interaction of small molecules such as substrates and inhibitors may modulate the function of the DAT through conformational alterations. **(D)** Phosphorylation of DAT or its accessory proteins controls the catalytic activity of the transporter by influencing protein kinase signaling cascades. **(E)** Activation of G-protien coupled receptors and **(F)** direct interaction with D2-like autoreceptors modulate the DAT function. **(G)** Post-translational modification such as ubiquitination of the DAT also dictates the number of active transporter molecules on the presynaptic plasma membrane. The figure was obtained from Schmitt and Reith (2010).

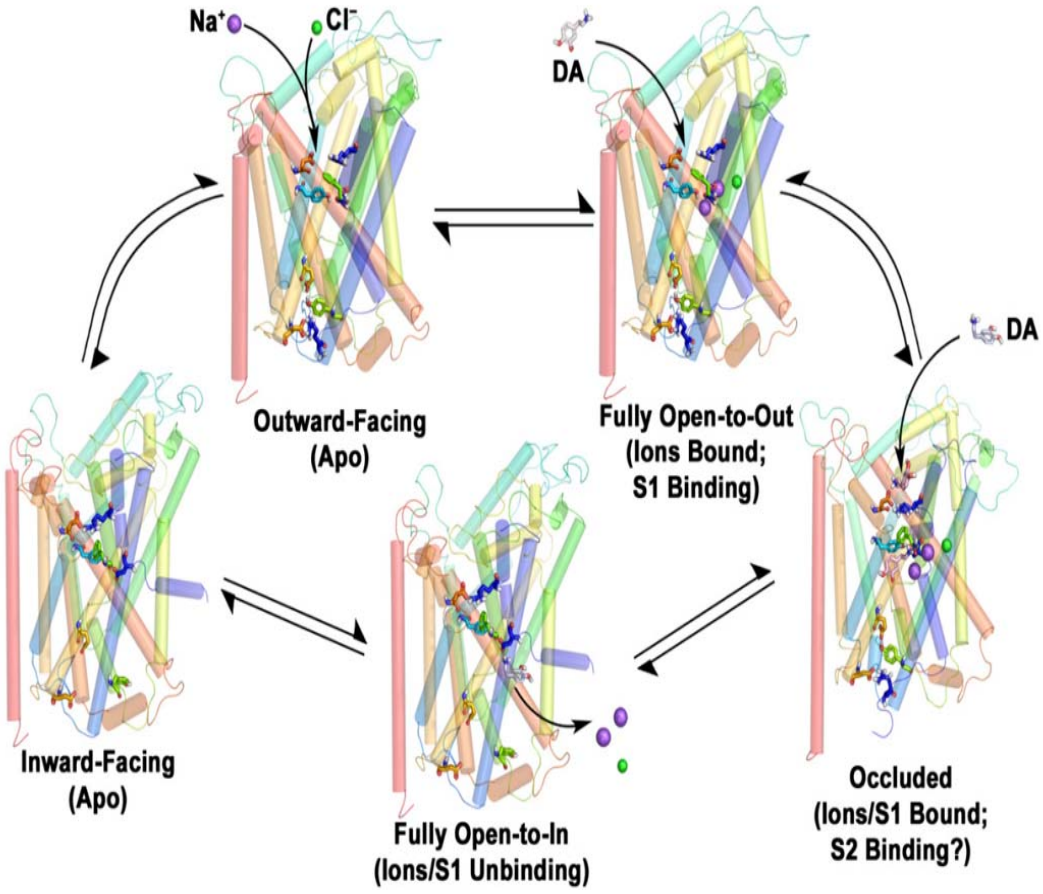

Figure 1.4 Model of substrate translocation cycle for DAT. Binding of the ions primes substrate-free (apo) DAT to fully stabilized outward-facing conformation with an open extracellular gate to bind to the substrate DA. Substrate binding at the S1 binding site promotes the formation of an occluded state and closure of the extracellular gate. Binding of a second substrate molecule at the S2 site induces the opening of an intracellular gating network leading to release of the S1-bound substrate from the inward-facing state of the DAT. The image was taken from Schmitt et al. (2013).

CHAPTER 2

MUTATION OF TYROSINE 470 OF HUMAN DOPAMINE TRANSPORTER IS CRITICAL FOR HIV-1 TAT-INDUCED INHIBITION OF DOPAMINE TRANSPORT AND TRANSPORTER CONFORMATIONAL TRANSITIONS[1]

ABSTRACT: HIV-1 Tat protein plays a crucial role in perturbations of the dopamine (DA) system. Our previous studies have demonstrated that Tat decreases DA uptake, and allosterically modulates DA transporter (DAT) function. In the present study, we have found that Tat interacts directly with DAT, leading to inhibition of DAT function. Through computational modeling and simulations, potential recognition binding site of human DAT (hDAT) for Tat was predicted. Mutation of tyrosine470 (Y470H) attenuated Tat-induced inhibition of DA transport, implicating the functional relevance of this residue for Tat binding to hDAT. Y470H reduced the maximal velocity of [^{3}H]DA uptake without changes in the K_m and IC_{50} values for DA inhibition of DA uptake but increased DA uptake potency for cocaine and GBR12909, suggesting that this residue does not overlap with the binding sites in hDAT for substrate but critical for these inhibitors. Furthermore, Y470H also led to transporter conformational transitions by affecting zinc modulation of DA uptake and WIN35,428 binding as well as enhancing basal DA efflux.

[1] Midde NM, Huang X, Gomez AM, Booze RM, Zhan CG, Zhu J (2013) Mutation of tyrosine 470 of human dopamine transporter is critical for HIV-1 Tat-induced inhibition of dopamine transport and transporter conformational transitions. Journal of neuroimmune pharmacology : the official journal of the Society on NeuroImmune Pharmacology 8:975-987. PMCID:PMC3740080

Collectively, these findings demonstrated Tyr470 as a functional recognition residue in hDAT for Tat-induced inhibition of DA transport and transporter conformational transitions. The consequence of mutation at this residue is to block the functional binding of Tat to hDAT without affecting physiological DA transport.

2.1 INTRODUCTION

The estimated prevalence of HIV-1-associated neurocognitive disorders (HAND) is about 70% of HIV-1 positive individuals with antiretroviral therapy (Robertson et al., 2007; Tozzi et al., 2007; Ernst et al., 2009). Cocaine has been shown to increase the incidence and exacerbate the severity of HAND by enhancing viral replication (Nath et al., 2001; Ferris et al., 2008). Antiretroviral agents cannot prevent the production of HIV-1 viral proteins, such as Tat protein, in HIV-1 infected brains in the early stage of HIV-1 infection (McArthur et al., 2010; Nath and Clements, 2011). Tat has been detected in the brains (Del Valle et al., 2000; Hudson et al., 2000; Lamers et al., 2010) and the sera (Westendorp et al., 1995; Xiao et al., 2000) of HIV-1 infected patients. Furthermore, Tat interacting with cocaine exacerbates the progression of the neurocognitive impairment (Buch et al., 2011; Gannon et al., 2011).

Accumulating clinical evidence supported by imaging (Chang et al., 2008; Meade et al., 2011a), neurocognitive (Kumar et al., 2011; Meade et al., 2011b), and postmortem examinations (Kumar et al., 2009; Gelman et al., 2012), reveals that abnormal neurocognitive function observed in HAND is associated with dysfunctions in dopamine (DA) neurotransmission (Berger and Arendt, 2000; Purohit et al., 2011). The DA transporter (DAT) terminates DA signaling and thus is central to control synaptic dopaminergic tone (Torres and Amara, 2007). DAT activity is strikingly reduced in HIV-

1-infected patients with a history of cocaine use (Wang et al., 2004; Chang et al., 2008). We have demonstrated that Tat allosterically modulates DAT function and reduces DAT cell surface expression in rat striatal synaptosomes (Zhu et al., 2009; Zhu et al., 2011; Midde et al., 2012).

Viral replication within HIV-1 infected brain regions results in Tat release, which elevates DA levels via inhibiting DAT function (Gaskill et al., 2009). Exposure of HIV-1 infected patients to cocaine further impairs DAT function and increases synaptic DA levels (Ferris et al., 2010). Importantly, the elevated DA induced by Tat and cocaine stimulates viral replication and Tat release (Gaskill et al., 2009), which has been implicated in the neuropathogenesis of HAND (Li et al., 2009). Considering oxidative stress-induced damage to dopaminergic neurons, long lasting exposure to viral proteins and elevated DA eventually lead to a DAT deficit that potentiates severity and accelerates the progression of HAND (Purohit et al., 2011). To the best of our knowledge, the mechanisms of Tat and cocaine interaction with hDAT have been virtually unexplored. In order to explore the molecular mechanism(s) underlying the interplay of Tat with cocaine in disrupting DAT-mediated DA neurotransmission, we performed computational modeling and simulations to predict potential recognition binding sites of human DAT (hDAT) for Tat. Identifying the functional recognition residues in hDAT for Tat may provide therapeutic insights into HAND in concurrent cocaine abusers. Upon prediction and validation of the functional relevance of tyrosine 470 (Tyr470) in hDAT, we determined the mechanisms that underlie mutation of Tyr470 in Tat-induced inhibition of DA transport and transporter conformational transitions.

2.2 MATERIALS AND METHODS

2.2.1 CONSTRUCTION OF PLASMIDS

Plasmid pcDNA3.1+/Tat_{1-72} that encodes Tat_{1-72} protein was provided by Dr. Avindra Nath (NINDS/NIH). Plasmid GFP-tagged Tat_{1-86} was a gift from by Dr. Mauro Giacca (Molecular Medicine Laboratory, ICGEB, Italy). Plasmids pcDNA3.1+/Tat_{1-101} that encodes Tat_{1-101} protein was provided by NIH AIDS Reagent Program. Mutation in hDAT (tyrosine to histidine, Y470H-hDAT) was generated based on WT hDAT sequence (NCBI, cDNA clone MGC:164608 IMAGE:40146999) by site-directed mutagenesis. Synthetic cDNA encoding hDAT subcloned into pcDNA3.1+ (provided by Dr. Haley E Melikian, University of Massachusetts) was used as a template to generate Y470H-hDAT using QuikChange™ site-directed mutagenesis Kit (Agilent Tech, Santa Clara CA). The sequence of the mutant construct was confirmed by restriction enzyme mapping and DNA sequencing.

2.2.2 CELL CULTURE AND DNA TRANSFECTION

CHO cells (ATCC #CCL-61) were maintained in F12 medium supplemented with 10% fetal bovine serum (FBS) and antibiotics (100 U/ml penicillin and 100 μg/mL streptomycin) at 37°C in a 5% CO_2 incubator. For hDAT transfection, cells were seeded into 24 well plates at a density of 1×10^5 cells/cm^2. After 24h, cells were transfected with WT or mutant DAT plasmids using Lipofactamine 2000 (Life Tech, Carlsbad, CA). Cells were used for the experiments after 24 h of transfection.

2.2.3 CO-IMMUNOPRECIPITATION (CO-IP) OF DAT AND TAT

To determine whether Tat directly binds to DAT, Co-IP of Tat and DAT assays were performed in rat synaptosomes after exposure to recombinant Tat_{1-86} as described

previously (Li et al., 2008). In brief, rat anti-DAT antibody (6 µg, MAB369, Millipore, Temecula, CA) was incubated with 20 µl protein A/G agarose beads (SC2003, Santa Cruz Biotechnology Inc., Santa Cruz, CA) for 5-6 h at 4°C with constant rotating and were centrifuged at 8,000 g for 5 min. The agarose-anti DAT antibody complex was washed five times with immunoprecipitation buffer (1% Triton X-100, 150 mM NaCl, 10 mM Tris, 1 mM EDTA, 1 mM EGTA, 0.2 mM sodium ortho-vanadate, 0.2 mM PMSF, 0.5% NP-40) to remove the unbound antibody. Rat synaptosomes from striatum and cerebellum, and spleen homogenates were prepared as described previously (Zhu et al., 2009) and adjusted to equal protein concentration (1.5 mg/ml) using the Bradford protein assay (Bradford, 1976). Then, aliquots (500 µg) of synaptosomes or homogenates were incubated in Krebs-Ringer-HEPES (KRH) buffer (final concentration in mM: 125 NaCl, 5 KCl, 1.5 $MgSO_4$, 1.25 $CaCl_2$, 1.5 KH_2PO_4, 10 D-glucose, 25 HEPES, 0.1 EDTA, 0.1 pargyline, and 0.1 L-ascorbic acid; pH 7.4) containing recombinant Tat_{1-86} (350 nM, final concentration, Clade B, # REP0002a, DIATHEVIA, Fano, Italy) for 1 h at room temperature and were then centrifuged at 8,000 g for 5 min. The resulting pellets were washed 5 times with KRH buffer. The pellets were resuspended and added to the agarose-antibody complex and incubated with agitation at 4°C overnight. These samples (agarose-antibody-protein complex) were centrifuged at 8,000 g for 1 min and the resulting pellets were washed with immunoprecipitation buffer for 5 times. These samples were then mixed with 2 × Laemmli sample buffer and boiled for 5 min. To detect immunoreactivity of DAT or Tat protein, the samples were then subjected to Western blotting with either goat polyclonal DAT antibody (1:200, Cat # SC-1433, Santa

Cruz Biotechnology Inc., Santa Cruz, CA) or mouse anti HIV-1 Tat (1:1000, Cat # ab24778, Abcam, Cambridge, MA) using our published method (Zhu et al., 2009).

2.2.4 GST-PULL-DOWN ASSAY

To confirm whether Tat interacts with DAT through a protein-protein interaction, GST-Tat fusion protein was used as bait for pull-down DAT to show their interaction as described previously (Li et al., 2008). In brief, BL21 *E*. coli expressing pGEX-Tat_{1-86} (obtained from Dr. Virginie W Gautier, University College Dublin, Ireland) and GST only (as negative control) were grown in liquid culture media and induced GST protein expression by 100 mM IPTG. These GST proteins were added to glutathione sepharose beads (17-0756-01, GE Healthcare) and then incubated with the cell lysates from CHO cells transfected with hDAT. The beads were washed with the immunoprecipitation buffer described above and mixed with protein sample buffer. The eluted proteins were subjected to immunoblotting with anti-DAT antibody (Cat # sc-1433, Santa Cruz Biotechnology Inc., Santa Cruz, CA).

2.2.5 PREDICTING THE SITE FOR HDAT BINDING WITH TAT

The binding structure of hDAT with HIV-1 clade B type Tat was modeled and simulated based on the nuclear magnetic resonance (NMR) structures of Tat (Peloponese et al., 2000) and the constructed structure of DAT(DA), as reported previously (Huang and Zhan, 2007; Huang et al., 2009). Briefly, Brownian dynamics (BD) simulations were performed to obtain the initial binding structure of the hDAT-Tat complex. Starting from the available 11 NMR structures of Tat, the BD simulations were launched from a spherical surface around the extracellular side of hDAT, and the electrostatic interaction energy was calculated for each BD trajectory by multiplying the electrostatic potential of

hDAT with the atomic charges of Tat. The initial complex for hDAT binding with Tat was identified from the BD trajectories, with the lowest interaction energy and the best geometric matching quality. The identified initial hDAT-Tat complex structures were energy-minimized in the same way as described in our previous studies on hDAT binding with DA and cocaine (Huang and Zhan, 2007; Huang et al., 2009). Molecular dynamics (MD) simulations were performed to further relax and equilibrate the energy-minimized structure of the hDAT-Tat binding complex. Finally, the MD-simulated hDAT-Tat binding structure was energy-minimized and analyzed.

2.2.6 PREPARATION OF RELEASED TAT FROM TAT-EXPRESSING CELLS

To generate released Tat from Tat-expressing cells, CHO cells were seeded into 60 mm plates at a density of $1 \times 10^6/cm^2$. After 24 h, cells were transfected with different amounts (5 and 10 μg) of plasmid DNAs for Tat_{1-72}, GFP-tagged Tat_{1-86} and Tat_{1-101} using Lipofactamine 2000. Cells transfected with pcDNA3.1+ were used as a negative control. After transfection, culture media from Tat- transfected cells were collected at 24, 48 and 72 h.

2.2.7 [^{3}H]DA UPTAKE ASSAY

Twenty four hours after transfection, [^{3}H]DA uptake in CHO cells transfected with wild type hDAT (WT hDAT) and Y470H-hDAT was performed in KRH buffer using a modified procedure as reported previously (Zhu et al., 2009). To determine whether mutated hDAT alters the maximal velocity (V_{max}) or Michaelis-Menten constant (K_m) of [^{3}H]DA uptake, kinetic analyses were conducted in WT hDAT versus Y470H-hDAT in the presence or absence of recombinant Tat_{1-86}. To generate saturation isotherms, [^{3}H]DA uptake was conducted in duplicate wells containing one of six

concentrations of unlabeled DA (final DA concentrations, 1.0 nM–5 μM) and a fixed concentration of [^{3}H]DA (500,000 dpm/well, specific activity, 31 Ci/mmol; PerkinElmer Life and Analytical Sciences, Boston, MA). In parallel, nonspecific uptake of each concentration of [^{3}H]DA (in the presence of 10 μM nomifensine, final concentration) was subtracted from total uptake to calculate DAT-mediated uptake. To determine the effect of Tat on DA uptake, cells transfected with WT or Y470H-hDAT were preincubated with each concentration of [^{3}H]DA in the presence or absence of the concentrations of released Tat or Tat_{1-86} (350 nM). The reaction was terminated by washing twice with ice cold uptake buffer. Cells were solubilized in 1% SDS and radioactivity was measured using a liquid scintillation counter (model Tri-Carb 2900TR; PerkinElmer Life and Analytical Sciences, Waltham, MA). Kinetic parameters (V_{max} and K_m) were determined using Prism 5.0 (GraphPad Software Inc., San Diego, CA).

For the competitive inhibition experiment, assays were performed in duplicate in a final volume of 500 μl. Cells in each well were incubated in 450 μl buffer containing 50 μl one of final concentrations of unlabeled DA (1 nM-1 mM), GBR12909 (1 nM-10 μM), cocaine (1 nM-1 mM), and $ZnCI_2$ (10 μM) at 37°C for 10 min and [^{3}H]DA uptake was determined by addition of 50 μl of [^{3}H]DA (0.1 μM, final concentration) for an additional 5 min.

2.2.8 IMMUNODEPLETION

Released Tat was prepared as described above. Seventy-two hours after transfection with Tat_{1-72} plasmid, aliquots (500 μl) of the conditioned media were incubated with mouse anti-Tat antibody (1:200, # ab6539, Abcam, Cambridge, MA) at 4°C for 2 h on a shaking platform, followed by incubation with 20 μl of Protein A/G –

PLUS Agarose beads (# SC2003, Santa Cruz Biotechnology Inc., Santa Cruz, CA) at 4°C for 2 h. After incubation, the agarose-antibody-Tat complex was pelleted at 12,000g for 2 min at 4°C and supernatants were collected. For the immunodepletion assay, CHO cells transfected with hDAT were incubated with either Tat-conditioned media or supernatant at 37°C for 2 h, followed by [^{3}H]DA uptake assay, as described above. Anti-Tat antibody specificity for the Tat protein was determined by using mouse IgG1 kappa monoclonal antibody (1:200, # ab18447, Abcam, Cambridge, MA) as an isotype control.

2.2.9 CELL SURFACE BIOTINYLATION

To determine whether decreased DA uptake in Y470H-hDAT is due to a reduction of cell surface DAT, biotinylation assays were performed, as described previously (Zhu et al., 2005). CHO cells expressing hDAT and Y470H-hDAT were plated on 6 well plates at a density of 10^5 cells/well. Cells were incubated with 1 ml of 1.5 mg/ml sulfo-NHS-SS biotin (Pierce, Rockford, IL) in PBS/Ca/Mg buffer (In mM: 138 NaCl, 2.7 KCl, 1.5 KH_2PO_4, 9.6 Na_2HPO_4, 1 $MgCl_2$, 0.1 $CaCl_2$, pH 7.3). After incubation, cells were washed 3 times with 1 ml of ice-cold 100 mM glycine in PBS/Ca/Mg buffer and incubated for 30 min at 4°C in 100 mM glycine in PBS/Ca/Mg buffer. Cells were then washed 3 times with 1 ml of ice-cold PBS/Ca/Mg buffer and then lysed by addition of 500 ml of Triton X-100, 1 µg/ml aprotinin, 1 µg/ml leupeptin, 1 µM pepstatin, 250 µM phenylmethysulfonyl fluoride), followed by incubation and continual shaking for 20 min at 4 °C. Cells were transferred to 1.5 ml tubes and centrifuged at 20,000g for 20 min. The resulting pellets were discarded, and 100 µl of the supernatants was stored at -20 °C for determination of immunoreactive total DAT. Remaining supernatants were incubated with continuous shaking in the presence of monomeric

avidin beads in Triton X-100 buffer (100 µl/tube) for 1 h at room temperature. Samples were centrifuged subsequently at 17,000g for 4 min at 4°C, and supernatants (containing the nonbiotinylated, intracellular protein fraction) were stored at -20°C. Resulting pellets containing the avidin-absorbed biotinylated proteins (cell-surface fraction) were resuspended in 1 ml of 1.0% Triton X-100 buffer and centrifuged at 17,000g for 4 min at 4°C, and pellets were resuspended and centrifuged twice. Final pellets consisted of the biotinylated proteins adsorbed to monomeric avidin beads. Biotinylated proteins were eluted by incubating with 50 µl of Laemmli sample buffer for 20 min at room temperature. If further assay was not immediately conducted, samples were stored at -20 °C.

2.2.10 [^{3}H]WIN 35,428 BINDING ASSAY

For the competitive inhibition experiment, cells transfected hDAT and Y470H-hDAT were incubated in KRH buffer containing 50 µl of [^{3}H]WIN 35,428 (5 nM, final concentration, specific activity, 85 Ci/mmol) and $ZnCI_2$ (10 µM) using our published method (Zhu et al., 2009). The reaction was terminated by washing twice with ice cold KRH buffer. Nonspecific binding at each concentration of [^{3}H]WIN 35,428 was determined in the presence of 30 µM cocaine (final concentration). Cells were solubilized in 1% SDS and radioactivity was measured using a liquid scintillation counter.

2.2.11 DA EFFLUX ASSAY

Basal efflux from CHO cell transfected with hDAT or mutated hDAT was measured, as described previously (Guptaroy et al., 2009). Cells were incubated in 24 well plates at a density of 10^5 cells/well for 24 h before assays were washed 3 times with

KRH buffer and preloaded with [^{3}H]DA (0.05 μM, final concentration) for 20 min at room temperature. After loading, cells were washed 3 times with KRH buffer. To obtain an estimate of the total amount of [^{3}H]DA in the cells at the zero time point, cells from a set of wells (four wells/sample) were lysed rapidly in 1% SDS after preloading with [^{3}H]DA. Buffer (500 μl) was added into separate set of cell wells and transferred to scintillation vials after 1 min as fractional efflux at 1 min, and another 500 μl buffer was added to the same wells (where the buffer was just removed for 1 min point) and collected to vials after 10 min. Additional fractional efflux at 20, 30, 40 and 50 min, respectively, was repeated under the same procedure. After 40 or 50 min, cells were lysed and counted as total amount of [^{3}H]DA remaining in the cells from each well. To determine whether exposure to Tat alters basal DA efflux, CHO cells transfected with hDAT were incubated with Tat- conditioned media from Tat-transfected cells collected at 72 h after transfection at 37°C for 2 h, followed by DA efflux assay.

2.2.12 DATA ANALYSIS

Descriptive statistics and graphical analyses were used as appropriate. Results are presented as mean ± SEM, and *n* represents the number of independent experiments for each experiment group. IC_{50} values for DA, cocaine and GBR12909 inhibiting specific [^{3}H]DA uptake were determined from inhibition curves by nonlinear regression analysis using a one-site model with variable slope. Kinetic parameters (V_{max} or K_m) of [^{3}H]DA uptake were determined from saturation curves by nonlinear regression analysis using a one-site model with variable slope. For experiments involving comparisons between unpaired samples, unpaired Student's *t* test was used to assess any difference in the kinetic parameters (IC_{50}, V_{max} or K_m) between WT and mutant; log-transformed values of

IC_{50} or K_m were used for the statistical comparisons. Significant differences between samples were analyzed with separate ANOVAs followed by post-hoc tests, as indicated in the results Section of each experiment. All statistical analyses were performed using IBM SPSS Statistics version 20, and differences were considered significant at $p, < 0.05$.

2.3 RESULTS

2.3.1 TAT PROTEIN DIRECTLY BINDS TO hDAT

Exposure of rat striatal synaptosomes to Tat protein inhibits DA uptake (Zhu et al., 2009). To determine whether Tat protein directly binds to DAT, we performed Co-IP of hDAT and Tat assays. As depicted in Fig. 2.1A, recombinant Tat_{1-86} bound to Tat antibody was able to immunoprecipitate hDAT in rat striatal synaptosomes but not in spleen and cerebellum where the density of DAT was low. To confirm this finding, we also used GST-Tat fusion protein (as bait) to pull down hDAT to show their interaction. Figure 2.1B shows that GST-Tat_{1-86} bound to hDAT protein. These data strongly suggest that the influence of Tat on DAT function involves a protein-protein interaction between Tat and DAT, which provides an experimental base for us to perform the following computational modeling analysis of the bindings between Tat and hDAT.

2.3.2 BINDING STRUCTURE OF hDAT WITH HIV-1 TAT

The energy-minimized binding structure of hDAT with Tat following the MD trajectory was shown in Fig. 2.1C and 1D. Tat protein is located on the gate of the vestibule of hDAT(DA). A loop (formed from residues #19 to #22) of Tat is plunged into the vestibule of hDAT(DA), blocking the central pore of the substrate-entry tunnel of hDAT(DA). Tat and DAT molecules bind with each other through both electrostatic interactions and shape complementarity. Particularly, the side chain of Cys22 (C22) of

Tat is located inside the vestibule of hDAT(DA), contacting closely with the side chain of Tyr470 residue of hDAT and Lys19 (K19) side chain of Tat. The positively charged head group of Lys19 side chain of Tat is hydrogen-bonded with the hydroxyl oxygen on Tyr470 side chain of hDAT(DA). The positively charged side chain of Lys19 also interacts with the aromatic side chain of Tyr470 through the cation-π interaction; the modeled distance between the N atom of Lys19 side chain and the center of the aromatic ring of Tyr470 side chain of hDAT(DA) is 4.55 Å. Based on the modeled hDAT-Tat complex structure, we predicted that residue Tyr470 is critical for the hDAT binding for Tat.

2.3.3 Extracellularly Released Tat is more potent than recombinant Tat in inhibiting hDAT function

Most previous studies of Tat-induced inhibition of DAT function have been performed using recombinant Tat. To mimic the nature of Tat released from HIV-1 infected cells, we have established a technique to ensure that clade B type Tat can be released from Tat-expressing cells and the effects of released Tat on DA uptake were examined. CHO cells were transfected with different amount of plasmid Tat_{1-72}, GFP-tagged Tat_{1-86}, and Tat_{1-101} DNA, and subsequently the conditioned media from these transfected cells were collected as a source of released Tat. The estimated amount (~1 ng/ml) of released Tat in culture media was measured by the density of immunoreactive bands and quantitated by comparison to a known amount of recombinant Tat_{1-86}.

To determine the effects of released Tat on DA uptake, we first performed the concentration and time-dependent studies for released Tat. Different amounts of released Tat from conditioned media collected at 24, 48 and 72 h were tested in [^{3}H]DA uptake in CHO expressing hDAT. A maximal effect of released Tat on DA uptake was observed

when 100 µl conditioned media collected at 72 h were used (data not shown). As shown in Fig. 2.2A, released Tat from cells transfected with Tat_{1-72}, Tat_{1-86} or Tat_{1-101} produced a similar magnitude of change from control in [^{3}H]DA uptake ($F_{(3, 12)} = 29.6$; $p < 0.01$, one-way ANOVA with Dunnett's Multiple comparison test), suggesting that Tat_{1-72}, Tat_{1-86} and full length Tat_{1-101} exhibit an equal ability in Tat-induced inhibitory effect on DA transport. We next determined whether the inhibitory effect on DA uptake was specific for released Tat by immunodepletion assay (Fig. 2.2B). Exposure to released Tat (1 ng/ml) produced a significant reduction (31 ± 2.7%) of specific [^{3}H]DA uptake compared to the control (media collected from cells transfected with vector alone). The released Tat-induced decrease in DA uptake was diminished by immunodepletion with anti-Tat antibody but not with an isotype control antibody ($F_{(3, 12)} = 13.4$; $p<0.001$, one-way ANOVA with Tukey's multiple comparison test). These data also confirmed that the inhibitory effect of incubation with conditioned media on DA uptake was specific for released Tat.

2.3.4 Mutation of Tyr470 alters DA uptake kinetics and potency of substrate and inhibitors

To validate the feasibility of the computational model of the DAT(DA)-Tat complex, we determined whether a specific residue (Tyr470, which was predicted by the computational modeling as one of favorable inter-molecular interactions between Tat and hDAT) in hDAT is important for intermolecular interaction between Tat and DAT. A mutation in hDAT (tyrosine to histidine, Y470H-hDAT) was generated by site-directed mutagenesis. We first determined the pharmacological profiles of [^{3}H]DA uptake in CHO cells transfected with equal amount of plasmid DNA for WT hDAT and mutated hDAT. As shown in Fig. 2.3A, the Y470H-hDAT displayed a decrease in the V_{max} values (2.8 ±

0.8 pmol/min/10^5 cells) compared with WT hDAT [15.7 ± 0.9 pmol/min/10^5 cells; t(3) = 15.6, $p<0.001$, unpaired Student's *t* test]; no difference in the K_m values was observed.

We have reported that Tat protein influences selective binding sites on the DAT, with differential impact on binding to GBR12935, WIN35,428 and cocaine (Zhu et al., 2009; Zhu et al., 2011). To explore the potential relationship between the binding sites of Tat in DAT and the binding sites of DAT substrate and inhibitors, we also tested the ability of DA, cocaine and GBR12909 to inhibit [^{3}H]DA uptake in WT hDAT and Y470H-hDAT (Table 1). The apparent affinity (IC_{50}) for DA was not significantly different between the WT hDAT (895 ± 80 nM) and Y470H-hDAT (737 ± 72 nM). However, the potencies of cocaine and GBR12909 for inhibition of [^{3}H]DA uptake were ~3.5-fold greater in Y470H-hDAT as compared with WT hDAT (unpaired Student's *t* test).

To assess whether the decreased V_{max} in this mutant was caused by decreased surface DAT expression, we determined DAT surface expression in CHO cells transfected with WT or Y470H-hDAT using cell surface biotinylation. As shown in Fig. 2.3B, despite no difference in the ratio of surface DAT to total DAT between WT and Y470-hDAT (biotinylated/total: WT, 0.70 ± 0.06; and Y479H, 0.68 ± 0.1; $p>0.05$, one-way ANOVA), the absolute surface DAT in the mutant hDAT was indeed decreased compared to WT hDAT (unpaired Student's *t* test). Thus, the reduction of available DAT on the cell surface could contribute to the decreased DA uptake actually measured in Y470H-hDAT, relative to WT DAT.

2.3.5 MUTATION OF TYR470 ATTENUATES TAT-INDUCED INHIBITORY EFFECTS ON DA TRANSPORT

To determine whether the mutation of Tyr470 alters inhibitory effects of Tat on DA uptake, we examined the specific [^{3}H]DA uptake in WT hDAT and Y470H-hDAT in the presence or absence of released Tat_{1-72} (1 ng/ml) or recombinant Tat_{1-86} (350 nM). As shown in Figure 2.4A, two-way ANOVA on the specific [^{3}H]DA uptake in WT and Y470H-hDAT revealed a significant main effect of mutation ($F_{(1, 24)} = 6.5$; $p < 0.05$), Tat treatment ($F_{(1, 24)} = 7.5$; $p < 0.05$) and a significant mutation × Tat interaction ($F_{(1, 24)} = 8.9$; $p < 0.05$). A subsequent simple effect analysis revealed a dramatic decrease (80%) in [^{3}H]DA uptake in Y470H-hDAT ($F_{(1, 12)} = 25$; $p < 0.001$) compared to WT hDAT in the absence of Tat. Exposure to Tat decreased [^{3}H]DA uptake by 50% in hDAT ($F_{(1, 12)} = 16.1$; $p < 0.01$; Fig. 2.4A); however, no effect of Tat was observed in Y470H-hDAT ($F_{(1, 12)} = 0.05$; $p > 0.05$), suggesting that mutation of Tyr470 in hDAT attenuates Tat-induced reduction of hDAT function.

With regard to the effect of recombinant Tat_{1-86} on DA uptake (Fig. 2.4B), a separate two-way ANOVA analysis revealed a significant main effect of mutation ($F_{(1, 24)} = 7.4$; $p < 0.05$) and Tat treatment ($F_{(1, 24)} = 9.5$; $p < 0.05$) as well as a significant mutation × Tat interaction ($F_{(1, 24)} = 12.9$; $p < 0.05$). [^{3}H]DA uptake in Y470H-hDAT was 19% of that in WT hDAT in cells transfected with equal amount of plasmid DNA for WT and mutated DAT, which is consistent with the low DAT expression observed in Fig. 2.3B**.** Exposure to Tat_{1-86} decreased [^{3}H]DA uptake by 38% in WT hDAT ($F_{(1, 12)} = 12.8$; $p < 0.01$); however, no effect of Tat on [^{3}H]DA uptake was observed in Y470H-hDAT. Since DA uptake is linear with DAT expression, in order to rule out whether the lack of effect of Tat on DA uptake in this mutant hDAT is due to a low DAT expression level in

Y470H-hDAT relative to WT hDAT, we corrected V_{max} value of Y470H-hDAT to 40% of that in WT hDAT using 3x amount of plasmid Y470H DNA in transfection (Fig. 2.4C), as reported previously (Chen et al., 2004). A two-way ANOVA revealed a significant main effect of mutation ($F_{(1, 24)} = 6.4$; $p < 0.05$) and Tat treatment ($F_{(1, 24)} = 5.5$; $p < 0.05$) as well as a significant mutation × Tat interaction ($F_{(1, 24)} = 11.2$; $p < 0.05$). Similarly, exposure to recombinant $Tat_{1\text{-}86}$ decreased V_{max} by 35% and 6% in WT hDAT and Y470H-hDAT, respectively. Thus, this result supports the inference that Tyr470 in hDAT is critical for HIV-1 Tat-induced inhibition of dopamine transport.

2.3.6 Mutation of Tyr470 affects Zinc regulation of DAT conformational transitions and basal DA efflux

We hypothesize that Tat, via allosteric modulation sites, alters conformational states of DAT, thereby decreasing DA transport. To test this possibility, we determined whether mutation of Tyr470 affects zinc regulation of DAT conformational transitions and basal DA efflux. In general, the conformational changes in DA transport process involve conversions between outward- and inward-facing conformations (Zhao et al., 2010). Occupancy of the endogenous Zn^{2+} binding site in WT hDAT (His193, His375, and Glu396) stabilizes the transporter in an outward-facing conformation, which allows DA to bind but inhibits its translocation, thereby increasing [^{3}H]WIN 35,428 binding (Norregaard et al., 1998; Moritz et al., 2013), but decreasing DA uptake (Loland et al., 2003). Addition of Zn^{2+} is able to partially reverse an inward-facing state to an outward-facing state (Norregaard et al., 1998; Loland et al., 2003). On the basis of this principle, the addition of Zn^{2+} to WT hDAT would inhibit DA uptake, whereas in a functional mutation in DAT Zn^{2+} might diminish the preference for the inward-facing conformation and thus enhance DA uptake. To explore this possibility, we examined the effects of

Tyr470 mutation on Zn^{2+} modulation of [^{3}H]DA uptake and [^{3}H]WIN35,428 binding that are thought to reflect stabilization of outwardly facing transporter forms (Richfield, 1993; Norregaard et al., 1998). For these experiments, CHO cells expressing WT and Y470H-hDAT were treated with 10 μM $ZnCI_2$ and assayed for both [^{3}H]DA uptake and [^{3}H]WIN 35,428 (Fig. 2.5A and 5B). As shown in Fig. 2.5A, two-way ANOVA on the specific [^{3}H]DA uptake in WT and Y470H-hDAT revealed a significant main effect of mutation ($F_{(1, 24)} = 11.5$; $p < 0.05$), zinc ($F_{(1, 24)} = 9.1$; $p < 0.05$) and a significant mutation × zinc interaction ($F_{(1, 24)} = 9.9$; $p < 0.05$). The addition of Zn^{2+} decreased [^{3}H]DA uptake in WT and Y470H-hDAT by 89% versus 32%, respectively (Fig. 2.5A, $p< 0.001$ relative to control, unpaired Student's *t* test). A two-way ANOVA on the specific [^{3}H]WIN35,428 binding in WT and Y470H-hDAT revealed a significant main effect of mutation ($F_{(1, 24)} = 6.5$; $p < 0.05$), zinc ($F_{(1, 24)} = 4.3$; $p < 0.05$) and a significant mutation × zinc interaction ($F_{(1, 24)} = 4.2$; $p < 0.05$). Zn^{2+} caused a 40% increase in [^{3}H]WIN 35,428 binding in WT but had no effect on Y470H-hDAT (Fig. 2.5B, $p< 0.001$ relative to control, unpaired Student's *t* test). The data suggest that Tyr 470 mutation disrupts an intermolecular interaction key for maintenance of the outward-facing conformation.

To further determine the role of Y470H-hDAT in the transition between outward-facing and inward-facing states, we also examined basal DA efflux in WT hDAT and this mutant. As shown in Fig. 2.5C, after preloading with 0.05 μM [^{3}H]DA for 20 min at room temperature, cells were washed and fractional DA efflux samples were collected at the indicated times. A two-way ANOVA revealed significant main effects of mutation ($F_{(1, 14)} = 170$; $p<0.001$) and time ($F_{(4, 56)} = 145$; $p<0.001$). A significant mutation × time interaction ($F_{(4, 56)} = 78$; $p<0.001$) was also found. Post-hoc analysis revealed robust

increases in DA efflux at 1, 10, 20, and 30 min compared to WT hDAT ($p < 0.05$, Bonferroni *t*-test). To determine whether exposure to Tat represents similar results, basal DA efflux in WT hDAT was determined in the presence or absence of released Tat_{1-72} (Fig. 2.5D). The fractional basal DA efflux data in WT hDAT were expressed as a percentage change in the respective controls of total DA content in cells with or without Tat. Analysis of two-way ANOVA revealed that a significant main effect of treatment ($F_{(1, 10)} = 18.7$; $p < 0.01$) and time ($F_{(5, 50)} = 291.9$; $p<0.001$) as well as a significant treatment × time interaction ($F_{(5, 50)} = 9.9$; $p<0.001$). Although a lower magnitude of DA efflux in response to Tat treatment was found in WT hDAT in comparison to DA efflux in Y470H-hDAT (Fig. 2.5D), post-hoc analysis revealed that exposure to released Tat_{1-72} significantly increased basal DA efflux at 1, 10, 20 and 30 min compared to control ($p < 0.05$, Bonferroni *t*-test). These data further support the possibility that Tyr 470 mutation causes a regional conformational change that affects hDAT associated with Tat.

2.4 DISCUSSION

In the current study, we used an integrated approach including computational modeling and simulations, protein mutagenesis and molecular pharmacological function assays to explore a key residue in the intermolecular interactions between HIV-1 Tat and hDAT. Our data provide additional evidence showing a direct interaction between Tat and hDAT as suggested in our previous report (Zhu et al., 2009). Through modeling and simulations, the site for Tat interaction with DAT has predicted that residue Tyr470 in hDAT is crucial for HIV-1 Tat-induced inhibition of DA transport. Tyr470 mutation did not alter the affinity for DA uptake but increased DA uptake potency for cocaine and GBR12909, suggesting that Tyr470 does not overlap with the substrate binding site but

disrupts the binding sites on DAT for these inhibitors. Importantly, mutation of Tyr470 alters Zn^{2+} modulation of DAT and basal DA efflux, compared to WT hDAT, implying a mechanistic context for the transporter conformational transitions by this mutant. Collectively, our results provide a relatively comprehensive molecular insight into this important residue for DA translocation and the underlying allosteric mechanism in DAT for Tat binding.

In response to the fundamental question how Tat interacts with hDAT through their recognition binding sites to interrupt DAT-mediated DA transmission, our computational model has predicted Tyr470 of hDAT and Cys22 as well as Lys19 in Tat as one of the favorable inter-molecular interactions between hDAT and Tat protein. Data from Co-IP and GST pull-down experiments demonstrate a direct interaction between Tat and DAT, which is consistent with the predictions from computational modeling and simulations. This study, based on the computational prediction, demonstrated that mutation of Tyr470 changes hDAT conformation and attenuates Tat-induced inhibition of DA transport. Despite the importance of Tyr470, our computational modeling does not anticipate that a single residue in hDAT is sufficient to control the interaction of Tat with hDAT. Therefore, once all recognition residues in hDAT are identified, an essential task in our future study will be to determine the influence of combined recognition residues on Tat-DAT interaction. The computational prediction of the binding mode was based on a series of computational modeling studies including homology modeling, Brownian dynamics simulations (Gabdoulline and Wade, 1998), and molecular dynamics simulations. Considering the fact that the Tat molecule has a large positive electrostatic potential, and hDAT(DA) bears negative charge, the long-range electrostatic attraction

can be viewed as the driving force for the association of Tat with hDAT. The binding mode of hDAT with Tat demonstrates that the Tat molecule is associated with DAT through inter-molecular electrostatic attractions and complementary hydrophobic interactions. In support of our proposed model, the current study and our previous report (Zhu et al., 2009) demonstrate that mutation of either Tyr470 in hDAT or Cys22 in Tat leads to attenuation of WT Tat-induced inhibitory effects on DA transport, implicating a structural and functional relationship between Tat and hDAT. Since Lys19 is also predicted as a critical residue for Tat interacting with the Tyr470 residue in DAT, we will also determine whether mutation of Lys19 produces a similar effect as mutation of Cys22 in Tat on DAT function in our future investigation. These data also qualitatively support that our computationally simulated model of the hDAT(DA)-Tat complex is reliable to be used to predict the intermolecular interactions between Tat and DAT.

Although both recombinant Tat and Tat released from cells expressing Tat produced a strong inhibitory effect on DA transport, released Tat was ~4000-fold more potent than recombinant Tat. This finding is consistent with a previous report showing this form of Tat was more neurotoxic than recombinant Tat protein (Li et al., 2008). We also found that Tat_{1-72}, Tat_{1-86} and full length Tat_{1-101} exhibited an equivalent inhibitory effect on DAT function, which is consistent with the previous studies showing that equal ability of Tat protein in Tat-induced neurotoxicity (Li et al., 2008; Aksenov et al., 2009). The concentration of released Tat (1 ng/ml) used in this study is similar to native HIV-1 Tat actually detected in the serum of patients with HIV infection (Westendorp et al., 1995) and in the conditioned medium of HIV-infected cells (Albini et al., 1998). Thus, our data support that physiologically secreted Tat is more neurotoxic to neuronal targets,

such as DAT. The advantage of this approach is feasible for further determination of the recognition sites of Tat (WT versus mutated) that functionally interact with hDAT.

The present results show that mutation of Tyr470 decreased the V_{max} with no changes in K_m value and IC_{50} value for DA inhibiting DA uptake compared to WT hDAT, demonstrating that the Tyr470 residue does not affect substrate transport characteristics. These data are consistent with the aforementioned computational prediction based on the modeled hDAT(DA)-Tat complex structure: Tat binding site in hDAT(DA) complex does not overlap with the binding site of substrate DA (Fig. 2.2). In contrast, the DA uptake potency of cocaine and GBR12909 was increased in Y470H-hDAT compared to WT hDAT. While GBR12909 labels the classic DA uptake site in rodent brain, binding to the piperazine acceptor site (Andersen et al., 1987) was affected much less by mutation of hDAT than cocaine (Loland et al., 2002; Guptaroy et al., 2011), consistent with the fact that cocaine preferentially stabilizes the hDAT in the outward-facing conformational state, resulting in a reduction of DA uptake (Reith et al., 2001; Loland et al., 2002). One interpretation of our finding is that Tat allosterically modulates DA transport rather than overlaps DA uptake sites on DAT as previously suggested (Zhu et al., 2011). However, the Tat binding site in hDAT may be close to the binding sites in hDAT for cocaine and GBR12909, increasing their DA uptake potency. Thus, the results may suggest synergistic influences of Tat and cocaine on DAT function: Tat, via allosteric modulation of the DAT, enhances the inhibitory effects of cocaine on DA transport. These findings also provide evidence to support our previous reports that Tat and cocaine synergistically inhibit DAT function *in vivo* and *in vitro* (Harrod et al., 2008; Ferris et al., 2010).

Our previous work provides evidence that Tat allosterically modulates DAT function (Zhu et al., 2009; Zhu et al., 2011). The allosteric modulation of DAT is responsible for conformational transitions via substrate- and ligand-binding sites on DAT (Zhao et al., 2010; Shan et al., 2011). In the present study, we found that mutation of Tyr470 diminished Zn^{2+}-induced inhibition of [^{3}H]DA uptake and attenuated increased [^{3}H]WIN 35,428 binding compared to WT hDAT. The endogenous Zn^{2+} binding sites in hDAT have been widely employed to investigate whether mutations of hDAT alter transporter conformational transitions in DA transport (Norregaard et al., 1998). The Zn^{2+}-mediated inhibition of DA transport and stimulation of WIN35,428 binding to DAT occur by stabilization of outwardly facing transporter conformations (Richfield, 1993; Norregaard et al., 1998; Moritz et al., 2013). Although analysis of Zn^{2+} regulation of DAT function only reflects one mechanistic aspect of DAT mutant-induced conformational change, our data provide strong evidence for the context of an allosteric mechanism responsible for conformational transitions in DAT. To explore the possible mechanism, we also examined the effects of mutant hDAT on basal DA efflux and observed extremely low accumulation of DA over time in Y470H-hDAT relative to WT hDAT. One possible explanation for the low accumulation of DA is that basal DA efflux can be elevated in this mutant, resulting in reduced accumulation of intracellular DA. One caveat is that DA efflux data may reflect not only DA moving out of the cell through the transporter, but also non-specific diffusion and reuptake. However, there is evidence (Guptaroy et al., 2009; Guptaroy et al., 2011) that this measurement largely reflects basal DA efflux through DAT because such basal DA efflux is consistent with amphetamine- or voltage-stimulated efflux of intracellular DA in cells expressing hDAT and its mutant.

Amphetamine, a substrate for DAT, competitively inhibits DA reuptake and elicits outward transport of DA by reversal of the transporter (Sulzer et al., 2005). Thus, it is possible that Y470H mutation shifts the conformation of DAT from physiologically favored substrate influx mode to an efflux one; a conformational switch promoted by Tat protein, and disturbs transition between inward- and outward-facing conformations. Taken together, these findings infer a potential mechanism that mutation of Tyr470 alters the transporter conformational transitions, which is consistent with our previous findings that Tat mediates allosteric modulation of DAT (Zhu et al., 2011). Additionally, the enhanced DA efflux was also observed in WT hDAT in the presence of Tat. Interestingly, the magnitude of DA efflux in WT hDAT was lower in response to Tat compared to that in Y470H-hDAT. One possible explanation for the discrepancy is that in addition to residue Y470, other recognition residues of the DAT may be involved in the effects of Tat on DA efflux. Therefore, to fully understand the mechanisms by which Tat inhibits DAT function, future studies based on the combined experimental and computational approaches will be necessary to further analyze the changes in the conformational transition attributed to the identified residues in DAT (i.e. an outward-facing form and an inward-facing form).

In conclusion, we have begun to identify the specific intermolecular interactions between Tat and DAT and the molecular mechanism(s) that underlies how Tat, via the recognition binding sites in DAT, interrupts DA transport. Particularly, our results provide relatively a broad molecular validation of this important residue of DA translocation and the underlying allosteric mechanism in DAT for Tat. We propose that multiple recognition residues in the DAT are involved in the dynamic and complex

interactions between Tat and DAT. Results obtained from Tyr470 only reflect the role of this residue in DAT-Tat interaction. The current findings have shed light on further mapping and validating the predicted sites for Tat interaction with DAT towards an ultimate goal to develop compounds that specifically block Tat binding site(s) in DAT without affecting physiological DA transport. Ideally, these compounds would be therapeutic candidates for stabilizing physiological dopaminergic tone.

Table 2.1 Summary of inhibitory activities in [^{3}H]DA uptake in WT and mutated hDAT in the presence of DA, cocaine or GBR12909

	DA	cocaine	GBR12909
	IC_{50} (nM)		
WT hDAT	895 ± 80	370 ± 40	160 ± 30
Y470H-hDAT	737 ± 72	100 ± 30*	50 ± 10*

Data are calculated as a percentage of DA uptake in the absence of substrate or inhibitor and analyzed by nonlinear regression. Data are presented as mean ± S.E.M. of IC_{50} values from three to four independent experiments performed in duplicate. * $p < 0.05$ compared with WT hDAT (unpaired Student's *t* test).

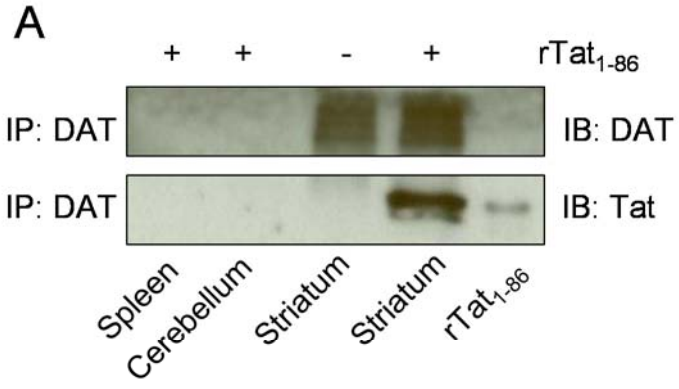
A
+ + - + rTat1-86
IP: DAT
IB: DAT
IP: DAT
IB: Tat
Spleen
Cerebellum
Striatum
Striatum
rTat1-86

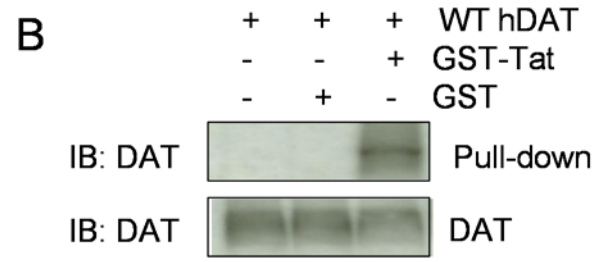
B
+ + + WT hDAT
- - + GST-Tat
- + - GST
IB: DAT
Pull-down
IB: DAT
DAT

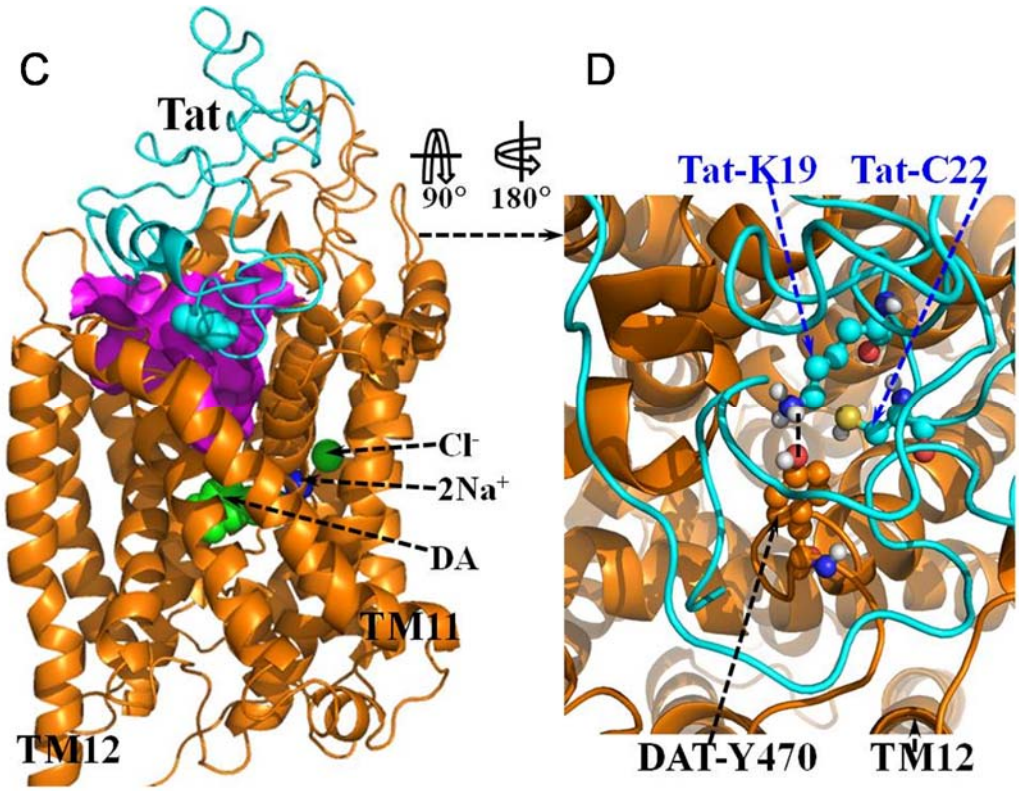
C
Tat
90°
180°
Cl-
2Na+
DA
TM11
TM12
D
Tat-K19
Tat-C22
DAT-Y470
TM12

Figure 2.1 A direct interaction between Tat and DAT and the energy-minimized hDAT(DA) binding complex following the MD simulation. Co-IP of DAT and Tat was performed by immunoprecipitation (IP) with anti-DAT antibody as bait and immunoblot (IB) with anti-Tat antibody. (**A**) Co-IP of DAT and Tat. Rat synaptosomes from spleen, cerebellum, striatum were preincubated with (+, lanes 1, 2 and 4, from left) or without (-, lane 3) 350 nM recombinant Tat_{1-86} ($rTat_{1-86}$). Top panel: DAT immunoreactivity was detected in striatum but not in spleen and cerebellum. Bottom panel: $rTat_{1-86}$ bound to agarose beads was able to immunoprecipitate DAT in rat striatum but not in spleen and cerebellum. $rTat_{1-86}$ (10 ng) was loaded in lane 5 as the positive control for Tat immunoreactivity. (**B**) GST-Tat_{1-86} bound to WT hDAT protein. Top panel: The GST-Tat_{1-86} fusion proteins were bound to glutathione-sepharose beads, and then incubated with cell lysates from CHO cells transfected with WT hDAT at room temperature for 1h following Western Blot using anti-DAT. GST-Tat fusion protein bound to glutathione-sepharose was able to pull down DAT, but GST alone was not. Bottom panel: DAT immunoreactivity in CHO cells expressing hDAT was shown in all lanes. (**C**) Side view of the complex structure. Tat is shown as ribbon in cyan color and hDAT(DA) as ribbon in gold color. Atoms of residue C22 (Cys22) of Tat are shown as overlapped balls in cyan color. Atoms of substrate dopamine (DA) and the Cl^- ion are shown as overlapped balls in green color. 2 Na^+ ions are shown as balls in blue color. The vestibule (colored in purple) is represented as molecular surface calculated by using program HOLLOW (Ho and Gruswitz, 2008). (**D**) Local view of the anchoring residues Lys 19 (K19) and Cys22 (C22) of Tat inside the vestibule of hDAT(DA). Residues K19 and C22 of Tat are shown in ball-and-stick style, and colored by the atom types. Residue Tyr470 (Y470) of hDAT(DA) is also shown in ball-and-stick style and colored by the atom types. The hydrogen bonding between the K19 side chain of Tat and the hydroxyl oxygen atom on Y470 side chain of hDAT(DA) is indicated with the dashed line. The non-polar hydrogen atoms are not shown for clarity. The positions of trans membrane domain11 and 12 (TM11 and TM12) of hDAT(DA) are also labeled.

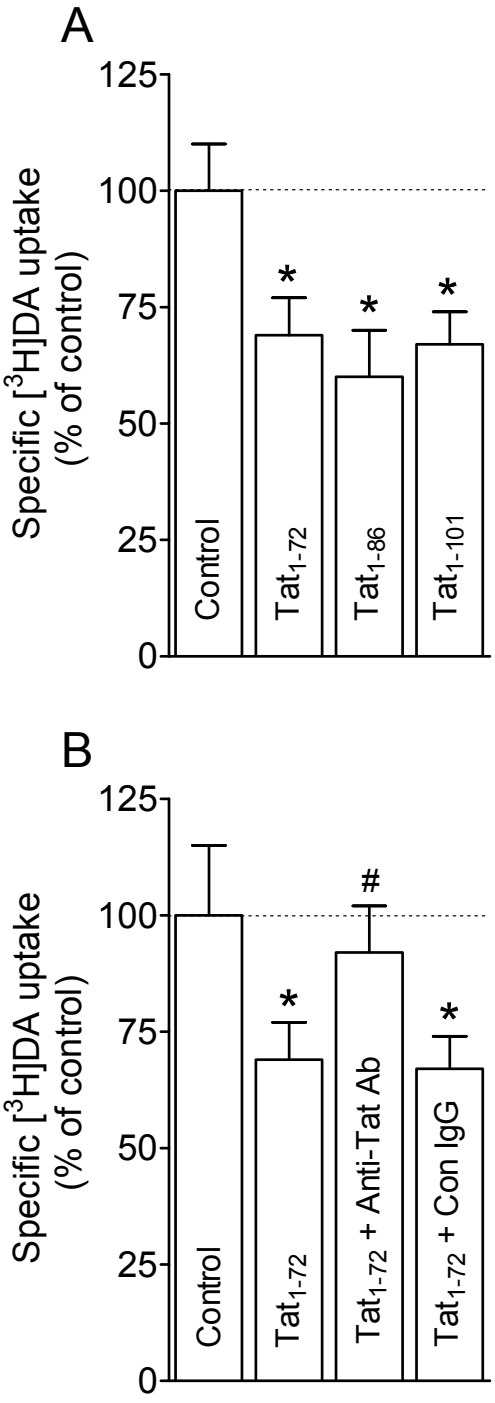

Figure 2.2 Inhibition of DA uptake by released Tat from Tat-expressing cells. (**A**) CHO cells transfected with WT hDAT were preincubated in KRH buffer including 100 µl conditioned media collected at 72 h from cells transfected with plasmid Tat_{1-72}, Tat_{1-86}, $Tat1_{-101}$ DNAs and vector alone (Control) followed by addition of [^{3}H]DA uptake. *$p <$ 0.05 different from control (Dunnett's Multiple comparison test). (**B**) Specificity of released Tat in inhibition of [^{3}H]DA uptake. Conditioned media collected at 72 h from

cells transfected with Tat_{1-72} were preincubated with anti-Tat antibody or isotype control IgG at 4°C for 3h, followed by incubation with protein A/G – Agarose beads 4°C for 2h. Media collected at same time from cells transfected with vector alone was used as control. Cells transfected with WT hDAT were preincubated in KRH buffer containing supernatants from the agarose-antibody-medium-beads complex, followed by [^{3}H]DA uptake. Released Tat_{1-72} caused significant decrease in [^{3}H]DA uptake, which was attenuated by immunodepletion with anti-Tat antibody but not isotype control antibody (one-way ANOVA followed by Tukey's multiple comparison test). * $p < 0.05$ different from control. # $p < 0.05$ different from Tat_{1-72} and Tat_{1-72} + Con IgG. (n = 4).

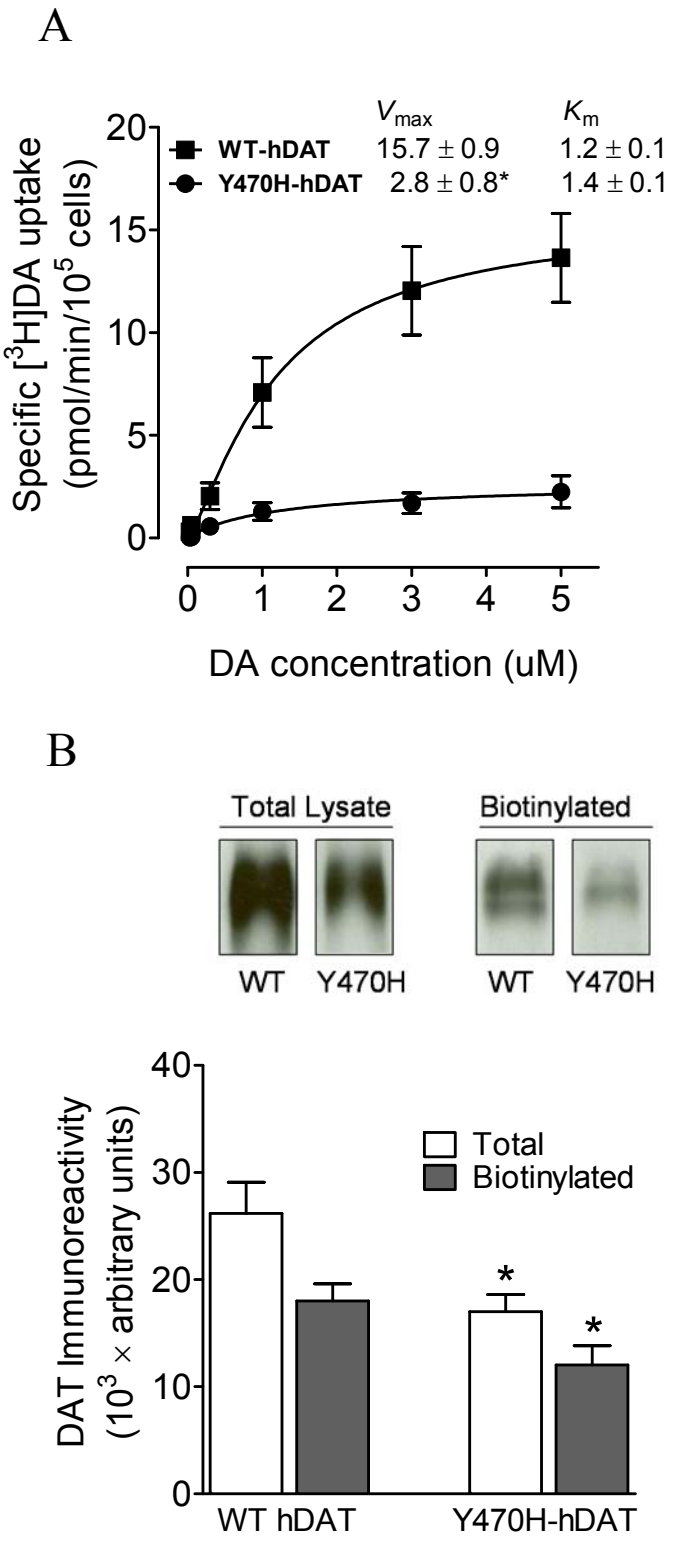

Figure 2.3 [^{3}H]DA uptake and DAT surface expression in WT hDAT and mutant. (A) Kinetic analysis of [^{3}H]DA uptake in WT hDAT and Y470H-hDAT. CHO cells transfected with WT hDAT or Y470H-hDAT were incubated with one of six mixed

concentrations of the [^{3}H]DA as total rate of DA uptake. In parallel, nonspecific uptake of each concentration of [^{3}H]DA (in the presence of 10 μM nomifensine, final concentration) was subtracted from total uptake to calculate DAT-mediated uptake. * $p <$ 0.05 compared to control value (unpaired Student's *t* test) (n = 5). (**B**) Cell surface of WT hDAT (WT) or Y470H-hDAT (Y470H) was analyzed by biotinylation. Top panel: representative immunoblots in CHO cells expressing WT hDAT or Y470H-hDAT. Bottom panel: DAT immunoreactivity is expressed as mean ± S.E.M. densitometry units from three independent experiments (n = 3). * $p < 0.05$ compared to WT hDAT (unpaired Student's *t* test).

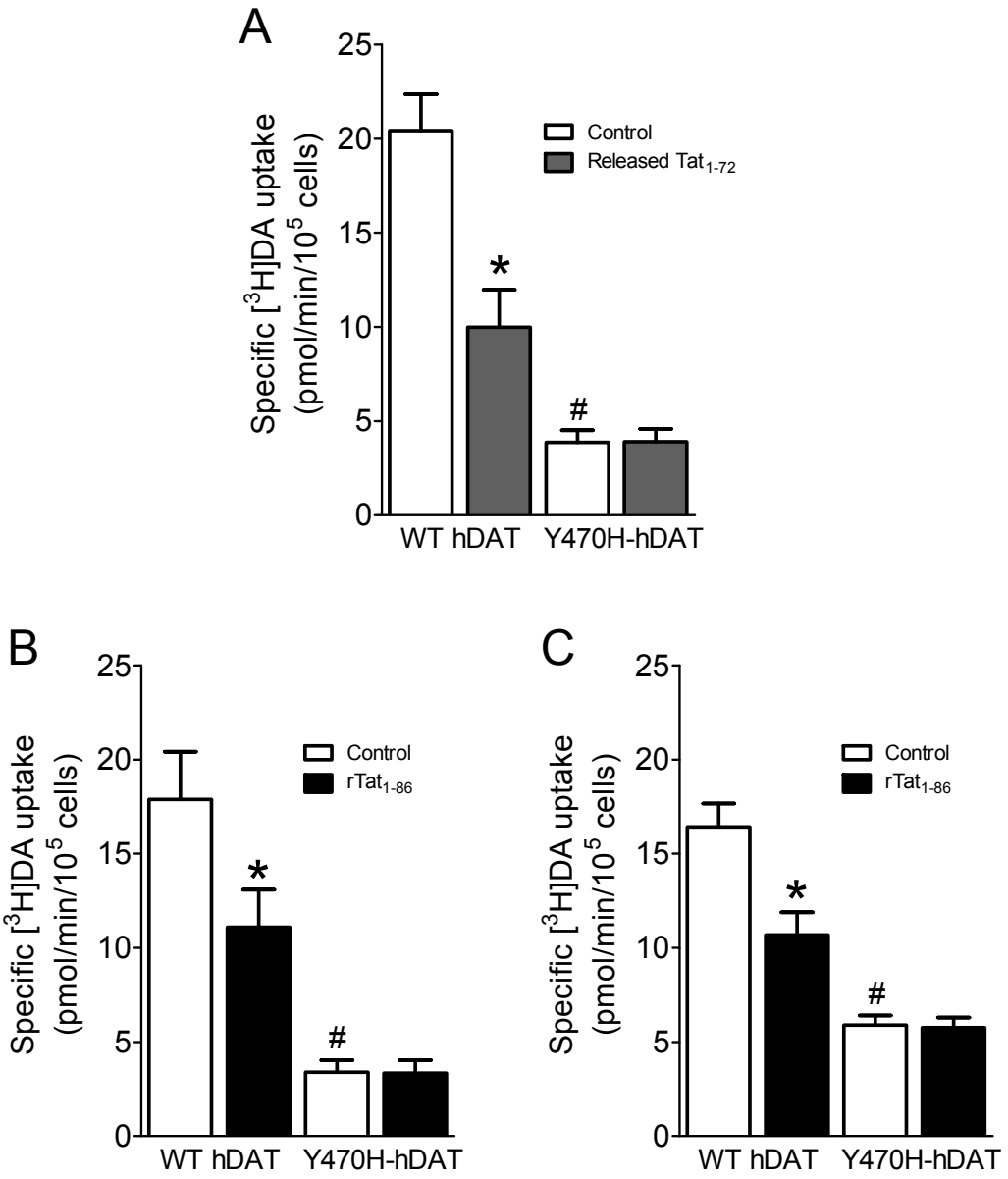

Figure 2.4 Effects of Tat on kinetic analysis of [^{3}H]DA uptake in WT hDAT and mutant. (**A**) CHO cells transfected with WT or Y470H-hDAT were preincubated with or without released Tat_{1-72} (1.0 ng/ml) at room temperature for 20 min followed by the addition of one of six mixed concentration of the [^{3}H]DA. In parallel, nonspecific uptake at each concentration of [^{3}H]DA (in the presence of 10 μM nomifensine, final concentration) was subtracted from total uptake to calculate DAT-mediated uptake. (**B**) [^{3}H]DA uptake in cells transfected with WT or Y470H-hDAT was determined in the presence or absence of recombinant Tat_{1-86} ($rTat_{1-86}$, 350 nM, final concentration). (**C**) [^{3}H]DA uptake in cells transfected with WT (0.8 μg plasmid cDNA) or Y470H-hDAT (2.4 μg plasmid cDNA) was determined in the presence or absence of $rTat_{1-86}$ (350 nM). Data are expressed as means from three independent experiments ± S.E.M. * $p < 0.05$ compared with the respective control values. # $p < 0.05$ compared to WT hDAT. (n = 5)

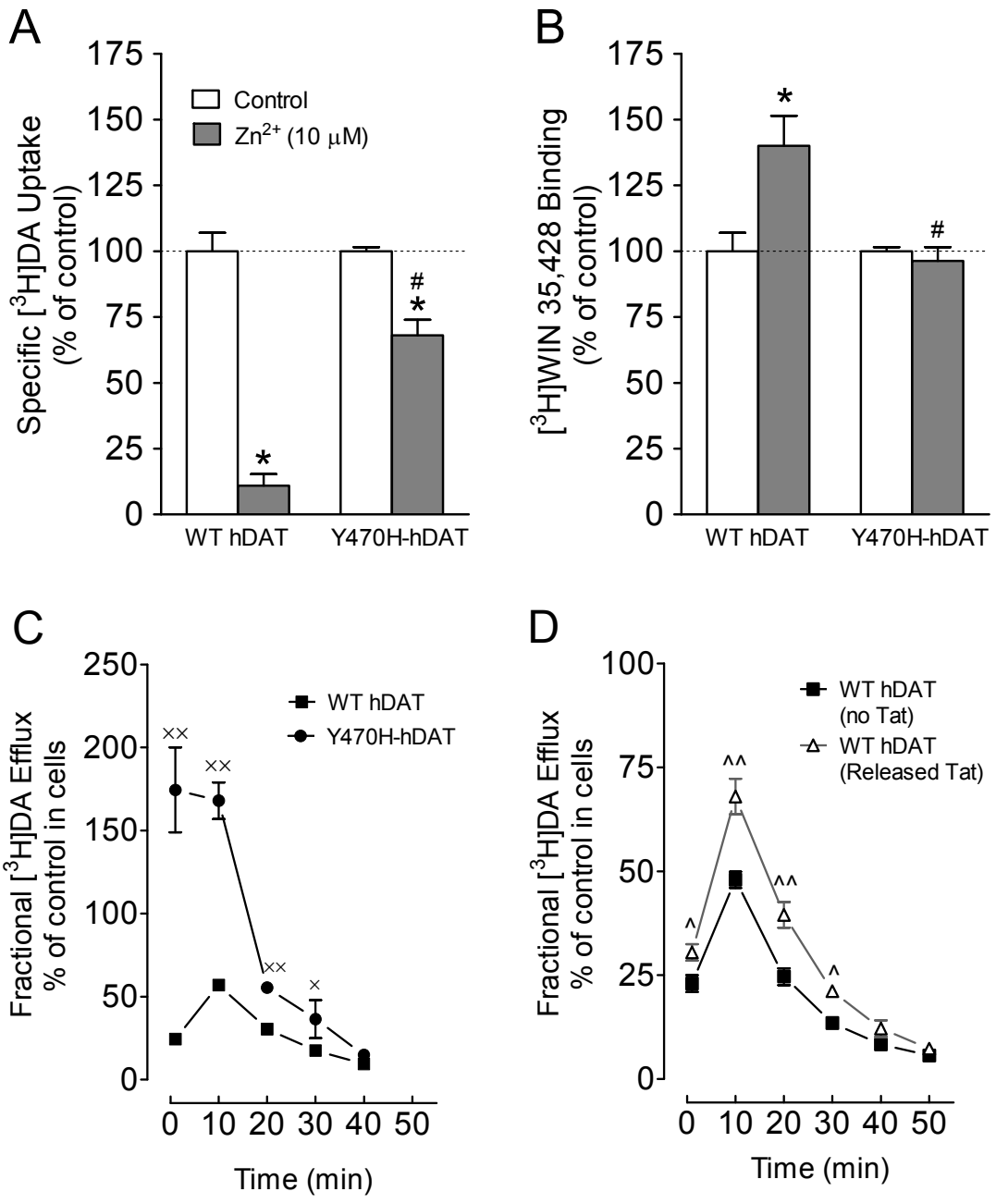

Figure 2.5 Mutation of Tyr470 alters transporter conformational transitions. Tyr470 mutation of DAT affects zinc regulation of DA uptake (**A**) and [^{3}H]WIN 35,428 binding (**B**). CHO cells transfected with WT or Y470H-hDAT were incubated with assay buffer alone (control) or $ZnCl_2$ (10 μM, final concentration) followed by [^{3}H]DA uptake or [^{3}H]WIN 35,428 binding (n = 4). The histogram shows [^{3}H]DA uptake and [^{3}H]WIN 35,428 binding expressed as mean ± S.E.M. of the respective controls set to 100% for the mutant. * $p < 0.05$ compared to control. $^{\#}$ $p < 0.05$ compared to WT hDAT with $ZnCl_2$.

(**C**) Functional DA efflux properties of WT hDAT and mutant. CHO cells transfected WT or Y470H-hDAT were preincubated with [^{3}H]DA (0.05 μM, final concentration) at room temperature for 20 min. After incubation, cells were washed and incubated with fresh buffer as indicated time points. Subsequently, the buffer was separated from cells, and radioactivity in the buffer and remaining in the cells was counted. Each fractional [^{3}H]DA efflux in WT hDAT and Y470H-hDAT was expressed as percentage of total [^{3}H] in the cells at the start of the experiment. Fractional [^{3}H]DA efflux at 1, 10, 20, 30 and 40 min are expressed as the percentage of total [^{3}H]DA with preloading with 0.05 μM (WT hDAT: 15379 ± 1800 dpm and Y470H-hDAT: 2488 ± 150 dpm) present in the cells at the start of the experiment ($n = 4$). $^{\times}p < 0.05$ and $^{\times\times}p < 0.01$, compared to WT hDAT (Bonferroni *t*-test). (**D**) Functional DA efflux properties of WT hDAT in the presence or absence of Tat_{1-72}. CHO cells transfected with WT hDAT were preincubated with released Tat_{1-72} (1 ng/mg) followed by DA efflux assay. Fractional [^{3}H]DA efflux at 1, 10, 20, 30, 40 and 50 min are expressed as the percentage of total [^{3}H]DA with preloading with 0.05 μM (control: 14200 ± 1448 dpm and released Tat: 10102 ± 1505 dpm) present in the cells at the start of the experiment ($n = 6$). $^{\wedge}p < 0.05$ and $^{\wedge\wedge}p < 0.01$, compared to WT hDAT in the absence of Tat (Bonferroni *t*-test).

Copyright Clearance Center RightsLink®

Home | Account Info | Help

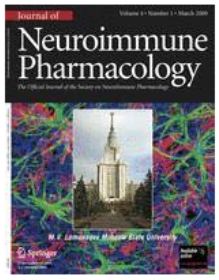

Title: Mutation of Tyrosine 470 of Human Dopamine Transporter is Critical for HIV-1 Tat-Induced Inhibition of Dopamine Transport and Transporter Conformational Transitions

Author: Narasimha M. Midde

Publication: Journal of NeuroImmune Pharmacology

Publisher: Springer

Date: Jan 1, 2013

Logged in as: Narasimha Midde

LOGOUT

Order Completed

Thank you very much for your order.

This is a License Agreement between Narasimha M Midde ("You") and Springer ("Springer"). The license consists of your order details, the terms and conditions provided by Springer, and the payment terms and conditions.

Get the printable license.

License Number	3333280564073
License date	Feb 20, 2014
Licensed content publisher	Springer
Licensed content publication	Journal of NeuroImmune Pharmacology
Licensed content title	Mutation of Tyrosine 470 of Human Dopamine Transporter is Critical for HIV-1 Tat-Induced Inhibition of Dopamine Transport and Transporter Conformational Transitions
Licensed content author	Narasimha M. Midde
Licensed content date	Jan 1, 2013
Volume number	8
Issue number	4
Type of Use	Thesis/Dissertation
Portion	Full text
Number of copies	10
Author of this Springer article	Yes and you are a contributor of the new work
Title of your thesis / dissertation	Effect of HIV-1 Tat protein on structure, function, and trafficking of the dopamine transporter
Expected completion date	May 2014
Estimated size(pages)	250
Total	0.00 USD

CLOSE WINDOW

CHAPTER 3

POINT MUTATIONS AT TYR 88, LYSINE 92 AND TYR 470 OF THE HUMAN DOPAMINE TRANSPORTER ATTENUATE TAT-INDUCED INHIBITION OF DOPAMINE TRANSPORTER FUNCTION

ABSTRACT: HIV-1 transactivator of transcription (Tat) protein disrupts the dopamine (DA) neurotransmission by inhibiting DA transporter (DAT) function, leading to increased neurocognitive impairment in HIV-1 infected individuals. Through computational modeling and simulations, three functional residues in human DAT (hDAT) were predicted as potential recognition binding sites for Tat. We previously showed that mutation of tyrosine470 (Y470H) of hDAT attenuates Tat-induced inhibition of DA uptake by changing the transporter conformational transitions. In the present study we examined the functional influences of other substitutions at tyrosine470 (Y470F and Y470A) and tyrosine88 (Y88F) and lysine92 (K92M), two other predicted residues for Tat binding to hDAT, in Tat-induced inhibitory effects on DA transport. Compared to wild type (WT) hDAT, K92M but not Y88F reduced V_{max} without changes in K_m. Both Y88F and K92M did not alter IC_{50} values for DA inhibition of [^{3}H]DA uptake but increased [^{3}H]DA uptake or [^{3}H]WIN35,428 binding potencies for cocaine and GBR12909, indicating that these residues do not overlap with the binding sites in hDAT for DA transport but are critical for these inhibitors. Besides, Y88F, K92M and Y470A attenuated Tat-induced inhibition of DA transport that is observed in WT hDAT. Y470F, Y470A, Y88F and K92M mutants reversed the zinc-induced increase of [^{3}H]WIN35,428 binding but not the [^{3}H]DA uptake. Moreover, Y470A and K92M mutants

displayed enhanced DA basal efflux compared to WT hDAT. Taken together, these results demonstrate that Tyr88 and Lys92 along with Tyr470 as functional recognition residues in hDAT for Tat interaction-induced inhibition of DA transport and provide mechanistic insights into identifying target residues on the DAT for Tat binding.

3.1 INTRODUCTION

HIV-associated neurocognitive disorder (HAND) that encompasses neurological and psychiatric complications has been on the considerably rise in people living with HIV-1 and AIDS even in the era of highly active antiretroviral therapy (HAART)(Heaton et al., 2010; Simioni et al., 2010; Mothobi and Brew, 2012). The growing body of evidence indicates that the HAND progression and severity is exacerbated by comorbid factors like widely abused drugs, particularly cocaine (Buch et al., 2011; Nair and Samikkannu, 2012). Lower adherence to medication regimen by HIV-1 positive people is also strongly associated with the active cocaine use (Arnsten et al., 2002; Norman et al., 2009). HAND is highly correlated with neurotoxic effects of HIV-1 viral proteins that are exuded from infected microglial cells (Bansal et al., 2000; Kaul et al., 2001; Mattson et al., 2005; Kaul and Lipton, 2006). Tat, a non-structural viral protein required for productive infection of virus, is one of the major neurotoxins responsible for neurotoxicity and oxidative stress in the central nervous system (Pocernich et al., 2005; Wallace et al., 2006). Studies have demonstrated that Tat protein and cocaine interaction have deleterious effects in HIV-1 positive brains by altering viral replication, neuropathogenesis and behavioral effects (Gandhi et al., 2010; Paris et al., 2013).

Dysregulation of dopamine (DA) neurotransmission in HIV-1 infected patients is greatly associated to HAND pathophysiology and has been reviewed extensively elsewhere (Koutsilieri et al., 2002; Ferris et al., 2008; Purohit et al., 2011). HIV-infection has been

shown to deplete intracellular DA levels in postmortem brains (Scheller et al., 2005; Kumar et al., 2009). Recently, enhanced DA levels were reported in cerebrospinal fluid of HIV-1 positive individuals with no treatment compared to normal subjects (Scheller et al., 2010). An explanation for this elevated level of DA is possibly due to impairment of DA transporter (DAT) function (Purohit et al., 2011). DAT is a presynaptic membrane protein that rapidly clears extracellular DA via rapid reuptake and is a primary determinant for the regulation of DA homeostasis in the brain (Vaughan and Foster, 2013). Clinical results using positron emission tomography imaging have demonstrated that HIV-associated dementia patients show a dramatic loss of DAT protein in the putamen and ventral striatum regions (Wang et al., 2004; Chang et al., 2008). Likewise, previous animal and *in vitro* studies including published data from our own laboratory indicated that the Tat manipulates the function of DAT (Ferris et al., 2009b; Ferris et al., 2009a; Zhu et al., 2009; Perry et al., 2010). Furthermore, we showed that Tat down regulates DAT function through allosteric mechanism (Zhu et al., 2011); also it decreases DAT cell surface expression in rat striatal synaptosomes (Midde et al., 2012). Therefore, it is expected that DAT would be a promising clinical target for therapeutic interventions to curb the damage of DA system instigated by the Tat protein.

It has been proposed that different ligands exert their actions on DAT by inducing specific conformational changes in the transporter that can influence DA uptake and efflux (Schmitt et al., 2013). DAT substrates and inhibitors initially recognize specific amino acids and are likely followed by a series of molecular changes to modulate DAT function (Tanda et al., 2009; Shan et al., 2011). Previous studies suggest that allosteric modulators of DAT differentially regulate transporter uptake and efflux properties (Pariser et al., 2008; Rothman

et al., 2009). Along these lines, our published report showed that Tat decreases DAT activity via binding to allosteric sites and also alters cocaine binding sites (Zhu et al., 2011), indicating different mode of Tat interaction that does not directly interfere with substrate translocation. Likewise, computational and experimental studies have focused to identify the binding mode and pocket of dopamine as well as cocaine (Li et al., 2002; Beuming et al., 2008; Huang et al., 2009; Shan et al., 2011). Having emerging evidence for additive and/or synergistic effects of Tat and cocaine (Gandhi et al., 2010; Paris et al., 2013), it is worth noting that molecular relationship between Tat binding site and the binding site of cocaine on the transporter remain unclear. Thus, in order to identify the binding pocket for Tat protein in DAT, it is necessary to identify the residues forming the crevice and understand the contribution of these recognition residues in substrate translocation, cocaine binding and conformational rearrangements in the transporter.

In the process of understanding the combined effects of Tat and cocaine on down regulation of DA transport through alteration of DAT function, using biophysical (Zhu et al., 2009) and biochemical methods (Midde et al., 2013), we demonstrated that Tat directly interacts with DAT. Based on predictions of computational modeling and simulations, as a proof of principle study we showed evidence that mutating Y470 of human DAT (hDAT) attenuates Tat-mediated inhibition of DA uptake but increases the potency of DAT inhibitor cocaine (Midde et al., 2013). It has also been demonstrated that Tyr470His-hDAT (Y470H-hDAT) mutant differentially modulates zinc-mediated regulation of DA uptake and WIN35,428 binding, and basal DA efflux properties, suggesting a role of Tyr470 in maintaining structural integrity of the transporter and mutating this amino acid resulted in a transporter that favors an inward facing conformation. As a follow up to this published data,

in the current study we investigated the role of additional substitutions at Tyr470 and other predicted potential Tat binding residues, Tyr88 and Lys92 of hDAT in Tat-induced decrease of DA translocation by generating points mutations Tyr470F (Y470F-hDAT), Tyr470A-hDAT (Y470A-hDAT), Tyr88Phe (Y88F-hDAT), Lys92Met (K92M-hDAT) and assessing their variability in function, surface expression, interaction with ligands and underlying mechanism for these alterations.

3.2 MATERIALS AND METHODS

3.2.1 PREDICTING THE SITE FOR hDAT BINDING WITH TAT

The binding structure of hDAT with HIV-1 clade B type Tat was modeled and simulated based on the nuclear magnetic resonance (NMR) structures of Tat (Peloponese et al., 2000) and the constructed structure of hDAT-DA complex. According to D-Y470 site-directed mutation experimental data as reported previously (Midde et al., 2013), Y470 of hDAT is a functional recognition residue for Tat-induced inhibition of DAT transport cycle. Therefore, Y470 of hDAT is expected to interact with Tat directly. The protein docking program ZDOCK (Pierce et al., 2011) was applied for obtaining the initial binding structure of the hDAT-Tat complex, with the constraint of contact between D-Y470 and Tat. Total 535 potential conformations were generated based on 11 NMR structures of Tat, then all of these conformations were evaluated and ranked by ZRANK (Pierce and Weng, 2007). Top 107 conformations (top 20%) were selected for further investigation by MD simulation. Then initial binding structure of the hDAT-Tat was identified from these simulations, with the best geometric matching quality and rational interaction between D-Y470 and Tat. With further relaxing and equilibrating the system, final MD-simulated hDAT-Tat binding structure was energy-minimized and analyzed.

3.2.2 Construction of plasmids

All point mutations of Tyr88, Lys92, and Tyr470 in hDAT were selected based on the predictions of the 3D-computational modeling and simulations. Mutations in hDAT at Tyr88 and Tyr470 (tyrosine to phenylalanine, Y88F-hDAT and Y470F-hDAT) are expected to destroy the hydrogen bond only. Since methionine is nearly isosteric with lysine, substitution at Lys92 (lysine to methionine, K92M-hDAT) should abolish hydrogen bond with minimal perturbations to the native structure of the transporter. Substitution of tyrosine at 470 with alanine or tryptophan (Y470A-hDAT and Y470W-hDAT) is expected to eliminate both hydrogen bond and cation-π interactions that is similar to Y470H-hDAT, but with different spatial effects on structural organization of the transporter. All mutations in hDAT were generated based on wild type human DAT (WT hDAT) sequence (NCBI, cDNA clone MGC: 164608 IMAGE: 40146999) by site-directed mutagenesis. Synthetic cDNA encoding hDAT subcloned into pcDNA3.1+ (provided by Dr. Haley E Melikian, University of Massachusetts) was used as a template to generate mutants using QuikChange™ site-directed mutagenesis Kit (Agilent Tech, Santa Clara CA). The sequence of the mutant construct was confirmed by DNA sequencing at University of South Carolina EnGenCore facility. Plasmid DNA were propagated and purified using plasmid isolation kit (Qiagen, Valencia, CA, USA)

3.2.3 Cell culture and DNA transfection

Chinese hamster ovary (CHO, ATCC #CCL-61) cells were maintained in F12 medium supplemented with 10% fetal bovine serum (FBS) and antibiotics (100 U/ml penicillin and 100 µg/mL streptomycin). Pheochromocytoma (PC12, ATCC #CRL-1721) cells were maintained in Dulbecco's modified eagle medium supplemented with 15 % horse serum, 2.5

% bovine calf serum, 2 mM glutamine and antibiotics (100 U/ml penicillin and 100 µg/mL streptomycin). Both cells were cultured at 37°C in a 5% CO_2 incubator. For hDAT transfection, cells were seeded into 24 well plates at a density of 1×10^5 cells/cm^2. After 24h, cells were transfected with WT or mutant DAT plasmids using Lipofectamine 2000 (Life Tech, Carlsbad, CA). Cells were used for the experiments after 24 h of transfection.

3.2.4 [^{3}H]DA UPTAKE ASSAY

Twenty four hours after transfection, [^{3}H]DA uptake in PC12 cells transfected with WT hDAT and mutants was performed as reported previously (Midde et al., 2013). To determine whether mutated hDAT alters the maximal velocity (V_{max}) or Michaelis-Menten constant (K_m) of [^{3}H]DA uptake, kinetic analyses were conducted in WT hDAT and mutants. To generate saturation isotherms, [^{3}H]DA uptake was measured in Krebs-Ringer-HEPES (KRH) buffer (final concentration in mM: 125 NaCl, 5 KCl, 1.5 $MgSO_4$, 1.25 $CaCl_2$, 1.5 KH_2PO_4, 10 D-glucose, 25 HEPES, 0.1 EDTA, 0.1 pargyline, and 0.1 L-ascorbic acid; pH 7.4) containing one of six concentrations of unlabeled DA (final DA concentrations, 1.0 nM–5 µM) and a fixed concentration of [^{3}H]DA (500,000 dpm/well, specific activity, 21.2 Ci/mmol; PerkinElmer Life and Analytical Sciences, Boston, MA). In parallel, nonspecific uptake of each concentration of [^{3}H]DA (in the presence of 10 µM nomifensine, final concentration) was subtracted from total uptake to calculate DAT-mediated uptake. The reaction was conducted at room temperature for 8 min and terminated by washing twice with ice cold uptake buffer. Cells were lysed in 500 µl of 1% SDS for an hour and radioactivity was measured using a liquid scintillation counter (model Tri-Carb 2900TR; PerkinElmer Life and Analytical Sciences, Waltham, MA). Kinetic parameters (V_{max} and K_m) were determined using Prism 5.0 (GraphPad Software Inc., San Diego, CA). To determine the

inhibitory effects of Tat on [^{3}H]DA uptake, cells transfected with WT hDAT or mutants were preincubated with Tat_{1-86} or Tat Cys22 (500 nM, final concentration) for 20 min. Tat Cyc22 was used as a negative control because our previous study shows that Tat Cyc22 has no effect on DA uptake (Zhu et al., 2009).

The competitive inhibition DA uptake experiments were performed in duplicate in a final volume of 500 µl. Cells in each well were incubated in 450 µl KRH buffer containing 50 µl one of final concentrations of unlabeled DA (1 nM-1 mM), GBR12909 (1 nM-10 µM), cocaine (1 nM-1 mM), WIN 35,428 (1 nM-1 mM) or $ZnCl_2$ (10 µM) at room temperature for 10 min and [^{3}H]DA uptake was determined by addition of 50 µl of [^{3}H]DA (0.1 µM, final concentration) for an additional 8 min.

3.2.5 [^{3}H]WIN 35,428 BINDING ASSAY

Binding assays were conducted to determine whether mutated hDAT alters the kinetic parameters (B_{max} or K_d) of [^{3}H]WIN 35,428 binding in PC12 cells transfected with WT hDAT and mutants. Twenty four hours after transfection, PC12 cells were dissociated with trypsin/EDTA (0.25%/0.1%, 1 mL for 100 mm dish) and resuspended in growth medium. After 10 min incubation at room temperature, the dissociated cells were harvested by centrifugation at 3000 rpm for 5 min and washed once with phosphate-buffered saline (PBS). The resulted cell pellets were resuspended in sucrose-phosphate buffer (final concentration in mM: 2.1 NaH_2PO_4, 7.3 $Na_2HPO_47H_2O$, and 320 sucrose, pH 7.4) for binding assay.

To generate saturation isotherms, aliquots of cell suspensions (100 µl) were incubated with one of the eight concentrations of [^{3}H]WIN 35,428 (84 Ci/mmol, PerkinElmer, 0.5 – 30 nM final concentrations) in a final volume of 250 µl on ice for 2 h. In parallel, nonspecific

binding at each concentration of [^{3}H]WIN 35,428 (in the presence of 30 μM cocaine, final concentration) was subtracted from total binding to calculate the specific binding. For the competitive inhibition experiment, assays were performed in duplicate in a final volume of 500 μl. Aliquots of the cell suspensions (50 μl) were added to the assay tubes containing 50 μl of [^{3}H]WIN 35,428 (final concentration, 5 nM) and one of seven concentrations of unlabeled substrate DA (1 nM – 100 μM), inhibitors cocaine (1 nM – 100 μM) or GBR12909 (0.01 nM – 1 μM) and incubated on ice for 2 h. Assays were terminated by rapid filtration onto Whatman GF/B glass fiber filters, presoaked for 2 h with assay buffer containing 0.5% polyethylenimine, using a Brandel cell harvester. Filters were rinsed three times with 3 ml of ice-cold assay buffer. Radioactivity remaining on the filters was determined by liquid scintillation spectrometry (model Tri-Carb 2900TR; PerkinElmer Life and Analytical Sciences, Waltham).

3.2.6 CELL SURFACE BIOTINYLATION

To determine whether DAT mutations alter DAT surface expression, biotinylation assays were performed as described previously (Zhu et al., 2005). CHO cells transfected with hDAT and mutants were plated on 6 well plates at a density of 10^5 cells/well. Cells were incubated with 1 ml of 1.5 mg/ml sulfo-NHS-SS biotin (Pierce, Rockford, IL) in PBS/Ca/Mg buffer (In mM: 138 NaCl, 2.7 KCl, 1.5 KH_2PO_4, 9.6 Na_2HPO_4, 1 $MgCl_2$, 0.1 $CaCl_2$, pH 7.3). After incubation, cells were washed 3 times with 1 ml of ice-cold 100 mM glycine in PBS/Ca/Mg buffer and incubated for 30 min at 4°C in 100 mM glycine in PBS/Ca/Mg buffer. Cells were then washed 3 times with 1 ml of ice-cold PBS/Ca/Mg buffer and then lysed by addition of 500 ml of Triton X-100, 1 μg/ml aprotinin, 1 μg/ml leupeptin, 1 μM pepstatin, 250 μM phenylmethysulfonyl fluoride), followed by incubation and continual shaking for 20 min at 4 °C. Cells were transferred to 1.5 ml tubes and centrifuged at 20,000g

for 20 min. The resulting pellets were discarded, and 100 µl of the supernatants was stored at -20 °C for determination of immunoreactive total DAT. Remaining supernatants were incubated with continuous shaking in the presence of monomeric avidin beads in Triton X-100 buffer (100 µl/tube) for 1 h at room temperature. Samples were centrifuged subsequently at 17,000g for 4 min at 4°C, and supernatants (containing the nonbiotinylated, intracellular protein fraction) were stored at -20°C. Resulting pellets containing the avidin-absorbed biotinylated proteins (cell-surface fraction) were resuspended in 1 ml of 1.0% Triton X-100 buffer and centrifuged at 17,000g for 4 min at 4°C, and pellets were resuspended and centrifuged twice. Final pellets consisted of the biotinylated proteins adsorbed to monomeric avidin beads. Biotinylated proteins were eluted by incubating with 75 µl of Laemmli sample buffer for 20 min at room temperature. If further assay was not immediately conducted, samples were stored at -20 °C.

3.2.7 BASAL EFFLUX ASSAY

DAT-mediated basal substrate efflux was carried out, as described previously (Guptaroy et al., 2009). We have reported that Y470H-hDAT significantly increased DA efflux compared to WT hDAT (Midde et al., 2013). In this study, we compared the effects of two types of substrates, DA or MPP+ on basal efflux in WT hDAT and mutants. The MPP+ was chosen because MPP+ has less diffusive properties than DA in heterologous expression systems (Scholze et al., 2001). CHO cells were seeded into 24 well plates and transfected with WT hDAT and mutants. Twenty four hours after transfection cells at a density of 10^5 cells/well were washed 3 times with KRH buffer and preloaded with [^{3}H]DA (50 nM, final concentration) or 5 nM final concentrations of [^{3}H]1-methyl-4-phenylpyridinium ([^{3}H]MPP+, 5 nM, final concentration, specific activity, 83.9 Ci/mmol; PerkinElmer Life and

Analytical Sciences, Boston, MA) at room temperature for 20 or 30 min, respectively. After incubation, cells were washed 3 times with KRH buffer. To obtain an estimate of the total amount of [^{3}H]DA or [^{3}H]MPP+ in the cells at the zero time point, cells from a set of wells (four wells/sample) were lysed rapidly in 1% SDS. To determine the time course of the fractional basal efflux, fresh buffer (500 µl) was added into separate set of cell wells (four wells/sample) and transferred to scintillation vials after 1 min as initial fractional efflux at 1 min, and another 500 µl buffer was added to the same wells (where the buffer was just removed for 1 min point) and collected to vials after 10 min. Additional fractional efflux at 20, 30, 40 and 50 min, respectively, was repeated under the same procedure. After last time point (50 min), cells were lysed in 1% SDS and counted as total amount of [^{3}H]DA remaining in the cells from each well.

3.2.8 DATA ANALYSES

Descriptive statistics and graphical analyses were used as appropriate. Results are presented as mean ± SEM, and *n* represents the number of independent experiments for each experiment group. Kinetic parameters (V_{max}, K_m, B_{max}, and K_d) were determined from saturation curves by nonlinear regression analysis using a one-site model with variable slope. IC_{50} values for substrate and inhibitors inhibiting [^{3}H]DA uptake or [^{3}H]WIN 35,428 were determined from inhibition curves by nonlinear regression analysis using a one-site model with variable slope. For experiments involving comparisons between unpaired samples, unpaired Student's *t* test was used to assess any difference in the kinetic parameters (V_{max}, K_m, B_{max}, K_d or IC_{50}) between WT and mutant; log-transformed values of IC_{50}, K_m or K_d were used for the statistical comparisons. Significant differences between samples were analyzed with separate ANOVAs followed by post-hoc tests, as indicated in the results

Section of each experiment. All statistical analyses were performed using IBM SPSS Statistics version 20, and differences were considered significant at $p < 0.05$.

3.3 RESULTS

3.3.1 STRUCTURAL INDICATIONS FROM MOLECULAR MODELING AND DYNAMICS SIMULATIONS

The transporting process of dopamine by DAT involves the conformational changes of DAT, typically from outward-open DAT (Figure 3.1A) bound with ions ($2Na^+$, and Cl^-) to outward-occluded DAT bound with both ions and substrate dopamine, and then to the inward-open DAT bound with Cl^- (Figure 3.1C). The mode of intra-molecular interactions guarantees the smooth conformational change of DAT during dopamine transporting. We could assume that the transporter is optimized via natural evolution and energy barrier of conformation change is relatively low for an efficient transporting process. Therefore any mutation of key residues that make the structure incline to certain state may decrease the efficiency of dopamine transporting process. Based on the results of molecular modeling and molecular dynamics simulations, we found that the Y470 is the key component of a hydrophobic core, which is critical to stabilize the compact structure of DAT and then reduce the barrier of conformation change between outward-open and outward-occlude state of DAT (Figure 3.1B). In addition, residues Y88, K92 and D313 also help to stabilize TM1b and TM6a through hydrophobic or electrostatic intra-molecular interactions, which make the outward-open and outward-occlude state of DAT keep compact and be ready for conformation changing. The hydroxyl group at the aromatic side chain of Y88 reduces the hydrophobicity and makes the hydrophobic core nearby Y88 less stable than Y88F mutation, as a result, the Y88F mutation is expected to make the TM1b and EL4 more compact and bring about positive effect on the transporting kinetics of dopamine, i.e. increasing the

Vmax. However, the compact conformation of TM1b also squeeze the vacant of dopamine binding site, which may bring about negative effect of binding affinity of dopamine, i.e., increasing the Kmax. Specifically, the positive charged side chain of K92 could interact with the negative charged side chain of residue D313 through electrostatic interaction, and hydrogen bonding which is mediated by surrounding water molecules. As observed in our simulation, TM1b and TM6a move together during the conformation change of transporting, therefore K92-D313 interaction could stabilize the connection between TM1b and TM6a and consequently decrease the energy barrier of conformation change. It can be expected that the K92M mutation would bring about negative effects on the transporting kinetics of dopamine, i.e. decreasing the Vmax. Moreover, the carboxyl of D79 in TM1b and carbonyl in main chain of F320 in TM6a interact directly with dopamine, so the K92M would pull away TM1b and TM6a, and these associated hydrogen bonding groups, which brings about negative effect of binding affinity of dopamine, i.e., increasing the K_{max} (Figure 3.1D). Besides, as shown in the binding structure of HIV-1 TAT-DAT complex (Figure 3.2), the D-Y470 interacts with the positive charged N-terminal of T-M1 through cation-π interaction. Hydroxyl of D-Y88 forms hydrogen bond with side chain of T-K19. Side chain of D-K92 of DAT forms hydrogen bond with carbonyl of main chain of T-P18. Based on the mode of interaction between DAT and HIV-1 TAT, it could be expected that the mutating of residues Y88 and K92 into residues without hydrogen-bonding capacity will weaken the interaction between DAT and TAT. This is why that the mutations of Y88F and K92M decrease the inhibitory potency of HIV-1 TAT against the function of dopamine uptake by DAT.

3.3.2 MUTATIONS OF TYR88 AND LYS92 ALTER DA UPTAKE KINETICS AND POTENCY OF SUBSTRATE AND INHIBITORS

To examine the functional relevance of Tyr88 and Lys92 residues of hDAT in intermolecular interaction between Tat and DAT, mutations in Tyr88 and Lys92 residues of hDAT (tyrosine to phenylalanine, Y88F-hDAT and lysine to methionine, K92M-hDAT) were generated by site-directed mutagenesis. We first determined the pharmacological profiles of [^{3}H]DA uptake in CHO cells transfected with WT hDAT or mutated hDAT. As shown in Table 3.1 and Fig. 3.4A, compared to WT hDAT (15.7 ± 0.9 pmol/min/10^5 cells), the Y88F-hDAT did not alter the V_{max} values, whereas the K92M-hDAT displayed a decrease in the V_{max} values (4.5 ± 1.7 pmol/min/10^5 cells, t(3) = 3.7, p<0.05, unpaired Student's *t* test); no difference in the K_m values was observed. WIN 35,428 binding site shares pharmacological identity with the DA uptake carrier and is part of the cocaine binding domain (Pristupa et al., 1994). We also determined the effects of these mutants on possible relationship between the binding site of Tat on DAT and the WIN 35,428 binding site. As shown in Table 3.1, the B_{max} values were not altered in Y88F-hDAT (5.8 ± 0.9 pmol/10^5 cells, t(8) = 2.1, p=0.07, unpaired Student's *t* test) but decreased in K92M-hDAT (2.4 ± 0.4 pmol/10^5 cells, t(8) = 4.4, p<0.01, unpaired Student's *t* test) compared with WT hDAT (9.7 ± 1.6 pmol/10^5 cells). However, the K_d values were significantly decreased in both in Y88F-hDAT (4.0 ± 0.6 nM, t(8) = 3.6, p<0.01, unpaired Student's *t* test) and K92M-hDAT (3.5 ± 1.1 nM, t(8) = 3.2, p<0.01, unpaired Student's *t* test) compared with WT hDAT (8.6 ± 1.1 nM).

We tested the ability of substrate and DAT inhibitors to inhibit [^{3}H]DA uptake in WT hDAT and its mutants (Table 3.2). The apparent affinity (IC_{50}) for DA was not significantly different among the WT hDAT (1730 ± 82 nM), Y88F-hDAT (3010 ± 60 nM) and K92M-

hDAT (2870 ± 48 nM). However, the potencies of cocaine and GBR12909 for inhibition of [^{3}H]DA uptake were 1.4 ~4.0-fold greater in Y88F-hDAT (Cocaine: 160 ± 9 nM and GBR12909: 95 ± 7 nM) and K92M-hDAT (Cocaine: 69 ± 4 nM and GBR12909: 101 ± 12 nM) as compared with WT hDAT (Cocaine: 285 ± 49 nM and GBR12909: 224 ± 41 nM). The apparent affinity (IC_{50}) for WIN 35,428 was not significantly different in Y88F-hDAT (20 ± 2 nM) but more potent in K92M-hDAT (10 ± 1.0 nM) compared to WT hDAT (39 ± 10 nM). The ability of substrate and DAT inhibitors to inhibit [^{3}H]WIN 35,428 binding in WT hDAT and its mutants was also examined (Table 3.2). The apparent affinity (IC_{50}) for DA was significantly lower in Y88F-hDAT (2071 ± 340 nM) and K92M-hDAT (4211 ± 118 nM) than the WT hDAT (827 ± 120 nM). In addition, the IC_{50} for cocaine was increased in Y88F-hDAT (85 ± 60 nM, $t(8)=5.8$, $p<0.01$) but not K92M-hDAT compared to WT hDAT (150 ± 8.6 nM).

To validate the relationship between the V_{max} values and surface DAT expression in these mutants, we determined DAT surface expression in CHO cells transfected with WT or Y88F-hDAT or K92M-hDAT using biotinylation assay. As shown in Fig. 3.4B, despite no difference in the ratio of surface DAT (biotinylated DAT) to total DAT between WT (1.0 ± 0.05), Y88F-hDAT (1.13 ± 0.13; $p>0.05$, one-way ANOVA) and K92M-hDAT (1.09 ± 0.09; $p>0.05$, one-way ANOVA). The biotinylated DAT was not altered but total DAT was significantly decreased in K92M-hDAT compared to WT hDAT ($t(8) = 4.6$, $p<0.01$, unpaired Student's *t* test). Thus, the decreased DA uptake in K92M-hDAT is not due to alteration of the available DAT on the cell surface.

3.3.3 Mutations of Tyr88, Lys92 and Tyr470 differentially influence Tat-induced inhibitory effects on DA transport

We have recently reported that mutation of either Tyr470 in hDAT or Cys22 in Tat attenuated Tat-induced decrease in DA uptake (Zhu et al., 2009; Midde et al., 2013). To determine whether other substitutions at Tyr470 residue show differential effects on Tat-induced decrease in DA uptake, we generated two mutations in Tyr470 residue of hDAT (tyrosine to phenylalanine, Y470F-hDAT and tyrosine to alanine, Y470A-hDAT) based on the predictions from computational modeling. We examined the specific [^{3}H]DA uptake in WT hDAT and mutants in the presence or absence of recombinant $Tat_{1\text{-}86}$ (500 nM) or recombinant Tat Cys22 (500 nM).

As shown in Fig. 3.5A, two-way ANOVA on the specific [^{3}H]DA uptake in WT hDAT and Tyr470 mutants revealed a significant main effect of mutation ($F_{(2, 36)} = 88.1$; $p < 0.001$) and Tat treatment ($F_{(2, 36)} = 15.5$; $p < 0.05$), as well as a significant mutation × Tat interaction ($F_{(4, 36)} = 5.2$; $p< 0.01$). The DA uptake was gradually decreased as Y470F (42%) > Y470H (72%) > Y470A (92%) compared to WT hDAT in the absence of Tat. Exposure to Tat decreased [^{3}H]DA uptake by 32% in WT hDAT ($F_{(1, 8)} = 23.6$; $p < 0.01$) and Y470F-hDAT (47%, $F_{(1, 8)} = 15.4$; $p < 0.01$); however, no effect of Tat was observed in Y470H-hDAT ($p > 0.05$) and Y470A-hDAT ($p > 0.05$), suggesting that the different substitutions at Tyr470 residue in hDAT differentially influence Tat-induced down regulation of DA uptake. We have demonstrated that mutation of Cys22 in Tat shows no inhibitory effect on [^{3}H]DA uptake (Zhu et al., 2009). As illustrated in Figure 3.5A, Tat Cyc22 did not alter DA uptake in WT hDAT and three Tyr470 mutants compared to respective controls, suggesting that Cyc22 residue in Tat plays a critical role in Tat-induced regulation DAT function.

As shown in Figure 3.5B, two-way ANOVA on the specific [^{3}H]DA uptake in WT and mutants revealed a significant main effect of mutation ($F_{(2, 54)} = 124$; $p < 0.001$) and Tat treatment ($F_{(2, 54)} = 4.7$; $p < 0.05$), however, mutation × Tat interaction ($F_{(4, 54)} = 1.9$; $p > 0.05$) was not significant. In control group, a subsequent simple effect analysis revealed decreased [^{3}H]DA uptake in Y88F-hDAT (40%, $p<0.05$) and K92M-hDAT (72%, $p<0.05$) compared to WT hDAT in the absence of Tat. Exposure to Tat decreased [^{3}H]DA uptake by 32% in WT hDAT ($F_{(1, 12)} = 8.0$; $p < 0.05$; Fig. 3.5B); however, no effect of Tat was observed in Y88F-hDAT ($F_{(1, 12)} = 1.1$; $p > 0.05$) and K92M-hDAT ($F_{(1, 12)} = 1.4$; $p > 0.05$), suggesting that mutation of either Tyr88 or Lys92 in hDAT attenuates Tat-induced reduction of hDAT function. With regard to the effect of recombinant Tat Cys22 on DA uptake (Fig. 3.5B), exposure to Tat Cyc22 did not alter DA uptake in Y88F-hDAT and K92M-hDAT compared to WT hDAT.

3.3.4 Effects of Tyr88, Lys92, and Tyr470 mutants on Zinc regulation of DAT conformational transitions and basal DA efflux

In general, occupancy of the endogenous Zn^{2+} binding site in WT hDAT (His193, His375, and Glu396) stabilizes the transporter in an outward-facing conformation, which allows DA to bind but inhibits its translocation, thereby increasing [^{3}H]WIN 35,428 binding (Norregaard et al., 1998; Moritz et al., 2013), but decreasing [^{3}H]DA uptake (Loland et al., 2003) . Addition of Zn^{2+} is able to partially reverse an inward-facing state to an outward-facing state (Norregaard et al., 1998; Loland et al., 2003). On the basis of this principle, the addition of Zn^{2+} to WT hDAT would inhibit DA uptake, whereas in a functional mutation in DAT Zn^{2+} might diminish the preference for the inward-facing conformation and thus enhance DA uptake. We recently reported that Y470H-hDAT exhibit an attenuation of Zn^{2+}-mediated decreased [^{3}H]DA uptake and increased [^{3}H]WIN35,428 binding observed in WT

hDAT, which demonstrates a preference for the inward-facing conformation of the transporter (Midde et al., 2013).

To investigate the role of additional substitutions at Tyr470 and Tyr88, Lys92 residues in DAT conformational transitions, we examined the effects of respective mutations on Zn^{2+} modulation of [^{3}H]DA uptake and [^{3}H]WIN35,428 binding. As described in Fig. 3.6A, two-way ANOVA on the specific [^{3}H]DA uptake in WT and Y470F-hDAT and Y470A-hDAT revealed a significant main effect of mutation ($F_{(2, 24)} = 99$; $p < 0.001$), zinc ($F_{(1, 24)} = 40$; $p < 0.001$) and a significant mutation × zinc interaction ($F_{(2, 24)} = 8.9$; $p < 0.02$). The addition of Zn^{2+} decreased [^{3}H]DA uptake in WT and Y470F-hDAT and Y470A-hDAT by 47%, 49% and 72% respectively (Fig. 3.6A, $p< 0.01$ relative to control, unpaired Student's *t* test). A two-way ANOVA on the specific [^{3}H]WIN35,428 binding in WT and Y470F-hDAT and Y470A-hDAT revealed a significant main effect of mutation ($F_{(2, 44)} = 38$; $p < 0.01$), zinc ($F_{(1, 44)} = 5$; $p < 0.04$); however, no significant mutation × zinc interaction ($F_{(2, 44)} = 2$; $p > 0.13$) was observed. Moreover, as presented in Fig. 3.6B. compared to respective control (in the absence of Zn^{2+}), Zn^{2+} caused a 48% increase in [^{3}H]WIN 35,428 binding in WT but 17% and 7% in Y470F-hDAT and Y470A-hDAT, respectively ($p< 0.05$ relative to control, unpaired Student's *t* test). Additionally, as shown in Fig. 3.7A, two-way ANOVA on the specific [^{3}H]DA uptake in WT and Y88F-hDAT and K92M-hDAT revealed a significant main effect of mutation ($F_{(1, 24)} = 170$; $p < 0.001$), zinc ($F_{(1, 24)} = 102$; $p < 0.001$) and a significant mutation × zinc interaction ($F_{(2, 24)} = 8.3$; $p < 0.01$). The addition of Zn^{2+} decreased [^{3}H]DA uptake in WT and Y88F-hDAT and K92M-hDAT by 48%, 73% and 81%, respectively (Fig. 3.6A, $p< 0.001$ relative to control, unpaired Student's *t* test). A two-way ANOVA on the specific [^{3}H]WIN35,428 binding in WT and Y88F-hDAT and K92M-hDAT

revealed a significant main effect of mutation ($F_{(1, 18)} = 7.8$; $p < 0.01$), zinc ($F_{(1, 18)} = 26$; $p < 0.001$); however, no significant mutation × zinc interaction ($F_{(2, 18)} = 0.9$; $p > 0.05$) was observed. As displayed in Fig. 3.7B. compared to respective control (in the absence of Zn^{2+}), Zn^{2+} caused a 54% increase in [^{3}H]WIN 35,428 binding in WT but 22% and 19% in Y88F-hDAT and K92M-hDAT respectively ($p< 0.001$ relative to control, unpaired Student's *t* test). These results suggest that Y88F, K92M, Y470F and Y470A mutants attenuate zinc modulation of [^{3}H]WIN 35,428 binding sites but not [^{3}H]DA uptake.

To further evaluate the effects of mutations on transporter conformational transitions, we examined the fractional efflux levels of [^{3}H]DA and [^{3}H]MPP+ in WT hDAT and these mutants. As shown in Fig. 3.6C, after preloading with 0.05 μM [^{3}H]DA for 20 min at room temperature, cells were washed and fractional DA efflux samples were collected at the indicated times. A two-way ANOVA revealed significant main effects of mutation ($F_{(2, 9)} = 10$; $p<0.05$), time ($F_{(5, 45)} = 175$; $p<0.001$) and significant mutation × time interaction ($F_{(10,45)} = 13$; $p<0.001$) for Y470F-hDAT and Y470A-hDAT compared to WT. Post-hoc analysis showed that compared to WT hDAT, DA efflux levels were elevated at 1 and 10 min in Y470A-hDAT only (Figure 3.6C; $p < 0.05$, Bonferroni *t*-test). Similarly, a two-way ANOVA revealed significant main effects of mutation ($F_{(3, 13)} = 45$; $p<0.001$) and time ($F_{(5, 65)} = 75$; $p<0.001$) for Y88F-hDAT and K92M-hDAT compared to WT. A significant mutation × time interaction ($F_{(15, 65)} = 24$; $p<0.001$) was also found. Post-hoc analysis revealed that compared to WT hDAT, DA efflux levels were at 1 and 10 min in K92M-hDAT (Figure 3.7C; $p < 0.05$, Bonferroni *t*-test) but not in Y88F-hDAT. With regarding to MPP+ efflux, a two-way ANOVA revealed significant main effects of mutation ($F_{(2, 9)} = 19$; $p<0.05$), time ($F_{(5, 45)} = 253$; $p<0.001$) and significant mutation × time interaction ($F_{(10, 45)} = 10$; $p<0.001$) for Y470F-

hDAT and Y470A-hDAT compared to WT. Post-hoc analysis displayed that compared to WT hDAT, MPP efflux levels were elevated at 1, 10, 20, 30, 40 and 50 min in Y470A-hDAT only (Figure 3.6D; $p < 0.05$, Bonferroni *t*-test). Taken together, this data suggest that Tyr470, Tyr88 and Lys92 residues differentially affect the basal efflux levels of either DA or MPP+.

3.4 DISCUSSION

Recently, we have demonstrated that Tyr470 in hDAT is a key residue in the intermolecular interaction between Tat and hDAT (Midde et al., 2013). In the current study, we extended characterization of Tyr470 by additional substitution mutations. Further, we pursued to characterize other predicted amino acids Tyr88 and Lys92 in the interaction of Tat with DAT. Tyr470 mutants exhibited differential impact on DAT uptake capacity and Tat-induced inhibition of DAT function, indicating the importance of Tyr470 in DAT interaction with Tat protein through cation-π interaction. Mutations at Tyr88 and Lys92 exhibited increased potencies for inhibitors to inhibit [^{3}H]DA uptake and [^{3}H]WIN 35,428 binding with less impact on potencies for DA substrate to inhibit [^{3}H]DA uptake and [^{3}H]WIN 35,428 binding, suggesting the influence of Tat interaction on inhibitors binding to DAT without interfering the DA uptake site. Notably, Y470F, Y470A, Y88F and K92M mutants did not reverse the Zn^{2+}-facilitated inhibition of DA uptake but decreased the zinc-mediated potentiation of WIN35,428 binding. In addition, Y470A and K92M displayed significant elevation in DA basal efflux compared to WT, suggesting the involvement of these residues in maintenance of conformational states of the transporter. Overall, our experimental evidence shows that Tyr88, Lys92 and Tyr470 play an essential role in

imparting Tat-induced conformational alterations in DAT and thereby inhibiting DA translocation process.

The current results show that K92M decreases V_{max} but not the Y88F, and both mutants failed to show appreciable change in K_m values compared to WT, reflecting that K92M indirectly involve in DA transport but not the Y88F. The likely reasons for impaired translocation in K92M would be either loss of transporter density on the membrane or alteration of DA turnover rate. Because of surface biotinylation data revealed similar amounts of WT and K92M mutant in the plasma membrane (Fig 3.4B) and K_m value for DA uptake was not changed, the turnover for DA is possibly decreased in this mutant. Furthermore, decreased binding capacity and increased affinity for [^{3}H]WIN35,428 binding (Table 3.2) were noted in both mutants. These observations indicate that Tat binding sites, Y88 and K92 are localized close to WIN35,428 binding site. Remarkably, our previous work showed that Tat protein decreases B_{max} for [^{3}H]WIN35,428 binding in dose dependent manner (Zhu et al., 2009). In addition, IC_{50} values for DA inhibiting [^{3}H]DA uptake were not significantly altered in both mutants supporting the view that Y88 and K92 residues do not manipulate the DA binding affinities for the transporter. In contrary, IC_{50} values for inhibitors cocaine, GBR12909 inhibiting [^{3}H]DA uptake are considerably decreased in both mutants compared to WT (Table 3.1), suggesting that increased potency for inhibitors observed in these mutants is a consequence of influence of Y88 and 92 on inhibitors binding sites. Similarly, this interpretation was further supported by increased potencies for inhibitors to inhibit [^{3}H]WIN35,428 binding in these mutants (Table 3.2). Cocaine and its analog WIN35,428, and atypical inhibitor GBR12909 represent different classes of DAT inhibitors. While cocaine-like compounds exhibit increased binding affinity, GBR12909 shows weaker

binding affinity for DAT mutants (W84L, D313N and Y335A) that influence the conformational states of the transporter (Chen et al., 2001; Loland et al., 2002; Chen et al., 2004). Unlike these reported mutants, Y88F and K92M displayed enhanced potencies for both cocaine and GBR12909, revealing that Tat may increase the effectiveness of cocaine through interaction at Tat binding sites. Furthermore, cocaine-like compounds were shown to interact with TM1 and TM6 of DAT, in the vicinity of substrate binding site (Beuming et al., 2008; Parnas et al., 2008). As our computational modeling data indicated Tat impacts TM1b and TM6a helices movement through interacting with Tyr 88, Lys 92 and Tyr 470 (Figure 3.2), it is conceivable that Tat and cocaine may have synergistic or additive effects on DAT function. In support of this interpretation, a recent study demonstrated that Tat expression in brain potentiates cocaine behavioral effects in mice (Paris et al., 2013) . Thus, these results support the idea of interactive effects of Tat and cocaine on DAT function.

We demonstrated that mutating Tyr470 to His attenuates the inhibitory effects of Tat on DA uptake by eliminating both hydrogen bond and cation-π interactions with Tat (Midde et al., 2013). To further validate Tyr470 residue, substitution mutants Y470A, Y470W and Y470F were generated with the expectation that Y470A and Y470W show characteristics similar to Y470H but with different sizes. Y470F mutant abolishes only hydrogen but not the cation-π interactions (Figure 3.3). We did not characterize Y470W mutant because our efforts failed to improve basal uptake in this mutant irrespective of increased DNA for transfections or protein concentration for assays. Y470A displayed mitigation of Tat inhibitory effects on DA translocation (Figure 3.5A), which is similar to our reported mutant Y470H (Midde et al., 2013). Interestingly, other mutant Y470F failed to diminish Tat-mediated effects on DA transport, indicating the important role of aromatic ring of Y470 in

DAT and Tat interaction. Moreover, Y88F and K92M mutants clearly showed attenuation of Tat-induced inhibition of DA uptake (Figure 3.5B) which is in line with Y470H and Y470A. Importantly, Tat Cys22 protein inhibitory effect was evidently attenuated by the mutant transporters irrespective of substitution, signifying the importance of physical interaction of Tat with DAT on transporter function. However, other residues of Tat protein that are involved in this interaction are needed to be evaluated. Taken together, this data demonstrate that Tat exploits Y470, Y88 and K92 amino acids of DAT to induce inhibitory effects on transporter function.

In our recent report we revealed that Y470H mutant transporter prefers inward-facing conformational state (Midde et al., 2013). Zinc, a DAT modulator that stabilizes the transporter in outward conformation by loosely binding to the transporter, is extensively used to study the conformational effects of mutants on transporter function (Loland et al., 2003). Accordingly, studies show that Zn^{2+} inhibits DA uptake and increases WIN35,428 binding in WT. In the present study, we showed that Y88F, K92M, Y470F and Y470A mutants do not attenuate Zn^{2+}-mediated inhibition of [^{3}H]DA transporter but decrease potentiation of [^{3}H]WIN 35,428 binding compared to WT. Established evidence indicate that transporters that prefer inward facing state reverse Zn^{2+} inhibitory effects on DA uptake and decrease Zn^{2+} -mediated WIN35,428 binding (Loland et al., 2002; Loland et al., 2004; Guptaroy et al., 2009; Liang et al., 2009; Midde et al., 2013). A possible explanation for Y88F, K92M, Y470F and Y470A mutants failing to reverse Zn^{2+} influence on DA uptake could be that these particular mutants induce an aberrant structure of the DAT that may not be suitable for Zn^{2+} inhibitory effects on DA translocation because Zn^{2+} binding require strict geometrical structural constraints (Alberts et al., 1998). However, our data strongly supports a modified

conformational change in the mutant transporters by attenuation of Zn^{2+} induced [^{3}H]WIN 35,428 binding (Figure 3.6B, 3.7B) and by showing increased inhibitor potency values for inhibiting [^{3}H]WIN 35,428 binding (Table 3.2). The effect of mutations on conformational states of DAT was further probed by measuring substrate basal efflux. We used both DA and MPP+ for efflux studies to produce more accurate outcomes as MPP+ has less diffusive properties than DA. In our recent study we showed that Y470H mutant robustly increases DA efflux compared to WT (Midde et al., 2013). In the present study, we found that Y470A exhibits increased efflux of both DA and MPP+ but not the Y470F mutant. The likely explanation for normal efflux in Y470F would be due to less impact of this substitution on the structural integrity of the transporter. Interestingly, K92M displayed increased DA efflux at two initial time points but failed to retain this ability when MPP+ efflux was measured. The possible reason for K92M not replicating elevated efflux levels in [^{3}H]MPP+ efflux assay as in [^{3}H]DA efflux may be due to assuming a putative conformation that is not favorable to MPP+ binding (Liang et al., 2009). This conformation may favor slower transition between inward and outward facing states and less effective at inducing DAT-mediated efflux at least for substrate MPP+. The alternative explanation would be quick loss of substrate DA but not MPP+ by diffusion after short period of accumulation. Taken together these findings infer that Y470A and K92M disrupt the inter-molecular interaction required to maintain transporter outward facing conformation. Nevertheless, we proposed that Tat promotes alterations in transporter conformation through allosteric regulation (Zhu et al., 2009; Zhu et al., 2011). Intriguingly, this mechanism is similar to the exogenous full substrates like amphetamines action on DAT (Robertson et al., 2009; Rothman et al., 2009). Therefore, it is important that systemic identification and characterization of all Tat binding

sites in DAT are required in order to pin point the mode of action of Tat on rearrangements of DAT conformational cycle.

In summary, we have evaluated different substitutions at 470 (Y470F and Y470A) and identified additional residues (Y88 and K92) in DAT that are predicted to be interact with Tat. All mutants attenuated the inhibitory action of Tat on DA translocation except Y470F and we reasoned that these alterations are the result of disruption of critical intramolecular interactions in DAT by Tat binding. As different substitutions at 470 consistently favored against Tat-induced decrease in DA uptake it is apparent that Tyr 470 of DAT plays central role in Tat and DAT interaction, and Tyr 88 and Lys 92 may work as supporting residues along with other unidentified residues. Because Tat-driven allosteric mechanism down regulates DA uptake (Zhu et al., 2011) and mutations at predicted amino acids show alterations in conformational distribution of DAT, future investigations that identify and validate other recognition residues will certainly improve our understanding of functional relevance of Tat binding sites on DAT. This information would be useful to develop therapeutics that alleviate imbalances of the DA system in HIV-infected individuals.

Table 3.1 Summary of kinetic properties and inhibitory activities in [^{3}H]DA uptake in CHO cells expressing WT and mutated hDATs.

	V_{max} (pmol/10^5 cells)	K_m (μM)	IC_{50} (nM)			
			DA	Cocaine	GBR12909	WIN35,428
WT-hDAT	12.4 ± 4.6	1.2 ± 0.4	1730 ± 82	285 ± 49	224 ± 41	39 ± 10
Y88F-hDAT	14.8 ± 3.7	1.9 ± 0.3	2010 ± 60	160 ± 9*	95 ± 7*	20 ± 2
K92M-hDAT	4.5 ± 1.7*	1.9 ± 0.4	2870 ± 48	69 ± 4*	101 ± 12*	10 ± 1*

Data are presented as mean ± S.E.M. values from 5-7 independent experiments performed in duplicate. * $p < 0.05$ compared with WT hDAT (unpaired Student's *t* test).

Table 3.2 Summary of kinetic properties and inhibitory activities in [^{3}H]WIN 35,428 binding in PC12 cells expressing WT and mutated hDATs.

	B_{max} (pmol/10^5 cells)	K_d (nM)	IC_{50} (nM)		
			DA	Cocaine	GBR12909
WT-hDAT	9.7 ± 1.6	8.6 ± 1.1	827 ± 102	150 ± 8.6	20.7 ± 6.3
Y88F-hDAT	5.8 ± 0.9	4.0 ± 0.6*	2071 ± 340*	85 ± 6.9	15.1 ± 5.1
K92M-hDAT	2.4 ± 0.4*	3.5 ± 1.1*	4211 ± 118*	106 ± 31.5	12.8 ± 14.3

Data are presented as mean ± S.E.M. of IC_{50} values from five independent experiments performed in duplicate. * $p < 0.05$ compared with WT hDAT (unpaired Student's *t* test).

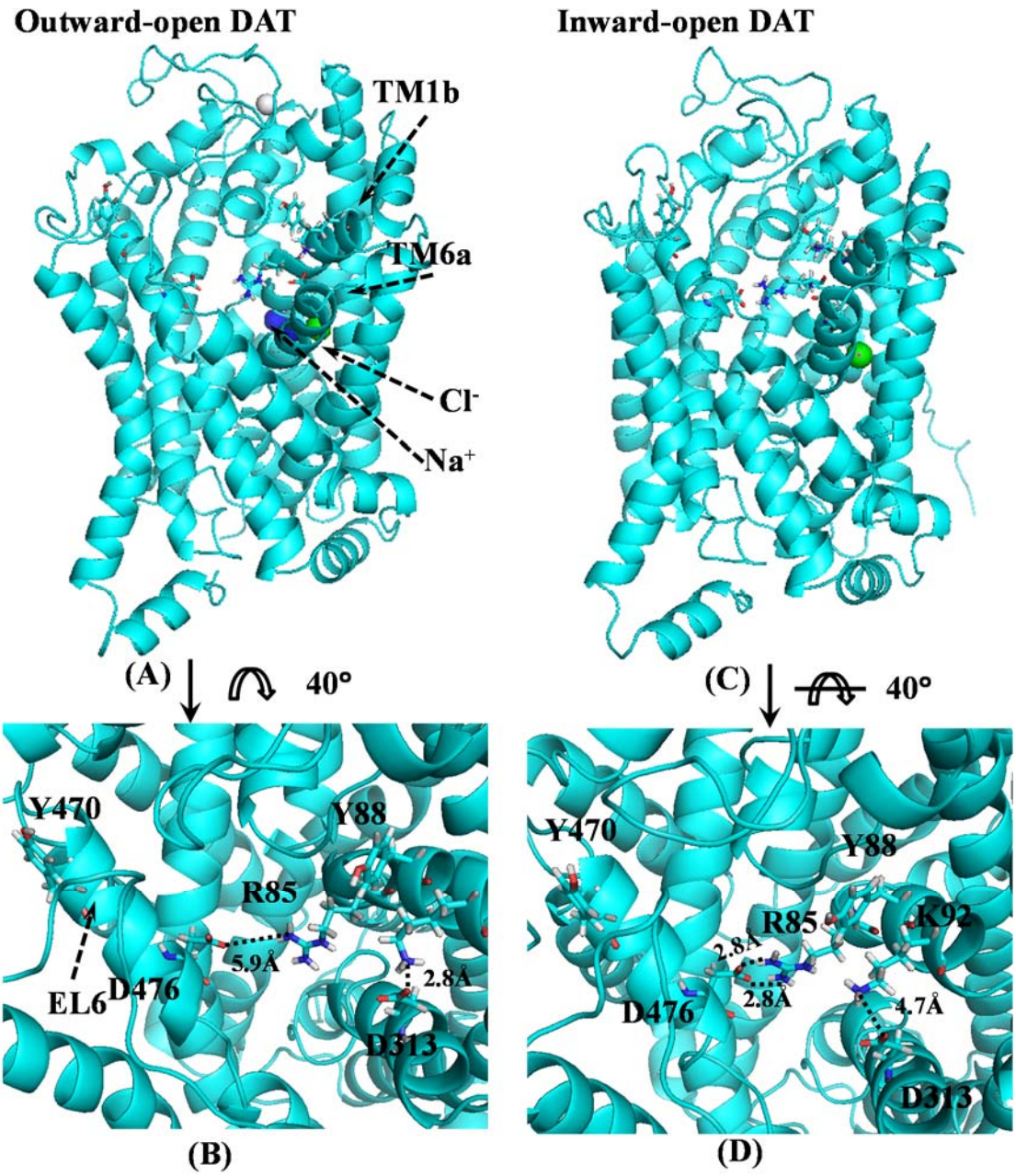

Figure 3.1 MD simulated structure of outward-open DAT (A and B) and structure of inward-open DAT (C and D). **(A)** Side view of outward-open state of DAT structure shown as cyan-colored ribbon. 2 Na^+ ions and 1 Cl^- ion are shown as spheres. **(B)** Local view of the residues around the mouth of the vestibule of outward-open state of DAT. These residues are R85, Y88, K92, D313, Y470 and D476 shown in stick-style. Hydrogen bond between K92 and D313 are represented as dashed lines with labeled distances (between hydrogen bond donor and acceptor, unit in Å), which stabilized the TM1b and TM6a. **(C)** Side view of inward-open state of DAT structure shown as colored ribbon. 1 Cl^- ion is shown as sphere.

(D) Local view of residues around the mouth of the vestibule of inward-open state of DAT. We also found that the salt bridge formed by the positive side chain of residue R85 and the negative side chain of D476 act as the gate for the entry of substrate dopamine into its biding pocket. The R85-D476 salt bridge are also labeled, which stabilized the inward-open state of DAT.

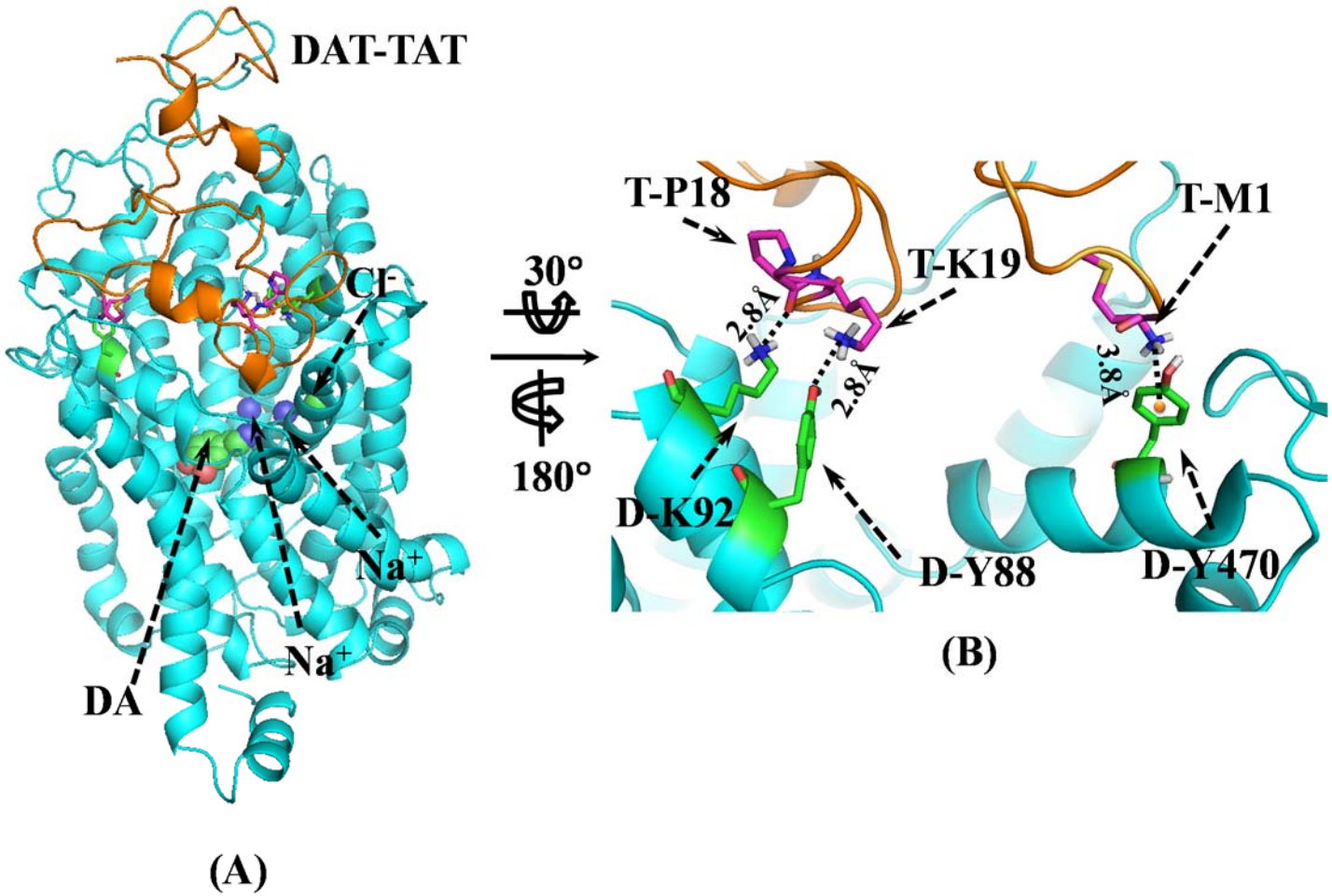

Figure 3.2 MD simulated structure of HIV-1 Tat-DAT binding complex. **(A)** HIV-1 Tat protein is shown as ribbon and colored in golden, and DAT is represented as cyan ribbon. Residues T-M1, T-P18 and T-K19 of HIV-1 Tat are represented as sticks and colored by atom types. Dopamine is shown as green spheres. One Cl- ion is shown as a green sphere, and two Na+ ions as blue spheres. **(B)** Atomic

interactions between HIV-1 Tat and DAT as observed from the binding structure. Critical residues of inter-molecular interactions from HIV-1 Tat and DAT are shown in stick style and colored by atom types. Two dashed lines on the left represent inter-molecular hydrogen bonds with labeled distances. The orange ball indicates the center of aromatic ring, and the dashed line pointing to the orange ball represents the cation-π interaction with labeled distance.

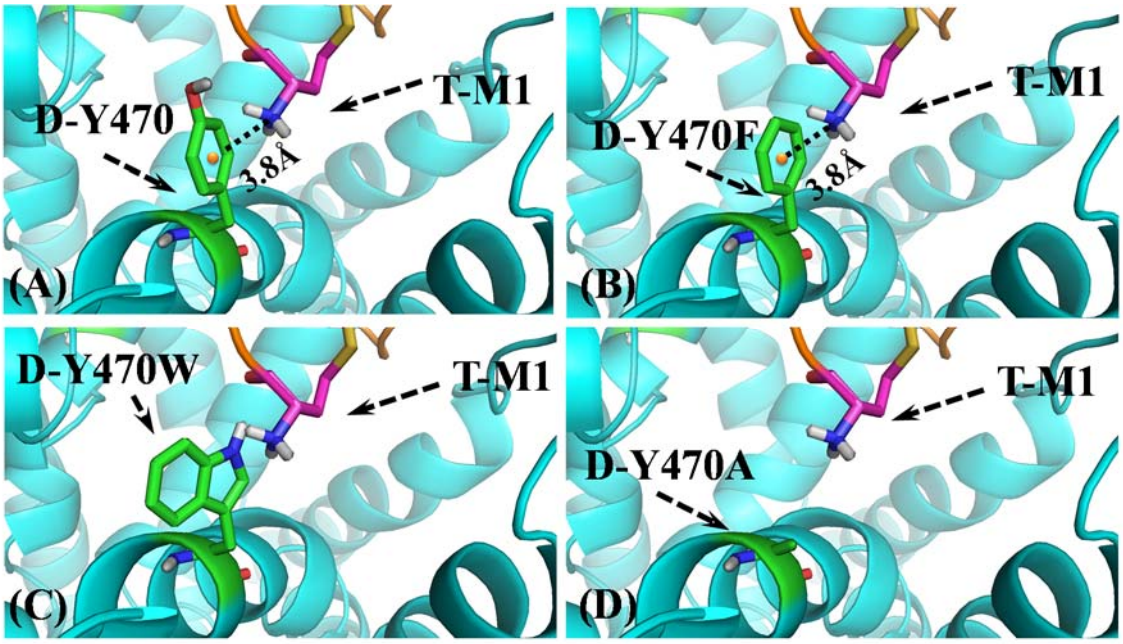

Figure 3.3 Interaction between TAT-M1 and DAT-Y470 mutations. **(A)** Residues T-M1 and D-Y470 are represented as sticks and colored by atom types. The orange ball indicates the center of aromatic ring, and the dashed line pointing to the orange ball represents the cation-π interaction with labeled distance. **(B)** Y470F mutation retains the cation-π interaction between T-M1 and D-Y470. It can be expected Y470F would bring little influence on the TAT effect, which is consist with experimental data. **(C)** Y470W would eliminate the cation-π interaction because of the unfavorable van der Waals interaction, which is expected to exhibit attenuation on DAT-TAT binding affinity. **(D)** Y470A would eliminate the cation-π interaction between T-M1 and D-Y470, which is also expected to exhibit attenuation on DAT-TAT binding affinity.

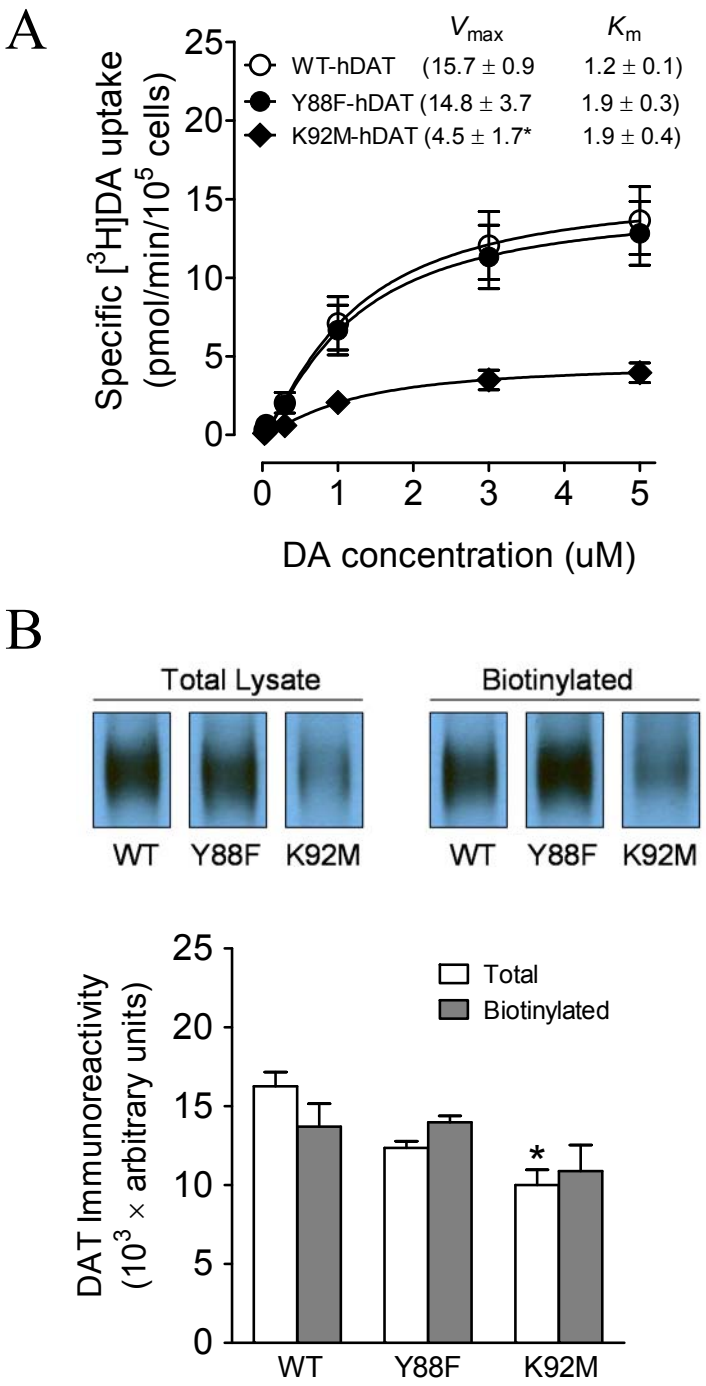

Figure 3.4 [^{3}H]DA uptake and DAT surface expression in WT hDAT and mutants. **(A)** Kinetic analysis of [^{3}H]DA uptake in WT hDAT, Y88F-hDAT and K92M-hDAT. CHO cells transfected with WT hDAT, Y88F-hDAT or K92M-hDAT were incubated with one of six mixed concentrations of the [^{3}H]DA as total rate of DA uptake. In parallel, nonspecific uptake of each concentration of [^{3}H]DA (in the presence of 10 μM nomifensine, final concentration) was subtracted from total uptake to calculate DAT-mediated uptake. * $p <$ 0.05 compared to control value (unpaired Student's *t* test) (n = 5). (**B**) Cell surface

expression of WT hDAT (WT), Y88F-hDAT (Y88F) and K92M-hDAT (K92M) was analyzed by biotinylation assay. Top panel: representative immunoblots in CHO cells expressing WT hDAT, Y88F-hDAT or K92M-hDAT. Bottom panel: DAT immunoreactivity is expressed as mean ± S.E.M. densitometry units from three independent experiments (n = 3). * $p < 0.05$ compared to WT hDAT (unpaired Student's *t* test).

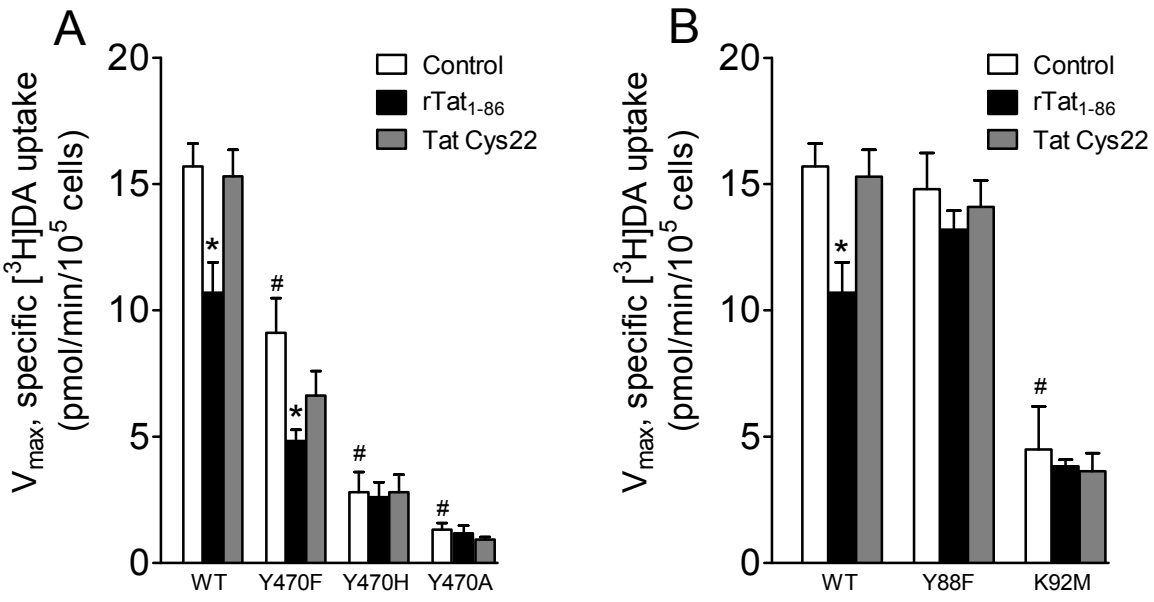

Figure 3.5 Effects of Tat or Tat Cys22 on [^{3}H]DA uptake in WT hDAT and mutants. (**A**) PC12 cells transfected with WT, Y470F-hDAT (Y470F), Y470H-hDAT (Y470H) or Y470A-hDAT (Y470A) were preincubated with or without recombinant Tat Cys22 or Tat$_{1-86}$ (rTat$_{1-86}$) at 500 nM final concentration at room temperature for 20 min followed by the addition of 0.05 μM final concentration of the [^{3}H]DA. Nonspecific uptake was determined in the presence of 10 μM final concentration of nomifensine. (**B**) [^{3}H]DA uptake in cells transfected with WT hDAT (WT), Y88F-hDAT (Y88F) and K92M-hDAT (K92M) was determined in the presence or absence of Tat Cys22 or rTat$_{1-86}$ (500 nM, final concentration). Data are expressed as means from seven independent experiments ± S.E.M. * $p < 0.05$ compared with the respective control values. # $p < 0.05$ compared to WT hDAT. (n = 5)

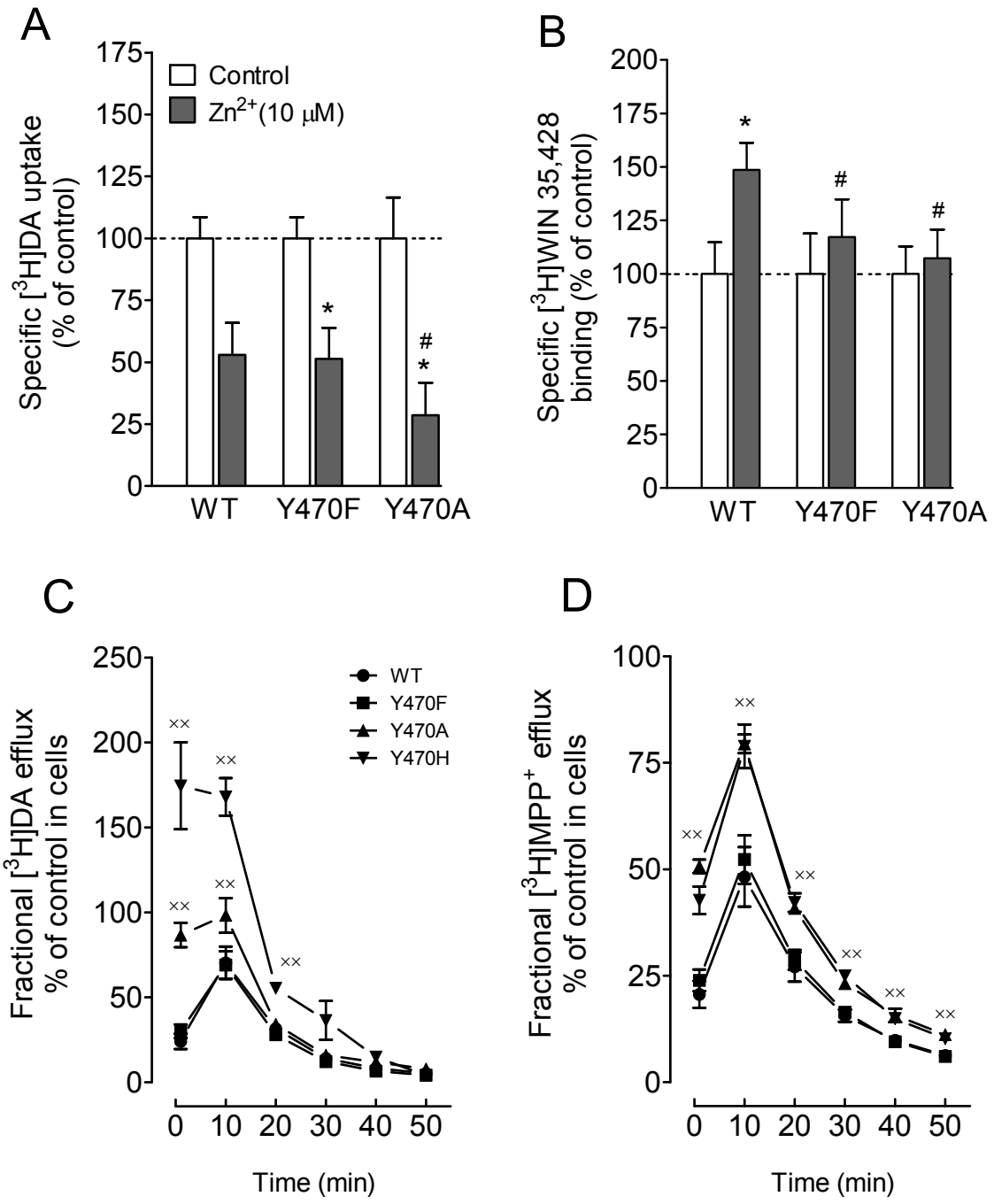

Figure 3.6 Effects of Y470F, Y470A and Y470H mutants on transporter conformational transitions. Mutations of Tyr470 affect zinc regulation of [^{3}H]DA uptake (**A**) and [^{3}H]WIN 35,428 binding (**B**). CHO cells transfected with WT hDAT (WT), Y470F-hDAT (Y470F) and Y470A-hDAT (Y470A) were incubated with assay buffer alone (control) or $ZnCl_2$ (10 μM, final concentration) followed by [^{3}H]DA uptake or [^{3}H]WIN 35,428 binding (n = 6). The histogram shows [^{3}H]DA uptake and [^{3}H]WIN 35,428 binding expressed as mean ± S.E.M. of the respective controls set to 100% for the mutant. * $p < 0.05$ compared to control. $^{\#}$ $p < 0.05$ compared to WT hDAT with $ZnCl_2$. Functional efflux of (**C**) DA and (**D**) MPP+

was determined in WT hDAT and mutants. CHO cells transfected with WT hDAT or mutants were preincubated with [^{3}H]DA (0.05 μM, final concentration) or [^{3}H]MPP+ (5 nM, final concentration) at room temperature for 20 or 30 min, respectively. After incubation, cells were washed and incubated with fresh buffer as indicated time points. Subsequently, the buffer was separated from cells, and radioactivity in the buffer and remaining in the cells was counted. Each fractional efflux of [^{3}H]DA or [^{3}H]MPP+ in WT hDAT (WT), Y470F-hDAT (Y470F), Y470A-hDAT (Y470A) or Y470H-hDAT was expressed as percentage of total [^{3}H]DA or [^{3}H]MPP+ in the cells at the start of the experiment. Fractional [^{3}H]DA efflux at 1, 10, 20, 30, 40 and 50 min are expressed as the percentage of total [^{3}H]DA with preloading with 0.05 μM (WT hDAT: 26837 ± 5089 dpm, Y470F-hDAT: 20908 ± 4209 dpm, Y470A-hDAT: 1158 ± 123 dpm and Y470H-hDAT: 2488 ± 150 dpm) present in the cells at the start of the experiment ($n = 3$). $^{\times\times}p < 0.05$ compared to WT hDAT (Bonferroni *t*-test). Fractional [^{3}H]MPP+ efflux at 1, 10, 20, 30, 40 and 50 min are expressed as the percentage of total [^{3}H]MPP+ with preloading with 0.05 μM (WT hDAT: 12120 ± 397 dpm, Y470F-hDAT: 7399 ± 359 dpm, Y470A-hDAT: 460 ± 46 dpm and Y470H-hDAT: 602 ± 28 dpm) present in the cells at the start of the experiment ($n = 3$). $^{\times\times}p < 0.05$, compared to WT hDAT (Bonferroni *t*-test).

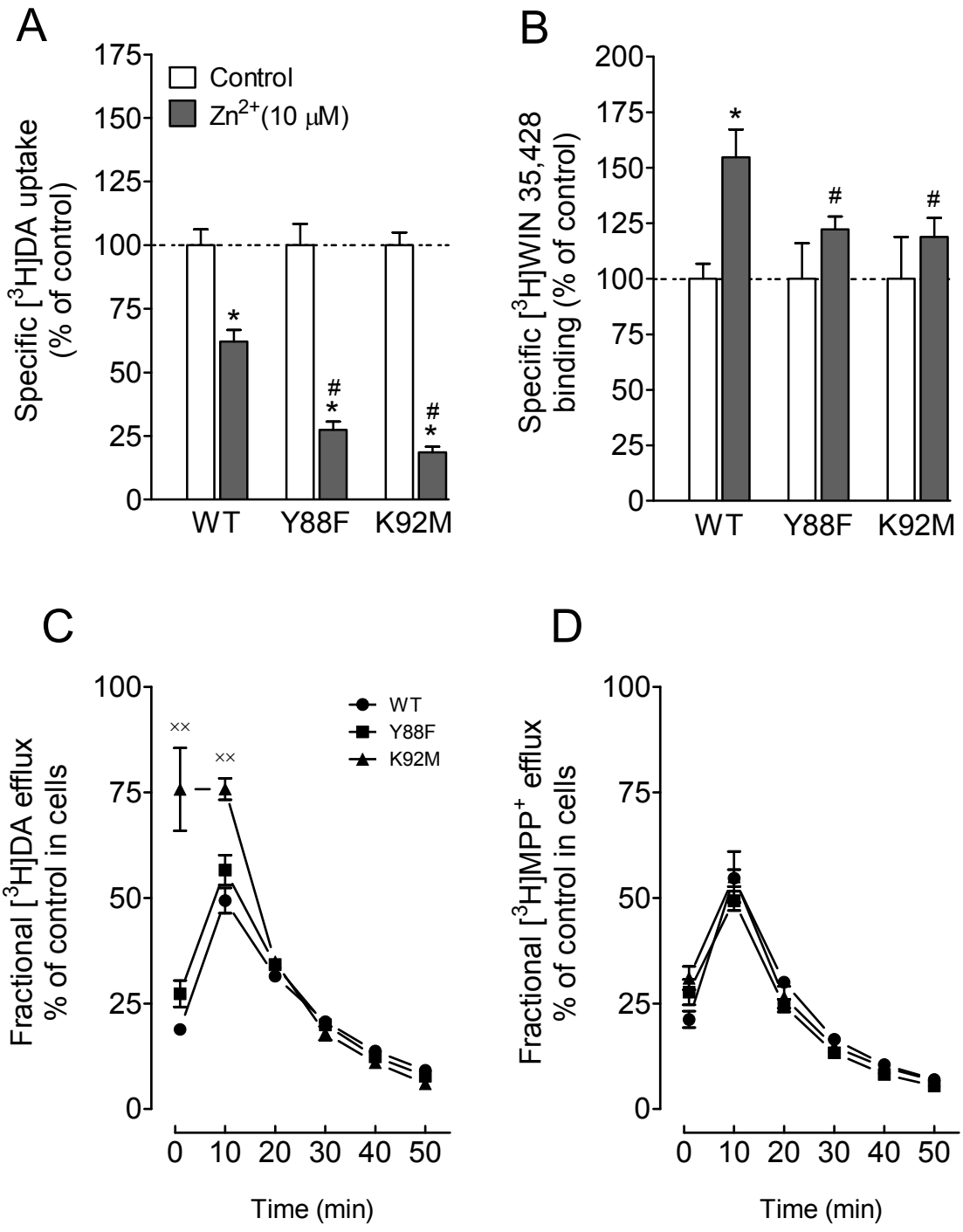

Figure 3.7 Effects of Y88F and K92M mutants on transporter conformational transitions. Mutations of Tyr88 and Lys92 affect zinc regulation of [^{3}H]DA uptake (**A**) and [^{3}H]WIN 35,428 binding (**B**). The histogram shows [^{3}H]DA uptake and [^{3}H]WIN 35,428 binding expressed as mean ± S.E.M. of the respective controls set to 100% for the mutant. * $p < 0.05$ compared to control. $^{\#}$ $p < 0.05$ compared to WT hDAT with $ZnCl_2$. Functional efflux of (**C**) DA and (**D**) MPP+ was determined in WT hDAT and mutants. Each fractional efflux of

[^{3}H]DA or [^{3}H]MPP+ in WT hDAT (WT), Y88F-hDAT (Y88F) or K92M-hDAT (K92M) was expressed as percentage of total [^{3}H]DA or [^{3}H]MPP+ in the cells at the start of the experiment. Fractional [^{3}H]DA efflux at 1, 10, 20, 30, 40 and 50 min are expressed as the percentage of total [^{3}H]DA with preloading with 0.05 μM (WT hDAT: 70082 ± 8256 dpm, Y88F-hDAT: 41805 ± 6887 dpm and K92M-hDAT: 9655 ± 2160 dpm) present in the cells at the start of the experiment (n = 3). $^{\times\times}$ $p < 0.05$ compared to WT hDAT (Bonferroni t-test). Fractional [^{3}H]MPP+ efflux at 1, 10, 20, 30, 40 and 50 min are expressed as the percentage of total [^{3}H]MPP+ with preloading with 0.05 μM (WT hDAT: 15516 ± 920 dpm, Y88F-hDAT: 5695 ± 450 dpm and K92M-hDAT: 967 ± 121 dpm) present in the cells at the start of the experiment (n = 3).

CHAPTER 4

HIV-1 TAT PROTEIN DECREASES DOPAMINE TRANSPORTER CELL SURFACE EXPRESSION AND VESICULAR MONOAMINE TRANSPORTER-2 FUNCTION IN RAT STRIATAL SYNAPTOSOMES[2]

ABSTRACT: The dopamine (DA) transporter (DAT) and vesicular monoamine transporter (VMAT2) proteins interact as a biochemical complex to regulate dopaminergic neurotransmission. We have reported that HIV-1 Tat_{1-86} decreases the specific [^{3}H]DA uptake and [^{3}H]WIN 35,428 binding sites without a change in total DAT immunoreactivity in rat striatum (Zhu et al., 2009b). The present study determined the effects of Tat on DAT phosphorylation and trafficking, and vesicular [^{3}H]DA uptake. Pre-incubation of rat striatal synaptosomes with the protein kinase C (PKC) inhibitor bisindolylmaleimide I (1 μM) completely blocked Tat_{1-86} -induced reduction of [^{3}H]DA uptake, indicating that Tat regulates DAT function through a PKC-dependent mechanism. After exposure of synaptosomes to Tat_{1-86} (1 μM), DAT immunoreactivity was decreased in plasma membrane enriched fractions (P3) and increased in vesicle-enriched fractions (P4) relative to controls without change in total synaptosomal fractions (P2), suggesting that Tat-induced inhibition of DA uptake is attributable to DAT internalization. Although both DAT and VMAT2 proteins are essential for the regulation of DA disposition in synapse and cytosol, Tat

[2] Midde NM, Gomez AM, Zhu J (2012) HIV-1 Tat Protein Decreases Dopamine Transporter Cell Surface Expression and Vesicular Monoamine Transporter-2 Function in Rat Striatal Synaptosomes. Journal of neuroimmune pharmacology : the official journal of the Society on NeuroImmune Pharmacology. PMCID: PMC3688268

inhibited the specific [^{3}H]DA uptake into vesicles (P4) and synaptosomes (P2) by 35% and 26%, respectively, inferring that the inhibitory effect of Tat was more profound in VMAT2 protein than in DAT protein. Taken together, the current study reveals that Tat inhibits DAT function through a PKC and trafficking-dependent mechanism and that Tat impacts the dopaminergic tone by regulating both DAT and VMAT2 proteins. These findings provide new insight into understanding the pharmacological mechanisms of HIV-1 viral protein-induced dysfunction of DA neurotransmission in HIV-infected patients.

4.1 INTRODUCTION

The prevalence of HIV-1-associated neurocognitive disorders (HAND) in HIV-1 positive individuals remains high (~50%), regardless of the success with treatments of anti-retroviral agents effectively controlling viral replication and dramatically improving longevity (Robertson et al., 2007; Tozzi et al., 2007; Ernst et al., 2009). Notably, the incidence and severity of HAND are greatly enhanced (~70%) due to concomitant use of drugs of abuse such as cocaine (Norman et al., 2009), which has been postulated as a co-morbid factor in the susceptibility and progression of HAND (Larrat and Zierler, 1993; Fiala et al., 1998; Webber et al., 1999; Buch et al., 2011). While HIV-1 virus enters the brain and produces proviral DNA in the early stage of HIV-1 infection (Nath and Clements, 2011), anti-retroviral agents cannot prevent the production of HIV-1 viral proteins in infected brain cells (McArthur et al., 2010; Nath and Clements, 2011). HIV-1 viral proteins, such as Tat, have been detected in brains of patients with HIV-1 infection (Del Valle et al., 2000; Hudson et al., 2000; Lamers et al., 2010), and have been implicated in the pathophysiology of HAND (Li et al., 2009). Moreover, Tat protein has been found to synergize with psychostimulant drugs in producing profound neural and behavioral impairments in preclinical models (Ferris

et al., 2008), consistent with the findings in the human HIV-1 positive drug abusing population (Larrat and Zierler, 1993). Unfortunately, there are no promising therapeutic approaches for such HIV-1-associated neurocognitive impairments.

The development of neurocognitive dysfunction in HAND patients is associated with perturbations of the central dopamine (DA) neurotransmission (Kumar et al., 2011; Meade et al., 2011a). The DA system is a clinically relevant HAND target as evidenced by recent human imaging (Chang et al., 2008; Meade et al., 2011a), neurocognitive (Kumar et al., 2011; Meade et al., 2011b), and post-mortem examinations (Silvers et al., 2007; Kumar et al., 2009), that HAND is associated with vulnerability of the DA system. Limited studies have reported that DA levels are decreased in DA-rich brain area (Sardar et al., 1996; Kumar et al., 2009), but increased in the CSF (Scheller et al., 2010) of HAND patients. The DA transporter (DAT) is critical for DA homeostasis, which is critical for neurocognitive function (Chudasama and Robbins, 2006). DAT is a target for HIV-1 viral proteins (Hu et al., 2009; Zhu et al., 2009b) and cocaine to impact the DA system (Zhu and Reith, 2008). We have demonstrated that Tat inhibits DA uptake in rat striatal synaptosomes and that influence of Tat on DAT ligand binding sites involves a protein-protein interaction (Zhu et al., 2009b). In particular, we have shown that Tat allosterically inhibits DAT function and modulates cocaine binding sites on DAT in rat striatal synaptosomes and heterologous cells expressing human DAT (Zhu et al., 2011).

The dynamic regulation of DAT function and cell surface localization of DAT are under the control of complex processes involving phosphorylation, protein-protein interaction, substrate pretreatment, and interaction with presynaptic receptors (Zhu and Reith, 2008). For example, activation of protein kinase C (PKC) results in reduced DA

transport activity, decreased transporter recycling and DAT cell surface expression, thereby causing reduced DA uptake (Daniels and Amara, 1999; Melikian, 2004; Zahniser and Sorkin, 2004). On one hand, dynamic cell surface localization of DAT is regulated by cellular signaling pathways and endocytotic trafficking (Zhu and Reith, 2008). On the other hand, the DAT and vesicular monoamine transporter (VMAT2) proteins interact as a biochemical complex to regulate dopaminergic tone in response to motivationally relevant stimuli, including abused drugs (Vergo et al., 2007; Zhu and Reith, 2008; Egana et al., 2009).

This study was aimed to understand the molecular mechanisms underlying Tat-induced decrease in DAT reuptake activity. The primary hypothesis tested here was that Tat-induced reduction of DA transport is attributable to acceleration of DAT endocytosis through the dynamic-trafficking and phosphorylation-dependent mechanisms and that both DAT and VMAT-2 function contribute to Tat-induced impairment of DA neurotransmission.

4.2 MATERIAL AND METHODS

4.2.1 ANIMALS

Adult male Sprague – Dawley rats (225-250g body weight) were obtained from Harlan Laboratories, Inc. (Indianapolis, IN). Rats were housed in standard polyurethane cages and provided normal rodent food (ProLab Rat/Mouse/Hamster Chow 3000) and water *ad libitum*. The colony was maintained at 21±2 °C, 50±10% relative humidity and a 12L: 12D cycle with lights on at 0700 h (EST).The animals were maintained according to the National Institute of Health (NIH) guidelines in AAALAC accredited facilities. The experimental protocol was approved by the Institutional Animal Care and Use Committee (IACUC) at the University of South Carolina.

4.2.2 Drugs and Chemicals

[^{3}H]DA (3,4-ethyl-2[N-3H]dihydroxyphenylethylamine; specific activity, 31 Ci/mmol) and [^{3}H]WIN 35,428 (specific activity, 85 Ci/mmol) were purchased from PerkinElmer Life and Analytical Sciences (Boston, MA). Recombinant HIV-1 transactivator of transcription ($Tat_{1–86}$, Clade B, REP0002a) protein and its mutant protein Tat Cys22 (cysteine 22 was substituted to glycine, REP0032) were purchased from Diatheva (Fano, Italy). D-amphetamine, cocaine and Bisindolylmaleimide-I (BIM-I) were purchased from Tocris Biosciences (Ellisville, MO). Tetrabenazine (TBZ) was provided by NIMH Chemical Synthesis and Drug Supply Program (Bethesda, MD). Antibodies recognizing rat DAT (C-20; goat polyclonal antibody) and actin (C-2; mouse monoclonal antibody) were purchased from Santa Cruz Biotechnology, Inc. (Santa Cruz, CA). Anti-goat IgG horseradish peroxidase was purchased from Jackson ImmunoResearch Laboratories Inc. (West Grove, PA). Goat anti-mouse IgG-horseradish peroxidase was purchased from Santa Cruz Biotechnology, Inc. D-Glucose, L-ascorbic acid, WIN35,428, L-leucine, L-lysine, bovine serum albumin, pyrocatechol, EDC, HEPES, isopropanol, nomifensine maleate, pargyline hydrochloride, polyethylene glycol, sucrose, and Tween 20 were purchased from Sigma-Aldrich (St. Louis, MO).

4.2.3 Preparation of Synaptosomes, Subfractions and Synaptic Vesicles

Striata from individual rats were homogenized in 20 ml of ice-cold 0.32 M sucrose containing 5 mM $NaHCO_3$, pH 7.4, with 16 up-and-down strokes using a Teflon pestle homogenizer (clearance, approximately 0.003 in.). Crude synaptosomal preparation was centrifuged at 2000g for 10 min at 4°C, and the resulting supernatants were then centrifuged at 20,000g for 15 min at 4°C. The resulting pellets (P2 fractions) were resuspended in 5 ml

of ice-cold Krebs-Ringer-HEPES assay buffer (final concentration in mM: 125 NaCl, 5 KCl, 1.5 $MgSO_4$, 1.25 $CaCl_2$, 1.5 KH_2PO_4, 10 D-glucose, 25 HEPES, 0.1 EDTA, 0.1pargyline, and 0.1 L-ascorbic acid, saturated with 95% O_2, 5% CO_2; pH 7.4) for the synaptosomal [^{3}H]DA uptake. To determine the distribution of DATs in subcellular fractions after exposure to Tat, striata from every two rats were pooled to achieve sufficient vesicles and the subcellular fractions were prepared using a previously published method with minor modifications (Middleton et al., 2007). Striata were homogenized in ice-cold 0.32 M sucrose buffer using a Teflon pestle homogenizer and then centrifuged at 800g for 12 min, 4°C. The resulting supernatant (S1) was centrifuged at 22,000g for 15 min at 4°C to yield a crude synaptosomal pellet (P2). The P2 pellet was then resuspended in DA uptake assay to obtain synaptosomes. In order to determine whether Tat (1 μM)-induced decreases of [^{3}H]DA uptake, as observed in our previous report (Zhu et al., 2009b), was associated with a reduction of DAT expression in plasma membrane, half of the synaptosomes were preincubated with Tat_{1-86} (1 μM), and the other half were preincubated without Tat_{1-86} as control at 34°C for 15 min. This concentration of Tat_{1-86} was chosen based on our previous report showing that the inhibitory effect of Tat (1 μM) on DA uptake was reversible (Zhu et al., 2009b). Subsequently, the synaptosomal samples were centrifuged at 22,000g for 15 min at 4°C and synaptosomes in the pellets (P2) were then lysed in ice-cold 25 mM HEPES, pH 7.5, and 100 mM potassium tartrate (pH 7.4) plus phosphatase inhibitor cocktails I (P2850, Sigma-Aldrich, St. Louis, MO) and protease inhibitor cocktail (P8340, Sigma-Aldrich, St. Louis, MO). After thorough mixing of all contents, the resulting mixture was centrifuged at 20,000g for 15 min at 4°C to get the plasma membrane enriched (P3) and vesicle-enriched supernatant (S3). The S3 was then centrifuged at 100,000g for 45 min at 4°C to yield the

cytoplasmic vesicles pellet (P4). The three fractions (P2, P3, and P4) were used for Western blot assay. Protein concentrations were determined by the Bradford protein assay (Bradford, 1976) using bovine serum albumin as the standard (Bio-Rad Laboratories, Hercules, CA).

4.2.4 SYNAPTOSOMAL [^{3}H]DA UPTAKE

[^{3}H]DA uptake was determined using previously described methods (Zhu et al., 2009b). Assays were performed in triplicate with a final volume of 1 mL. Aliquots of striatal synaptosomes were preincubated in assay buffer containing BIM-I (100 μM, final concentration) at 34 °C for 5 min in an oxygenated metabolic shaker, and then incubated with amphetamine (20 μM, final concentration) or Tat (0.7 μM) for an additional 15 min. The concentration of BIM-I was chosen based on the previous report showing that BIM-I (100 μM) alone did not show inhibitory effect on [^{3}H]DA into rat striatal synaptosomes (Richards and Zahniser, 2009). A low concentration of Tat (0.7 μM) was chosen because our previously published study (Zhu et al., 2009b) has demonstrated that Tat at both 0.7 and 1.0 μM concentrations significantly decreases [^{3}H]DA uptake by 21% and 26%, respectively. The purpose of the experiment was to determine whether Tat-induced decrease in DAT function is PKC-dependent. We selected the low concentration because it was sufficient to elicit a significant decrease in DA uptake for the PKC experiment. Subsequently, the synaptosomes were centrifuged at 20,000g for 15 min and the resulting pellets were resuspended with ice cold assay buffer. Aliquots of the well-washed synaptosomes were incubated with 5 nM [^{3}H]DA (final concentration) at 34 °C for 10 min. The reactions were terminated by the addition of 3 ml of ice-cold assay buffer. Nonspecific uptake was determined in duplicate at each [^{3}H]DA concentration by including 10 μM nomifensine in the assay buffer. Samples were filtered through Whatman GF/B glass fiber filters (Whatman,

Maidstone, UK), presoaked with assay buffer containing 1 mM pyrocatechol. Filters were washed three times with 3 ml of ice-cold assay buffer containing 1 mM pyrocatechol using a Brandel cell harvester (model M-48; Biochemical Research and Development Laboratories Inc., Gaithersburg, MD). Pyrocatechol (catechol) is a catechol-O-methyltransferase inhibitor. In the current study, pyrocatechol (1 mM) was included in the DA uptake assay buffer to prevent the degradation of [^{3}H]DA during the processes of washes and harvesting (Zhu et al., 2004). Radioactivity was determined using liquid scintillation spectrometry (model Tri-Carb 2900TR; PerkinElmer Life and Analytical Sciences).

4.2.5 VESICULAR [^{3}H]DA UPTAKE

To determine inhibitory effects of Tat on VMAT-2 function, vesicular [^{3}H]DA uptake was measured using previously described methods (Volz et al., 2007). In brief, assays were performed in duplicate with a final volume of 250 µl. For the competitive inhibition experiment, aliquots of P4 suspensions were preincubated in VMAT-2 assay buffer (final concentration in mM: 25 HEPES, 100 potassium tartrate, 0.05 EGTA, and 0.1 EDTA, 1.7 ascorbic acid, and 2 ATP-Mg^{2+}, pH 7.5) containing Tat, Tat Cys22 or TBZ (final concentration, 0.1 nM-10 µM) at 34 ºC for 15 min in an oxygenated metabolic shaker and subsequently incubated with a fixed concentration of [^{3}H]DA (1 µM, final concentration) at 34 ºC for additional 8 min. To determine if Tat differentially inhibits DAT and VMAT-2 function, in a separate experiment, synaptosomes were preincubated with 1 µM Tat at 34 ºC for 15 min. Subsequently the synaptosomes were washed with fresh ice-cold assay buffer, and P2 and P4 fractions were then separated as described above. Aliquots of P4 fractions were incubated in the assay buffer with 1 to 8 concentrations of [^{3}H]DA (0.03-5 µM) at 34 ºC for 8 min. Nonspecific uptake was determined in the presence of 10 µM TBZ. Reactions

were terminated by addition of 1 ml of cold wash buffer (assay buffer containing 2 mM $MgSO_4$ substituted for the ATP-Mg^{2+}, pH 7.5) and rapid filtration through Whatman GF/B filters soaked previously in 0.5% polyethylenimine. Filters were washed 3 times with the VMAT-2 assay buffer and radioactivity was measured using a liquid scintillation counter.

4.2.6 WESTERN BLOTS

Proteins were extracted from each fraction (P2, P3 and P4) as described above with the Laemmli sample buffer (Sigma-Aldrich, St. Louis, MO) containing phosphatase inhibitor cocktail 1 (P2850, Sigma-Aldrich, St. Louis, MO) and protease inhibitors (P8340, Sigma-Aldrich, St. Louis, MO) and boiled for 5 min. To detect the immunoreactive DAT protein in these fractions, samples were subjected to gel electrophoresis and Western blotting. Proteins were separated by 10% SDS-polyacrylamide gel electrophoresis for 90 min at 150 V and transferred to Immobilon-P transfer membranes (Millipore, Billerica, MA) in transfer buffer (50 mM Tris, 250 mM glycine, and 3.5 mM SDS) using a Mini Trans-Blot Electrophoretic Transfer Cell (Bio-Rad Laboratories) for 110 min at 72 V. Transfer membranes were incubated with blocking buffer (5% dry milk powder in phosphate-buffered saline containing 0.5% Tween 20) for 1 h at room temperature, followed by incubation with goat polyclonal DAT antibody (1 μg/ml in blocking buffer) overnight at 4°C. Transfer membranes were washed five times with wash buffer (phosphate-buffered saline containing 0.5% Tween 20) at room temperature and then incubated with rabbit anti-goat DAT antibody (1:2500 dilution in blocking buffer) for 1 h at 22°C. Blots on transfer membranes were detected using enhanced chemiluminescence and developed on Hyperfilm ECL-Plus (GE Healthcare, Chalfont St. Giles, Buckinghamshire, UK). After detection and quantification of the DAT protein, each blot was stripped in 10% Re-blot plus mild antibody stripping

solution (Millipore Bioscience Research Reagents, Temecula, CA) for 20 min at room temperature and reprobed for detection of actin. Actin was used as an intracellular control protein to monitor protein loading between samples and determined using a mouse monoclonal antibody (1:1000 dilution in blocking buffer). Multiple autoradiographs were obtained using different exposure time, and immunoreactive bands within the linear range of detection were quantified with densitometric scanning (Scion Image software; Scion Corporation, Frederick, MD). Band density measurements, expressed as relative optical density, were used to determine levels of the DAT immunoreactivity in synaptosomes.

4.2.7 [^{3}H]WIN 35,428 BINDING ASSAY

To determine whether Tat-induced inhibition of [^{3}H]DA uptake was the result of alterations in the maximal number of binding sites (B_{max}) or affinity (K_d) for [^{3}H]WIN 35,428 binding in P3 fraction, kinetic analysis of [^{3}H]WIN 35,428 binding was determined using a previously described method (Zhu et al., 2009b). After exposure of synaptosomes to Tat (1 μM) or vehicle (control) as described above, the P3 pellets were resuspended in ice-cold sodium-phosphate buffer (2.1 mM NaH_2PO_4, 7.3 mM $Na^2HPO_47H_2O$, and 320 mM sucrose, pH 7.4). Aliquots of P3 fractions were incubated with one of the eight concentrations of [^{3}H]WIN 35,428 (final concentration, 0.5–30 nM) on ice for 2 h. In parallel, nonspecific binding at each concentration of [^{3}H]WIN 35,428 (in the presence of 30 μM cocaine, final concentration) was subtracted from total binding to calculate the specific binding. Assays were terminated by rapid filtration onto Whatman GF/B glass fiber filters, presoaked for 2 h with the assay buffer containing 0.5% polyethylenimine, using a Brandel cell harvester. Filters were rinsed three times with 3 ml of ice-cold assay buffer. Radioactivity remaining on the filters was determined by liquid scintillation spectrometry.

4.2.8 DATA ANALYSIS

Data are presented as mean ± S.E.M., and *n* represents the number of independent experiments for each experiment. The effect of BIM-I on Tat-induced changes in DA uptake was analyzed by one-way ANOVA. Student-Newman-Keuls comparisons were made for *post hoc* analyses. Separate paired Student's *t* test was conducted on DAT immunoreactivity for comparisons between control and Tat treated samples. Kinetic parameters (B_{max} and K_d) of [^{3}H]WIN 35,428 binding were determined from saturation curves by nonlinear regression analysis using a one-site model with variable slope. For experiments involving comparisons between two paired samples, paired Student's *t* test was used to determine the ability of Tat to alter the kinetic parameters [K_m and V_{max} for [^{3}H]DA uptake; K_d and B_{max} for [^{3}H]WIN 35,428 compared with control (the absence of Tat)]; log-transformed values of K_m or K_d were used for these statistical comparisons. IC_{50} values for Tat-induced inhibition in specific vesicular [^{3}H]DA uptake were determined from inhibition curves by nonlinear regression analysis using a one-site model with variable slope. All statistical analyses were performed using SPSS, standard version 19.0 (SPSS Inc., Chicago, IL), and differences were considered significant at $p < 0.05$.

4.3 RESULTS

4.3.1 INVOLVEMENT OF PKC IN TAT-INDUCED DOWN-REGULATION OF DAT FUNCTION IN RAT STRIATAL SYNAPTOSOMES

To determine whether the Tat-induced down-regulation of DAT function was mediated by activation of PKC, synaptosomes were preincubated with the PKC inhibitor BIM-I (1 μM) for 5 min prior to preincubation with Tat (0.7 μM) or amphetamine (20 μM) for additional 15 min. Amphetamine was used as a positive control, because the previous report has shown that amphetamine-induced down-regulation of DAT activity was blocked

by preincubation of BIM-I (Richards and Zahniser, 2009). As shown in Figure 4.1, amphetamine ($F(3, 15) = 8.83$, $p < 0.01$) or Tat ($F(3, 15) = 8.28$, $p < 0.05$) alone significantly reduced [^{3}H]DA uptake, and preincubation of BIM-I completely blocked both amphetamine- and Tat-induced reductions.

4.3.2 Tat Protein Decreased Cell Surface DAT Expression in Rat Striatal Synaptosomes

To determine if the Tat-induced decrease in [^{3}H]DA uptake of DAT function was attributed to a reduction in the plasma membrane of the DATs, DAT expression in subfractions was examined. As shown in Figure 4.2, after exposure of synaptosomes to Tat (1 μM), DAT immunoreactivity was decreased by 46% in P3 fractions ($t(3) = 3.22$, $p<0.05$) and increased by 49% in P4 fractions ($t(3) = 5.64$, $p<0.05$) without changes in P2 fractions. To verify the Tat-induced decreases in P3 fractions, the B_{max} of [^{3}H]WIN 35,428 in P3 fractions was determined. Figure 4.3 shows that 15 min preincubation of synaptosomes with Tat (1 μM) led to a significant decrease of the B_{max} value by 64% (3.99 ± 0.6 pmol/mg protein) compared with the control [11.2 ± 1.3 pmol/mg protein; $t(3) = 5.6$, $p<0.05$, paired Student's *t* test]. There was no change in the K_d value between Tat-treated and control samples (38.9 ± 8.7 and 33.9 ± 11.4 nM).

4.3.3 Inhibitory Effects of Tat on VMAT-2 and DAT Function

To determine whether Tat differentially inhibited DAT and VMAT-2 function, the ability of Tat protein to inhibit vesicular [^{3}H]DA uptake or synaptosomal [^{3}H]DA uptake was measured. As shown in Figure 4.4, 15 min preincubation of synaptosomes with Tat (1 μM) caused a 35 ± 1.8 and 26 ± 1.5% reduction in [^{3}H]DA uptake into vesicles and synaptosomes, respectively.

To determine the concentration-dependent inhibitory effect of Tat on specific [^{3}H]DA uptake into striatal vesicles, vesicular [^{3}H]DA uptake was examined in the presence of various concentrations of Tat. Specific [^{3}H]DA uptake was substantially inhibited by Tat (IC_{50} = 210 ± 19 nM; Figure 4.5). TBZ was used as a positive control for the [^{3}H]DA uptake assay and had a IC_{50} value of 9.8 ± 0.7 nM. Tat Cys22 was a negative control for the assay, which showed no inhibitory effect on vesicular [^{3}H]DA uptake across the concentration range from 0.1 nM to 10 μM.

4.4 DISCUSSION

We have reported previously that Tat protein induced decrease of [^{3}H]DA uptake in rat striatal synaptosomes (Zhu et al., 2009b). The current study investigated the mechanism of this Tat-induced impairment of DAT activity. This study also determined the effect of Tat on VMAT-2 function. The results provide evidence that the Tat-induced decrease in DA uptake is ascribed to a DAT trafficking- and phosphorylation-dependent mechanism. Further, we demonstrated that Tat inhibited not only DAT activity but also VMAT-2 function. These findings provide new insight into understanding the molecular mechanisms of HIV-1 viral protein-induced dysfunction of DA neurotransmission in HIV-1 infected patients.

The present results are in agreement with previous work showing that *in vitro* exposure of rat striatal synaptosomes to Tat protein leads to a decrease in DAT uptake function (Wallace et al., 2006; Zhu et al., 2009b). In this study, while a PKC inhibitor, BIM-I, alone had no effect on DA uptake, Tat (0.7 μM)-induced decrease (21%) in specific [^{3}H]DA uptake was ablated by BIM-I. Similarly, preincubation of the synaptosomes with BIM-I completely blocked amphetamine-induced decrease (31%) in [^{3}H]DA uptake, which is consistent with a previous report (Richards and Zahniser, 2009). Therefore, compared to

amphetamine, Tat produces a similar regulatory effect on DAT uptake function through a PKC-dependent mechanism. It has been well documented that exposure to amphetamine results in DAT internalization or reduced DA uptake in cell lines expressing DAT and synaptosomes (Chen et al., 2010). Also, DAT shows a time-dependent, biphasic trafficking pattern *in vitro* and *in vivo* upon short- and long-exposure to amphetamine (Chen et al., 2010). For example, rapid treatment (less than 1 min) of rat striatal synaptosomes with amphetamine increased DAT surface expression (Furman et al., 2009), whereas a prolonged stimulation (30-60 min) led to reductions of surface DAT (Gulley et al., 2002; Johnson et al., 2005; Thwar et al., 2007), indicating that rapid amphetamine-induced DAT surface expression may contribute to amphetamine-induced DA efflux. While the current results and previous studies (Cervinski et al., 2005; Gorentla and Vaughan, 2005; Richards and Zahniser, 2009) have demonstrated that amphetamine-induced reduction of DA uptake can be blocked by pretreatment of BIM-I, it was reported that amphetamine-induced reduction in surface DAT in human DAT-PC12 cells was not inhibited by BIM-I (Boudanova et al., 2008), suggesting that amphetamine regulates DAT activity through a PKC-independent pathway. In contrast, this study shows that Tat decreased DA uptake via activation of PKC pathway. Importantly, we have demonstrated that the influence of Tat on DAT function involves a protein-protein interaction between Tat and DAT (Zhu et al., 2009b) and that Tat acts as an allosteric modulator of DAT rather than as either a reuptake inhibitor (e.g. cocaine) or a substrate releaser (e.g. amphetamine) (Zhu et al., 2011). Allosterism has been shown to be responsible for the conformational transitions via substrate- and ligand-binding sites on the DAT (Shan et al., 2011). Tat-induced inhibition of DA transporting may involve a change in the DAT conformation that requires DAT phosphorylation. Previous studies

suggest that Tat protein and amphetamine synergistically impair DAT function *in vitro* (Cass et al., 2003; Theodore et al., 2006) and *in vivo* (Kass et al., 2010); however, underlying mechanism(s) are unclear. To investigate the synergistic effects of Tat and amphetamine on DAT function and trafficking will be an essential task in our future study.

In the current study, exposure to Tat (0.7 μM) for 15 min decreased [^{3}H]DA uptake activity in rat synaptosomes. In general, Tat-induced decrease of DA transport could be accomplished in several manners: increased DAT protein degradation, decreased turnover rates of DAT, or changes in DAT trafficking on the cell surface expression without changes in total DAT immunoreactivity. To validate these potential mechanisms, first, we have demonstrated that a 15-min exposure to $Tat_{1\text{-}86}$ induced a rapid and reversible decrease in V_{max} of [^{3}H]DA uptake without changes in total DAT levels (Zhu et al., 2009b), suggesting that Tat-induced reduction in V_{max} of DA uptake is not caused by DAT degradation. Second, transporter turnover rate, which reflects the number of DA molecules transported per second per site (Lin et al., 2000), was determined and shown that 15-min exposure of synaptosomes to 1 μM Tat did not alter the ratio of V_{max} for [^{3}H]DA uptake/B_{max} for [^{3}H]WIN 35,428 binding. This result provides evidence that Tat does not decrease the turnover rates of DAT (Zhu et al., 2009b). The current results display that the levels of DAT immunoreactivity were increased by 49% in vesicle-enriched fractions (P4) and decreased by 46% in plasma membrane enriched fractions (P3) without changes in total synaptosomal fractions (P2) in Tat-exposed samples compared to the respective controls. These data indicate that exposure to Tat results in a redistribution of DAT from the cell surface to intracellular compartments (*i.e.* internalization) and that loss of DAT from the plasma membrane is responsible for the decrease in V_{max} observed after Tat exposure.

The efficiency of DA transport depends on the number of DAT molecules expressed on the plasma membrane, which is regulated by a dynamic-trafficking mechanism (Zhu and Reith, 2008). This has been consistently reported in a number of studies using cells expressing DAT (Saunders et al., 2000; Chi and Reith, 2003) and rat striatal synaptosomes (Chi and Reith, 2003; Zhu et al., 2005; Zhu et al., 2009a). Changes in DAT dynamics in plasma membranes can be detected using either biotinylation assay (Zhu et al., 2005; Zhu et al., 2009a) or subfractionation method (Middleton et al., 2007). In the current study, a 49% decrease in DAT surface expression (P3) was not comparable to the magnitude (26%) of the decrease in V_{max} for [^{3}H]DA uptake in rat striatal synaptosomes demonstrated in our previous report (Zhu et al., 2009b). This result is also supported by [^{3}H]WIN 35,428 binding experiment showing that the B_{max} was decreased in P3 of Tat-treated samples compared to controls. As reported in our previous studies, levels of the changes in DAT cell surface expression were less than (Zhu et al., 2009a) or similar (Zhu et al., 2005) to the magnitude of the changes in V_{max} for [^{3}H]DA uptake. Trafficking of plasma membrane transporters is associated with changes in posttranslational modifications of the DAT protein, including phosphorylation states and protein-protein interactions (Sager and Torres, 2011). Therefore, the current results infer that Tat-induced great decrease of DAT expression in plasma membranes could be regulated by both phosphorylation (i.e. PKC-dependent mechanism) and protein-protein interactions (e.g. allosteric modulation). In contradiction with our results, 30-min exposure of PC12 cells expressing human DAT to 120 nM Tat_{1-86} increased (24%) DA uptake using measurement of the fluorescence ASP+, which was accompanied by a profound increase (177%) in plasma membranes and a minor decrease (14%) in cytoplasmic membranes compared to respective controls (Perry et al., 2010). The

contrasting results might be due to differences in DAT expression models (rat synaptosomes versus a human DAT cell line), Tat concentration, exposure time and methodology. Tat-induced changes in DAT surface levels could arise from increased PKC-mediated endocytosis, decreased DAT recycling rates, or both. Rat synaptosomes express DAT endogenously and have less surface DAT expression compared to DAT expressed in heterologous cells such as PC12 cells (Johnson et al., 2005; Boudanova et al., 2008). In addition, synaptosomes exhibit fast DAT recycling rates for basal DAT levels in plasma membranes, whereas the PC12 cells overexpressing DAT have slow DAT recycling rates (Johnson et al., 2005; Boudanova et al., 2008). These differences may, at least in part, contribute to the contrasting results between the current study and the previous report (Perry et al., 2010). Nevertheless, the results from Perry et al's study demonstrate that increased membrane DAT may be a compensatory response to decreased transporting efficiency of individual DAT (Perry et al., 2010).

Another important finding from this study is that Tat inhibited not only DAT function and trafficking but also VMAT-2 function. Although both DAT and VMAT-2 proteins are essential for the regulation of DA disposition in the synapse and cytosol, our data show that the inhibitory effects of Tat are more profound in VMAT2 protein than in DAT protein. Moreover, the potency of Tat for inhibiting synaptosomal [^{3}H]DA uptake (IC_{50} = 3.1 μM) (Zhu et al., 2009b) is 15-fold higher than that for inhibiting vesicular [^{3}H]DA uptake (IC_{50} = 0.21 μM). Thus, VMAT-2 protein may play a more critical role in Tat-induced alterations of extracellular DA concentrations. In the current study, the affinity of TBZ, a highly selective compound for VMAT-2 (Erickson et al., 1996) was about 20-fold greater than that of Tat protein. Interestingly, our recent study shows that the influence of Tat on DAT ligand

binding sites involves a protein-protein interaction and that a mutation of Tat (Cys22Gly) significantly attenuates Tat-induced inhibitory effects on DA transport (Zhu et al., 2009b). In addition to influencing DAT function, the current study demonstrates that this mutant of Tat (Cys22Gly) also attenuates Tat-induced decrease in VMAT-2 function. Together, these findings suggest that the residue (Cys22) of Tat may share a favorable inter-molecular interaction between Tat protein and human DAT (or VMAT-2). Furthermore, this result also suggests that Tat protein may cause synergistic effects on impairing DA neurotransmission by inhibition of both DAT and VMAT-2 proteins. At the functional level, plasma membrane DAT translocates substrates through a sodium- and chloride-dependent mechanism (Rudnick and Clark, 1993; Gu et al., 1994), whereas vesicular transporters use the proton electrochemical gradient across the vesicular membrane to transport monoamines (Johnson, 1988). Many DAT inhibitors have an ability to rapidly regulate VMAT-2 localization and function (Fleckenstein et al., 2009). For example, methamphetamine leads to releases of DA from synaptic vesicles into the cytosol via an interaction with the VMAT2 and by disruption of the vesicular proton gradient (Sulzer et al., 1995; Fleckenstein et al., 2007). Subsequently, available cytosolic DA is reversely transported by the DAT into the extracellular space (Sulzer et al., 1995). Co-exposure to Tat and methamphetamine produces synergistic effects on impairing DA terminals (Theodore et al., 2006) and methamphetamine-mediated behavior (Kass et al., 2010). Thus, the current results provide a mechanistic basis to interpret the synergistic effects of Tat and methamphetamine.

HIV-1 associated dementia and neurocognitive disorder progress gradually over months or years. Such long time intervals are not practical or feasible for *in vitro* determination of long-term alteration of DAT function. Hence, we investigated acute effects

of Tat exposure on DAT dynamics. Using this *in vitro* model, we have found that 15-min exposure of synaptosomes to Tat (1 μM) caused a reversible reduction of DA uptake, whereas 60-min Tat exposure greatly inhibited DA uptake that was not reversible (Zhu et al., 2009b). It is possible that reduction of DA uptake and plasma membrane DAT in response to a short-term Tat exposure is a protective mechanism against the build-up of toxic levels of DA, whereas a long-term Tat exposure accelerates DAT degradation. Excessive levels of cytosolic DA and its oxidative products can be toxic to dopaminergic neurons and are postulated to contribute to the development of HIV-associated dementia and neurocognitive disorders (Mosharov et al., 2009). HIV-1 infection causes the hallmark decrease in $CD4^+$ T cells, which results from programmed cell death, apoptosis (McCune, 2001). Tat protein released from infected cells can induce apoptosis in uninfected bystander T cells (Ma and Nath, 1997) or neurons (New et al., 1997) and these cells subsequently become toxic cells and can destroy other bystander cells (Campbell and Loret, 2009). While the present study has provided evidence that *in vitro* exposure of rat synaptosomes to Tat functionally regulates DAT function and trafficking, it also indicates potential roles of Tat in dynamic regulation of DAT *in vivo*. Given that Tat can be absorbed by non-infected neurons, our results infer that Tat-induced decrease in DAT function and cell surface expression in this *in vitro* model may continue to produce long-term impairments of dopaminergic terminals in *in vivo* models. Several studies have reported that continued presence of HIV-1 viral proteins may be not required for Tat-induced long-term process of neurotoxicity. For example, an exposure to Tat for a few minutes was sufficient for sustained releases of cytokines for several hours (Nath et al., 1999); following a single intraventricular injection of Tat in rats, progressive glial activation and macrophage infiltration could maintain for several days,

whereas Tat was undetectable in the brain a few hours after the injection (Jones et al., 1998). Further, an exposure of Tat for only milliseconds is adequate to induce prolonged depolarization in neurons (Magnuson et al., 1995). Therefore, it is possible that a transient exposure to Tat in dopaminergic target proteins, such as DAT, may share a similar "hit and run" phenomenon to initiate a cascade of events, leading to progressive neuropathogenesis, such as HIV-1 associated dementia (Wang et al., 2004).

In conclusion, Tat protein exposure led to changes of DAT and VMAT2 function and expression in rat striatal synaptosomes. The Tat-induced reduction of DAT uptake function is mediated by DAT trafficking- and PKC-dependent mechanisms. These findings may have important implication for preclinical studies of the role of DAT and VMAT-2 in drugs of abuse in HIV-1 infected individuals. Future studies will be necessary to investigate how DAT interacts with VMAT-2 to promote Tat-induced dysfunction of DA neurotransmission and which DAT residues are required for interactions of Tat and DAT.

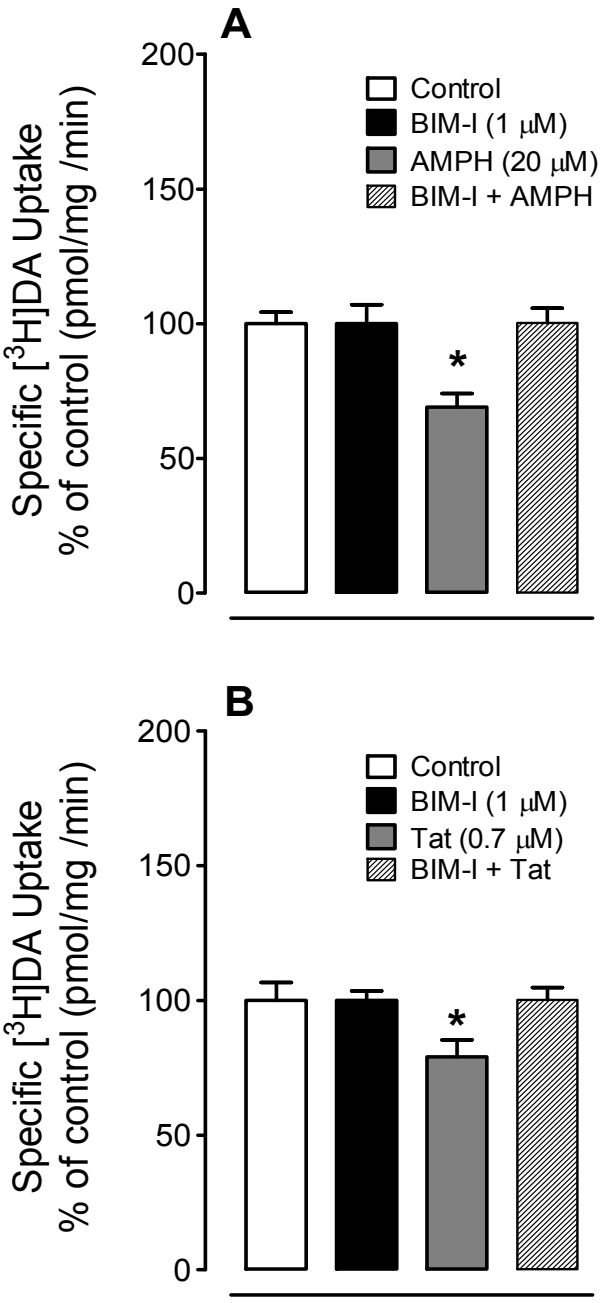

Figure 4.1 PKC inhibition attenuated Tat- and d-amphetamine (AMPH)-induced reduction of [^{3}H]DA uptake in rat striatal synaptosomes. After pre-incubation of synaptosomes with 1 μM BIM-I for 5 min, Tat (0.7 μM, A) or AMPH (20 μM, B) were added for another 15 min and subsequently all reagents were washed off, specific uptake of 5 nM [^{3}H]DA uptake was measured. * $P < 0.05$ versus Tat or AMPH only.

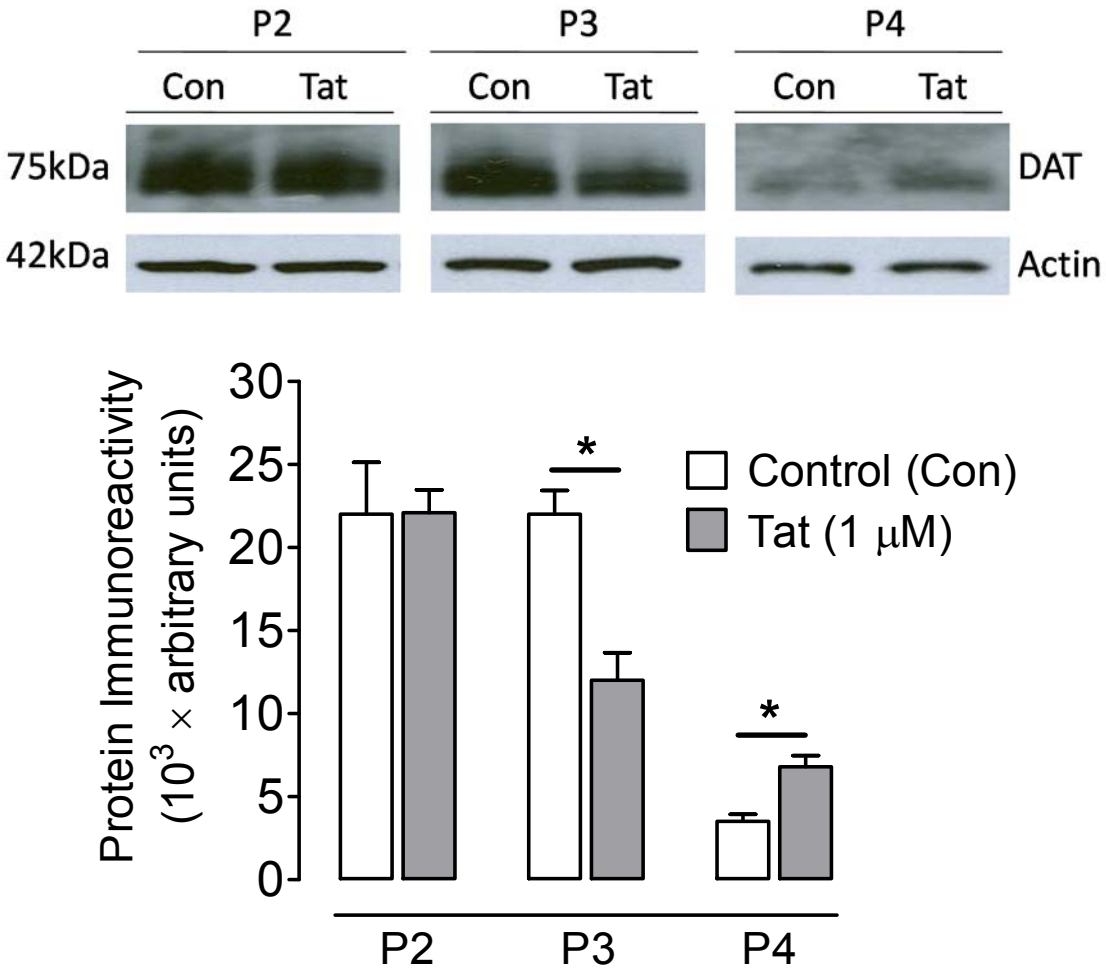

Figure 4.2 Tat protein decreased DAT cell surface expression. Rat striatal synaptosomes were incubated with or without Tat (1 μM). Subsequently, total synaptosomal fractions (P2), plasma membrane enriched fractions (P3), and vesicle-enriched fractions (P4) were prepared for western blot analysis. The same portion of P3 fraction were used in [^{3}H]WIN 35,428 binding assay (see Figure 4.3). The levels of DAT immunoreactivity are increased in P4 and decreased in P3 without changes in P2 in Tat-exposed samples compared to the respective controls. * $P < 0.05$, paired Student's *t*-test.

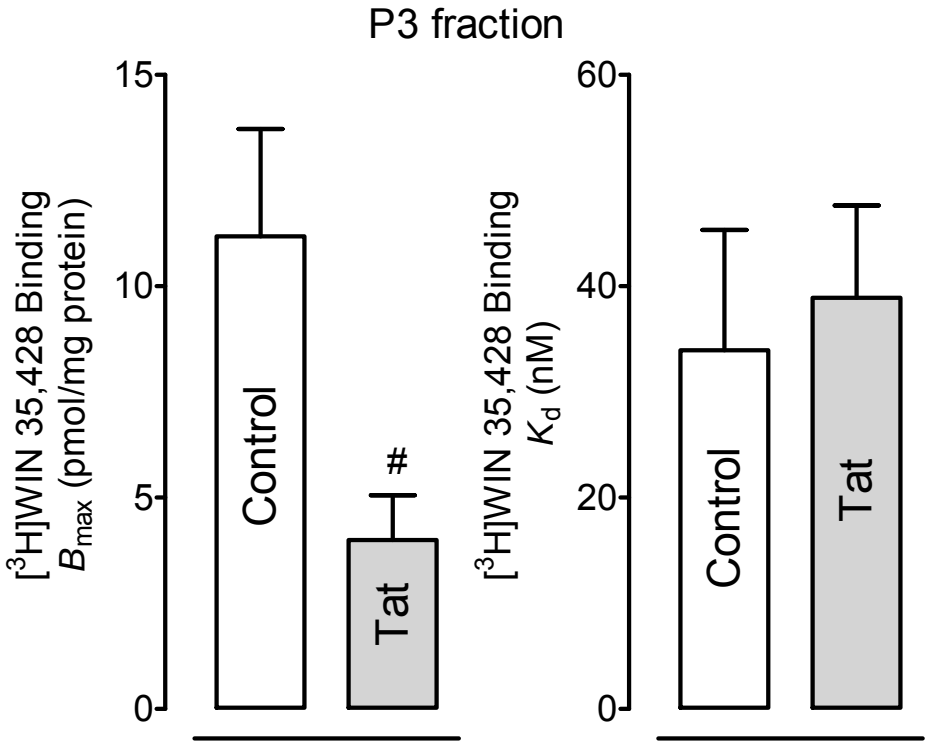

Figure 4.3 Tat protein decreased the specific [^{3}H]WIN35,428 binding in plasma membrane enriched fraction. Rat striatal synaptosomes were incubated with or without Tat (1 μM), and then total synaptosomal fractions (P2), plasma membrane enriched fractions (P3) and vesicle-enriched fractions (P4) were prepared and used for the specific [^{3}H]WIN35,428 binding. * P <0.05, paired Student's t-test.

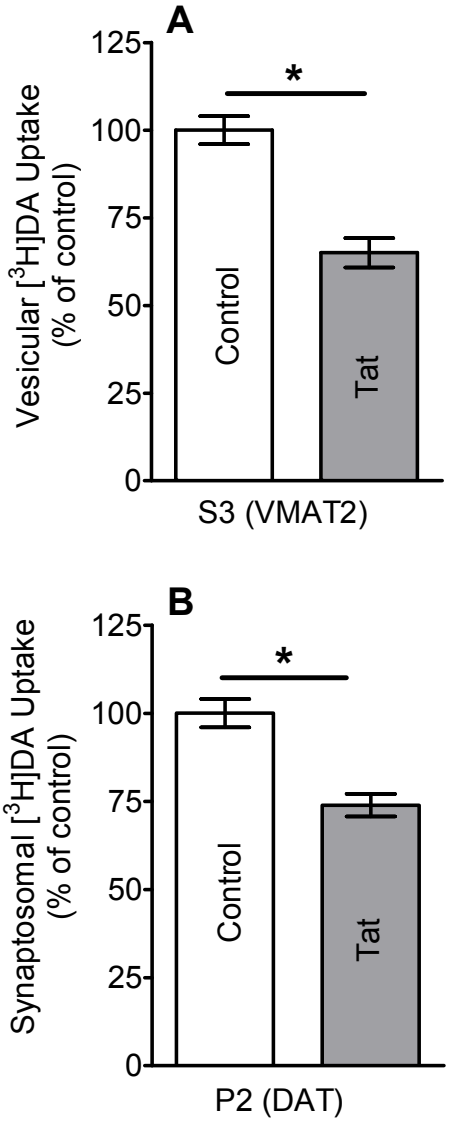

Figure 4.4 Inhibitory effects of Tat on synaptosomal [^{3}H]DA uptake and vesicular [^{3}H]DA uptake in rat striatum. Rat striatal synaptosomes were preincubated with or without Tat (1 μM) for 15 min. Drug was then washed off, and specific synaptosomal and vesicular uptake of 0.1 μM [^{3}H]DA uptake were measured. Tat inhibited the specific [^{3}H]DA uptake into vesicles (A; via VMAT2) and synaptosomes (B; via DAT) by 35% and 26%, respectively, compared to the respective control values (**P* <0.05, paired Student's *t*-test).

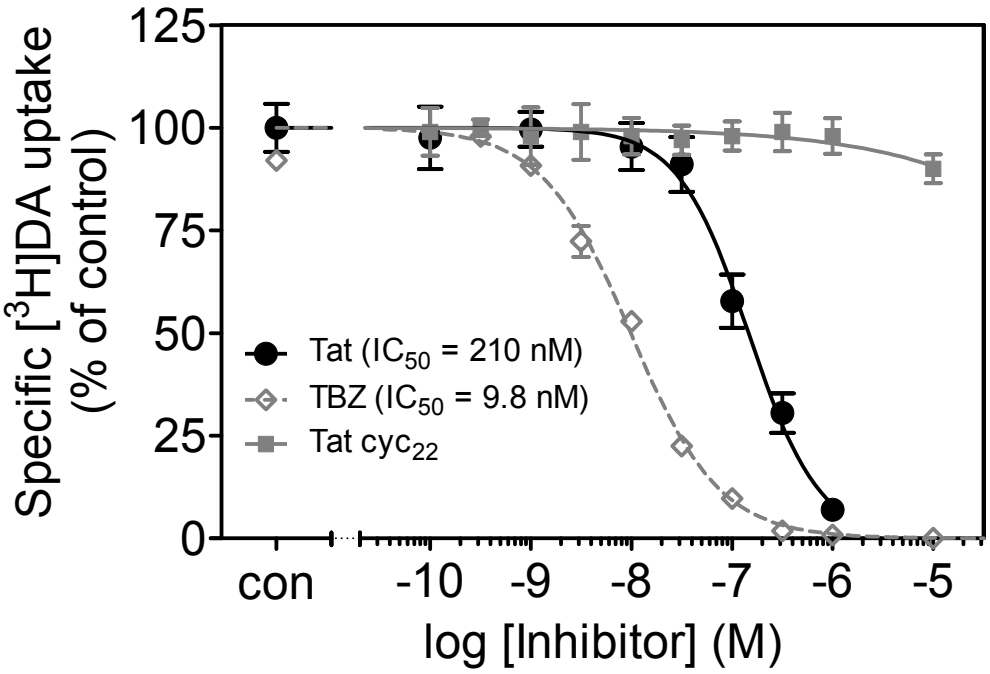

Figure 4.5 Pharmacological profiles of vesicular [^{3}H]DA uptake in rat striatum in the presence of $Tat_{1–86}$, Tat Cys22, or tetrabenazine (TBZ, a VMAT2 inhibitor). Striatal synaptosomes were preincubated with various concentrations of $Tat_{1–86}$, Tat Cys22, or TBZ (0.1 nM–10 μM) at 34°C for 15 min followed by the addition of [^{3}H]DA (final concentration, 0.1 μM) for 8 min. Tat Cys22 and TBZ were used as negative and positive controls, respectively. Data are expressed as mean ± S.E.M. as percentage of control (CON) values (28,205 ± 1965 dpm) from five independent experiments performed in duplicate. Nonspecific [^{3}H]DA uptake was determined in the presence of 10 μM nomifensine. All curves were best fit to a single class of binding site and generated by nonlinear regression.

Copyright Clearance Center RightsLink®

Home Account Info Help

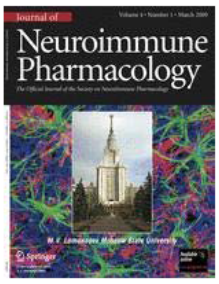

Title: HIV-1 Tat Protein Decreases Dopamine Transporter Cell Surface Expression and Vesicular Monoamine Transporter-2 Function in Rat Striatal Synaptosomes

Author: Narasimha M. Midde

Publication: Journal of NeuroImmune Pharmacology

Publisher: Springer

Date: Jan 1, 2012

Logged in as:
Narasimha Midde
LOGOUT

Order Completed

Thank you very much for your order.

This is a License Agreement between Narasimha M Midde ("You") and Springer ("Springer"). The license consists of your order details, the terms and conditions provided by Springer, and the payment terms and conditions.

Get the printable license.

License Number	3333280363282
License date	Feb 20, 2014
Licensed content publisher	Springer
Licensed content publication	Journal of NeuroImmune Pharmacology
Licensed content title	HIV-1 Tat Protein Decreases Dopamine Transporter Cell Surface Expression and Vesicular Monoamine Transporter-2 Function in Rat Striatal Synaptosomes
Licensed content author	Narasimha M. Midde
Licensed content date	Jan 1, 2012
Volume number	7
Issue number	3
Type of Use	Thesis/Dissertation
Portion	Full text
Number of copies	10
Author of this Springer article	Yes and you are a contributor of the new work
Title of your thesis / dissertation	Effect of HIV-1 Tat protein on structure, function, and trafficking of the dopamine transporter
Expected completion date	May 2014
Estimated size(pages)	250
Total	0.00 USD

CLOSE WINDOW

CHAPTER 5

GENETICALLY EXPRESSED HIV-1 VIRAL PROTEINS ATTENUATE NICOTINE-INDUCED BEHAVIORAL SENSITIZATION AND ALTER MESOCORTICOLIMBIC ERK AND CREB SIGNALING IN RATS[3]

Abstract: The prevalence of tobacco smoking in HIV-1 positive individuals is 3-fold greater than that in the HIV-1 negative population; however, whether HIV-1 viral proteins and nicotine together produce molecular changes in mesolimbic structures that mediate psychomotor behavior has not been studied. This study determined whether HIV-1 viral proteins changed nicotine-induced behavioral sensitization in HIV-1 transgenic (HIV-1Tg) rats. Further, we examined cAMP response element binding protein (CREB) and extracellular regulated kinase (ERK1/2) signaling in the prefrontal cortex (PFC), nucleus accumbens (NAc) and ventral tegmental area (VTA). HIV-1Tg rats exhibited a transient decrease of activity during habituation, but showed attenuated nicotine (0.35 mg/kg, s.c.)-induced behavioral sensitization compared to Fisher 344 (F344) rats. The basal levels of phosphorylated CREB and ERK2 were lower in the PFC of HIV-1Tg rats, but not in the NAc and VTA, relative to the controls. In the nicotine-treated groups, the levels of phosphorylated CREB and ERK2 in the PFC were increased in HIV-1Tg rats, but decreased in F344 animals. Moreover, repeated nicotine administration reduced phosphorylated ERK2 in VTA of HIV-1Tg rats and in the NAc of F344 rats, but had no effect on phosphorylated

[3] Midde NM, Gomez AM, Harrod SB, Zhu J (2011) Genetically expressed HIV-1 viral proteins attenuate nicotine-induced behavioral sensitization and alter mesocorticolimbic ERK and CREB signaling in rats. Pharmacology, Biochemistry, and Behavior 98:587-597. PMCID: PMC3091851

CREB, indicating a region-specific change of intracellular signaling. These results demonstrate that HIV-1 viral proteins produce differences in basal and nicotine-induced alterations in CREB and ERK signaling that may contribute to the alteration in psychomotor sensitization. Thus, HIV-1 positive smokers are possibly more vulnerable to alterations in CREB and ERK signaling and this has implications for motivated behavior, including tobacco smoking, in HIV-1 individuals who self-administer nicotine.

5.1 INTRODUCTION

Tobacco smoking prevalence among HIV-1 positive population is 3-fold greater than that in HIV-1 negative population, according to Centers for Disease Control and Prevention (2007). HIV-1 infected patients are more likely to become dependent on nicotine, and less likely to quit than HIV-1 negative individuals (Hershberger et al., 2004; Fuster et al., 2009; Nahvi and Cooperman, 2009). There is an increasing body of clinical and experimental evidence that tobacco smoking is associated with a more rapid progression to AIDS (Nieman et al., 1993; Crothers et al., 2005; Furber et al., 2007; Zhao et al., 2010) and HIV-1 associated dementia (Burns et al., 1996; Manda et al., 2010). Considering that the HIV-1 positive population exhibits a greater risk for tobacco-associated morbidity and mortality (Palella et al., 2006; Triant et al., 2007), there is a critical need to define the molecular mechanisms underlying the enhanced susceptibility to nicotine dependence in this population.

HIV-1 infection is associated with a variety of neurological impairments that result, in part, from the presence of HIV-1 viral proteins, such as Tat and gp120. Some of the neurological deficits caused by these viral proteins reflect an apparent dysfunction of the mesocorticolimbic dopamine (DA) system (Nath et al., 1987; Berger and Arendt, 2000;

Koutsilieri et al., 2002), the motivation pathway of the brain (Wise and Bozarth, 1987; Everitt and Robbins, 2005; Berridge, 2007). Indeed, long-term viral protein exposure can accelerate damage in this DA system (Del Valle et al., 2000; Ferris et al., 2008; Hudson et al., 2010; Nath, 2010). For example, a significant reduction in DA transporter (DAT) density in striatum was observed in HIV-1 positive patients (Wang et al., 2004; Chang et al., 2008), and *in vitro* Tat and gp120 *in vitro* decreased the specific [^{3}H]DA uptake in rat striatum (Wallace et al., 2006; Zhu et al., 2009). Importantly, the use of addictive drugs by HIV-1 positive individuals results in greater neurological impairments relative to individuals who are infected with HIV-1 but do not abuse drugs (Del Valle et al., 2000; Ferris et al., 2008; Hudson et al., 2010; Nath, 2010). Furthermore, the mesocorticolimbic DA pathway is compromised in HIV-1 positive individuals that exhibit co-morbid drug abuse (Kumar et al., 2009; Norman et al., 2009; Obermann et al., 2009). The extent to which HIV-1 related viral proteins and drugs of abuse alter motivation in humans is not well understood.

Our laboratory uses a rodent model to investigate the neurobehavioral and neurochemical changes induced by the combination of HIV-1 viral proteins and abused drugs. Several approaches are utilized to study these viral proteins because experimental rodents cannot be infected with HIV-1: 1) *in vitro* exposure to Tat (Zhu et al., 2009), 2) direct microinjection of Tat into rat brain (Fitting et al., 2008; Harrod et al., 2008), 3) transgenic mice that express Tat protein (Kim et al., 2003; Duncan et al., 2008), and 4) HIV-1 transgenic (HIV-1Tg) rats, which express HIV-1 viral proteins (Reid et al., 2001). These models mimic different aspects of viral protein-induced neurotoxicity, although none of these models fully represent the spectrum of HIV-1 viral protein insult in humans (Nath, 2010). We are using the HIV-1Tg model in combination with basic behaviors that are

mediated by the mesocorticolimbic system. This pathway organizes motivated behaviors that range various levels of complexity. For example, psychomotor behavior, such as locomotor/exploratory activity, represents the integration of sensory and motor information (Wise and Bozarth, 1987; Berridge, 2007), whereas drug maintained responding is a combination of Pavlovian and operant conditioning processes (Rescorla, 1991; Robinson and Berridge, 2003; Everitt and Robbins, 2005), and is a relatively more complex form of motivated behavior. Insult to this pathway produces significant changes in both types of responding (Kelly and Iversen, 1976; Roberts et al., 1977; Fink and Smith, 1980; Joyce and Koob, 1981; Koob et al., 1981; Kubos et al., 1987; Corrigall et al., 1992).

Nicotine activates nicotinic acetylcholine receptors (nAChRs) located throughout the mesocorticolimbic DA system, specifically in the prefrontal cortex (PFC), nucleus accumbens (NAc) and ventral tegmental area (VTA) (Kita et al., 1992; Panagis and Spyraki, 1996; Mansvelder et al., 2002; Laviolette and van der Kooy, 2004). Nicotine increases DA levels in the NAc (Nisell et al., 1994b, a), and repeated nicotine treatment induces a progressive increase in psychomotor behavior, which represents the initiation of behavioral sensitization (Post, 1980; Clarke and Kumar, 1983b, a; Kalivas, 1995). Accordingly, the locomotor stimulant properties of nicotine are blocked by lesion of mesolimbic DA neurons (Louis and Clarke, 1998) or by nicotinic receptor antagonists (Clarke and Kumar, 1983b; Corrigall et al., 1994). The behavioral sensitization procedure is sensitive to behavioral changes produced by the psychostimulant effects of abused drugs, however, it is not a measure of drug reward (Wise and Bozarth, 1987; Robinson and Berridge, 1993; Berridge and Robinson, 1998). This procedure was used in the present experiment to determine whether HIV-1 Tg rats exhibited deficits in locomotor sensitization to nicotine.

Furthermore, HIV-1 viral proteins alter dopaminergic pathways that medaite behavioral sensitization. For example, intra-accumbal or striatal Tat rats show decreased DAT activity in striatum (Maragos et al., 2002), decreased DA levels (Cass et al., 2003), and attenuated behavioral sensitization to cocaine (Harrod et al., 2008). Moreover, HIV-1Tg rats show enhanced behavioral sensitization to methamphetamine (Liu et al., 2009; Kass et al., 2010). However, whether the combination of nicotine and HIV-1 viral proteins alters psychomotor behavior has not been investigated.

The extracellular regulated protein kinase (ERK) and its downstream transcriptional signaling protein, the cyclic AMP response element-binding protein (CREB), appear critical for long-term adaptations in individuals who exhibit drug abuse (Berhow et al., 1996; Carlezon et al., 1998; Nestler, 2001; Girault et al., 2007). ERK is one of the mitogen-activated protein kinases involved in numerous cellular processes, including long-term neuronal plasticity and survival (Hetman and Gozdz, 2004; Subramaniam and Unsicker, 2010). Abundant evidence suggests that ERK is an essential component of the signaling pathways involved in synaptic plasticity and the long-term effects of drugs of abuse (Berhow et al., 1996; Valjent et al., 2006; Girault et al., 2007; Lu et al., 2009). Two major isoforms of ERK, ERK1 and ERK2, are very similar in sequence (Yoon and Seger, 2006), but have distinct functions (Lloyd, 2006; Lu et al., 2009). It has implicated that ERK2 is more strikingly changed than ERK1 in the long-term effects of drugs of abuse (Valjent et al., 2005; Girault et al., 2007; Iniguez et al., 2010). Moreover, acute nicotine treatment increases CREB phosphorylation in the NAc, striatum and VTA (Walters et al., 2005; Jackson et al., 2009). Chronic nicotine exposure in mice decreases CREB phosphorylation in the NAc, whereas nicotine withdrawal increases CREB phosphorylation in the VTA (Brunzell et al.,

2003). In addition, the levels of CREB and phosphorylated CREB are decreased in the cortex and amygdala after withdrawal from repeated nicotine administration (Pandey et al., 2001). Thus, long-term nicotine exposure leads to neural adaptations in intracellular signaling through the changes of ERK and CREB signaling (Brunzell et al., 2003; Brunzell et al., 2009; Mineur et al., 2009). To date, the effects of HIV-1 viral proteins on ERK and CREB signaling are unknown.

It was hypothesized that the combination of HIV-1 viral proteins and nicotine would alter nicotine-induced behavioral sensitization, and would also produce changes in the expression of intracellular signaling proteins. To test these hypotheses, HIV-1Tg rats and Fischer 344/NHsd (F344) non-transgenic, wild-type control rats were used to determine if genetically expressed HIV-1 viral proteins produce altered nicotine-induced behavioral sensitization. To investigate a potential mechanism, the modulation of ERK and CREB signaling following repeated nicotine exposure was determined in the PFC, NAc and VTA regions of the mesocorticolimbic DA system.

5.2 Materials and Methods

5.2.1 Subjects

Male HIV-1Tg Fisher 344/NHsd rats and age-matched male nontransgenic Fisher 344/NHsd rats were obtained from Harlan Laboratories, Inc. (Indianapolis, IN). The HIV-1Tg rat model carries a *gag-pol*-deleted HIV-1 provirus regulated by the viral promoter expressing seven of the nine HIV-1 viral proteins (Reid et al., 2001). Since the HIV-1Tg rat model is developed from F344 strain, F344 rats were used as the control animals. Rats at age of 7-9 weeks arrived in the animal care facilities and were pair housed throughout the experiment. Rodent food (Pro-Lab Rat, Mouse Hamster Chow #3000) and water were

provided *ad libitum*. The colony was maintained at 21 ± 2 °C, 50 ± 10% relative humidity and a 12L:12D cycle with lights on at 0700 h (EST). The animals were weighed daily. The animals were maintained according to the National Institute of Health (NIH) guidelines in AAALAC accredited facilities. The experimental protocol was approved by the Institutional Animal Care and Use Committee (IACUC) at the University of South Carolina.

5.2.2 DRUGS

Nicotine hydrogen tartrate salt was purchased from Sigma-Aldrich (St. Louis, MO, USA) and dissolved in sterile saline (0.9% sodium chloride). Nicotine was prepared immediately prior to injection. The nicotine solution was neutralized to pH 7.0 with $NaHCO_3$. Nicotine (0.35 mg/kg, freebase) was administered subcutaneously (s.c.) in a volume of 1 ml/kg once daily for 20 days.

5.2.3 LOCOMOTOR ACTIVITY PROCEDURE

5.2.3.1 BEHAVIORAL APPARATUS

The activity monitors were square (40 × 40 cm) locomotor activity chambers (Hamilton-Kinder Inc., Poway, CA) that detect free movement of animals by infrared photocell interruptions. This equipment uses an infrared photocell grid (32 emitter/ detector pairs) to measure locomotor activity. The chambers were converted into round (~ 40 cm in diameter) compartments by adding clear Plexiglas inserts; photocell emitter/detector pairs were tuned by the manufacturer to handle the extra perspex width. Total horizontal activity represents all beam breaks in the horizontal plane. All activity monitors were located in an isolated room.

5.2.3.2 HABITUATION

Rats in the HIV-1Tg-Saline (HIV1Tg-Sal; n = 8/group), HIV-1Tg-Nicotine (HIV-1Tg-Nic; n = 8/group), F344-Saline (F344-Sal; n = 8/group) and the F344-Nicotine (F344-

Nic; n = 8/group) groups were habituated to the locomotor activity chambers for two 60-min sessions, once/day. No injections were administered on the habituation days. Twenty four hours after the second habituation session, all rats were habituated to the chambers for 30 min prior to injection, and then injected (s.c.) with saline and placed into the activity chambers for 60-min to measure baseline activity.

5.2.3.3 PRE-INJECTION HABITUATION AND NICOTINE-INDUCED BEHAVIORAL SENSITIZATION

The behavioral sensitization procedure began 24 hours after the saline baseline measurement. First, all rats received a 30-minute habituation period in the testing chamber prior to nicotine (0.35 mg/kg) or saline injection as previously reported (Addy et al., 2007). This was done so that the onset of nicotine's effects did not overlap with the period that rats showed the most exploratory behavior in the chamber, which was during the first 15 min. Previous research indicates that control rats exhibit asymptotic levels of within-session habituation by 20 to 30 min, according to similar procedures and use of the same automated chambers (Harrod et al., 2008; Harrod and Van Horn, 2009). Rats were administered nicotine or saline subcutaneously every day for a total of 20 days. Locomotor activity was assessed every other day, i.e., on days 1, 3, 5, 7, 9, 11, 13, 15, 17, and 19, for 60 min. On alternate days, nicotine and saline administered in the home cage.

5.2.4 WESTERN BLOT ANALYSIS

Following completion of the behavioral study, brains were removed by rapid decapitation 4 hours after the last injection on day 20. Brains were placed in ice-cold PBS and dissected in a chilled matrix. PFC, NAc and VTA were dissected and immediately sonicated on ice in a homogenization buffer containing 20 mM HEPES, 0.5 mM EDTA, 0.1 mM EGTA, 0.4 M NaCI, 5 mM MgCI2, 20% glycerol, 1 mM PMSF, phosphatase inhibitor

cocktails I (Sigma, P2850) and protease inhibitors (Sigma, P8340). Samples were centrifuged at 12000 g for 15 min. The supernatant was stored at -80°C. Protein concentrations were determined in duplicate using Bio-Rad DC protein detection reagent. Proteins (30, 10 or 15 μg per sample in the PFC, NAc or VTA) were loaded for ERK, phosphorylated ERK (pERK), CREB, phosphorylated CREB (pCREB) and Tyrosine Hydroxylase (TH) immunoreactivity.

Proteins were separated by 10% SDS-polyacrylamide gel electrophoresis (SDS-PAGE) for 90 min at 150 V, and subsequently transferred to Immobilon-P transfer membranes (Cat # IPVH00010, 0.45 μm pore size; Millipore Co., Bedford, MA) in transfer buffer (50 mM Tris, 250 mM glycine, 3.5 mM SDS) using a Mini Trans-Blot Electrophoretic Transfer Cell (Bio-Rad, Hercules, CA) for 110 min at 72 V. Transfer membranes were incubated with blocking buffer (5% dry milk powder in PBS containing 0.5% Tween 20) for 1 h at room temperature followed by incubation with primary antibodies diluted in blocking buffer overnight at 4 ºC. Antisera against ERK½ (V114A, Promega, Madison, WI) and pERK½ (SC-16982R, Santa cruz biotechnology, inc, Santa Cruz, CA) were used at a dilution of 1:2000 and 1:1000, respectively. Anti-CREB (9104, Cell signaling, Danvers, MA) and anti-pCREB (9196, Cell signaling, Danvers, MA) antibodies were used at a dilution of 1:1000 and 1:500, respectively. Anti-TH (2792) was diluted 1:2000 (Cell signaling, Danvers, MA). Blots were washed 5 min × 5 times with wash buffer (PBS containing 0.5% Tween 20) at room temperature, and then incubated for 1 h in affinity-purified, peroxidase-labeled, anti-rabbit IgG (1:10000 for ERK½, 1:5000 for pERK½, 1:20000 for TH, Jackson ImmunoResearch, West Grove, PA) and 1:2000 anti-mouse IgG (7076, Bio-Rad, Hercules, CA) in blocking buffer for 1 h at room temperature. Blots on the

transfer membranes were detected using enhanced chemiluminescence and developed on Hyperfilm (ECL-plus; Amersham Biosciences UK Ltd., Little Chalfont Buckinghamshire UK). After detection and quantification of these proteins, each blot was stripped in 10% of Re-blot plus mild antibody stripping solution (CHEMICON, Temecula, CA) for 20 min at room temperature and reprobed for detection of β-tubulin (sc-9104, Santa cruz biotechnology, inc, Santa Cruz, CA). β-tubulin was used to monitor protein loading among samples. Multiple autoradiographs were obtained using different exposure times, and immunoreactive bands within the linear range of detection were quantified by densitometric scanning using Scion image software (Scion Corp., Frederick, MD).

5.2.5 Data analyses

The data are presented as mean values ± standard error of the mean (S.E.M.). In order to analyze the effects of nicotine exposure on body weight gain, the body weights of the rats were expressed as a percentage of the body weights on the day prior to nicotine injection. The effect of nicotine administration on body weight gain was analyzed with a (2 × 2 × 20) mixed factorial analysis of variance (ANOVA), with genotype (HIV1-Tg or F344) and treatment (nicotine or saline) as the between-subjects factors, and day as the within-subjects factor. A genotype × day × time (2 × 2 × 12) mixed factorial ANOVA was used to analyze data from the 2 habituation days, and a genotype x time (2 × 12) factorial ANOVA was conducted on the saline baseline day. The pre-injection habituation part of the experiment was analyzed using a genotype × treatment × day × time (2 × 2 × 10 × 12) ANOVA. The effect of repeated nicotine injection on total horizontal activity was analyzed using a genotype × treatment × day × time (2 × 2 × 10 × 12) factorial ANOVA, with genotype and treatment as between-subjects factors, and day and time as within-subjects

factors. To determine the effects of repeated nicotine administration on the activity of signaling proteins (ERK, CREB and TH), separate genotype x treatment (2 × 2) factorial ANOVAs were performed on the data from the PFC, NAc, and VTA. Simple effect comparisons were made for post hoc analyses. All statistical analyses were performed using SPSS (standard version 18.0, Chicago, IL) and differences were considered significant at $p < 0.05$.

5.3 RESULTS

5.3.1 EFFECT OF NICOTINE ON BODY WEIGHT

Daily body weights were analyzed using a genotype × treatment × day ANOVA. There were significant main effects of genotype ($F(1,28) = 25.71$; $p < 0.001$) and day ($F(19,532) = 384.28$; $p < 0.001$), indicating that HIV-1Tg rats weighed less than F344 controls, and that all animals gained weight over days. Body weight gain across days was not different between HIV-1Tg rats and F344 rats ($F(19,532) = 1.24$; $p = 0.22$): these groups showed 11 and 12% increase in weight gain from day 1 to day 20, respectively (Figure 5.1).

5.3.2 HABITUATION, PRE-INJECTION HABITUATION, AND NICOTINE-INDUCED LOCOMOTOR ACTIVITY IN HIV-1TG AND F344 RATS

Habituation and Saline Baseline

Animals were habituated to the chambers for two days, 60 min per day. The total horizontal activity that occurred during the two habituation days is shown on Figures 5.2A and 2B. A genotype × day × time ANOVA (2 × 2 × 12) revealed main effects of day ($F(1, 30) = 55.95$, $p < 0.001$) and time ($F(11, 330) = 147.6$, $p < 0.001$), and a significant genotype × day × time interaction ($F(11, 330) = 2.14$, $p < 0.05$). Both genotypes showed the most activity at the beginning of the habituation session, and the activity decreased over the 30-min period, and both groups of rats were at asymptote for the remaining 30 min of the

session. HIV-1Tg rats exhibited less locomotor activity than did F344 rats in the first 30 min of the first habituation session ($p < 0.01$ Bonferroni *t*-test), and this is observed as a downward, and leftward shift in the habituation curve (Figure 5.2B). No significant differences in total horizontal activity during second habituation session were detected (Fig. 5.2B). On the third day, total horizontal activity was recorded for all groups after a saline injection to determine baseline activity prior to the induction of sensitization phase of the experiment. The genotype × time ANOVA revealed a main effect of time ($F(11, 330) = 41.77$, $p < 0.001$), and a genotype × time interaction ($F(11, 330) = 2.41$, $p < 0.05$). No main effect of genotype was found. In general, both genotypes showed lower activity during the first 5 min of the saline baseline day, acquired asymptotic levels of activity more quickly, and showed a lower asymptote compared to that of the habituation sessions (Fig. 5.2C). Within the first 30 min period, the F344 habituation curve crosses and slightly goes below that of the HIV-1Tg curve. The habituation curve crosses again at minute 30, and this was observed again at the end of the session within the last 30 min (data not shown). None of the comparisons indicated differences between the HIV-1Tg and F344 rats (all $p > .05$).

Pre-injection habituation

Animals were placed into locomotor chambers for 30 min prior to the activity measurement to produce within-session habituation of activity prior to nicotine or saline injection. Total horizontal activity during the 30 min habituation period across the 19-day treatment was recorded and is shown in Figure 5.3A. A mixed-factor genotype × treatment × day × time ANOVA (2 × 2 × 10 × 12) revealed main effects of treatment ($F(1, 28) = 4.76$, $p < 0.05$), day ($F(9, 252) = 9.15$, $p < 0.05$), time ($F(5, 140) = 705.56$, $p < 0.05$) and a significant day × treatment interaction ($F(9, 252) = 2.74$, $p < 0.01$). There was no main

effect of genotype and there were no significant interactions containing this factor. The treatment × day interaction indicates that, regardless of genotype, animals treated with nicotine show increased activity during the pre-injection habituation measures as the number of habituation/injection days increased. To test this, activity from the first and last pre-injection habituation days were compared using a within-subjects comparison of the saline (HIV-1Tg Sal and F344 Sal) and nicotine (HIV-1Tg Nic and F344 Nic) treated groups. The saline treated rats showed activity counts of 652.6 (± 39.3) and 586.4 (± 20.3) on days 1 and 19, respectively; no change in pre-injection habituation activity was observed ($F(1, 15) = 2.6$, $p > 0.05$). The nicotine treated animals exhibited 640.3 (± 29.9) and 764.6 (± 35.5) activity counts on days 1 and 19, respectively, and this increase in locomotor activity during pre-injection habituation sessions was significant ($F(1, 15) = 25.0$, $p < 0.001$). These data indicate that animals injected with nicotine, but not saline, exhibit a significant increase in activity during the pre-injection observation.

Nicotine-induced behavioral sensitization

To determine the effect of HIV-1 viral proteins on nicotine-mediated locomotor sensitization, we measured horizontal activity following administration of nicotine (0.35 mg/kg, s.c.) or saline in HIV-1Tg and F344 rats (Fig. 5.3B). A genotype × treatment × day × time ANOVA revealed significant main effects of genotype ($F(1, 27) = 4.37$, $p < 0.05$), treatment ($F(1, 27) = 965.71$, $p < 0.001$), day ($F(9, 243) = 23.52$, $p < 0.001$) and time ($F(11, 297) = 536.04$, $p < 0.001$). A significant treatment × day interaction ($F(9, 243) = 37.40$, $p < 0.05$) was found, indicating that repeated nicotine injection produced behavioral sensitization. Rats treated with saline exhibited decreased activity across treatment days, from a mean (±S.E.M.) of 357 (±27) activity counts on day 1, to 245 (±32) on day 19.

Nicotine treated rats exhibited 763 (±28) activity counts on day 1, but showed increased locomotor counts of 1287 (±33) on day 19. The genotype × treatment ($F(1, 27) = 4.40$, $p < 0.05$) and genotype × day ($F(9, 243) = 2.76$, $p < 0.05$) interactions indicate that genotype significantly interacted with the effects of repeated nicotine administration. The pattern of nicotine-induced sensitization was similar for the HIV-1Tg and F344 rats following the first ten nicotine injections; however, the nicotine-induced behavioral sensitization was attenuated in HIV-1Tg rats compared to F344 rats during treatment days 11-19. The HIV-1Tg rats showed decreased nicotine-induced activity on four of the remaining five nicotine behavioral assessments, thus suggesting that transgenic animals do not acquire the same magnitude of nicotine-induced behavioral sensitization.

A genotype × treatment × day ANOVA was conducted on the first and final injection days to determine if HIV-1Tg rats exhibited attenuated nicotine-induced behavioral sensitization (Figures. 5.4A and 4B). There were significant main effects of genotype ($F(1,28) = 6.27$; $p < 0.05$), treatment ($F(1,28) = 192.05$; $p < 0.001$) and day ($F(1,28) = 14.97$; $p < 0.01$). A significant genotype × day interaction ($F(1,28) = 5.29$; $p < 0.05$) and a significant treatment × day interaction ($F(1,28) = 40.96$; $p < 0.001$) were found. On day 1, the HIV-1Tg and F344 rats in nicotine-treated groups exhibited more activity than their saline controls ($p < 0.001$; $p < 0.001$, Bonferroni *t*-test, respectively). No differences between the HIV-1Tg-Nic and F344-Nic groups were observed ($p > 0.05$). Similarly, there were no differences between HIV-1Tg-Sal and F344-Sal groups on day 1 ($p > 0.05$). On day 19, HIV-1Tg and F344 rats injected with nicotine displayed greater activity compared to their saline controls ($p < 0.001$), however, both groups showed enhanced activity following repeated nicotine injection relative to day 1 ($F(1,6) = 136.5$; $p < 0.001$), and day 19 ($F(1,7) =$

98.8; $p < 0.001$, respectively). The HIV-1Tg-Nic group, however, exhibited less locomotor activity relative to the F344-Nic group ($p < 0.01$), suggesting that the HIV-1Tg rats exhibited attenuated psychomotor sensitization relative to the F344 rats.

The time course data from Day 1 and Day 19 are illustrated in Figures 5.4C and 4D. Figure 5.4C shows that rats treated with nicotine and saline had the same amount of activity in the first five min of the session, and that nicotine injected rats showed more activity than did the rats administered saline. Figure 5.4D, which represents day 19, clearly shows that animals treated with nicotine exhibited higher activity counts in the first 5 min relative to the saline groups, and although both groups showed within-session habitua-tion, animals in the nicotine conditions exhibited higher activity counts throughout the remainder of the hour. Furthermore, HIV-1Tg rats treated with nicotine showed less activity than the F344 rats treated with nicotine throughout the remainder of the hour measurement.

5.3.3 Levels and activity of ERK and CREB signaling proteins in HIV-1Tg and F344 rats

To determine whether the nicotine-induced behavioral change is associated with mesocorticolimbic DA signaling, we examined the effects of repeated nicotine administration on the levels and the phosphorylation state of CREB and ERK in the PFC, NAc and VTA from the HIV-1Tg and F344 rats used in the behavioral experiment.

Prefrontal Cortex (PFC)

Separate two-way ANOVAs were performed to determine the effect of nicotine on the levels and phosphorylation state of the signaling proteins. As shown in Figure 5.5, no significant differences in total CREB, ERK1, ERK2 and TH were found in the PFC among the groups. With respect to the ratio of pCREB /β-tubulin, a main effect of genotype ($F(1, 27) = 4.34$, $p < 0.05$) and a significant genotype × treatment interaction ($F(1, 27) = 9.47$, $p <$

0.05) were found. Post hoc analysis revealed that the ratio of pCREB /β-tubulin was lower in the HIV-1Tg rats than that in the F344 rats in saline-control groups ($F(1, 13) = 5.64$, $p < 0.05$). The level of pCREB was greater in the nicotine-treated HIV-1Tg group than that in the saline-treated HIV-1Tg group ($F(1, 13) = 4.69$, $p < 0.05$). In contrast, pCREB levels were decreased in the nicotine-treated F344 group compared to the saline-treated F344 group ($F(1, 13) = 4.31$, $p < 0.05$).

With respect to the ratio of pERK2/β-tubulin in the PFC, a main effect of genotype ($F(1, 27) = 4.32$, $p < 0.05$) and a significant genotype × treatment interaction were found ($F(1, 27) = 8.81$, $p < 0.05$). Post hoc analysis revealed that the ratio of pERK2/β-tubulin in the PFC was lower in HIV-1Tg rats than that in F344 rats in saline-treated group ($F(1, 13) = 13.2$, $p < 0.05$). Nicotine increased the ratio in HIV-1Tg rats compared to the saline-treated group ($F(1, 13) = 6.64$, $p < 0.05$). There was a trend toward a decrease in the ratio of pERK2/β-tubulin in F344 rats after repeated nicotine injection ($F(1,13) = 3.31$; $p = 0.07$). The ratio of pERK2/β-tubulin was greater in HIV-1Tg-Nic group than that in F344-Nic group ($p < 0.05$).

Nucleus Accumbens (NAc)

There were no changes in total and phosphorylated CREB, in total ERK and pERK1, or in the levels of TH observed in NAc of HIV-1Tg and F344 rats following nicotine or saline injection. With respect to ratio of pERK2/β-tubulin, the two-way ANOVA revealed a significant main effect of treatment ($F(1, 27) = 5.31$, $p < 0.05$), but neither the main effect of genotype nor the genotype × treatment interaction was significant (Fig. 5.6). Repeated nicotine administration decreased the ratio of pERK2/β-tubulin in F344 rats ($F(1, 14) = 7.05$, $p < 0.05$), but not in the HIV-1Tg rats ($F(1.14) = 0.51$, $p > 0.05$).

Ventral Tegmental Area (VTA)

There was no change in total and phosphorylated ERK and CREB, or in the levels of TH observed in the VTA following nicotine administration. Regarding the ratio of pERK2/β-tubulin, two-way ANOVA revealed a significant main effect of treatment ($F(1, 27) = 4.45$, $p < 0.05$), but neither the main effect of genotype nor the genotype × treatment interaction was not significant (Fig. 5.7). Repeated nicotine administration produced a decreased ratio of pERK2/β-tubulin in HIV-1Tg rats ($F(1, 14) = 6.74$, $p < 0.05$), but not in the F344 rats ($F(1.14) = 0.34$, $p > 0.05$).

5.4 DISCUSSION

The present findings demonstrate that genetically expressed HIV-1 viral proteins alter the sensitivity of the locomotor effects of repeated nicotine administration. HIV-1Tg rats exhibited diminished locomotor activity during habituation to a novel context and showed an attenuation of nicotine-induced behavioral sensitization. Importantly, the basal levels of pCREB and pERK2 in the PFC were lower in the HIV-1Tg saline group compared to F344 saline controls. Following repeated nicotine administration, the levels of pCREB and pERK2 in PFC were decreased in F344 rats, but increased in HIV-1Tg rats, suggesting opposite effects of nicotine on these phosphorylated signaling proteins. In addition, repeated nicotine administration decreased pERK2 levels in the NAc of F344 rats and this effect was also observed in the VTA of HIV-1Tg rats. Thus, HIV-1 viral protein-induced alterations in the CREB and ERK signaling pathway in the mesocorticolimbic DA system appear to have played a role in the locomotor effects of repeated nicotine in HIV-1Tg rats.

Regarding the behavioral portion of the experiment, we observed that HIV-1Tg rats exhibited alterations in locomotor activity during both the habituation and behavioral

sensitization phases of the experiment. First, the transgenic rats showed less activity during day 1 of habituation compared to F344 rats, indicating that the novelty of the initial context exposure produced less activity in the transgenics relative to control rats. This difference in habituation between the HIV-1Tg and F344 rats was transient, as the transgenic rats did not continue to exhibit the blunted locomotor response, relative to F344 controls, on either day 2 of habituation or on the saline baseline measure. A recent study reported HIV-1Tg rats exhibited less rearing and head movement activity compared to F344 rats following repeated saline injections (Liu et al., 2009), but these differences did not reach significance in another report (Kass et al., 2010). The lower baseline activity exhibited by HIV-1Tg rats in the present study and reported by Liu et al. (2009) appear to be the result of manipulation of dopaminergic system by genetically expressed viral proteins (Fink and Smith, 1980). Indeed, HIV-1Tg rats exhibited increased expression of D1 receptors in the PFC (Liu et al., 2009) and a decrease in DAT mRNA (Webb et al., 2010). These studies are consistent with clinical studies showing a significant reduction of DAT density in the putamen and ventral striatum in HIV-1 infected patients (Wang et al., 2004; Chang et al., 2008). In addition, D1 expression has been reported to be negatively correlated with baseline locomotor activity observed in D1 receptor-deficient mice (El-Ghundi et al., 2010). Thus, our behavioral data indicate that the attenuated habituation curve in HIV-1Tg rats is related to neural adaptations produced by HIV-1 viral proteins, and that this transient effect represents an attenuation of activity in response to the novelty of the locomotor activity chambers.

The induction of nicotine-induced behavioral sensitization was altered in transgenic rats as well. In this study, enhanced locomotor activity was observed in both genotypes across days following repeated nicotine administration. Although no difference in acute

nicotine-induced activity between the two genotypes was observed on day 1, the HIV-1Tg group displayed reduced nicotine-induced locomotor activity during the later days, i.e., 13-19, relative to the nicotine-treated F344 group. Thus, although transgenic rats showed a blunted response to repeated nicotine exposure during the induction of sensitization, those animals did not exhibit a deficit in developing behavioral sensitization. Rather, HIV-1Tg rats exhibited less sensitivity to the repeated effects of nicotine, and this deficit may contribute to an alteration in nAChR-mediated dopamine neurotransmission. In accord with these behavioral data, we recently found that HIV-1Tg rats had lower IC_{50} values for [^{3}H]nicotine binding with 5-fold rightward shift of the nicotine concentration curve, compared to F344 controls (unpublished data). Similarly, previous research showed that intra-accumbal Tat infusion attenuated cocaine-induced behavioral sensitization in rats (Harrod et al., 2008), suggesting that the viral protein Tat is involved in the altered behavioral response to psychostimulant drugs. Together, the results indicate that the HIV-1Tg rats are a pertinent model to investigate how chronic exposure to viral proteins and nicotine alter dopaminergic pathways that mediate motivated behavior.

Notably, although behavioral sensitization is a sensitive measure for the influence of psychostimulants on the mesocorticolimbic system (Berridge, 2007), it does not measure drug reward. Thus, predictions regarding cigarette smoking in HIV-1 positive individuals are limited. Given that two behavioral models of viral protein exposure produced diminished psychostimulant-induced behavioral sensitization (Harrod et al., 2008), it is suggested that cigarette smoking by HIV-1 positive individuals will produce alterations in motivated behavior due to the interplay of nicotine exposure and HIV viral proteins within the mesocorticolimbic DA system.

Previous research suggests the possibility that the sensitization of one type of behavior, like rearing, could result in the decrease of another behavior, such as horizontal activity (Iwamoto, 1984; Jerome and Sanberg, 1987; Ksir, 1994; Reid et al., 1998). That the attenuation of total horizontal activity exhibited by the HIV-1Tg rats was diminished in response to the emergence of a competing behavior like rearing or stereotypy, however, is not likely. First, our automated activity chambers measure rearing as all beam breaks in the vertical plane. In the present experiment, there were no effects or interactions with the factor of genotype so the data are not shown; however, animals progressively exhibited sensitization and both genotypes showed asymptotic levels by day 7. Thus, rearing did not emerge on days 11-19, which corresponds to the treatment days that transgenic rats exhibited less nicotine-induced total horizontal activity. Although nicotine-induced sensitization of stereotypy has been reported (Reid et al., 1998), it is not a consistent finding (Jerome and Sanberg, 1987; Ksir, 1994; Harrod et al., 2004; Harrod et al., 2008). We did not use observational procedures in the present experiment, so the levels of nicotine-induced stereotypy were not determined. Our previous studies, which used a combination of automated and observational procedures, show that repeated nicotine or cocaine injection induced sensitization of horizontal activity and rearing incidence, but not of stereotypy (Harrod et al., 2004; Harrod et al., 2008). It is unlikely that the attenuation of total horizontal activity observed for the HIV-1Tg rats is attributable to an emergence of stereotypic behavior.

The present results show that animals injected with nicotine, regardless of genotype, exhibited increased locomotor activity during pre-injection habituation, which was particularly evident on days 13-15. Rats in the saline control groups showed steady activity

across the 19 day period. The increase in activity in the nicotine treated groups likely represents drug-induced conditioned hyperactivity, which is well documented to be mediated by Pavlovian conditioning processes (Anagnostaras and Robinson, 1996; Bevins and Palmatier, 2003). Repeated psychostimulant injection within the same context allows for contextual cues to function as a conditional stimulus, and the drug effect, e.g., hyperactivity, to act as an unconditional stimulus (Anagnostaras and Robinson, 1996). In the present experiment, repeated context-nicotine pairings support the standard associative model described above, and exposure to the chamber prior to daily drug injection represents presentation of the conditional stimulus, or the context alone, without the influence of the unconditional stimulus. Our results indicate that after being placed in the context, hyperactivity, which is similar to the unconditional stimulus effects of repeated nicotine, was observed and there were no effects of genotype on this effect.

The second part of the experiment determined levels of transcriptional factors throughout the mesocorticolimbic DA system in nicotine sensitized HIV-1 rats relative to F344 controls. First, HIV-1Tg-saline rats exhibited lower basal levels of pCREB and pERK2 in the PFC, but not in the VTA or NAc, compared to F344-saline controls. These findings suggest that viral proteins produced a neurobiological adaptation in ERK and CREB signaling in the PFC. The observed changes in signaling have implications for the functionality of the mesocorticolimbic DA system. For example, neuronal firing elicits ERK activity in the brain of rats (Davis et al., 2000; Thiels et al., 2002; Ying et al., 2002), whereas blocking ERK activity decreases the firing rate of DA neurons (Iniguez et al., 2010). Increased tonic release of DA enhances ERK activity, which is attenuated in DA D1 receptor mutant mice (Chen and Xu, 2010). Further, deletion of DA D1 receptors in mice produces

higher pCREB levels in the striatum (El-Ghundi et al., 2010), suggesting that CREB phosphorylation is stimulated by DA D1 receptor activation. ERK activation is coupled to activation of CREB (Nakayama et al., 2001; Ying et al., 2002) and, in turn, supports adaptive processes such as long-term potentiation and psychostimulant-induced sensitization (Ying et al., 2002; DiRocco et al., 2009). It has been reported that Tat, gp120 and other viral proteins have higher expression in the PFC compared to other brain regions of HIV-1Tg rats (Peng et al., 2010). Thus, the lower basal levels of pERK2 and pCREB could contribute to the differences in DA D1 receptor expression that was previously reported between HIV-1Tg rats and the F344 controls (Liu et al., 2009). Moreover, although the regional high expression of these viral proteins may contribute to the PFC-specific changes of pERK2 and pCREB, it is also possible that these signaling proteins in PFC are more sensitive to HIV-1 viral protein insult. Together, the molecular data show that the basal levels of particular transcriptional factors, which are implicated in the regulation of mesocorticolimbic function, are altered in HIV-1Tg animals.

Repeated nicotine administration significantly decreased pCREB in the PFC of F344-nicoitne rats compared to F344-saline group. Although delivering chronic nicotine through drinking water increased the ratio of pCREB/CREB in the PFC in C57BI/6J mice (Brunzell et al., 2003), another report showed that the levels of CREB and pCREB were decreased in the cortex of rats 18 h after withdrawal from repeated administration of 2 mg/kg of nicotine (Pandey et al., 2001). Thus, nicotine-mediated regulation of CREB activity is largely dependent on the species, dosage, route of administration, and the time needed to harvest brains (Pandey et al., 2001; Brunzell et al., 2003). The current results show that repeated nicotine increased pCREB in cortical tissue of HIV-1Tg rats, with no change in

CREB. This finding is interesting for two reasons. First, F344 rats exhibited decreased pCREB following repeated nicotine administration, and second, the nicotine-induced increase in pCREB occurred despite lower basal levels of this transcription factor in HIV-1Tg rats relative to F344 controls. This suggests that the processes that mediate the lower basal levels of pCREB in the transgenic rats do not prevent repeated nicotine from regulating CREB signaling. Rather, the current results suggest that nicotine and HIV-1 viral proteins act synergistically to alter CREB signaling in the PFC. Decreased CREB activity is associated with an increase in drug reward and food preference (Carlezon et al., 1998). In general, this suggests that an aberrant decrease in CREB activity, as is shown in the present experiment, may negatively impact normal function of the mesocorticolimbic DA system. Determining if PFC CREB activity is also implicated in the reduced rate of nicotine-induced reward in HIV-1Tg rats is of future interest.

Regarding the ERK experiments, we observed significant alterations in pERK2 levels in the PFC, NAc, and VTA with no change in ERK1, ERK2, or pERK1 in either HIV-1Tg or F344 rats. Notably, the overall levels of pERK2 in the PFC were similar to those changes observed with pCREB in the PFC. Basal levels of pERK2 from the HIV-1Tg-Saline rats were lower than that of the F344-Saline rats, which indicates that the presence of viral proteins reduces pERK2 in the PFC. Following repeated nicotine injection, F344 animals exhibited a trend for decreased pERK2 relative to F344-Saline rats, whereas HIV-1Tg showed increased pERK2 relative to their saline controls. Regarding the VTA, basal pERK2 levels did not differ by genotype in the saline control group, but repeated nicotine decreased this transcriptional factor in HIV-1Tg rats relative to the saline controls. In the NAc, however, there were no differences between levels of pERK2 in the HIV-1Tg-Nic and HIV-

1Tg-Saline rats, but the nicotine sensitized F344 rats exhibited decreased pERK2 relative to controls. This is consistent with the diminished pCREB levels observed in the PFC of HIV-1Tg rats, and this result indicates that viral proteins manipulate ERK signaling in a region specific manner.

Our results suggest that viral protein-induced changes in ERK phosphorylation may exacerbate the plasticity related to the magnitude of the attenuated nicotine-induced sensitization observed in the behavioral part of our experiment. This conclusion is supported by recent reports (Valjent et al., 2005; Valjent et al., 2006; Girault et al., 2007; Iniguez et al., 2010). For example, blocking ERK1/2 activity by SL327, a selective inhibitor of mitogen-activated protein kinase, prevented the induction of locomotion sensitization by repeated injection of cocaine or amphetamine (Valjent et al., 2005; Valjent et al., 2006). Further, discrete manipulation of ERK2 within the VTA, using viral-mediated dominant negative mutant of ERK2, blunted the expression of cocaine-induced behavioral sensitization (Iniguez et al., 2010). The current findings suggest that low levels of prefrontal pERK2 may contribute to the blunted nicotine-induced locomotor activity observed in transgenic rats. Thus, the present study provides evidence that HIV-1 viral proteins impair ERK signaling, thereby contributing to the long-term behavioral changes induced by repeated nicotine. Additional research is needed to elucidate the role of HIV-1 viral proteins on ERK and CREB signaling in the PFC on nicotine reward. As mentioned above, whether the combined effects of nicotine and HIV-1 viral proteins alter the rewarding effects of nicotine cannot be inferred from the present experiment. Nonetheless, these findings further indicate that HIV-1 positive individuals who smoke cigarettes may experience a synergistic effect of viral proteins and nicotine on transcriptional factors that regulate mesocorticolimbic function.

The current study found no differences in basal TH levels regardless of region or genotype, which is consistent with the findings of a recent report showing no change in protein levels of TH in the striatum of naive HIV-1Tg rats (Webb et al., 2010). Notably, regardless of the nicotine-induced changes in pCREB and pERK in the PFC, repeated nicotine injection did not alter the level of TH in any region. This is in contrast to the findings of Brunzell et al. who reported that chronic nicotine exposure in drinking water increased TH levels in the PFC in mice 1.5 h after the last nicotine injection; an increase that returned to normal levels 24 h after withdrawal (Brunzell et al., 2003). The discrepant findings between the current and previous experiments may be related to differences in species and in the route of nicotine administration. However, a recent report showed that *in vitro* exposure to nicotine only increased TH mRNA levels of mouse midbrain slices within 1 hour, but did not change TH protein for different periods of time up to 48 hours (Radcliffe et al., 2009). Hence, it is possible that nicotine stimulation transiently changes transcriptional TH levels, without changing the protein levels of TH.

In conclusion, the current results suggest that genetically expressed HIV-1 viral proteins in rats diminish basal expression levels of pERK2 and pCREB in the PFC, which may explain, at least in part, the low baseline locomotor activity of HIV-1Tg rats. The opposite effects of nicotine on pERK2 and pCREB in the PFC between HIV-1Tg rats and F344 rats may play a role in the blunted locomotor response to repeated administration of nicotine noted in HIV-1Tg rats. Determining how HIV-1 viral proteins and nicotine influence ERK and CREB signaling in the mesocorticolimbic system will be important to understand why HIV-1 positive individuals exhibit increased vulnerability for nicotine addiction.

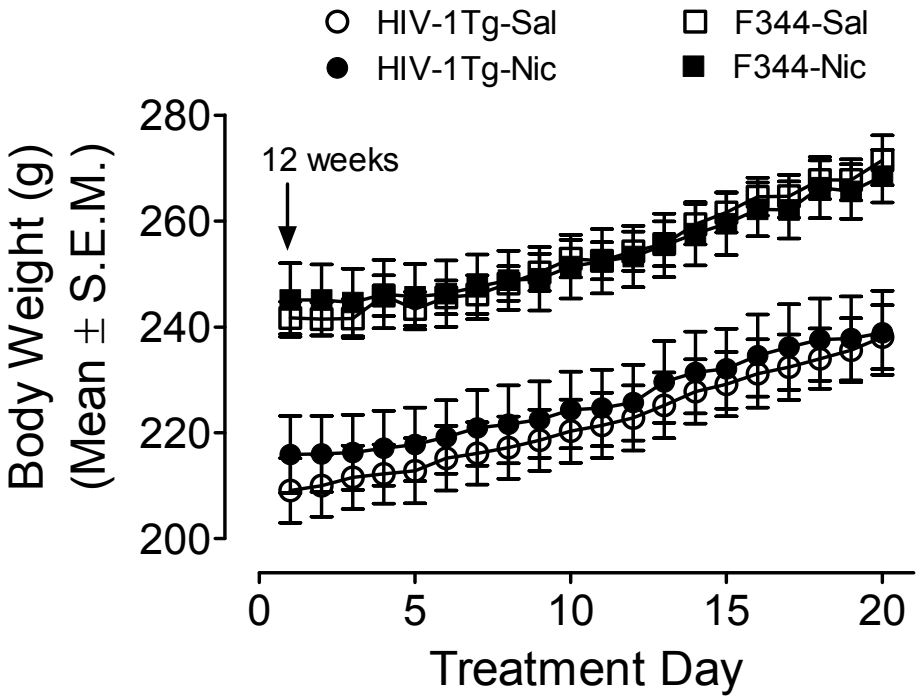

Figure 5.1 Body weights of HIV-1Tg and F344 rats during the nicotine or saline treatment period. Beginning at 12 weeks of age, rats were injected subcutaneously with nicotine or saline prior to locomotor measurement. Data are presented as the mean ± S.E.M. *n*=8 rats per group.

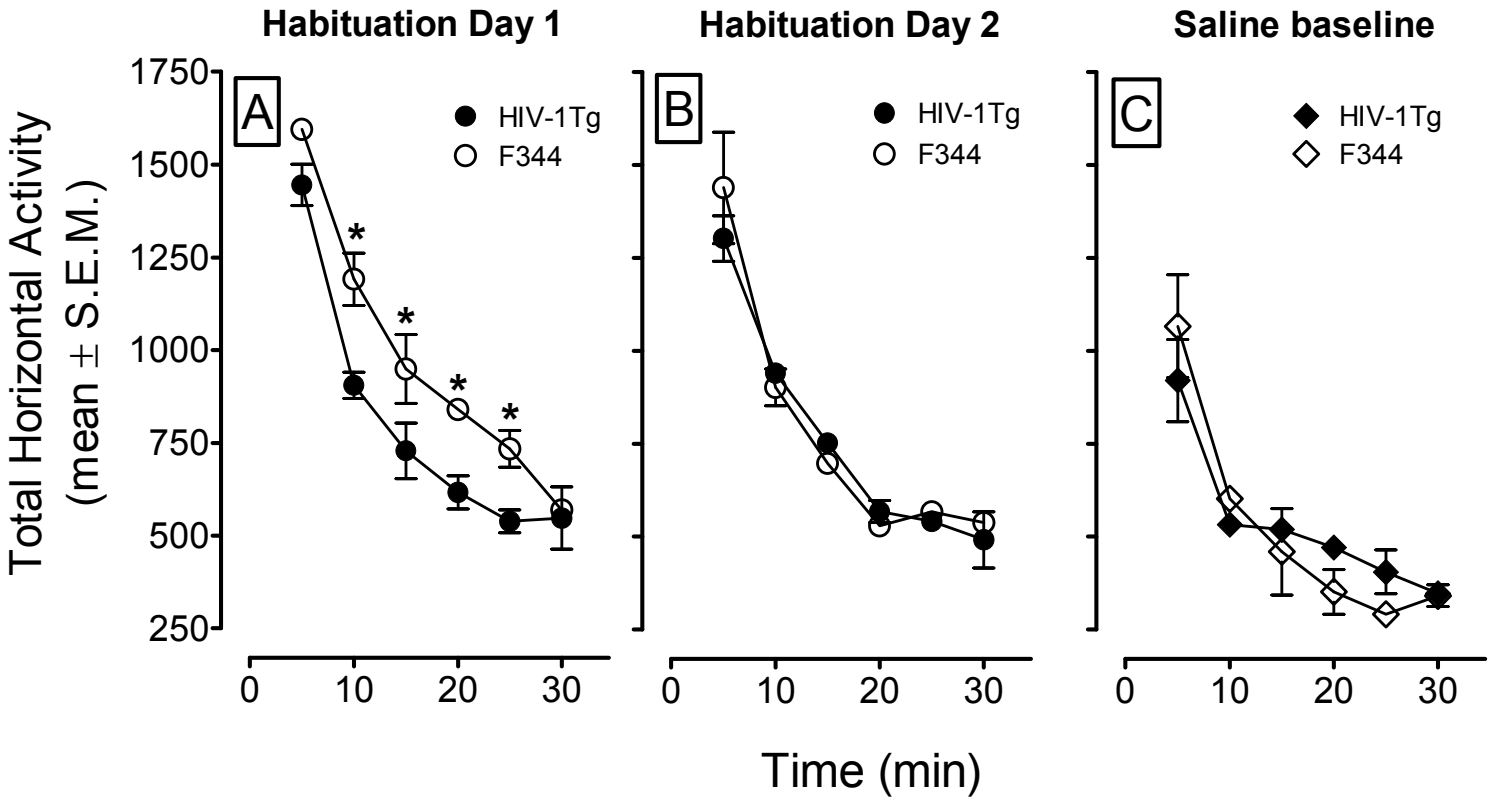

Figure 5.2 The time-course data during the habituation and the saline baseline sessions. **Panels A and B** show the total horizontal activity (mean ± S.E.M.) during the first 30 min of the habituation period. **Panel C** shows the total horizontal activity (mean ± S.E.M.) across the first 30 min of the session following saline injection. * $p < 0.05$, difference between HIV-1Tg and F344 rats at the corresponding time interval. *n*=8 rats per group.

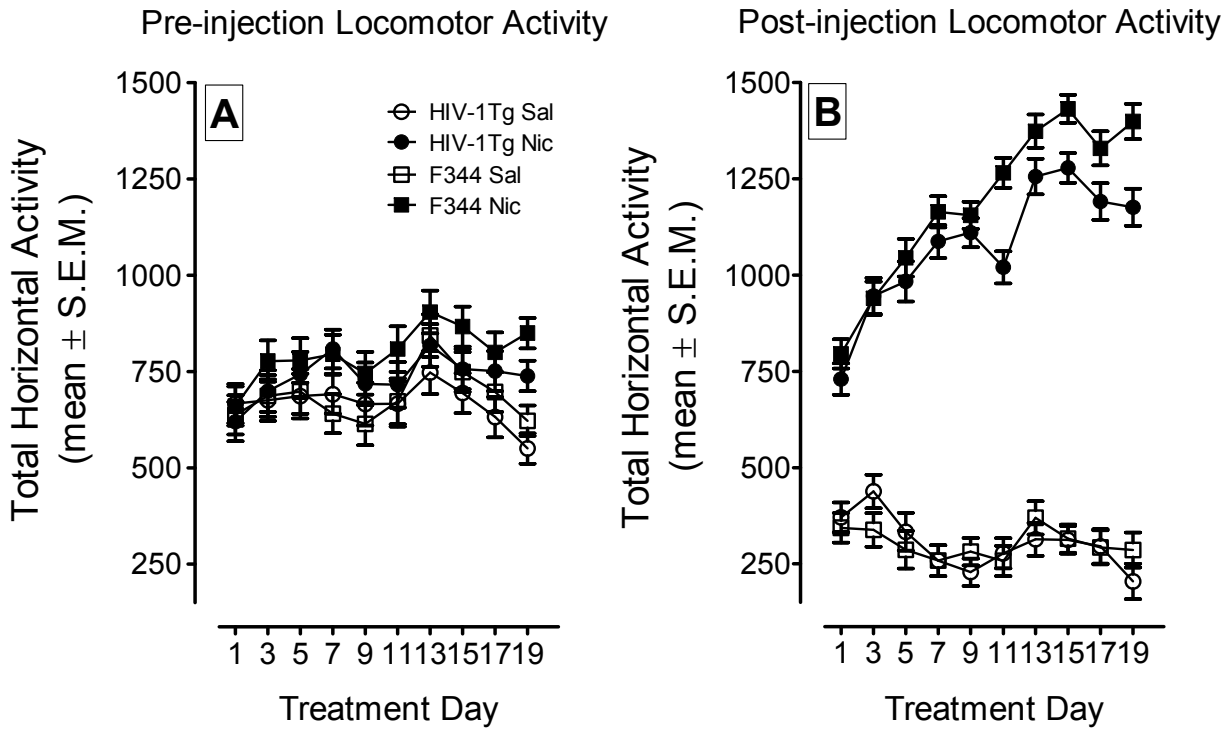

Figure 5.3 The time-course data during the behavioral sensitization phase. HIV-1Tg and F344 rats were administered nicotine (Nic; 0.35 mg/kg; s.c.) or saline (Sal) on Days 1-19. **Panel A** shows the total horizontal activity (mean ± S.E.M.) during the 30 min pre-injection habituation period. **Panel B** shows the total horizontal activity (mean ± S.E.M.) during 60 min following nicotine or saline injection. *n*=8 rats per group.

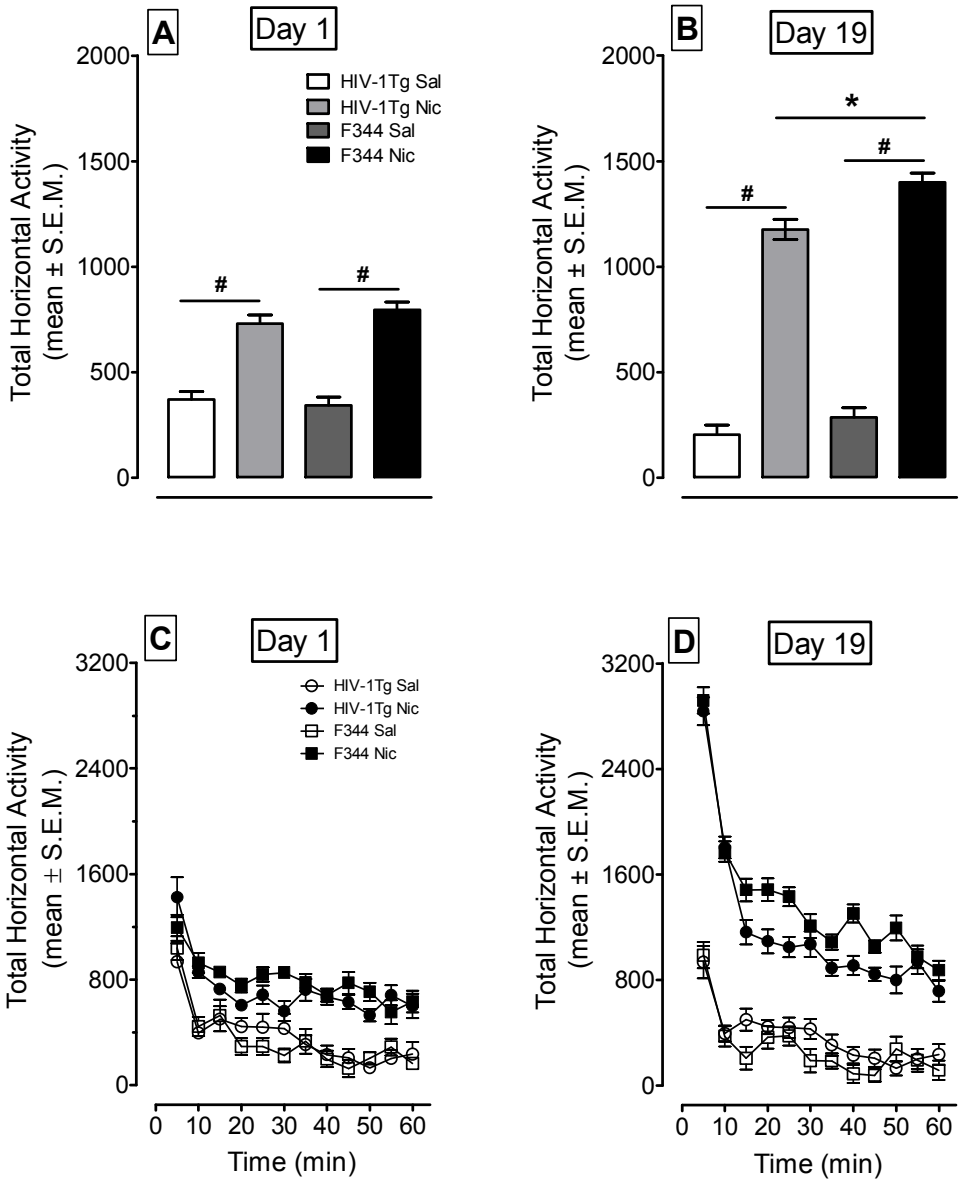

Figure 5.4 The time-course data for total horizontal activity during day 1 and day 19 of the behavioral sensitization phase. Panels A and B show the total horizontal activity (mean ± S.E.M.) across the 60-min session. Panels C and D show the time course of the total horizontal activity (mean ± S.E.M.) during each 5-min time interval. * $p < 0.05$ difference between HIV-1Tg and F344 rats. # $p < 0.05$ difference between nicotine- and saline-treatment group. n=8 rats per group.

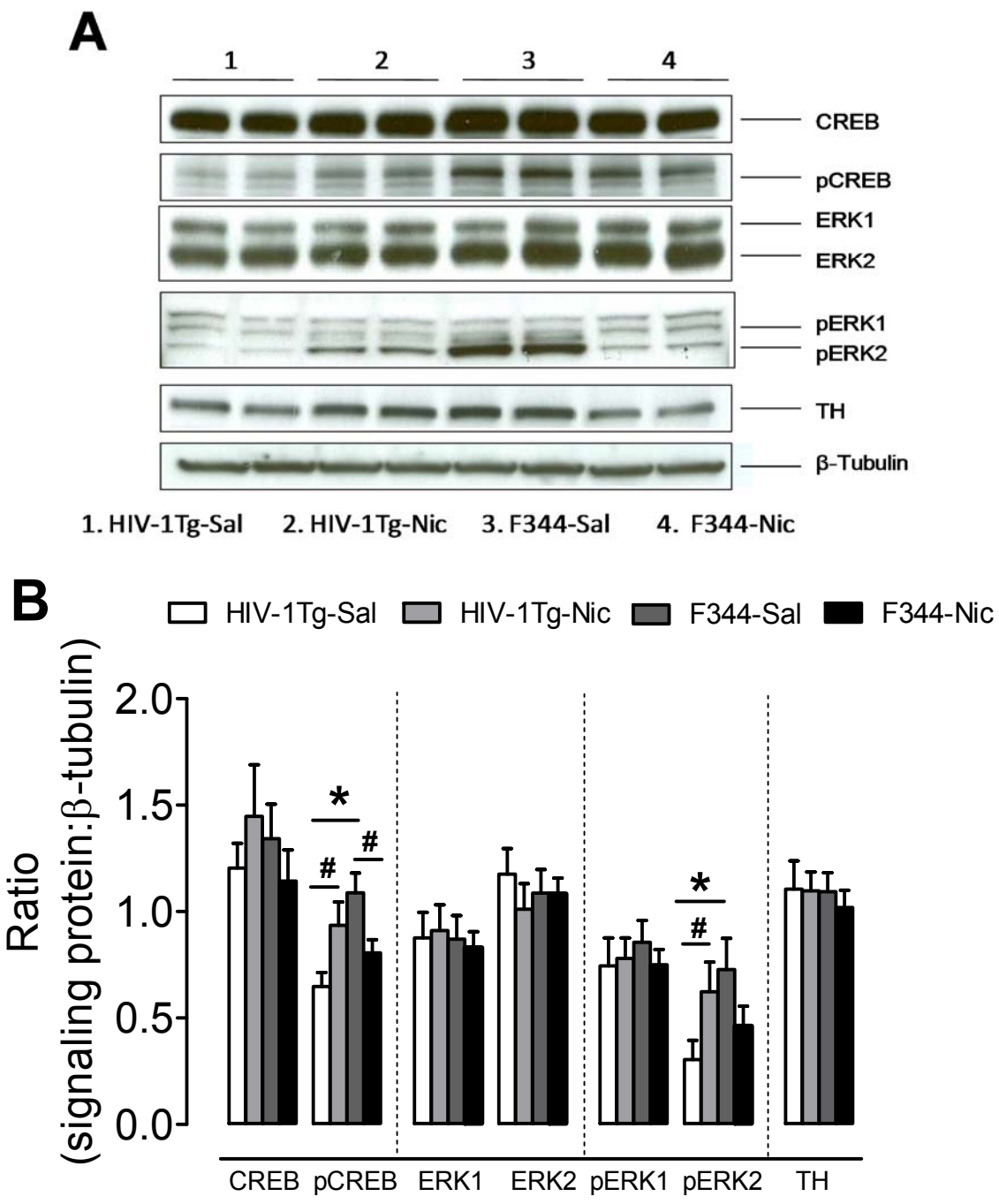

Figure 5.5 Levels of ERK, CREB and TH proteins in the PFC in HIV-1Tg and F344 rats. **(A)** Representative western blots showing the protein density of CREB, pCREB, ERK1/2, pERK1/2, TH and β-tubulin in nicotine or saline treated HIV-1Tg (HIV-1Tg-Nic, HIV-1Tg-Sal) and F344 rats (F344-Nic, F344-Sal). **(B)** Total and phosphorylated protein levels of ERK1, ERK2 and CREB along with levels of TH after chronic nicotine or saline injection.

Ratios are presented as the mean percentage of β-tubulin ± S.E.M. * $p < 0.05$ difference between HIV-1Tg and F344 rats. # $p < 0.05$ difference between the nicotine- and saline-treatment groups. n=8 rats per group.

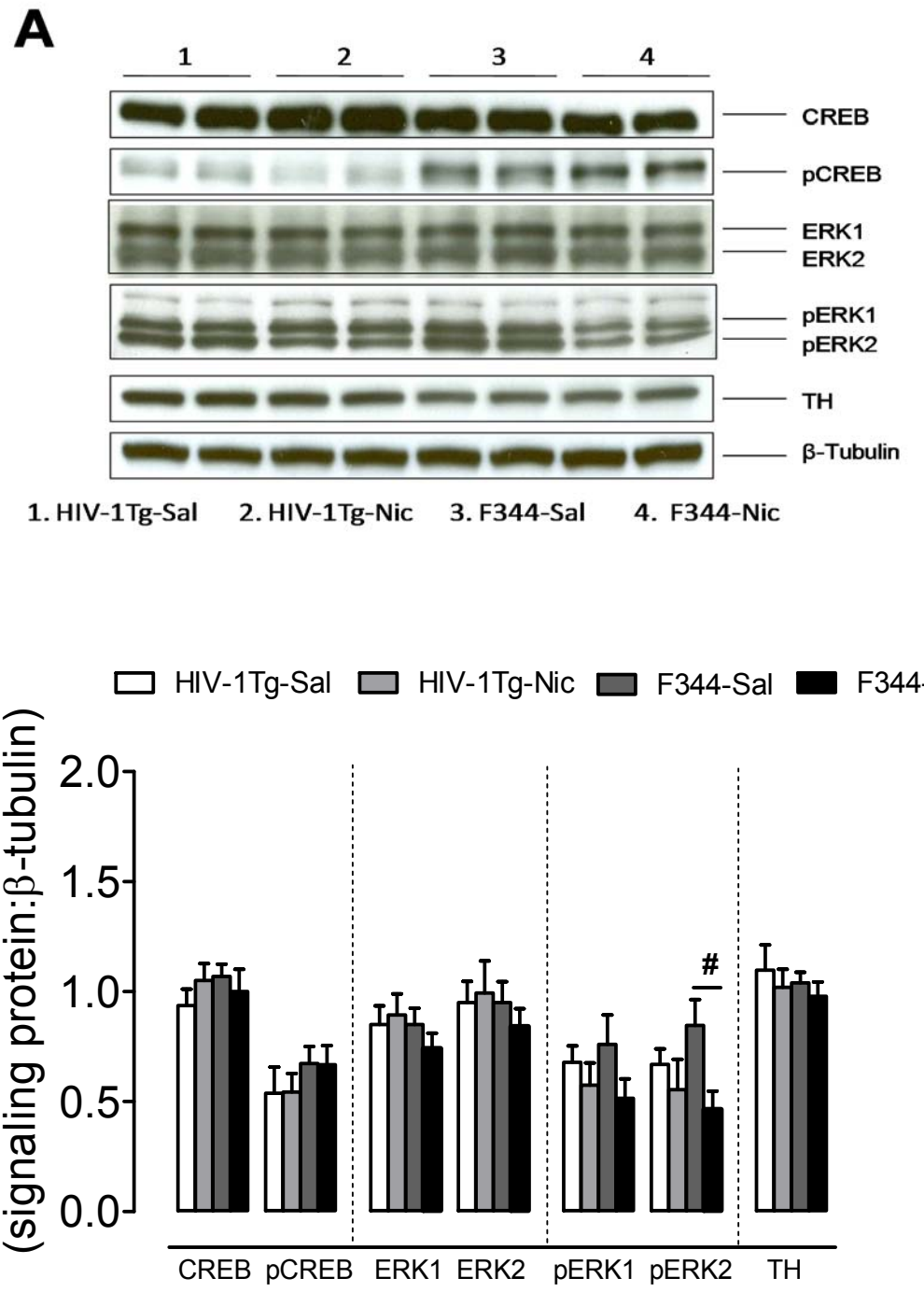

Figure 5.6 Levels of ERK, CREB and TH proteins in the NAc in HIV-1Tg and F344 rats. **(A)** Representative western blots showing the protein density of CREB, pCREB, ERK1/2, pERK1/2, TH and β-tubulin in the nicotine or saline treated HIV-1Tg (HIV-1Tg-Nic, HIV-1Tg-Sal) and F344 rats (F344-Nic, F344-Sal). **(B)** Total and phosphorylated protein levels of ERK1, ERK2 and CREB along with levels of TH after chronic nicotine or saline injection.

Ratios are presented as the mean percentage of β-tubulin ± S.E.M. # $p < 0.05$ difference between the nicotine- and saline-treatment groups. n=8 rats per group.

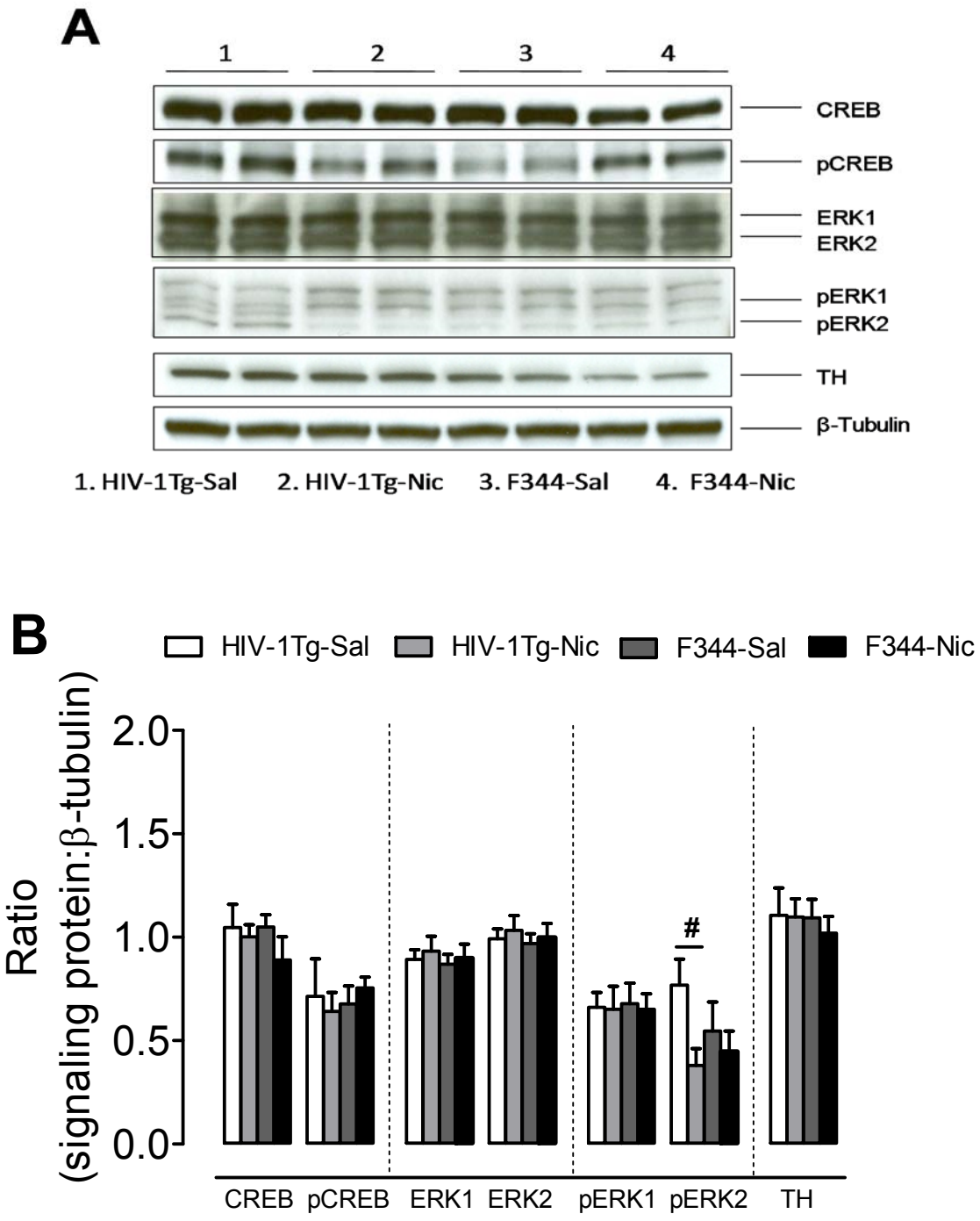

Figure 5.7 Levels of ERK, CREB and TH proteins in the VTA in HIV-1Tg and F344 rats. **(A)** Representative western blots showing the protein density of CREB, pCREB, ERK1/2, pERK1/2, TH and β-tubulin in the nicotine or saline treated HIV-1Tg (HIV-1Tg-Nic, HIV-1Tg-Sal) and F344 rats (F344-Nic, F344-Sal). **(B)** Total and phosphorylated protein levels of

ERK1, ERK2 and CREB along with levels of TH after chronic nicotine or saline injection. Ratios are expressed as the mean percentage of β-tubulin ± S.E.M. # $p < 0.05$ difference between the nicotine- and saline-treatment group. n=8 rats per group.

Copyright Clearance Center RightsLink®

Home | Account Info | Help

Title: Genetically expressed HIV-1 viral proteins attenuate nicotine-induced behavioral sensitization and alter mesocorticolimbic ERK and CREB signaling in rats

Author: Narasimha M. Midde,Adrian M. Gomez,Steven B. Harrod,Jun Zhu

Publication: Pharmacology Biochemistry and Behavior

Publisher: Elsevier

Date: June 2011

Logged in as:
Narasimha Midde
LOGOUT

Order Completed

Thank you very much for your order.

This is a License Agreement between Narasimha M Midde ("You") and Elsevier ("Elsevier"). The license consists of your order details, the terms and conditions provided by Elsevier, and the payment terms and conditions.

Get the printable license.

License Number	3333271228586
License date	Feb 20, 2014
Licensed content publisher	Elsevier
Licensed content publication	Pharmacology Biochemistry and Behavior
Licensed content title	Genetically expressed HIV-1 viral proteins attenuate nicotine-induced behavioral sensitization and alter mesocorticolimbic ERK and CREB signaling in rats
Licensed content author	Narasimha M. Midde,Adrian M. Gomez,Steven B. Harrod,Jun Zhu
Licensed content date	June 2011
Licensed content volume number	98
Licensed content issue number	4
Number of pages	11
Type of Use	reuse in a thesis/dissertation
Portion	full article
Format	both print and electronic
Are you the author of this Elsevier article?	Yes
Will you be translating?	No
Title of your thesis/dissertation	Effect of HIV-1 Tat protein on structure, function, and trafficking of the dopamine transporter
Expected completion date	May 2014
Estimated size (number of pages)	250
Elsevier VAT number	GB 494 6272 12
Permissions price	0.00 USD
VAT/Local Sales Tax	0.00 USD / 0.00 GBP
Total	0.00 USD

ORDER MORE... CLOSE WINDOW

CHAPTER 6

CONCLUSIONS AND FUTURE DIRECTIONS

6.1 SUMMARY AND CONCLUSIONS

Increasing evidence suggest that the alarming rise in HIV-1 associated neurocognitive disorder is, at least in part, associated with HIV-1 viral proteins shed from infected macrophages/microglia, including the nonstructural viral protein Tat, despite the success of anti-retroviral therapies. Tat enhances extra synaptic DA levels by inhibiting DAT, and the concerted effects of Tat and cocaine escalate the severity and amelioration of the HAND. In order to develop adjunctive therapies that can stabilize the altered DA system in the HIV-1 positive brains, it is crucial to understand the underlying mechanism for Tat inhibitory effects on DAT function. The research described in this dissertation focused on addressing the central hypothesis- 'HIV-1 Tat protein via allosteric modulation of DAT induces inhibition of DA transport, leading to dysfunction of the DA system'. This chapter summarizes the findings that were presented in earlier chapters with the following subheadings: (1) protein-protein interactions between Tat and DAT, (2) molecular dynamics simulated structure of HIV-1 Tat and DAT binding complex, (3) mutational analysis of DAT residues involved in HIV-1 Tat-DAT binding complex, (4) effect of HIV-1 Tat protein on trafficking dependent regulation of DAT, (5) effect of HIV-1 Tat protein on VMAT2 function, and (6) released Tat is more potent than synthetic Tat. Finally, the chapter concludes with the proposed model for HIV-1 Tat protein effects on DAT and VMAT2

functions, and future directions for this work.

PROTEIN-PROTEIN INTERACTIONS BETWEEN TAT AND DAT

The preliminary evidence for protein-protein interaction between Tat and DAT comes from Zhu et al. (2009), using a biophysical technique, surface plasmon resonance. This real time measurement using immobilized membranes that overexpress hDAT-GFP revealed that the transporter interacts with Tat protein but not with Tat Cys22. This proposed biomolecular interaction was further strengthened by the lack of inhibitory effects of Tat mutant proteins $Tat_{\Delta 31\text{-}61}$ and Tat Cys 22 on DA transport. However, there is lack of evidence for this protein-protein interaction from a biochemical perspective. In the current dissertation work, I addressed this gap by performing Co-IP and GST-pull down assays to confirm the direct interaction between Tat and DAT proteins (Chapter 2) (Midde et al., 2013). In Chapter 2, it was shown that recombinant Tat protein can immuneprecipitate DAT from the rat striatal synaptosomes and *Glutathione S-transferases* (GST)-tagged Tat protein was able to pull-down DAT (Figure 2.1B and C). Taken together, these results strongly support that Tat-mediated inhibitory effect on DAT function is triggered by a protein-protein interaction between these two proteins.

MOLECULAR DYNAMICS SIMULATED STRUCTURE OF HIV-1 TAT AND DAT BINDING COMPLEX

The above described experimental evidence provides a strong base to further evaluate the mechanism of Tat binding and to predict molecular determinants for DAT and Tat interaction. Binding structure of DAT-Tat-DA-Cocaine was constructed based on the crystallized structure of the leucine transporter (Yamashita et al., 2005) – the bacterial homolog of NSS family proteins, modeling studies of DA substrate and inhibitor cocaine binding to DAT (Huang and Zhan, 2007; Beuming et al., 2008; Huang et al., 2009), and

nuclear magnetic resonance structure of Tat (Peloponese et al., 2000). As displayed in Figure 2.1C (Chapter 2) and Figure 6.1, the proposed binding of Tat protein at the substrate entry tunnel region through electrostatic inter-molecular interactions does not directly interfere with DA binding sites. However, the cocaine binding site is located inside the substrate transport path in the vicinity of DA binding site, and cocaine binding has a direct impact on affinity and transport kinetics of substrate.

According to the most embraced model, the alternating access model of Jardetzky (1966), the substrate binding site is only available to either side of membrane surface at a given time during the DA translocation process. This model proposes that the transporter exists primarily in an outward facing conformation and stabilization of this conformation require a network of intra-molecular interactions. Binding of substrate, two Na^+ and one Cl^- ions trigger allosteric rearrangements of the transporter to the inward facing conformation followed by initiation of substrate release into the intracellular milieu. A schematic showing the outward open state structure of DAT is depicted in Figure 3.3A and B (Chapter 3). According to this model and Singh et al. (2008), residues located in TM1b (TM, transmembrane) and TM6a helices are highly required for conformational transitions during functional DA translocation. These two helices move as group to the inner side of transporter during conversion from outward-open to inward-open state of DAT. TM1b and TM6a involve in a direct interaction with TM11 and EL4 (EL, extracellular) helices. As part of extracellular gating creation Arg85 and Asp476 form a salt-bridge (joint hydrogen and ionic interactions), which drives EL6 to stabilize the TM10 by hydrophobic interaction with Tyr470. Tyr470 is critical to overcome the impermeable barrier of conformational alterations between outward-open and outward-occluded state. Furthermore, this salt-bridging enhances

the flexibility of TM1b for easy movement than TM6a. As a result salt-bridge between Lys92 and Asp313 play an essential role for synchronizing motion of TM1b and TM6a. Thus, residues Tyr88, Lys92 and Asp313 support to stabilize TM1b and TM6a through hydrophobic or electrostatic intra-molecular interactions, and Tyr470 is the key residue in the hydrophobic core of the central cavity of the plasma membrane.

Molecular modeling and molecular dynamics simulations predict the plausible interaction of Tat protein with DAT as presented in Figure 3.2 (Chapter 3). According to this model, the aromatic ring of Tyr470 of DAT interacts with the amino terminal of Met1 of Tat through cation-π interaction. Hydroxyl group of Tyr88 of DAT participates in hydrogen bond attractions with ε-amino group of Tat Lys19. Besides, the side chain of Lys92 of DAT forms hydrogen bond with carbonyl group of main chain of Pro18 of Tat protein. This initial binding structure of Tat and DAT binding complex demonstrates that Tat molecule is associated with DAT through inter molecular electrostatic attractions and complementary hydrophobic interactions.

MUTATIONAL ANALYSIS OF DAT RESIDUES INVOLVED IN HIV-1 TAT-DAT BINDING COMPLEX

As described above, DAT residues that are involved in favorable inter-molecular interaction with Tat are part of the conformational stabilizing network that is critical for smooth conformational transitions during DA transport cycle. Consequently, mutation of these residues may cause alterations in the conformation of the transporter that will manipulate affinity and kinetics of DA transporting process. The research shown in this dissertation uses a systemic mutagenesis approach to define the predicted binding sites in DAT for Tat binding. As a proof of concept, initially Y470H mutant was generated in DAT with the expectation that Y470H disrupts critical cation-π interaction required for Tat

binding (Chapter 2) (Midde et al., 2013). In Y470H mutant, the effect of recombinant Tat_{1-86} on DA uptake was attenuated compared to 38% decrease in WT-hDAT transfected cells that are exposed to Tat_{1-86}, suggesting the antagonistic nature of Tat to inhibit transporter function through direct interaction with Tyr470 of hDAT (Figure 2.4). As our hypothesis regarding role of Tyr470 in Tat interaction with DAT was verified to be correct, additional substitutions at 470 – Y470F, Y470A and mutation of other predicted residues such as Tyr88 and Lys92 of DAT would be expected to show similar attenuation in response to Tat treatment (Chapter 3). Indeed, all other mutants exhibited similar diminution in Tat-induced inhibition of DA uptake except Y470F (Figure 3.5) emphasizing the importance of aromatic ring of Tyr470 in Tat binding with DAT, and the involvement of Y88 and K92 in Tat and DAT interaction. Thus, these observations further confirm our prediction that Tyr470, Tyr88 and Lys92 are part of the critical network that is required for DA transport and Tat reduces the transporter efficiency by altering the conformation of the transporter by interacting with these residues.

Pharmacological characterization revealed that Y470H and K92M mutations were not only accompanied by decreased V_{max} with no noticeable change in K_m for DA uptake, but also by significant increase in apparent affinities (IC_{50}) for inhibitors (Chapter 2 and 3). Whereas the apparent affinity for substrate DA was not significantly different from WT, the apparent affinities for cocaine and GBR12909 inhibitors were significantly increased to inhibit [^{3}H]DA uptake (Table 2.1 and 3.1). These results indicate that Tat binding sites do not overlap with the binding sites of substrate DA and do not influence the affinity for DA uptake. However, increased apparent inhibitor affinities suggest the direct involvement of Tat binding sites with cocaine binding. This close proximity of Tat and cocaine binding sites

was further supported by Tat-induced decrease in B_{max} for [^{3}H]WIN35,428 binding (Chapter 3, Table 3.2 and (Zhu et al., 2009)). These observations are in line with previous report demonstrating that Tat protein allosterically interacts with the transporter and modulates cocaine binding sites (Zhu et al., 2011). In addition, Y88F and K92M mutants displayed decreased IC_{50} values for cocaine and GBR12909 to inhibit [^{3}H]WIN35,428 binding, a structural derivative of cocaine. Cocaine and GBR12909 belong to different DAT inhibitor classes that are structurally distinct and label different binding sites on the transporter. Furthermore, substantial evidence indicate that inhibitor binding require a specific conformational state of the DAT and cocaine –like compounds prefer the outward facing conformation (Reith et al., 2001; Schmitt et al., 2013). It is interesting to note that mutants increased both cocaine and GBR12909 apparent affinities similarly but with varying degrees of impact. One possible explanation for this variability is that Tat-mediated allosteric effects cause subtle conformational alterations in the transporter which consequently enhances DA uptake potencies for cocaine. An alternative possibility is that GBR12909 can bind to several conformations or is less dependent on conformation of the DAT (Schmitt and Reith, 2011). Nevertheless, these inferences underscore the importance of extensive characterization of predicted Tat recognition residues before concluding the influence of Tat binding on inhibitors affinities. Taken together, it is evident that Tat through allosteric modulation of transporter function escalates the inhibitory action of cocaine on DA translocation.

To explore the molecular basis for mutants altered pharmacological properties and thereby to substantiate our hypothesis that Tat down regulates DAT function through allosteric regulation, this research employed DA uptake and WIN35,428 binding studies in the presence of zinc, a noncompetitive DAT inhibitor that blocks the DA uptake but

potentiates WIN35,428 binding by stabilizing the transporter in the outward facing state (Norregaard et al., 1998; Loland et al., 2003). Ample evidence indicates that specific conformational effects in DAT that differ in response to bound ligand or mutations can be investigated by Zn^{2+}. In the presence of zinc, the uptake ability in Y470H was increased but not in all other four mutants (Chapter 2 and 3). Interestingly, zinc-induced increase in WIN35,428 binding was attenuated not only in Y470H but in all tested mutants with different proportions. It was reasoned that Y470H mutation may cause the transporter to stay principally in an extreme inward facing conformation that is highly suitable to reverse Zn^{2+}-mediated effects on DA uptake and WIN35,428 binding (Guptaroy et al., 2009; Liang et al., 2009). In the case of Y88F, K92M, Y470F and Y470A mutations induce an inward conformation that is able to abolish the binding preference for WIN35,428 without interfering with zinc stimulated down regulation in DA uptake. These conformational preferences of the mutants were further screened by measuring basal efflux (DAT-mediated release of preloaded substrate). Y470H and Y470A displayed significant increase in both DA and MPP+ efflux but not the Y470F and Y88F (Chapter 3). The most likely reason for the low retention of substrate is that elevation of efflux without improving the uptake capacity i.e. forward transport. Curiously, the K92M mutant exhibited considerable increase in the DA basal efflux but not MPP+ efflux. It was interpreted that this may be due to K92M inclination for a conformation that is not suitable for MPP+ binding (Liang et al., 2009). Alternatively, the observed DA efflux in K92M is merely a quick leakage of substrate by non-specific diffusion as MPP+ was showed to exhibit less diffusive properties compared to DA in heterologous expression systems (Scholze et al., 2001). However, provided that the effect of mutants on kinetic differences, increased inhibitor apparent affinities and the

attenuation of zinc-mediated increase in WIN35,428 binding, it was deduced that the reported mutants adopt similar molecular mechanisms that are ranging from closed-to-out (occluded) to open-to-in (inward) conformational states. While these results strongly support the allosteric mode of regulation by Tat protein to inhibit DAT function, further strategies are required to confirm specific conformational states that are attributed to the identified residues in transporter. For example substituted-cysteine accessibility method (Javitch, 1998; Norregaard et al., 2003; Loland et al., 2008) and amphetamine-induced substrate efflux (Khoshbouei et al., 2004; Guptaroy et al., 2011) can be used to further support the above stated inferences for Tat induced effects on DAT structure and function.

EFFECT OF HIV-1 TAT PROTEIN ON TRAFFICKING DEPENDENT REGULATION OF DAT

A recent NMR spectroscopy study has shown Tat as a "natively unfolded" protein with no distinctive three-dimensional structure but with fast dynamics (Shojania and O'Neil, 2006). Moreover, the unique genetic arrangement of Tat sequence and post-translational modifications (Hetzer et al., 2005) enhances the likelihood of Tat protein interaction with multiple cellular proteins. As described earlier, due to the complex nature of the DAT regulation it is possible that Tat may impact other regulatory partners of DAT because of its flexible and versatile nature, which ultimately leads to the reduction in DA uptake. As previous studies (Aksenova et al., 2006; Zhu et al., 2009) indicated exposure to Tat reduces V_{max} of [^{3}H]DA uptake with no change in the total DAT immunoreactivity levels. It clearly suggests that there is no degradation of DAT protein due to Tat treatment at least in the acute treatment time periods. However, it remains uncertain whether Tat causes any alterations in the surface expression levels of the transporter. Ample experimental evidence has demonstrated that redistribution of DAT proteins to and away from the presynaptic

membrane is a predominant mechanism of DAT regulation (Chen et al., 2010). In an attempt to understand the effects of Tat on DAT surface localization, rat striatal synaptosomes were exposed to Tat protein for 15 min and it was found that DAT immunoreactivity levels were decreased by 46% in the plasma membrane enriched fractions (P3) with no changes in the total synaptosomal fractions (P2) (Chapter 4) (Midde et al., 2012). It was reasoned that Tat could promote the redistribution of surface DAT to intracellular compartments possibly through manipulating trafficking events, results in the reduction of DAT density at the surface, which causes the observed decrease in V_{max} of DA uptake. This hypothesis was further supported by the decrease in B_{max} of [^{3}H]WIN 35,428 binding in P3 of Tat-treated samples.

These findings raise vital questions, what is underlying mechanism for Tat-induced shift in the surface DAT? Is it due to acceleration of endocytosis or diminution of recycling to the membrane, or a combination of both? Numerous studies have demonstrated that DAT undergo both constitutive and regulated endocytic trafficking. Following internalization, DAT can be recycled back to the plasma membrane via the endocytic recycling pathways, or targeted to lysosomal degradation pathways (Sorkina et al., 2009). Since PKC has been shown as a key mediator for regulating recycling to the plasmalemma and internalization of DAT to the early/late endosomes (Loder and Melikian, 2003; Chen et al., 2010), we exposed rat striatal synaptosomes to the Tat protein that were pre-treated with PKC inhibitor, bisindoylmaleimide-I (BIM-I) and observed the attenuation of Tat inhibitory effects on DA uptake (Chapter 4). This outcome indicates that Tat exploits PKC-dependent signaling pathway to modulate the functional regulation of the DAT. However, it is worth noting that residues 587-596 at carboxyl-terminal of the DAT are required for the PKC-mediated

internalization of the transporter (Holton et al., 2005). Furthermore, studies suggest that mutating classical PKC consensus serine and threonine sites (Chang et al., 2001) and truncation of amino-terminal of DAT (Granas et al., 2003) prevent direct phosphorylation of the transporter but not the internalization. Collectively, these findings suggest that Tat may manipulate the structural determinants that lead to rapid PKC-stimulated internalization of DAT. Alternatively, Tat potentially interferes with functions of other downstream kinases and/or scaffolding proteins in the PKC signaling cascade (Yang et al., 2010). Future studies are necessary to address whether Tat-mediated influences on DAT endocytic trafficking is phosphorylation dependent or independent.

EFFECT OF HIV-1 TAT PROTEIN ON VMAT2 FUNCTION

In the central nervous system, vesicular monoamine transporter 2 (VMAT2, Slc18a2) is the only transporter that sequesters cytoplasmic monoamines, in particular DA, into synaptic vesicles for storage and subsequent release (Zheng et al., 2006; Vergo et al., 2007). This packaging process is highly regulated and dysfunction plays a role in a variety of disorders including Parkinson's disease (Caudle et al., 2008; Taylor et al., 2009; Rilstone et al., 2013), Huntington's disease (Ondo et al., 2002; Paleacu et al., 2004; Morrow, 2008), and neuropsychiatric disorders (Zubieta et al., 2001; Zucker et al., 2001; Eiden and Weihe, 2011). Moreover, VMAT2 is one of the principal targets for amphetamine-derived psychoactive drugs (Sulzer et al., 2005; Fleckenstein et al., 2007; Fleckenstein et al., 2009). Having proven evidence for Tat induced effects on dopaminergic neurons especially on DAT it was hypothesized that Tat may follow a similar mode of action to impair VMAT2 function.

To test this hypothesis, synaptic vesicular uptake in the presence of 1 μM Tat was performed and demonstrated that inhibitory effects of Tat are more profound in VMAT2 (35%) than DAT (25%) protein. Importantly, current data show that Tat potency for inhibiting vesicular DA uptake (IC_{50} =0.21 μM) (Chapter 4) is 15-fold higher than that for inhibiting synaptosomal DA uptake (IC_{50} = 3.1 μM) (Zhu et al., 2009). These results visibly imply the essential role played by Tat protein in the impairment of VMAT2 that results in the reduction of the loading and storage of DA into the synaptic vesicles. Moreover, mutant Tat Cys22 (Cys22Glys) protein attenuates Tat-induced decrease in VMAT2 function, which is similar to reported attenuation of Tat effects on DAT function (Zhu et al., 2009). Along these lines, Theodore et al. (2012) using *in vivo* microdialysis reported that striatal synaptic vesicles incubated with Tat show ~35% decrease in DA uptake and ~30% reduction in K^+ - evoked total DA overflow in rats injected with Tat. Taken together, these findings tempting to speculate that Tat may directly influence VMAT2 structure through protein-protein interactions. However, future investigations are necessary to delineate this possible mechanism. Furthermore, recent studies proposed a physical and functional coupling between DAT and VMAT2 to regulate dopaminergic tone in response to normal and drug-induced stimuli (Zhu and Reith, 2008; Egaña et al., 2009; Sager and Torres, 2011), suggesting that Tat protein may increase the neurodegeneration of dopaminergic terminal by simultaneously targeting both DAT and VMAT2. In addition, it was reported that simultaneous exposure of Tat protein and amphetamine synergistically impairs DAT function *in vitro* (Cass et al., 2003; Theodore et al., 2006) and *in vivo* (Kass et al., 2010). Having established evidence for VMAT2 as a target for amphetamine class of drugs (Sulzer et al., 2005; Sulzer, 2011), it is conceivable that co-exposure of Tat protein and abused drugs

by complementing each other may further deteriorate neuronal terminal loss that eventually contribute to HAND (Purohit et al., 2011; Purohit et al., 2013).

RELEASED TAT IS MORE POTENT THAN SYNTHETIC TAT

Unconventional secretion of Tat (Pugliese et al., 2005; Rayne et al., 2010; Bachani et al., 2013) by infected cells without cell lysis causes neurotoxicity to the neighboring uninfected cells including neurons (Li et al., 2009). This extracellularly released Tat is biologically active and can interact with DAT (Zhu et al., 2009; Midde et al., 2013) suggesting that Tat protein is very flexible and can assume a unique conformation to bind with the target molecule. It was demonstrated that a point mutation in Tat that substitutes cysteine with alanine at 22 (Tat Cys22) attenuates Tat-mediated inhibition of DA uptake (Zhu et al., 2009). In addition, this study also showed that deletion of residues 31-61 ($Tat_{\Delta 31-61}$) abolishes inhibitory effects of Tat on DAT function indicating that specific recognition residues of Tat are responsible for Tat and DAT interaction. However, one caveat here is that synthetic Tat used for these experiments is substantially less potent than Tat released from Tat-expressing astrocytes (Li et al., 2008). Degradation of Tat during purification process, high susceptibility of Tat to freeze/thaw cycles, and ability to get oxidized easily are the most likely reasons for less Tat activity (Nath et al., 2000). As a part of this dissertation work, Tat-conditioned medium which was obtained from the cells that were transiently transfected with Tat plasmid DNA was evaluated to confirm whether it can be substituted for commercially available recombinant Tat in the proposed experiments (Chapter 2) (Midde et al., 2013). This approach was chosen because extracellularly released Tat exhibits more relevant constitutively produced Tat effects than recombinant protein (Nath et al., 2000). As shown in Figure 2.5B secreted Tat_{1-72}, Tat_{1-86} or Tat_{1-101} variants exhibited a similar inhibitory pattern

which decreased DA uptake in heterologous cells that were expressing hDAT, and this diminished effect was attenuated when released Tat was immunodepleted with anti-Tat antibodies (Figure 2.5C). Furthermore, released Tat displayed ~4000 times more potent inhibitory effects on DA uptake than recombinant Tat (Chapter 2). Therefore, these results indicate that secreted Tat is more neurotoxic and Tat-conditioned media can be used as a source of extracellular Tat (by producing different Tat mutant proteins) to characterize unique binding sites of Tat that are required for functional interaction with DAT.

OVERALL CONCLUSIONS

In summary, the Tat protein plays a significant role in the impairment of DA system by affecting regulatory pathways that control the functional attributes of DAT and VMAT2. A graphical representation of potential ways by which Tat protein exerts its actions are depicted in Figure 6.2 that include (1) direct protein-protein interaction with DAT, (2) stimulation of PKC-mediated endocytosis, (3) diminution of recycling of DAT to the plasma membrane, (4) alteration of direct phosphorylation state of the DAT, and (5) direct protein-protein interaction with VMAT2 protein. Even though most of these regulatory components are interconnected, here they were shown separately for the sake of clarity. It is quite possible that Tat interaction or influence at one molecular component can trigger activation of other factors or cellular events that ultimately lead to dysregulation of the DA system. As described in this work, it appears that Tat will have a profound impact on DA translocation process principally by altering the conformational states of the DAT through direct protein-protein interaction. We do not know whether this Tat-mediated impact on structure of DAT could also prompt increased endocytosis to early/recycling endosomes or diminished recycling to the surface. Curiously, recent findings suggest that modifications in the

conformational equilibrium of the DAT influence the endocytic trafficking of the transporter molecules (Sorkina et al., 2009).

6.2 FUTURE DIRECTIONS

Several studies with various approaches and models tried to explain the evolution of neuroAIDS. HAND begins as HIV-1 enters the brain and ARTs have little impact on viral reservoir in the CNS, insisting the need to develop adjunctive therapies to treat neurological complications associated with HIV-1 infection that can improve the HIV-1 positive individual's capability to perform daily activities. With increasing evidence it is almost certain that HIV-1 viral proteins dysregulate the dopaminergic system and cause subsequent neurodegeneration (Purohit et al., 2011; Barreto et al., 2014). However, delineating the mechanism of action of Tat protein on target molecules, such as DAT, is a key step forward to combat the progression of neuronal damage in HIV-1 infected brains. As described above, the initial findings show that Tat recognition residues Tyr88, Lys92 and Tyr470 of DAT are part of the crucial framework of substrate permeation pathway in DAT. Nonetheless, this information is not sufficient to completely understand Tat and DAT interaction. Doubtlessly, identification and characterization of other recognition residues is necessary to construct a ligand-binding pocket for the functional interaction of Tat with DAT. Moreover, the fundamental role of these DAT domains involved in DAT-Tat interaction are subject of great debate, and shedding light on these regions will greatly improve our understanding of the basic functionality of DA transport process. As it is hypothesized that neurocognitive deficits and alterations in DA homeostasis are more severe in HIV-1 positive drug abusers (Nath, 2010; Gaskill et al., 2013), understanding how concerted effects of Tat and cocaine manipulate the structural and functional attributes of the transporter is an important goal for

future research in this area. Finally, the major obstacle would be how to translate these computational and *in vitro* findings into a preclinical setting. This is very important because evaluating the molecular mechanisms in a relevant model system is a key step before exploiting them as clinically effective strategies. Hence, HIV-1 Tg rat model that was utilized to demonstrate that genetically expressed HIV-1 viral proteins modify the locomotor sensitization in response to nicotine administration (Chapter 5) (Midde et al., 2011) could be used to investigate perturbations of DA neurotransmission that are present in HIV-infected brains. Considering the alteration in dopaminergic biomarkers and behavioral evaluations (Persidsky and Fox, 2007; Vigorito et al., 2007; Lashomb et al., 2009; Webb et al., 2010; Rao et al., 2011), HIV-1 Tg rat model may be an appropriate model to evaluate the ligand-binding pocket in DAT for Tat binding and to screen potential small molecules that can block Tat-specific effects on DAT functional regulation.

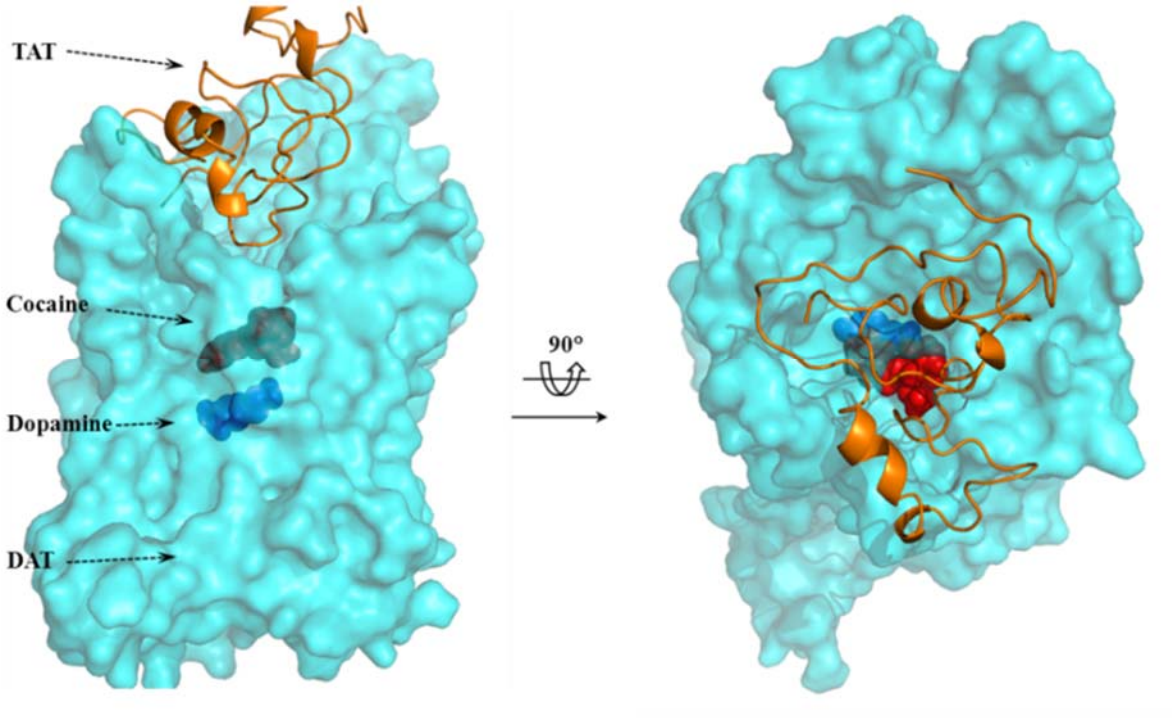

Figure 6.1 Structure of DAT-Tat-Dopamine-Cocaine complex. DAT, Tat, cocaine, and dopamine are colored in cyan, orange, red and blue respectively. Tat, cocaine and dopamine bind to different region of DAT. Cocaine can block the entry of substrate dopamine, but not Tat protein.

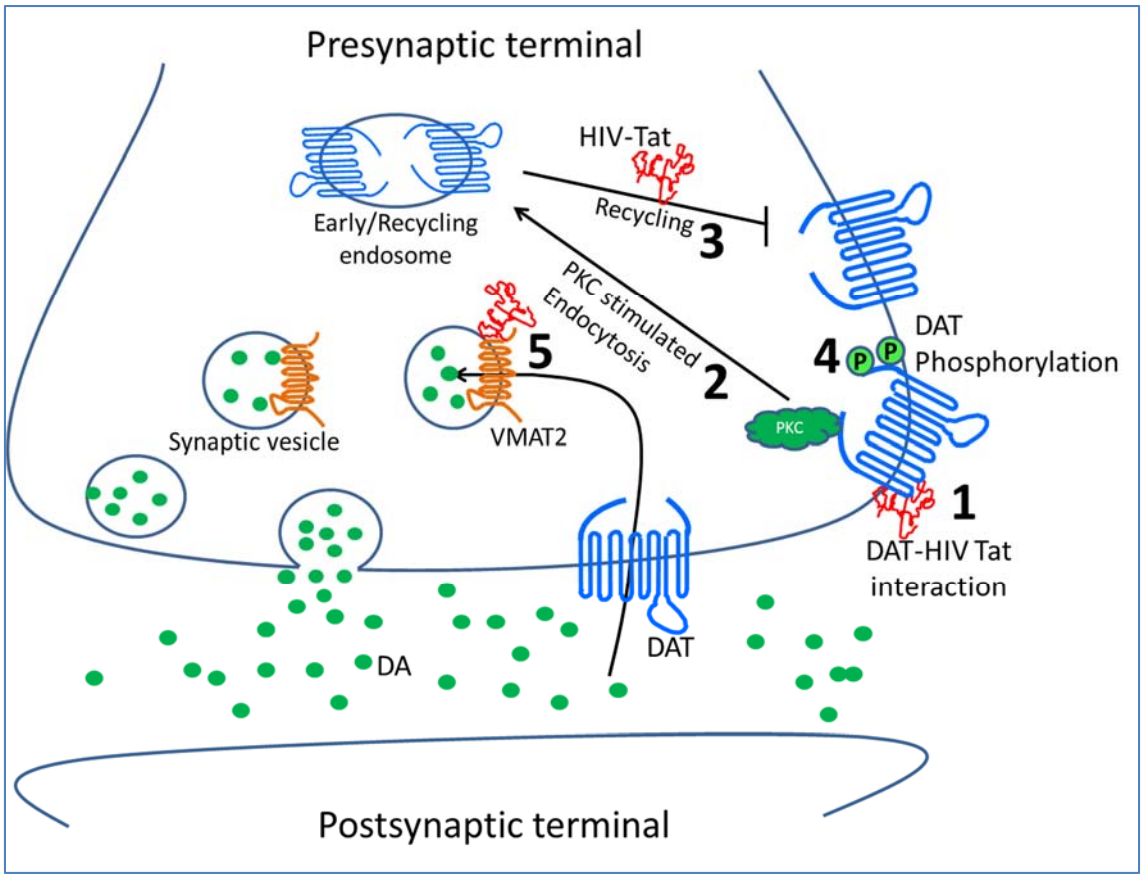

Figure 6.2 Proposed model of HIV-1 Tat protein effects on DAT and VMAT2 proteins. Tat protein may elicit its effects on DA system by influencing the structure, function and endocytic trafficking of the DAT. (1) physical interaction of Tat with DAT induces transporter down regulation and this physical coupling may encourage (2) PKC-stimulated endocytosis and/or, (3) reduced recycling to the surface. Tat may also play a role in alterations of (4) phosphorylation status of the DAT. (5) The direct interaction of Tat with VMAT2 is also an important mechanism to dysregulate DA synaptic vesicular loading through VMAT2.

REFERENCES

Addy NA, Fornasiero EF, Stevens TR, Taylor JR, Picciotto MR (2007) Role of calcineurin in nicotine-mediated locomotor sensitization. J Neurosci 27:8571-8580.

Aksenov MY, Aksenova MV, Mactutus CF, Booze RM (2009) Attenuated neurotoxicity of the transactivation-defective HIV-1 Tat protein in hippocampal cell cultures. Exp Neurol 219:586-590.

Aksenov MY, Hasselrot U, Bansal AK, Wu G, Nath A, Anderson C, Mactutus CF, Booze RM (2001) Oxidative damage induced by the injection of HIV-1 Tat protein in the rat striatum. Neuroscience Letters 305:5-8.

Aksenova MV, Silvers JM, Aksenov MY, Nath A, Ray PD, Mactutus CF, Booze RM (2006) HIV-1 Tat neurotoxicity in primary cultures of rat midbrain fetal neurons: changes in dopamine transporter binding and immunoreactivity. Neuroscience Letters 395:235-239.

Alberts IL, Nadassy K, Wodak SJ (1998) Analysis of zinc binding sites in protein crystal structures. Protein science : a publication of the Protein Society 7:1700-1716.

Albini A, Ferrini S, Benelli R, Sforzini S, Giunciuglio D, Aluigi MG, Proudfoot AE, Alouani S, Wells TN, Mariani G, Rabin RL, Farber JM, Noonan DM (1998) HIV-1 Tat protein mimicry of chemokines. Proc Natl Acad Sci U S A 95:13153-13158.

Anagnostaras SG, Robinson TE (1996) Sensitization to the psychomotor stimulant effects of amphetamine: modulation by associative learning. Behav Neurosci 110:1397-1414.

Andersen PH, Jansen JA, Nielsen EB (1987) [3H]GBR 12935 binding in vivo in mouse brain: labelling of a piperazine acceptor site. Eur J Pharmacol 144:1-6.

Antinori A et al. (2007) Updated research nosology for HIV-associated neurocognitive disorders. Neurology 69:1789-1799.

Antiretroviral Therapy Cohort C (2008) Life expectancy of individuals on combination antiretroviral therapy in high-income countries: a collaborative analysis of 14 cohort studies. Lancet 372:293-299.

Arnsten JH, Demas PA, Grant RW, Gourevitch MN, Farzadegan H, Howard AA, Schoenbaum EE (2002) Impact of active drug use on antiretroviral therapy adherence and viral suppression in HIV-infected drug users. J Gen Intern Med 17:377-381.

Aylward EH, Henderer JD, McArthur JC, Brettschneider PD, Harris GJ, Barta PE, Pearlson GD (1993) Reduced basal ganglia volume in HIV-1-associated dementia: results from quantitative neuroimaging. Neurology 43:2099-2104.

Bachani M, Sacktor N, McArthur JC, Nath A, Rumbaugh J (2013) Detection of anti-tat antibodies in CSF of individuals with HIV-associated neurocognitive disorders. J Neurovirol 19:82-88.

Bansal AK, Mactutus CF, Nath A, Maragos W, Hauser KF, Booze RM (2000) Neurotoxicity of HIV-1 proteins gp120 and Tat in the rat striatum. Brain Research 879:42-49.

Barré-Sinoussi F, Chermann JC, Rey F, Nugeyre MT, Chamaret S, Gruest J, Dauguet C, Axler-Blin C, Vézinet-Brun F, Rouzioux C, Rozenbaum W, Montagnier L (2004) Isolation of a T-lymphotropic retrovirus from a patient at risk for acquired immune deficiency syndrome (AIDS). 1983. Rev Invest Clin 56:126-129.

Barreto ICG, Viegas P, Ziff EB, Konkiewitz EC (2014) Animal models for depression associated with HIV-1 infection. Journal of Neuroimmune Pharmacology: The Official Journal of the Society on NeuroImmune Pharmacology 9:195-208.

Berger JR, Arendt G (2000) HIV dementia: the role of the basal ganglia and dopaminergic systems. Journal of psychopharmacology 14:214-221.

Berger JR, Kumar M, Kumar A, Fernandez JB, Levin B (1994) Cerebrospinal fluid dopamine in HIV-1 infection. AIDS (London, England) 8:67-71.

Berhow MT, Hiroi N, Nestler EJ (1996) Regulation of ERK (extracellular signal regulated kinase), part of the neurotrophin signal transduction cascade, in the rat mesolimbic dopamine system by chronic exposure to morphine or cocaine. J Neurosci 16:4707-4715.

Berridge KC (2007) The debate over dopamine's role in reward: the case for incentive salience. Psychopharmacology (Berl) 191:391-431.

Berridge KC, Robinson TE (1998) What is the role of dopamine in reward: hedonic impact, reward learning, or incentive salience? Brain Research Reviews 28:309-369.

Beuming T, Kniazeff J, Bergmann ML, Shi L, Gracia L, Raniszewska K, Newman AH, Javitch JA, Weinstein H, Gether U, Loland CJ (2008) The binding sites for cocaine and dopamine in the dopamine transporter overlap. Nature Neuroscience 11:780-789.

Bevins RA, Palmatier MI (2003) Nicotine-conditioned locomotor sensitization in rats: assessment of the US-preexposure effect. Behav Brain Res 143:65-74.

Bilgrami M, O'Keefe P (2014) Neurologic diseases in HIV-infected patients. Handb Clin Neurol 121:1321-1344.

Bonavia R, Bajetto A, Barbero S, Albini A, Noonan DM, Schettini G (2001) HIV-1 Tat causes apoptotic death and calcium homeostasis alterations in rat neurons. Biochemical and biophysical research communications 288:301-308.

Boudanova E, Navaroli DM, Melikian HE (2008) Amphetamine-induced decreases in dopamine transporter surface expression are protein kinase C-independent. Neuropharmacology 54:605-612.

Bradford MM (1976) A rapid and sensitive method for the quantitation of microgram quantities of protein utilizing the principle of protein-dye binding. Anal Biochem 72:248-254.

Bratanich AC, Liu C, McArthur JC, Fudyk T, Glass JD, Mittoo S, Klassen GA, Power C (1998) Brain-derived HIV-1 tat sequences from AIDS patients with dementia show increased molecular heterogeneity. Journal of Neurovirology 4:387-393.

Bruce-Keller AJ, Chauhan A, Dimayuga FO, Gee J, Keller JN, Nath A (2003) Synaptic transport of human immunodeficiency virus-Tat protein causes neurotoxicity and gliosis in rat brain. The Journal of Neuroscience: The Official Journal of the Society for Neuroscience 23:8417-8422.

Brunzell DH, Russell DS, Picciotto MR (2003) In vivo nicotine treatment regulates mesocorticolimbic CREB and ERK signaling in C57Bl/6J mice. J Neurochem 84:1431-1441.

Brunzell DH, Mineur YS, Neve RL, Picciotto MR (2009) Nucleus accumbens CREB activity is necessary for nicotine conditioned place preference. Neuropsychopharmacology 34:1993-2001.

Buch S, Yao H, Guo M, Mori T, Su TP, Wang J (2011) Cocaine and HIV-1 interplay: molecular mechanisms of action and addiction. Journal of neuroimmune pharmacology : the official journal of the Society on NeuroImmune Pharmacology 6:503-515.

Burns DN, Hillman D, Neaton JD, Sherer R, Mitchell T, Capps L, Vallier WG, Thurnherr MD, Gordin FM (1996) Cigarette smoking, bacterial pneumonia, and other clinical outcomes in HIV-1 infection. Terry Beirn Community Programs for Clinical Research on AIDS. J Acquir Immune Defic Syndr Hum Retrovirol 13:374-383.

Campbell GR, Loret EP (2009) What does the structure-function relationship of the HIV-1 Tat protein teach us about developing an AIDS vaccine? Retrovirology 6:50.

Carlezon WA, Jr., Thome J, Olson VG, Lane-Ladd SB, Brodkin ES, Hiroi N, Duman RS, Neve RL, Nestler EJ (1998) Regulation of cocaine reward by CREB. Science 282:2272-2275.

Carpenter CJ, Fischl MA, Hammer SM, et al. (1996) Antiretroviral therapy for hiv infection in 1996: Recommendations of an international panel. JAMA 276:146-154.

Cass WA, Harned ME, Peters LE, Nath A, Maragos WF (2003) HIV-1 protein Tat potentiation of methamphetamine-induced decreases in evoked overflow of dopamine in the striatum of the rat. Brain Res 984:133-142.

Caudle WM, Colebrooke RE, Emson PC, Miller GW (2008) Altered vesicular dopamine storage in Parkinson's disease: a premature demise. Trends in Neurosciences 31:303-308.

Cervinski MA, Foster JD, Vaughan RA (2005) Psychoactive substrates stimulate dopamine transporter phosphorylation and down-regulation by cocaine-sensitive and protein kinase C-dependent mechanisms. J Biol Chem 280:40442-40449.

Chang JR, Mukerjee R, Bagashev A, Del Valle L, Chabrashvili T, Hawkins BJ, He JJ, Sawaya BE (2011) HIV-1 Tat protein promotes neuronal dysfunction through disruption of microRNAs. The Journal of Biological Chemistry 286:41125-41134.

Chang L, Wang G-J, Volkow ND, Ernst T, Telang F, Logan J, Fowler JS (2008) Decreased brain dopamine transporters are related to cognitive deficits in HIV patients with or without cocaine abuse. NeuroImage 42:869-878.

Chang MY, Lee SH, Kim JH, Lee KH, Kim YS, Son H, Lee YS (2001) Protein kinase C-mediated functional regulation of dopamine transporter is not achieved by direct phosphorylation of the dopamine transporter protein. Journal of Neurochemistry 77:754-761.

Chen L, Xu M (2010) Dopamine D1 and D3 receptors are differentially involved in cue-elicited cocaine seeking. J Neurochem 114:530-541.

Chen N, Reith ME (2000) Structure and function of the dopamine transporter. European Journal of Pharmacology 405:329-339.

Chen N, Vaughan RA, Reith ME (2001) The role of conserved tryptophan and acidic residues in the human dopamine transporter as characterized by site-directed mutagenesis. Journal of Neurochemistry 77:1116-1127.

Chen N, Zhen J, Reith MEA (2004a) Mutation of Trp84 and Asp313 of the dopamine transporter reveals similar mode of binding interaction for GBR12909 and benztropine as opposed to cocaine. Journal of Neurochemistry 89:853-864.

Chen N, Rickey J, Berfield JL, Reith ME (2004b) Aspartate 345 of the dopamine transporter is critical for conformational changes in substrate translocation and cocaine binding. J Biol Chem 279:5508-5519.

Chen R, Furman CA, Gnegy ME (2010) Dopamine transporter trafficking: rapid response on demand. Future Neurology 5:123-123.

Chi L, Reith ME (2003) Substrate-Induced Trafficking of the Dopamine Transporter in Heterologously Expressing Cells and in Rat Striatal Synaptosomal Preparations. The Journal of pharmacology and experimental therapeutics.

Chudasama Y, Robbins TW (2006) Functions of frontostriatal systems in cognition: comparative neuropsychopharmacological studies in rats, monkeys and humans. Biological psychology 73:19-38.

Clarke PB, Kumar R (1983a) The effects of nicotine on locomotor activity in non-tolerant and tolerant rats. Br J Pharmacol 78:329-337.

Clarke PB, Kumar R (1983b) Characterization of the locomotor stimulant action of nicotine in tolerant rats. Br J Pharmacol 80:587-594.

Clifford DB, Ances BM (2013) HIV-associated neurocognitive disorder. Lancet Infect Dis 13:976-986.

Corrigall WA, Coen KM, Adamson KL (1994) Self-administered nicotine activates the mesolimbic dopamine system through the ventral tegmental area. Brain Res 653:278-284.

Corrigall WA, Franklin KB, Coen KM, Clarke PB (1992) The mesolimbic dopaminergic system is implicated in the reinforcing effects of nicotine. Psychopharmacology (Berl) 107:285-289.

Cowley D, Gray LR, Wesselingh SL, Gorry PR, Churchill MJ (2011) Genetic and functional heterogeneity of CNS-derived tat alleles from patients with HIV-associated dementia. Journal of Neurovirology 17:70-81.

Cremona ML, Matthies HJG, Pau K, Bowton E, Speed N, Lute BJ, Anderson M, Sen N, Robertson SD, Vaughan RA, Rothman JE, Galli A, Javitch JA, Yamamoto A (2011) Flotillin-1 is essential for PKC-triggered endocytosis and membrane microdomain localization of DAT. Nature Neuroscience 14:469-477.

Crothers K, Griffith TA, McGinnis KA, Rodriguez-Barradas MC, Leaf DA, Weissman S, Gibert CL, Butt AA, Justice AC (2005) The impact of cigarette smoking on mortality, quality of life, and comorbid illness among HIV-positive veterans. J Gen Intern Med 20:1142-1145.

D'Hooge R, Franck F, Mucke L, De Deyn PP (1999) Age-related behavioural deficits in transgenic mice expressing the HIV-1 coat protein gp120. The European journal of neuroscience 11:4398-4402.

Daniels GM, Amara SG (1999) Regulated trafficking of the human dopamine transporter. Clathrin-mediated internalization and lysosomal degradation in response to phorbol esters. J Biol Chem 274:35794-35801.

Davis LE, Hjelle BL, Miller VE, Palmer DL, Llewellyn AL, Merlin TL, Young SA, Mills RG, Wachsman W, Wiley CA (1992) Early viral brain invasion in iatrogenic human immunodeficiency virus infection. Neurology 42:1736-1739.

Davis S, Vanhoutte P, Pages C, Caboche J, Laroche S (2000) The MAPK/ERK cascade targets both Elk-1 and cAMP response element-binding protein to control long-term potentiation-dependent gene expression in the dentate gyrus in vivo. J Neurosci 20:4563-4572.

Deeks SG, Lewin SR, Havlir DV (2013) The end of AIDS: HIV infection as a chronic disease. Lancet 382:1525-1533.

Del Arco A, Segovia G, Canales JJ, Garrido P, de Blas M, Garcia-Verdugo JM, Mora F (2007) Environmental enrichment reduces the function of D1 dopamine receptors in the prefrontal cortex of the rat. J Neural Transm 114:43-48.

Del Valle L, Croul S, Morgello S, Amini S, Rappaport J, Khalili K (2000) Detection of HIV-1 Tat and JCV capsid protein, VP1, in AIDS brain with progressive multifocal leukoencephalopathy. Journal of Neurovirology 6:221-228.

DiRocco DP, Scheiner ZS, Sindreu CB, Chan GC, Storm DR (2009) A role for calmodulin-stimulated adenylyl cyclases in cocaine sensitization. J Neurosci 29:2393-2403.

Duncan MJ, Bruce-Keller AJ, Conner C, Knapp PE, Xu R, Nath A, Hauser KF (2008) Effects of chronic expression of the HIV-induced protein, transactivator of transcription, on circadian activity rhythms in mice, with or without morphine. Am J Physiol Regul Integr Comp Physiol 295:R1680-1687.

Egaña LA, Cuevas RA, Baust TB, Parra LA, Leak RK, Hochendoner S, Peña K, Quiroz M, Hong WC, Dorostkar MM, Janz R, Sitte HH, Torres GE (2009) Physical and functional interaction between the dopamine transporter and the synaptic vesicle protein synaptogyrin-3. The Journal of Neuroscience: The Official Journal of the Society for Neuroscience 29:4592-4604.

Eiden LE, Weihe E (2011) VMAT2: a dynamic regulator of brain monoaminergic neuronal function interacting with drugs of abuse. Annals of the New York Academy of Sciences 1216:86-98.

El-Ghundi MB, Fan T, Karasinska JM, Yeung J, Zhou M, O'Dowd BF, George SR (2010) Restoration of amphetamine-induced locomotor sensitization in dopamine D1 receptor-deficient mice. Psychopharmacology (Berl) 207:599-618.

Ensoli B, Barillari G, Salahuddin SZ, Gallo RC, Wong-Staal F (1990) Tat protein of HIV-1 stimulates growth of cells derived from Kaposi's sarcoma lesions of AIDS patients. Nature 345:84-86.

Erickson JD, Schafer MK, Bonner TI, Eiden LE, Weihe E (1996) Distinct pharmacological properties and distribution in neurons and endocrine cells of two isoforms of the human vesicular monoamine transporter. Proc Natl Acad Sci U S A 93:5166-5171.

Eriksen J, Jørgensen TN, Gether U (2010) Regulation of dopamine transporter function by protein-protein interactions: new discoveries and methodological challenges. Journal of Neurochemistry 113:27-41.

Ernst T, Yakupov R, Nakama H, Crocket G, Cole M, Watters M, Ricardo-Dukelow ML, Chang L (2009) Declined neural efficiency in cognitively stable human immunodeficiency virus patients. Ann Neurol 65:316-325.

Everitt BJ, Robbins TW (2005) Neural systems of reinforcement for drug addiction: from actions to habits to compulsion. Nat Neurosci 8:1481-1489.

Faul F, Erdfelder E, Lang AG, Buchner A (2007) G*Power 3: a flexible statistical power analysis program for the social, behavioral, and biomedical sciences. Behavior research methods 39:175-191.

Feinberg MB, Baltimore D, Frankel AD (1991) The role of Tat in the human immunodeficiency virus life cycle indicates a primary effect on transcriptional elongation. Proceedings of the National Academy of Sciences of the United States of America 88:4045-4049.

Ferris MJ, Mactutus CF, Booze RM (2008) Neurotoxic profiles of HIV, psychostimulant drugs of abuse, and their concerted effect on the brain: current status of dopamine system vulnerability in NeuroAIDS. Neuroscience and Biobehavioral Reviews 32:883-909.

Ferris MJ, Frederick-Duus D, Fadel J, Mactutus CF, Booze RM (2009a) The human immunodeficiency virus-1-associated protein, Tat1-86, impairs dopamine transporters and interacts with cocaine to reduce nerve terminal function: a no-net-flux microdialysis study. Neuroscience 159:1292-1299.

Ferris MJ, Frederick-Duus D, Fadel J, Mactutus CF, Booze RM (2009b) In vivo microdialysis in awake, freely moving rats demonstrates HIV-1 Tat-induced alterations in dopamine transmission. Synapse (New York, NY) 63:181-185.

Ferris MJ, Frederick-Duus D, Fadel J, Mactutus CF, Booze RM (2010) Hyperdopaminergic tone in HIV-1 protein treated rats and cocaine sensitization. J Neurochem 115:885-896.

Fiala M, Gan XH, Zhang L, House SD, Newton T, Graves MC, Shapshak P, Stins M, Kim KS, Witte M, Chang SL (1998) Cocaine enhances monocyte migration across the blood-brain barrier. Cocaine's connection to AIDS dementia and vasculitis? Adv Exp Med Biol 437:199-205.

Fink JS, Smith GP (1980) Mesolimbic and mesocortical dopaminergic neurons are necessary for normal exploratory behavior in rats. Neurosci Lett 17:61-65.

Fitting S, Booze RM, Hasselrot U, Mactutus CF (2008) Differential long-term neurotoxicity of HIV-1 proteins in the rat hippocampal formation: a design-based stereological study. Hippocampus 18:135-147.

Fleckenstein A, Volz TJ, Riddle EL, Gibb JW, Hanson GR (2007) New insights into the mechanism of action of amphetamines. Annu Rev Pharmacol Toxicol 47:681-698.

Fleckenstein AE, Volz TJ, Hanson GR (2009) Psychostimulant-induced alterations in vesicular monoamine transporter-2 function: neurotoxic and therapeutic implications. Neuropharmacology 56 Suppl 1:133-138.

Foster JD, Vaughan RA (2011) Palmitoylation controls dopamine transporter kinetics, degradation, and protein kinase C-dependent regulation. The Journal of Biological Chemistry 286:5175-5186.

Foster JD, Cervinski MA, Gorentla BK, Vaughan RA (2006) Regulation of the dopamine transporter by phosphorylation. Handbook of Experimental Pharmacology:197-214.

Foster JD, Adkins SD, Lever JR, Vaughan RA (2008) Phorbol ester induced trafficking-independent regulation and enhanced phosphorylation of the dopamine transporter associated with membrane rafts and cholesterol. Journal of Neurochemistry 105:1683-1699.

Furber AS, Maheswaran R, Newell JN, Carroll C (2007) Is smoking tobacco an independent risk factor for HIV infection and progression to AIDS? A systemic review. Sex Transm Infect 83:41-46.

Furman CA, Chen R, Guptaroy B, Zhang M, Holz RW, Gnegy M (2009) Dopamine and amphetamine rapidly increase dopamine transporter trafficking to the surface: live-cell imaging using total internal reflection fluorescence microscopy. J Neurosci 29:3328-3336.

Fuster M, Estrada V, Fernandez-Pinilla MC, Fuentes-Ferrer ME, Tellez MJ, Vergas J, Serrano-Villar S, Fernandez-Cruz A (2009) Smoking cessation in HIV patients: rate of success and associated factors. HIV Med 10:614-619.

Gabdoulline RR, Wade RC (1998) Brownian dynamics simulation of protein-protein diffusional encounter. Methods 14:329-341.

Gallo R, Wong-Staal F, Montagnier L, Haseltine WA, Yoshida M (1988) HIV/HTLV gene nomenclature. Nature 333.

Gandhi N, Saiyed ZM, Napuri J, Samikkannu T, Reddy PVB, Agudelo M, Khatavkar P, Saxena SK, Nair MPN (2010) Interactive role of human immunodeficiency virus type 1 (HIV-1) clade-specific Tat protein and cocaine in blood-brain barrier dysfunction: implications for HIV-1-associated neurocognitive disorder. Journal of Neurovirology 16:294-305.

Gannon P, Khan MZ, Kolson DL (2011) Current understanding of HIV-associated neurocognitive disorders pathogenesis. Current Opinion in Neurology 24:275-283.

Gaskill PJ, Calderon TM, Coley JS, Berman JW (2013) Drug induced increases in CNS dopamine alter monocyte, macrophage and T cell functions: implications for HAND. Journal of neuroimmune pharmacology : the official journal of the Society on NeuroImmune Pharmacology 8:621-642.

Gaskill PJ, Calderon TM, Luers AJ, Eugenin EA, Javitch JA, Berman JW (2009) Human immunodeficiency virus (HIV) infection of human macrophages is increased by dopamine: a bridge between HIV-associated neurologic disorders and drug abuse. The American Journal of Pathology 175:1148-1159.

Gelman BB, Spencer JA, Holzer CE, 3rd, Soukup VM (2006) Abnormal striatal dopaminergic synapses in National NeuroAIDS Tissue Consortium subjects with HIV encephalitis. Journal of Neuroimmune Pharmacology: The Official Journal of the Society on NeuroImmune Pharmacology 1:410-420.

Gelman BB, Lisinicchia JG, Chen T, Johnson KM, Jennings K, Freeman DH, Jr., Soukup VM (2012) Prefrontal Dopaminergic and Enkephalinergic Synaptic Accommodation in HIV-associated Neurocognitive Disorders and Encephalitis. Journal of neuroimmune pharmacology : the official journal of the Society on NeuroImmune Pharmacology 7:686-700.

Girault JA, Valjent E, Caboche J, Herve D (2007) ERK2: a logical AND gate critical for drug-induced plasticity? Curr Opin Pharmacol 7:77-85.

González-Lugo OE, Ceballos-Huerta F, Jiménez-Capdeville ME, Arankowsky-Sandoval G, Góngora-Alfaro JL (2010) Synergism of theophylline and anticholinergics to inhibit haloperidol-induced catalepsy: a potential treatment for extrapyramidal syndromes. Prog Neuropsychopharmacol Biol Psychiatry 34:1465-1471.

Gorantla S, Poluektova L, Gendelman HE (2012) Rodent models for HIV-associated neurocognitive disorders. Trends in Neurosciences.

Gorentla BK, Vaughan RA (2005) Differential effects of dopamine and psychoactive drugs on dopamine transporter phosphorylation and regulation. Neuropharmacology 49:759-768.

Göttlinger HG, Sodroski JG, Haseltine WA (1989) Role of capsid precursor processing and myristoylation in morphogenesis and infectivity of human immunodeficiency virus type 1. Proceedings of the National Academy of Sciences of the United States of America 86:5781-5785.

Granas C, Ferrer J, Loland CJ, Javitch JA, Gether U (2003) N-terminal truncation of the dopamine transporter abolishes phorbol ester- and substance P receptor-stimulated phosphorylation without impairing transporter internalization. The Journal of Biological Chemistry 278:4990-5000.

Grovit-Ferbas K, Harris-White ME (2010) Thinking about HIV: the intersection of virus, neuroinflammation and cognitive dysfunction. Immunol Res 48:40-58.

Gu H, Wall SC, Rudnick G (1994) Stable expression of biogenic amine transporters reveals differences in inhibitor sensitivity, kinetics, and ion dependence. J Biol Chem 269:7124-7130.

Gulley JM, Doolen S, Zahniser NR (2002) Brief, repeated exposure to substrates down-regulates dopamine transporter function in Xenopus oocytes in vitro and rat dorsal striatum in vivo. J Neurochem 83:400-411.

Guptaroy B, Fraser R, Desai A, Zhang M, Gnegy ME (2011) Site-directed mutations near transmembrane domain 1 alter conformation and function of norepinephrine and dopamine transporters. Molecular Pharmacology 79:520-532.

Guptaroy B, Zhang M, Bowton E, Binda F, Shi L, Weinstein H, Galli A, Javitch JA, Neubig RR, Gnegy ME (2009) A juxtamembrane mutation in the N terminus of the dopamine transporter induces preference for an inward-facing conformation. Molecular Pharmacology 75:514-524.

Hanna Z, Kay DG, Rebai N, Guimond A, Jothy S, Jolicoeur P (1998) Nef harbors a major determinant of pathogenicity for an AIDS-like disease induced by HIV-1 in transgenic mice. Cell 95:163-175.

Harrod SB, Van Horn ML (2009) Sex differences in tolerance to the locomotor depressant effects of lobeline in periadolescent rats. Pharmacology Biochemistry and Behavior 94:296-304.

Harrod SB, Mactutus CF, Fitting S, Hasselrot U, Booze RM (2008) Intra-accumbal Tat1-72 alters acute and sensitized responses to cocaine. Pharmacol Biochem Behav 90:723-729.

Harrod SB, Mactutus CF, Bennett K, Hasselrot U, Wu G, Welch M, Booze RM (2004) Sex differences and repeated intravenous nicotine: behavioral sensitization and dopamine receptors. Pharmacol Biochem Behav 78:581-592.

Haughey NJ, Mattson MP (2002) Calcium dysregulation and neuronal apoptosis by the HIV-1 proteins Tat and gp120. Journal of Acquired Immune Deficiency Syndromes (1999) 31 Suppl 2:S55-61.

Hayman M, Arbuthnott G, Harkiss G, Brace H, Filippi P, Philippon V, Thomson D, Vigne R, Wright A (1993) Neurotoxicity of peptide analogues of the transactivating protein tat from Maedi-Visna virus and human immunodeficiency virus. Neuroscience 53:1-6.

Heaton RK et al. (2010) HIV-associated neurocognitive disorders persist in the era of potent antiretroviral therapy: CHARTER Study. Neurology 75:2087-2096.

Hershberger SL, Fisher DG, Reynolds GL, Klahn JA, Wood MM (2004) Nicotine dependence and HIV risk behaviors among illicit drug users. Addict Behav 29:623-625.

Hetman M, Gozdz A (2004) Role of extracellular signal regulated kinases 1 and 2 in neuronal survival. Eur J Biochem 271:2050-2055.

Hetzer C, Dormeyer W, Schnölzer M, Ott M (2005) Decoding Tat: the biology of HIV Tat posttranslational modifications. Microbes and Infection 7:1364-1369.

Hoaglin DC, Iglewicz B (1987) Fine-Tuning Some Resistant Rules for Outlier Labeling. Journal of the American Statistical Association 82:1147-1149.

Hoenig JM, Heisey DM (2001) The Abuse of Power. The American Statistician 55:19-24.

Holton KL, Loder MK, Melikian HE (2005) Nonclassical, distinct endocytic signals dictate constitutive and PKC-regulated neurotransmitter transporter internalization. Nat Neurosci 8:881-888.

Hong WC, Amara SG (2013) Differential targeting of the dopamine transporter to recycling or degradative pathways during amphetamine- or PKC-regulated endocytosis in dopamine neurons. FASEB journal : official publication of the Federation of American Societies for Experimental Biology 27:2995-3007.

Hu S, Sheng WS, Lokensgard JR, Peterson PK, Rock RB (2009) Preferential sensitivity of human dopaminergic neurons to gp120-induced oxidative damage. J Neurovirol 15:401-410.

Huang X, Zhan CG (2007) How dopamine transporter interacts with dopamine: insights from molecular modeling and simulation. Biophysical journal 93:3627-3639.

Huang X, Gu HH, Zhan CG (2009) Mechanism for cocaine blocking the transport of dopamine: insights from molecular modeling and dynamics simulations. The journal of physical chemistry B 113:15057-15066.

Hudson L, Liu J, Nath A, Jones M, Raghavan R, Narayan O, Male D, Everall I (2000) Detection of the human immunodeficiency virus regulatory protein tat in CNS tissues. Journal of Neurovirology 6:145-155.

Hudson LG, Gale JM, Padilla RS, Pickett G, Alexander BE, Wang J, Kusewitt DF (2010) Microarray analysis of cutaneous squamous cell carcinomas reveals enhanced expression of epidermal differentiation complex genes. Mol Carcinog 49:619-629.

Iniguez SD, Warren BL, Neve RL, Russo SJ, Nestler EJ, Bolanos-Guzman CA (2010) Viral-mediated expression of extracellular signal-regulated kinase-2 in the ventral tegmental area modulates behavioral responses to cocaine. Behav Brain Res 214:460-464.

Iwamoto ET (1984) An assessment of the spontaneous activity of rats administered morphine, phencyclidine, or nicotine using automated and observational methods. Psychopharmacology (Berl) 84:374-382.

Jackson KJ, McIntosh JM, Brunzell DH, Sanjakdar SS, Damaj MI (2009) The role of alpha6-containing nicotinic acetylcholine receptors in nicotine reward and withdrawal. The Journal of pharmacology and experimental therapeutics 331:547-554.

Jacobs MM, Murray J, Byrd DA, Hurd YL, Morgello S (2013) HIV-related cognitive impairment shows bi-directional association with dopamine receptor DRD1 and DRD2 polymorphisms in substance-dependent and substance-independent populations. Journal of Neurovirology 19:495-504.

Jaeger LB, Nath A (2012) Modeling HIV-associated neurocognitive disorders in mice: new approaches in the changing face of HIV neuropathogenesis. Dis Model Mech 5:313-322.

Jardetzky O (1966) Simple allosteric model for membrane pumps. Nature 211:969-970.

Javitch JA (1998) Probing structure of neurotransmitter transporters by substituted-cysteine accessibility method. Meth Enzymol 296:331-346.

Jeang KT, Xiao H, Rich EA (1999) Multifaceted activities of the HIV-1 transactivator of transcription, Tat. The Journal of Biological Chemistry 274:28837-28840.

Jerome A, Sanberg PR (1987) The effects of nicotine on locomotor behavior in non-tolerant rats: a multivariate assessment. Psychopharmacology (Berl) 93:397-400.

Johnson LA, Furman CA, Zhang M, Guptaroy B, Gnegy ME (2005) Rapid delivery of the dopamine transporter to the plasmalemmal membrane upon amphetamine stimulation. Neuropharmacology 49:750-758.

Johnson RG, Jr. (1988) Accumulation of biological amines into chromaffin granules: a model for hormone and neurotransmitter transport. Physiological reviews 68:232-307.

Jones GJ, Barsby NL, Cohen EA, Holden J, Harris K, Dickie P, Jhamandas J, Power C (2007) HIV-1 Vpr causes neuronal apoptosis and in vivo neurodegeneration. The Journal of Neuroscience: The Official Journal of the Society for Neuroscience 27:3703-3711.

Jones M, Olafson K, Del Bigio MR, Peeling J, Nath A (1998) Intraventricular injection of human immunodeficiency virus type 1 (HIV-1) tat protein causes inflammation, gliosis, apoptosis, and ventricular enlargement. Journal of Neuropathology and Experimental Neurology 57:563-570.

Joyce EM, Koob GF (1981) Amphetamine-, scopolamine- and caffeine-induced locomotor activity following 6-hydroxydopamine lesions of the mesolimbic dopamine system. Psychopharmacology (Berl) 73:311-313.

Kalivas PW (1995) Interactions between dopamine and excitatory amino acids in behavioral sensitization to psychostimulants. Drug Alcohol Depend 37:95-100.

Kass MD, Liu X, Vigorito M, Chang L, Chang SL (2010) Methamphetamine-induced behavioral and physiological effects in adolescent and adult HIV-1 transgenic rats. Journal of neuroimmune pharmacology : the official journal of the Society on NeuroImmune Pharmacology 5:566-573.

Katzenschlager R, Sampaio C, Costa J, Lees A (2003) Anticholinergics for symptomatic management of Parkinson's disease. The Cochrane Database of Systematic Reviews.

Kaul M, Lipton SA (2006) Mechanisms of neuroimmunity and neurodegeneration associated with HIV-1 infection and AIDS. Journal of Neuroimmune Pharmacology: The Official Journal of the Society on NeuroImmune Pharmacology 1:138-151.

Kaul M, Garden GA, Lipton SA (2001) Pathways to neuronal injury and apoptosis in HIV-associated dementia. Nature 410:988-994.

Kelly PH, Iversen SD (1976) Selective 6OHDA-induced destruction of mesolimbic dopamine neurons: abolition of psychostimulant-induced locomotor activity in rats. Eur J Pharmacol 40:45-56.

Khoshbouei H, Sen N, Guptaroy B, Johnson LA, Lund D, Gnegy ME, Galli A, Javitch JA (2004) N-Terminal Phosphorylation of the Dopamine Transporter Is Required for Amphetamine-Induced Efflux. PLoS Biol 2.

Kieburtz K, Ketonen L, Cox C, Grossman H, Holloway R, Booth H, Hickey C, Feigin A, Caine ED (1996) Cognitive performance and regional brain volume in human immunodeficiency virus type 1 infection. Archives of neurology 53:155-158.

Kim BO, Liu Y, Ruan Y, Xu ZC, Schantz L, He JJ (2003) Neuropathologies in transgenic mice expressing human immunodeficiency virus type 1 Tat protein under the regulation of the astrocyte-specific glial fibrillary acidic protein promoter and doxycycline. The American Journal of Pathology 162:1693-1707.

King SR (1994) HIV: virology and mechanisms of disease. Ann Emerg Med 24:443-449.

Kita T, Okamoto M, Nakashima T (1992) Nicotine-induced sensitization to ambulatory stimulant effect produced by daily administration into the ventral tegmental area and the nucleus accumbens in rats. Life Sci 50:583-590.

Kitayama S, Shimada S, Xu H, Markham L, Donovan DM, Uhl GR (1992) Dopamine transporter site-directed mutations differentially alter substrate transport and cocaine binding. Proceedings of the National Academy of Sciences of the United States of America 89:7782-7785.

Koob GF, Stinus L, Le Moal M (1981) Hyperactivity and hypoactivity produced by lesions to the mesolimbic dopamine system. Behav Brain Res 3:341-359.

Koutsilieri E, Sopper S, Scheller C, ter Meulen V, Riederer P (2002a) Involvement of dopamine in the progression of AIDS Dementia Complex. J Neural Transm 109:399-410.

Koutsilieri E, Sopper S, Scheller C, ter Meulen V, Riederer P (2002b) Parkinsonism in HIV dementia. Journal of Neural Transmission (Vienna, Austria: 1996) 109:767-775.

Koutsilieri E, Scheller C, Sopper S, ter Meulen V, Riederer P (2002c) Psychiatric complications in human immunodeficiency virus infection. Journal of Neurovirology 8 Suppl 2:129-133.

Kristensen AS, Andersen J, Jørgensen TN, Sørensen L, Eriksen J, Loland CJ, Strømgaard K, Gether U (2011) SLC6 neurotransmitter transporters: structure, function, and regulation. Pharmacological Reviews 63:585-640.

Kruman II, Nath A, Mattson MP (1998) HIV-1 protein Tat induces apoptosis of hippocampal neurons by a mechanism involving caspase activation, calcium overload, and oxidative stress. Experimental Neurology 154:276-288.

Ksir C (1994) Acute and chronic nicotine effects on measures of activity in rats: a multivariate analysis. Psychopharmacology (Berl) 115:105-109.

Kubos KL, Moran TH, Robinson RG (1987) Differential and asymmetrical behavioral effects of electrolytic or 6-hydroxydopamine lesions in the nucleus accumbens. Brain Res 401:147-151.

Kumar AM, Ownby RL, Waldrop-Valverde D, Fernandez B, Kumar M (2011) Human immunodeficiency virus infection in the CNS and decreased dopamine availability: relationship with neuropsychological performance. Journal of Neurovirology 17:26-40.

Kumar AM, Fernandez JB, Singer EJ, Commins D, Waldrop-Valverde D, Ownby RL, Kumar M (2009) Human immunodeficiency virus type 1 in the central nervous system leads to decreased dopamine in different regions of postmortem human brains. Journal of Neurovirology 15:257-274.

Lamers SL, Salemi M, Galligan DC, Morris A, Gray R, Fogel G, Zhao L, McGrath MS (2010) Human immunodeficiency virus-1 evolutionary patterns associated with pathogenic processes in the brain. J Neurovirol 16:230-241.

Larrat EP, Zierler S (1993) Entangled epidemics: cocaine use and HIV disease. J Psychoactive Drugs 25:207-221.

Larsson M, Hagberg L, Forsman A, Norkrans G (1991) Cerebrospinal fluid catecholamine metabolites in HIV-infected patients. Journal of neuroscience research 28:406-409.

Lashomb AL, Vigorito M, Chang SL (2009) Further characterization of the spatial learning deficit in the human immunodeficiency virus-1 transgenic rat. Journal of Neurovirology 15:14-24.

Laviolette SR, van der Kooy D (2004) The neurobiology of nicotine addiction: bridging the gap from molecules to behaviour. Nat Rev Neurosci 5:55-65.

Lee S-K, Potempa M, Swanstrom R (2012) The choreography of HIV-1 proteolytic processing and virion assembly. The Journal of Biological Chemistry 287:40867-40874.

Levine M, Ensom MH (2001) Post hoc power analysis: an idea whose time has passed? Pharmacotherapy 21:405-409.

Li LB, Cui XN, Reith MA (2002) Is Na(+) required for the binding of dopamine, amphetamine, tyramine, and octopamine to the human dopamine transporter? Naunyn Schmiedebergs Arch Pharmacol 365:303-311.

Li W, Galey D, Mattson MP, Nath A (2005) Molecular and cellular mechanisms of neuronal cell death in HIV dementia. Neurotoxicity Research 8:119-134.

Li W, Li G, Steiner J, Nath A (2009) Role of Tat protein in HIV neuropathogenesis. Neurotox Res 16:205-220.

Li W, Huang Y, Reid R, Steiner J, Malpica-Llanos T, Darden TA, Shankar SK, Mahadevan A, Satishchandra P, Nath A (2008) NMDA receptor activation by HIV-Tat protein is clade dependent. The Journal of Neuroscience: The Official Journal of the Society for Neuroscience 28:12190-12198.

Liang Y-J, Zhen J, Chen N, Reith MEA (2009) Interaction of catechol and non-catechol substrates with externally or internally facing dopamine transporters. Journal of Neurochemistry 109:981-994.

Lin Z, Uhl GR (2005) Proline mutations induce negative-dosage effects on uptake velocity of the dopamine transporter. Journal of Neurochemistry 94:276-287.

Lin Z, Itokawa M, Uhl GR (2000) Dopamine transporter proline mutations influence dopamine uptake, cocaine analog recognition, and expression. FASEB journal : official publication of the Federation of American Societies for Experimental Biology 14:715-728.

Liu X, Chang L, Vigorito M, Kass M, Li H, Chang SL (2009) Methamphetamine-induced behavioral sensitization is enhanced in the HIV-1 transgenic rat. Journal of Neuroimmune Pharmacology: The Official Journal of the Society on NeuroImmune Pharmacology 4:309-316.

Lloyd AC (2006) Distinct functions for ERKs? J Biol 5:13.

Loder MK, Melikian HE (2003) The dopamine transporter constitutively internalizes and recycles in a protein kinase C-regulated manner in stably transfected PC12 cell lines. The Journal of Biological Chemistry 278:22168-22174.

Loland CJ, Norgaard-Nielsen K, Gether U (2003) Probing dopamine transporter structure and function by Zn2+-site engineering. European Journal of Pharmacology 479:187-197.

Loland CJ, Norregaard L, Litman T, Gether U (2002) Generation of an activating Zn(2+) switch in the dopamine transporter: mutation of an intracellular tyrosine constitutively alters the conformational equilibrium of the transport cycle. Proc Natl Acad Sci U S A 99:1683-1688.

Loland CJ, Grånäs C, Javitch JA, Gether U (2004) Identification of intracellular residues in the dopamine transporter critical for regulation of transporter conformation and cocaine binding. The Journal of Biological Chemistry 279:3228-3238.

Loland CJ, Desai RI, Zou M-F, Cao J, Grundt P, Gerstbrein K, Sitte HH, Newman AH, Katz JL, Gether U (2008) Relationship between conformational changes in the dopamine transporter and cocaine-like subjective effects of uptake inhibitors. Molecular Pharmacology 73:813-823.

Lopez OL, Smith G, Meltzer CC, Becker JT (1999) Dopamine systems in human immunodeficiency virus-associated dementia. Neuropsychiatry Neuropsychol Behav Neurol 12:184-192.

Louis M, Clarke PB (1998) Effect of ventral tegmental 6-hydroxydopamine lesions on the locomotor stimulant action of nicotine in rats. Neuropharmacology 37:1503-1513.

Lu L, Wang X, Wu P, Xu C, Zhao M, Morales M, Harvey BK, Hoffer BJ, Shaham Y (2009) Role of ventral tegmental area glial cell line-derived neurotrophic factor in incubation of cocaine craving. Biol Psychiatry 66:137-145.

Lyon GJ, Abi-Dargham A, Moore H, Lieberman JA, Javitch JA, Sulzer D (2011) Presynaptic regulation of dopamine transmission in schizophrenia. Schizophr Bull 37:108-117.

Ma M, Nath A (1997) Molecular determinants for cellular uptake of Tat protein of human immunodeficiency virus type 1 in brain cells. J Virol 71:2495-2499.

Magnuson DS, Knudsen BE, Geiger JD, Brownstone RM, Nath A (1995) Human immunodeficiency virus type 1 tat activates non-N-methyl-D-aspartate excitatory amino acid receptors and causes neurotoxicity. Ann Neurol 37:373-380.

Manda VK, Mittapalli RK, Geldenhuys WJ, Lockman PR (2010) Chronic exposure to nicotine and saquinavir decreases endothelial Notch-4 expression and disrupts blood-brain barrier integrity. J Neurochem 115:515-525.

Mansvelder HD, Keath JR, McGehee DS (2002) Synaptic mechanisms underlie nicotine-induced excitability of brain reward areas. Neuron 33:905-919.

Maragos WF, Young KL, Turchan JT, Guseva M, Pauly JR, Nath A, Cass WA (2002) Human immunodeficiency virus-1 Tat protein and methamphetamine interact synergistically to impair striatal dopaminergic function. J Neurochem 83:955-963.

Mattson MP, Haughey NJ, Nath A (2005) Cell death in HIV dementia. Cell Death and Differentiation 12 Suppl 1:893-904.

McArthur JC, Steiner J, Sacktor N, Nath A (2010) Human immunodeficiency virus-associated neurocognitive disorders: Mind the gap. Ann Neurol 67:699-714.

McCune JM (2001) The dynamics of CD4+ T-cell depletion in HIV disease. Nature 410:974-979.

McPhail ME, Robertson KR (2011) Neurocognitive impact of antiretroviral treatment: thinking long-term. Current HIV/AIDS Reports 8:249-256.

Meade CS, Conn NA, Skalski LM, Safren SA (2011a) Neurocognitive impairment and medication adherence in HIV patients with and without cocaine dependence. J Behav Med 34:128-138.

Meade CS, Lowen SB, MacLean RR, Key MD, Lukas SE (2011b) fMRI brain activation during a delay discounting task in HIV-positive adults with and without cocaine dependence. Psychiatry Res 192:167-175.

Melikian HE (2004) Neurotransmitter transporter trafficking: endocytosis, recycling, and regulation. Pharmacology & Therapeutics 104:17-27.

Merk A, Subramaniam S (2013) HIV-1 envelope glycoprotein structure. Curr Opin Struct Biol 23:268-276.

Midde NM, Gomez AM, Zhu J (2012) HIV-1 Tat Protein Decreases Dopamine Transporter Cell Surface Expression and Vesicular Monoamine Transporter-2 Function in Rat Striatal Synaptosomes. Journal of neuroimmune pharmacology : the official journal of the Society on NeuroImmune Pharmacology 7:629-639.

Midde NM, Gomez AM, Harrod SB, Zhu J (2011) Genetically expressed HIV-1 viral proteins attenuate nicotine-induced behavioral sensitization and alter mesocorticolimbic ERK and CREB signaling in rats. Pharmacology, Biochemistry, and Behavior 98:587-597.

Midde NM, Huang X, Gomez AM, Booze RM, Zhan CG, Zhu J (2013) Mutation of tyrosine 470 of human dopamine transporter is critical for HIV-1 Tat-induced inhibition of dopamine transport and transporter conformational transitions. Journal of neuroimmune pharmacology : the official journal of the Society on NeuroImmune Pharmacology 8:975-987.

Middleton LS, Apparsundaram S, King-Pospisil KA, Dwoskin LP (2007) Nicotine increases dopamine transporter function in rat striatum through a trafficking-independent mechanism. Eur J Pharmacol 554:128-136.

Mineur YS, Brunzell DH, Grady SR, Lindstrom JM, McIntosh JM, Marks MJ, King SL, Picciotto MR (2009) Localized low-level re-expression of high-affinity mesolimbic nicotinic acetylcholine receptors restores nicotine-induced locomotion but not place conditioning. Genes Brain Behav 8:257-266.

Money KM, Stanwood GD (2013) Developmental origins of brain disorders: roles for dopamine. Front Cell Neurosci 7.

Moran LM, Aksenov MY, Booze RM, Webb KM, Mactutus CF (2012) Adolescent HIV-1 transgenic rats: evidence for dopaminergic alterations in behavior and neurochemistry revealed by methamphetamine challenge. Current HIV Research 10:415-424.

Moritz AE, Foster JD, Gorentla BK, Mazei-Robison MS, Yang JW, Sitte HH, Blakely RD, Vaughan RA (2013) Phosphorylation of dopamine transporter serine 7 modulates cocaine analog binding. J Biol Chem 288:20-32.

Morrow T (2008) Gene therapy offers HD patients relief from some symptoms. Tetrabenazine inhibits the transport of a molecule called vesicular monoamine transporter type 2 or VMAT2. Manag Care 17:46-47.

Mosharov EV, Larsen KE, Kanter E, Phillips KA, Wilson K, Schmitz Y, Krantz DE, Kobayashi K, Edwards RH, Sulzer D (2009) Interplay between cytosolic dopamine, calcium, and alpha-synuclein causes selective death of substantia nigra neurons. Neuron 62:218-229.

Mothobi NZ, Brew BJ (2012) Neurocognitive dysfunction in the highly active antiretroviral therapy era. Curr Opin Infect Dis 25:4-9.

Nahvi S, Cooperman NA (2009) Review: the need for smoking cessation among HIV-positive smokers. AIDS Educ Prev 21:14-27.

Nair MPN, Samikkannu T (2012) Differential regulation of neurotoxin in HIV clades: role of cocaine and methamphetamine. Current HIV Research 10:429-434.

Nakayama H, Numakawa T, Ikeuchi T, Hatanaka H (2001) Nicotine-induced phosphorylation of extracellular signal-regulated protein kinase and CREB in PC12h cells. J Neurochem 79:489-498.

Nath A (2002) Human immunodeficiency virus (HIV) proteins in neuropathogenesis of HIV dementia. The Journal of infectious diseases 186 Suppl 2:S193-198.

Nath A (2010) Human immunodeficiency virus-associated neurocognitive disorder: pathophysiology in relation to drug addiction. Annals of the New York Academy of Sciences 1187:122-128.

Nath A, Clements JE (2011) Eradication of HIV from the brain: reasons for pause. AIDS (London, England) 25:577-580.

Nath A, Jankovic J, Pettigrew LC (1987) Movement disorders and AIDS. Neurology 37:37-41.

Nath A, Conant K, Chen P, Scott C, Major EO (1999) Transient exposure to HIV-1 Tat protein results in cytokine production in macrophages and astrocytes. A hit and run phenomenon. J Biol Chem 274:17098-17102.

Nath A, Maragos WF, Avison MJ, Schmitt FA, Berger JR (2001) Acceleration of HIV dementia with methamphetamine and cocaine. J Neurovirol 7:66-71.

Nath A, Haughey NJ, Jones M, Anderson C, Bell JE, Geiger JD (2000a) Synergistic neurotoxicity by human immunodeficiency virus proteins Tat and gp120: protection by memantine. Annals of Neurology 47:186-194.

Nath A, Anderson C, Jones M, Maragos W, Booze R, Mactutus C, Bell J, Hauser KF, Mattson M (2000b) Neurotoxicity and dysfunction of dopaminergic systems

associated with AIDS dementia. Journal of Psychopharmacology (Oxford, England) 14:222-227.

Nestler EJ (2001) Molecular neurobiology of addiction. Am J Addict 10:201-217.

New DR, Ma M, Epstein LG, Nath A, Gelbard HA (1997) Human immunodeficiency virus type 1 Tat protein induces death by apoptosis in primary human neuron cultures. Journal of Neurovirology 3:168-173.

Nieman RB, Fleming J, Coker RJ, Harris JR, Mitchell DM (1993) The effect of cigarette smoking on the development of AIDS in HIV-1-seropositive individuals. Aids 7:705-710.

Nisell M, Nomikos GG, Svensson TH (1994a) Infusion of nicotine in the ventral tegmental area or the nucleus accumbens of the rat differentially affects accumbal dopamine release. Pharmacol Toxicol 75:348-352.

Nisell M, Nomikos GG, Svensson TH (1994b) Systemic nicotine-induced dopamine release in the rat nucleus accumbens is regulated by nicotinic receptors in the ventral tegmental area. Synapse 16:36-44.

Norman LR, Basso M, Kumar A, Malow R (2009) Neuropsychological consequences of HIV and substance abuse: a literature review and implications for treatment and future research. Current drug abuse reviews 2:143-156.

Norregaard L, Loland CJ, Gether U (2003) Evidence for distinct sodium-, dopamine-, and cocaine-dependent conformational changes in transmembrane segments 7 and 8 of the dopamine transporter. The Journal of Biological Chemistry 278:30587-30596.

Norregaard L, Frederiksen D, Nielsen EO, Gether U (1998) Delineation of an endogenous zinc-binding site in the human dopamine transporter. The EMBO journal 17:4266-4273.

Obermann M, Kuper M, Kastrup O, Yaldizli O, Esser S, Thiermann J, Koutsilieri E, Arendt G, Diener HC, Maschke M (2009) Substantia nigra hyperechogenicity and CSF dopamine depletion in HIV. J Neurol 256:948-953.

Ondo WG, Tintner R, Thomas M, Jankovic J (2002) Tetrabenazine treatment for Huntington's disease-associated chorea. Clin Neuropharmacol 25:300-302.

Paleacu D, Giladi N, Moore O, Stern A, Honigman S, Badarny S (2004) Tetrabenazine treatment in movement disorders. Clin Neuropharmacol 27:230-233.

Palella FJ, Jr., Baker RK, Moorman AC, Chmiel JS, Wood KC, Brooks JT, Holmberg SD (2006) Mortality in the highly active antiretroviral therapy era: changing causes of death and disease in the HIV outpatient study. Journal of acquired immune deficiency syndromes 43:27-34.

Panagis G, Spyraki C (1996) Neuropharmacological evidence for the role of dopamine in ventral pallidum self-stimulation. Psychopharmacology (Berl) 123:280-288.

Pandey SC, Roy A, Xu T, Mittal N (2001) Effects of protracted nicotine exposure and withdrawal on the expression and phosphorylation of the CREB gene transcription factor in rat brain. J Neurochem 77:943-952.

Paris JJ, Carey AN, Shay CF, Gomes SM, He JJ, McLaughlin JP (2013) Effects of Conditional Central Expression of HIV-1 Tat Protein to Potentiate Cocaine-Mediated Psychostimulation and Reward Among Male Mice. Neuropsychopharmacology.

Pariser JJ, Partilla JS, Dersch CM, Ananthan S, Rothman RB (2008) Studies of the biogenic amine transporters. 12. Identification of novel partial inhibitors of amphetamine-induced dopamine release. The Journal of Pharmacology and Experimental Therapeutics 326:286-295.

Parnas ML, Gaffaney JD, Zou MF, Lever JR, Newman AH, Vaughan RA (2008) Labeling of dopamine transporter transmembrane domain 1 with the tropane ligand N-[4-(4-azido-3-[125I]iodophenyl)butyl]-2beta-carbomethoxy-3beta-(4-chlorophenyl) tropane implicates proximity of cocaine and substrate active sites. Mol Pharmacol 73:1141-1150.

Peloponese JM, Jr., Gregoire C, Opi S, Esquieu D, Sturgis J, Lebrun E, Meurs E, Collette Y, Olive D, Aubertin AM, Witvrow M, Pannecouque C, De Clercq E, Bailly C, Lebreton J, Loret EP (2000) 1H-13C nuclear magnetic resonance assignment and structural characterization of HIV-1 Tat protein. Comptes rendus de l'Academie des sciences Serie III, Sciences de la vie 323:883-894.

Peng J, Vigorito M, Liu X, Zhou D, Wu X, Chang SL (2010) The HIV-1 transgenic rat as a model for HIV-1 infected individuals on HAART. J Neuroimmunol 218:94-101.

Penmatsa A, Wang KH, Gouaux E (2013) X-ray structure of dopamine transporter elucidates antidepressant mechanism. Nature.

Perry SW, Barbieri J, Tong N, Polesskaya O, Pudasaini S, Stout A, Lu R, Kiebala M, Maggirwar SB, Gelbard HA (2010) Human immunodeficiency virus-1 Tat activates calpain proteases via the ryanodine receptor to enhance surface dopamine transporter levels and increase transporter-specific uptake and Vmax. J Neurosci 30:14153-14164.

Persidsky Y, Fox H (2007) Battle of Animal Models. Jrnl Neuroimmune Pharm 2:171-177.

Pierce B, Weng Z (2007) ZRANK: reranking protein docking predictions with an optimized energy function. Proteins 67:1078-1086.

Pierce BG, Hourai Y, Weng Z (2011) Accelerating protein docking in ZDOCK using an advanced 3D convolution library. PLoS ONE 6:e24657.

Pocernich CB, Sultana R, Mohmmad-Abdul H, Nath A, Butterfield DA (2005) HIV-dementia, Tat-induced oxidative stress, and antioxidant therapeutic considerations. Brain Res Brain Res Rev 50:14-26.

Post RM (1980) Intermittent versus continuous stimulation: effect of time interval on the development of sensitization or tolerance. Life Sci 26:1275-1282.

Pramod AB, Foster J, Carvelli L, Henry LK (2013) SLC6 transporters: structure, function, regulation, disease association and therapeutics. Mol Aspects Med 34:197-219.

Pristupa ZB, Wilson JM, Hoffman BJ, Kish SJ, Niznik HB (1994) Pharmacological heterogeneity of the cloned and native human dopamine transporter: disassociation of [3H]WIN 35,428 and [3H]GBR 12,935 binding. Mol Pharmacol 45:125-135.

Pugliese A, Vidotto V, Beltramo T, Petrini S, Torre D (2005) A review of HIV-1 Tat protein biological effects. Cell biochemistry and function 23:223-227.

Purohit V, Rapaka R, Shurtleff D (2011) Drugs of Abuse, Dopamine, and HIV-Associated Neurocognitive Disorders/HIV-Associated Dementia. Molecular Neurobiology 44:102-110.

Purohit V, Rapaka R, Frankenheim J, Avila A, Sorensen R, Rutter J (2013) National Institute on Drug Abuse symposium report: drugs of abuse, dopamine, and HIV-associated neurocognitive disorders/HIV-associated dementia. Journal of Neurovirology 19:119-122.

Radcliffe PM, Sterling CR, Tank AW (2009) Induction of tyrosine hydroxylase mRNA by nicotine in rat midbrain is inhibited by mifepristone. J Neurochem 109:1272-1284.

Ramamoorthy S, Shippenberg TS, Jayanthi LD (2011) Regulation of monoamine transporters: Role of transporter phosphorylation. Pharmacol Ther 129:220-238.

Rao JS, Kim H-W, Kellom M, Greenstein D, Chen M, Kraft AD, Harry GJ, Rapoport SI, Basselin M (2011) Increased neuroinflammatory and arachidonic acid cascade markers, and reduced synaptic proteins, in brain of HIV-1 transgenic rats. Journal of Neuroinflammation 8:101-101.

Ratner L, Haseltine W, Patarca R, Livak KJ, Starcich B, Josephs SF, Doran ER, Rafalski JA, Whitehorn EA, Baumeister K (1985) Complete nucleotide sequence of the AIDS virus, HTLV-III. Nature 313:277-284.

Rayne F, Debaisieux S, Bonhoure A, Beaumelle B (2010) HIV-1 Tat is unconventionally secreted through the plasma membrane. Cell Biology International 34:409-413.

Reid MS, Ho LB, Berger SP (1998) Behavioral and neurochemical components of nicotine sensitization following 15-day pretreatment: studies on contextual conditioning. Behav Pharmacol 9:137-148.

Reid W et al. (2001) An HIV-1 transgenic rat that develops HIV-related pathology and immunologic dysfunction. Proceedings of the National Academy of Sciences of the United States of America 98:9271-9276.

Reith ME, Berfield JL, Wang LC, Ferrer JV, Javitch JA (2001) The uptake inhibitors cocaine and benztropine differentially alter the conformation of the human dopamine transporter. J Biol Chem 276:29012-29018.

Reith MEA, Ali S, Hashim A, Sheikh IS, Theddu N, Gaddiraju NV, Mehrotra S, Schmitt KC, Murray TF, Sershen H, Unterwald EM, Davis FA (2012) Novel C-1 Substituted Cocaine Analogs Unlike Cocaine or Benztropine. The Journal of Pharmacology and Experimental Therapeutics 343:413-425.

Rescorla RA (1991) Associative Relations in Instrumental Learning - the 18th Bartlett Memorial Lecture. Quarterly Journal of Experimental Psychology Section B-Comparative and Physiological Psychology 43:1-23.

Richards TL, Zahniser NR (2009) Rapid substrate-induced down-regulation in function and surface localization of dopamine transporters: rat dorsal striatum versus nucleus accumbens. J Neurochem 108:1575-1584.

Richfield EK (1993) Zinc modulation of drug binding, cocaine affinity states, and dopamine uptake on the dopamine uptake complex. Mol Pharmacol 43:100-108.

Rilstone JJ, Alkhater RA, Minassian BA (2013) Brain dopamine-serotonin vesicular transport disease and its treatment. The New England journal of medicine 368:543-550.

Roberts DC, Corcoran ME, Fibiger HC (1977) On the role of ascending catecholaminergic systems in intravenous self-administration of cocaine. Pharmacol Biochem Behav 6:615-620.

Robertson KR, Smurzynski M, Parsons TD, Wu K, Bosch RJ, Wu J, McArthur JC, Collier AC, Evans SR, Ellis RJ (2007) The prevalence and incidence of neurocognitive impairment in the HAART era. Aids 21:1915-1921.

Robertson SD, Matthies HJG, Galli A (2009) A closer look at amphetamine-induced reverse transport and trafficking of the dopamine and norepinephrine transporters. Molecular Neurobiology 39:73-80.

Robinson TE, Berridge KC (1993) The neural basis of drug craving: an incentive-sensitization theory of addiction. Brain Res Brain Res Rev 18:247-291.

Robinson TE, Berridge KC (2003) Addiction. Annu Rev Psychol 54:25-53.

Rothman RB, Dersch CM, Ananthan S, Partilla JS (2009) Studies of the biogenic amine transporters. 13. Identification of "agonist" and "antagonist" allosteric modulators

of amphetamine-induced dopamine release. The Journal of Pharmacology and Experimental Therapeutics 329:718-728.

Ruben S, Perkins A, Purcell R, Joung K, Sia R, Burghoff R, Haseltine WA, Rosen CA (1989) Structural and functional characterization of human immunodeficiency virus tat protein. Journal of Virology 63:1-8.

Rudnick G, Clark J (1993) From synapse to vesicle: the reuptake and storage of biogenic amine neurotransmitters. Biochimica et biophysica acta 1144:249-263.

Sabatier JM, Vives E, Mabrouk K, Benjouad A, Rochat H, Duval A, Hue B, Bahraoui E (1991) Evidence for neurotoxic activity of tat from human immunodeficiency virus type 1. Journal of Virology 65:961-967.

Sager JJ, Torres GE (2011) Proteins Interacting with Monoamine Transporters: Current State and Future Challenges. Biochemistry.

Santoro TJ, Bryant JL, Pellicoro J, Klotman ME, Kopp JB, Bruggeman LA, Franks RR, Notkins AL, Klotman PE (1994) Growth failure and AIDS-like cachexia syndrome in HIV-1 transgenic mice. Virology 201:147-151.

Sardar AM, Czudek C, Reynolds GP (1996) Dopamine deficits in the brain: the neurochemical basis of parkinsonian symptoms in AIDS. Neuroreport 7:910-912.

Saunders C, Ferrer JV, Shi L, Chen J, Merrill G, Lamb ME, Leeb-Lundberg LM, Carvelli L, Javitch JA, Galli A (2000) Amphetamine-induced loss of human dopamine transporter activity: an internalization-dependent and cocaine-sensitive mechanism. Proc Natl Acad Sci U S A 97:6850-6855.

Scheller C, Sopper S, Jassoy C, ter Meulen V, Riederer P, Koutsilieri E (2000) Dopamine activates HIV in chronically infected T lymphoblasts. Journal of Neural Transmission (Vienna, Austria: 1996) 107:1483-1489.

Scheller C, Sopper S, Jenuwein M, Neuen-Jacob E, Tatschner T, Grünblatt E, ter Meulen V, Riederer P, Koutsilieri E (2005) Early impairment in dopaminergic neurotransmission in brains of SIV-infected rhesus monkeys due to microglia activation. Journal of Neurochemistry 95:377-387.

Scheller C, Arendt G, Nolting T, Antke C, Sopper S, Maschke M, Obermann M, Angerer A, Husstedt IW, Meisner F, Neuen-Jacob E, Müller HW, Carey P, Ter Meulen V, Riederer P, Koutsilieri E (2010b) Increased dopaminergic neurotransmission in therapy-naïve asymptomatic HIV patients is not associated with adaptive changes at the dopaminergic synapses. Journal of Neural Transmission (Vienna, Austria: 1996) 117:699-705.

Schmitt KC, Reith MEA (2010) Regulation of the dopamine transporter: aspects relevant to psychostimulant drugs of abuse. Annals of the New York Academy of Sciences 1187:316-340.

Schmitt KC, Reith MEA (2011) The atypical stimulant and nootropic modafinil interacts with the dopamine transporter in a different manner than classical cocaine-like inhibitors. PloS One 6:e25790-e25790.

Schmitt KC, Rothman RB, Reith MEA (2013) Nonclassical pharmacology of the dopamine transporter: atypical inhibitors, allosteric modulators, and partial substrates. The Journal of Pharmacology and Experimental Therapeutics 346:2-10.

Scholze P, Sitte HH, Singer EA (2001) Substantial loss of substrate by diffusion during uptake in HEK-293 cells expressing neurotransmitter transporters. Neuroscience Letters 309:173-176.

Shan J, Javitch JA, Shi L, Weinstein H (2011) The substrate-driven transition to an inward-facing conformation in the functional mechanism of the dopamine transporter. PloS One 6:e16350-e16350.

Shi L, Quick M, Zhao Y, Weinstein H, Javitch JA (2008) The mechanism of a neurotransmitter:sodium symporter--inward release of Na+ and substrate is triggered by substrate in a second binding site. Mol Cell 30:667-677.

Shojania S, O'Neil JD (2006) HIV-1 Tat is a natively unfolded protein: the solution conformation and dynamics of reduced HIV-1 Tat-(1-72) by NMR spectroscopy. The Journal of Biological Chemistry 281:8347-8356.

Silvers JM, Aksenova MV, Aksenov MY, Mactutus CF, Booze RM (2007) Neurotoxicity of HIV-1 Tat protein: involvement of D1 dopamine receptor. Neurotoxicology 28:1184-1190.

Silvers JM, Aksenov MY, Aksenova MV, Beckley J, Olton P, Mactutus CF, Booze RM (2006) Dopaminergic marker proteins in the substantia nigra of human immunodeficiency virus type 1-infected brains. Journal of Neurovirology 12:140-145.

Simioni S, Cavassini M, Annoni J-M, Rimbault Abraham A, Bourquin I, Schiffer V, Calmy A, Chave J-P, Giacobini E, Hirschel B, Du Pasquier RA (2010) Cognitive dysfunction in HIV patients despite long-standing suppression of viremia. AIDS (London, England) 24:1243-1250.

Singh SK, Piscitelli CL, Yamashita A, Gouaux E (2008) A competitive inhibitor traps LeuT in an open-to-out conformation. Science 322:1655-1661.

Sorkina T, Caltagarone J, Sorkin A (2013) Flotillins Regulate Membrane Mobility of the Dopamine Transporter but Are Not Required for Its Protein Kinase C Dependent Endocytosis. Traffic 14:709-724.

Sorkina T, Richards TL, Rao A, Zahniser NR, Sorkin A (2009) Negative regulation of dopamine transporter endocytosis by membrane-proximal N-terminal residues. The Journal of Neuroscience: The Official Journal of the Society for Neuroscience 29:1361-1374.

Sporer B, Linke R, Seelos K, Paul R, Klopstock T, Pfister HW (2005) HIV-induced chorea: evidence for basal ganglia dysregulation by SPECT. Journal of Neurology 252:356-358.

Strazza M, Pirrone V, Wigdahl B, Nonnemacher MR (2011) Breaking down the barrier: the effects of HIV-1 on the blood-brain barrier. Brain Research 1399:96-115.

Strebel K (2013) HIV accessory proteins versus host restriction factors. Curr Opin Virol 3:692-699.

Subramaniam S, Unsicker K (2010) ERK and cell death: ERK1/2 in neuronal death. FEBS J 277:22-29.

Sulzer D (2011) How addictive drugs disrupt presynaptic dopamine neurotransmission. Neuron 69:628-649.

Sulzer D, Sonders MS, Poulsen NW, Galli A (2005) Mechanisms of neurotransmitter release by amphetamines: a review. Prog Neurobiol 75:406-433.

Sulzer D, Chen TK, Lau YY, Kristensen H, Rayport S, Ewing A (1995) Amphetamine redistributes dopamine from synaptic vesicles to the cytosol and promotes reverse transport. J Neurosci 15:4102-4108.

Tanda G, Newman AH, Ebbs AL, Tronci V, Green JL, Tallarida RJ, Katz JL (2009) Combinations of cocaine with other dopamine uptake inhibitors: assessment of additivity. The Journal of Pharmacology and Experimental Therapeutics 330:802-809.

Taylor TN, Caudle WM, Shepherd KR, Noorian A, Jackson CR, Iuvone PM, Weinshenker D, Greene JG, Miller GW (2009) Nonmotor symptoms of Parkinson's disease revealed in an animal model with reduced monoamine storage capacity. The Journal of Neuroscience: The Official Journal of the Society for Neuroscience 29:8103-8113.

Teoh L, Allen H, Kowalenko N (2002) Drug-induced extrapyramidal reactions. J Paediatr Child Health 38:95-97.

Theodore S, Cass WA, Maragos WF (2006) Methamphetamine and human immunodeficiency virus protein Tat synergize to destroy dopaminergic terminals in the rat striatum. Neuroscience 137:925-935.

Theodore S, Cass WA, Dwoskin LP, Maragos WF (2012) HIV-1 protein Tat inhibits vesicular monoamine transporter-2 activity in rat striatum. Synapse 66:755-757.

Thiels E, Kanterewicz BI, Norman ED, Trzaskos JM, Klann E (2002) Long-term depression in the adult hippocampus in vivo involves activation of extracellular signal-regulated kinase and phosphorylation of Elk-1. J Neurosci 22:2054-2062.

Thomas FP, Chalk C, Lalonde R, Robitaille Y, Jolicoeur P (1994) Expression of human immunodeficiency virus type 1 in the nervous system of transgenic mice leads to neurological disease. Journal of Virology 68:7099-7107.

Thwar PK, Guptaroy B, Zhang M, Gnegy ME, Burns MA, Linderman JJ (2007) Simple transporter trafficking model for amphetamine-induced dopamine efflux. Synapse 61:500-514.

Toggas SM, Masliah E, Rockenstein EM, Rall GF, Abraham CR, Mucke L (1994) Central nervous system damage produced by expression of the HIV-1 coat protein gp120 in transgenic mice. Nature 367:188-193.

Torres GE, Amara SG (2007) Glutamate and monoamine transporters: new visions of form and function. Current opinion in neurobiology 17:304-312.

Torres GE, Gainetdinov RR, Caron MG (2003) Plasma membrane monoamine transporters: structure, regulation and function. Nature Reviews Neuroscience 4:13-25.

Tozzi V, Balestra P, Bellagamba R, Corpolongo A, Salvatori MF, Visco-Comandini U, Vlassi C, Giulianelli M, Galgani S, Antinori A, Narciso P (2007) Persistence of neuropsychologic deficits despite long-term highly active antiretroviral therapy in patients with HIV-related neurocognitive impairment: prevalence and risk factors. Journal of acquired immune deficiency syndromes 45:174-182.

Triant VA, Lee H, Hadigan C, Grinspoon SK (2007) Increased acute myocardial infarction rates and cardiovascular risk factors among patients with human immunodeficiency virus disease. J Clin Endocrinol Metab 92:2506-2512.

Trono D (1995) HIV accessory proteins: leading roles for the supporting cast. Cell 82:189-192.

UNAIDS (2011) Global report: UNAIDS report on the global AIDS epidemic. In: UNAIDS.

Valjent E, Corvol JC, Trzaskos JM, Girault JA, Herve D (2006) Role of the ERK pathway in psychostimulant-induced locomotor sensitization. BMC Neurosci 7:20.

Valjent E, Pascoli V, Svenningsson P, Paul S, Enslen H, Corvol JC, Stipanovich A, Caboche J, Lombroso PJ, Nairn AC, Greengard P, Herve D, Girault JA (2005) Regulation of a protein phosphatase cascade allows convergent dopamine and glutamate signals to activate ERK in the striatum. Proc Natl Acad Sci U S A 102:491-496.

Van Duyne R, Pedati C, Guendel I, Carpio L, Kehn-Hall K, Saifuddin M, Kashanchi F (2009) The utilization of humanized mouse models for the study of human retroviral infections. Retrovirology 6.

van Maanen M, Sutton RE (2003) Rodent models for HIV-1 infection and disease. Current HIV Research 1:121-130.

Vaughan RA, Foster JD (2013) Mechanisms of dopamine transporter regulation in normal and disease states. Trends Pharmacol Sci.

Vercruysse T, Daelemans D (2014) HIV-1 Rev Multimerization: Mechanism and Insights. Current HIV Research.

Vergo S, Johansen JL, Leist M, Lotharius J (2007) Vesicular monoamine transporter 2 regulates the sensitivity of rat dopaminergic neurons to disturbed cytosolic dopamine levels. Brain Res 1185:18-32.

Vigorito M, LaShomb AL, Chang SL (2007) Spatial learning and memory in HIV-1 transgenic rats. Journal of Neuroimmune Pharmacology: The Official Journal of the Society on NeuroImmune Pharmacology 2:319-328.

Volz TJ, Hanson GR, Fleckenstein AE (2007) The role of the plasmalemmal dopamine and vesicular monoamine transporters in methamphetamine-induced dopaminergic deficits. J Neurochem 101:883-888.

Wallace DR, Dodson S, Nath A, Booze RM (2006) Estrogen attenuates gp120- and tat1-72-induced oxidative stress and prevents loss of dopamine transporter function. Synapse 59:51-60.

Walters CL, Cleck JN, Kuo YC, Blendy JA (2005) Mu-opioid receptor and CREB activation are required for nicotine reward. Neuron 46:933-943.

Wang G-J, Chang L, Volkow ND, Telang F, Logan J, Ernst T, Fowler JS (2004) Decreased brain dopaminergic transporters in HIV-associated dementia patients. Brain: A Journal of Neurology 127:2452-2458.

Webb KM, Aksenov MY, Mactutus CF, Booze RM (2010) Evidence for developmental dopaminergic alterations in the human immunodeficiency virus-1 transgenic rat. Journal of Neurovirology 16:168-173.

Webber MP, Schoenbaum EE, Gourevitch MN, Buono D, Klein RS (1999) A prospective study of HIV disease progression in female and male drug users. Aids 13:257-262.

Westendorp MO, Frank R, Ochsenbauer C, Stricker K, Dhein J, Walczak H, Debatin KM, Krammer PH (1995) Sensitization of T cells to CD95-mediated apoptosis by HIV-1 Tat and gp120. Nature 375:497-500.

Wiley CA, Baldwin M, Achim CL (1996) Expression of HIV regulatory and structural mRNA in the central nervous system. AIDS (London, England) 10:843-847.

Williams DW, Calderon TM, Lopez L, Carvallo-Torres L, Gaskill PJ, Eugenin EA, Morgello S, Berman JW (2013) Mechanisms of HIV entry into the CNS: increased sensitivity of HIV infected CD14+CD16+ monocytes to CCL2 and key roles of CCR2, JAM-A, and ALCAM in diapedesis. PloS One 8.

Wise RA, Bozarth MA (1987) A psychomotor stimulant theory of addiction. Psychol Rev 94:469-492.

Xiao H, Neuveut C, Tiffany HL, Benkirane M, Rich EA, Murphy PM, Jeang KT (2000) Selective CXCR4 antagonism by Tat: implications for in vivo expansion of coreceptor use by HIV-1. Proc Natl Acad Sci U S A 97:11466-11471.

Yamashita A, Singh SK, Kawate T, Jin Y, Gouaux E (2005) Crystal structure of a bacterial homologue of Na+/Cl--dependent neurotransmitter transporters. Nature 437:215-223.

Yang Y, Wu J, Lu Y (2010) Mechanism of HIV-1-TAT induction of interleukin-1beta from human monocytes: Involvement of the phospholipase C/protein kinase C signaling cascade. J Med Virol 82:735-746.

Ying SW, Futter M, Rosenblum K, Webber MJ, Hunt SP, Bliss TV, Bramham CR (2002) Brain-derived neurotrophic factor induces long-term potentiation in intact adult hippocampus: requirement for ERK activation coupled to CREB and upregulation of Arc synthesis. J Neurosci 22:1532-1540.

Yoon S, Seger R (2006) The extracellular signal-regulated kinase: multiple substrates regulate diverse cellular functions. Growth Factors 24:21-44.

Zahniser NR, Sorkin A (2004) Rapid regulation of the dopamine transporter: role in stimulant addiction? Neuropharmacology 47:80-91.

Zapp ML, Green MR (1989) Sequence-specific RNA binding by the HIV-1 Rev protein. Nature 342:714-716.

Zauli G, Secchiero P, Rodella L, Gibellini D, Mirandola P, Mazzoni M, Milani D, Dowd DR, Capitani S, Vitale M (2000) HIV-1 Tat-mediated inhibition of the tyrosine hydroxylase gene expression in dopaminergic neuronal cells. The Journal of Biological Chemistry 275:4159-4165.

Zhang L, Meissner E, Chen J, Su L (2010) Current humanized mouse models for studying human immunology and HIV-1 immuno-pathogenesis. Sci China Life Sci 53:195-203.

Zhao L, Li F, Zhang Y, Elbourkadi N, Wang Z, Yu C, Taylor EW (2010a) Mechanisms and genes involved in enhancement of HIV infectivity by tobacco smoke. Toxicology 278:242-248.

Zhao Y, Terry D, Shi L, Weinstein H, Blanchard SC, Javitch JA (2010b) Single-molecule dynamics of gating in a neurotransmitter transporter homologue. Nature 465:188-193.

Zheng G, Dwoskin LP, Crooks PA (2006) Vesicular monoamine transporter 2: role as a novel target for drug development. AAPS J 8:E682-692.

Zhou Z, Zhen J, Karpowich NK, Law CJ, Reith MEA, Wang D-N (2009) Antidepressant specificity of serotonin transporter suggested by three LeuT-SSRI structures. Nature structural & molecular biology 16:652-657.

Zhou Z, Zhen J, Karpowich NK, Goetz RM, Law CJ, Reith MEA, Wang D-N (2007) LeuT-desipramine structure reveals how antidepressants block neurotransmitter reuptake. Science (New York, NY) 317:1390-1393.

Zhu J, Reith ME (2008) Role of the dopamine transporter in the action of psychostimulants, nicotine, and other drugs of abuse. CNS Neurol Disord Drug Targets 7:393-409.

Zhu J, Apparsundaram S, Dwoskin LP (2009a) Nicotinic receptor activation increases [3H]dopamine uptake and cell surface expression of dopamine transporters in rat prefrontal cortex. The Journal of pharmacology and experimental therapeutics 328:931-939.

Zhu J, Green T, Bardo MT, Dwoskin LP (2004) Environmental enrichment enhances sensitization to GBR 12935-induced activity and decreases dopamine transporter function in the medial prefrontal cortex. Behav Brain Res 148:107-117.

Zhu J, Apparsundaram S, Bardo MT, Dwoskin LP (2005) Environmental enrichment decreases cell surface expression of the dopamine transporter in rat medial prefrontal cortex. J Neurochem 93:1434-1443.

Zhu J, Mactutus CF, Wallace DR, Booze RM (2009b) HIV-1 Tat protein-induced rapid and reversible decrease in [3H]dopamine uptake: dissociation of [3H]dopamine uptake and [3H]2beta-carbomethoxy-3-beta-(4-fluorophenyl)tropane (WIN 35,428) binding in rat striatal synaptosomes. J Pharmacol Exp Ther 329:1071-1083.

Zhu J, Ananthan S, Mactutus CF, Booze RM (2011) Recombinant human immunodeficiency virus-1 transactivator of transcription1-86 allosterically modulates dopamine transporter activity. Synapse (New York, NY) 65:1251-1254.

Zubieta JK, Taylor SF, Huguelet P, Koeppe RA, Kilbourn MR, Frey KA (2001) Vesicular monoamine transporter concentrations in bipolar disorder type I, schizophrenia, and healthy subjects. Biological psychiatry 49:110-116.

Zucker M, Weizman A, Harel D, Rehavi M (2001) Changes in vesicular monoamine transporter (VMAT2) and synaptophysin in rat Substantia nigra and prefrontal cortex induced by psychotropic drugs. Neuropsychobiology 44:187-191.

APPENDIX A

GENERAL STATISTICAL ANALYSES CONSIDERATIONS

1. Replicates

For all the experiments performed in this dissertation, I used a minimum of two or three technical replicates. These replicates were either cell culture wells or tubes carrying same amount cell suspension. The reason for such technical replicates was to establish the validity of the method (e.g. pipetting errors). Three to eight biological replicates (sample size) were used to differentiate the random effect from "true" biological difference that is triggered by the treatment. The major advantage with the replicates is that they provide the ability to run various statistics to evaluate the variability. Ability to detect smaller but important changes and the capacity to spot the outliers in a dataset are the other benefits that can be achieved from the replicates. Using both technical and biological replicates in the experimental design increases the confidence of conclusions drawn from these experiments.

2. Power Analyses

A priori type power analysis was conducted for behavioral experiments for HIV-1 Tg and nicotine project using G*power software (Faul et al. 2007). This analysis indicated that a total sample of 32 animals would be needed to detect medium effects (0.40) with 80% power using an analysis of variance with alpha set at 0.05. A detailed statistical design for behavioral assays was described in the data analysis section of chapter 5. For the *in vitro* assays a priori power analysis was not estimated, however 0.75 to 0.99 'observed

power' was noted after experimental data was analyzed. Nevertheless, this post-hoc power analyses doesn't convey any new information as the significant p value (<0.05) indicates actually observed effect (Hoenig and Heisey, 2001; Levine and Ensom, 2001). Factorial design and statistical methods used for analysis of pharmacological data were elaborated in respective chapters in the dissertation.

3. Outlier detection

The outlier labeling rule (Hoaglin and Iglewicz, 1987) was used to identify the outliers in the data set. The formulae Upper limit = Q3 + (2.2 * (Q3 - Q1)); Lower limit = Q1 - (2.2 * (Q3 - Q1)) were used to detect extreme values from both ends. If an outlier was spotted, a root cause analysis was performed to determine the potential reason (e.g. measurement error). The data points were trimmed which accounts for only less than 5% of total data set for further analyses.

4. Randomization

To minimize the possibility of bias in the behavioral experiments, both HIV-1 Tg and F344 rats were randomly assigned to two treatment groups such as nicotine and saline. Sixteen HIV-1 Tg and 16 F344 animals were randomized into blocks of 8, 8 respectively. The randomization scheme was generated by using the Web site Randomization.com (http://www.randomization.com). Animal handling, drug treatment and placing the animals into locomotor chambers were performed by three technicians to further insure against human introduced bias into the procedure. Overall, randomization eliminates the selection bias and assures equality of treatments for accurate statistical analyses.